



**Downstream Signaling Pathway in Bone Stromal Cells Induced with
Basic Fibroblast Growth Factor (FGF2)**

Paweena Wongwitwichot

**A Thesis Submitted in Partial Fulfillment of the Requirements for the Degree of
Doctor of Philosophy in Pharmaceutical Sciences**

Prince of Songkla University

2015

Copyright of Prince of Songkla University

Thesis Title Downstream Signaling Pathway in Bone Stromal Cells Induced with Basic Fibroblast Growth Factor (FGF2)
Author Miss Paweena Wongwitwichot
Major Program Pharmaceutical Sciences

Major Advisor

Examining Committee:

.....Chairperson
(Assoc. Prof. Dr. Jasadee Kaewsrichan) (Asst. Prof. Dr. Bhutorn Canyuk)

Co-advisor

.....
(Dr. Danai Tiwawech)

.....
(Asst. Prof. Dr. Potchanapond Graidist) (Assoc. Prof. Dr. Chua Kien Hui)

.....
(Assoc. Prof. Dr. Jasadee Kaewsrichan)

.....
(Asst. Prof. Dr. Potchanapond Graidist)

The Graduate School, Prince of Songkla University, has approved this thesis as partial fulfillment of the requirements for the Degree of Doctor of Philosophy in Pharmaceutical Sciences.

.....
(Assoc. Prof. Dr. Teerapol Srichana)

Dean of Graduate School

This is to certify that the work here submitted is the result of the candidate's own investigations. Due acknowledgement has been made of any assistance received.

.....Signature

(Assoc. Prof. Dr. Jasadee Kaewsrichan)

Major Advisor

.....Signature

(Miss Paweena Wongwitwichot)

Candidate

I hereby certify that this work has not been accepted in substance for any degree, and is not being currently submitted in candidature for any degree.

.....Signature

(Miss Paweena Wongwitwichot)

Candidate

ชื่อวิทยานิพนธ์	การส่งต่อสัญญาณในเซลล์ต้นกำเนิดกระดูกเมื่อถูกเหนี่ยวนำด้วย Basic Fibroblast Growth Factor (FGF2)
ผู้เขียน	นางสาวปวีณา วงศ์วิทย์วิโชติ
สาขาวิชา	เภสัชศาสตร์
ปีการศึกษา	2557

บทคัดย่อ

วิศวกรรมเนื้อเยื่อกระดูกจากเซลล์ต้นกำเนิด เป็นเทคโนโลยีที่ถูกพัฒนาขึ้นเพื่อการรักษาและทดแทนกระดูกที่สูญเสียไปในปริมาณมาก เกินความสามารถของร่างกายที่จะซ่อมแซมได้เอง เซลล์ต้นกำเนิดจากไขกระดูกเป็นแหล่งที่มาของเซลล์ที่เข้าถึงได้ง่าย และหากเป็นของผู้ป่วยเองก็ จะไม่มีปัญหาเรื่องการเข้ากันไม่ได้ของเนื้อเยื่อ แต่มีข้อจำกัดที่สำคัญคือปริมาณเซลล์ต้นกำเนิดในไขกระดูกมีน้อยมาก กล่าวคือน้อยกว่า 0.01 เปอร์เซ็นต์ สำหรับการรักษาด้วยเทคนิคนี้ซึ่งต้องใช้เซลล์ ปริมาณมากจึงเป็นข้อเสียเปรียบที่สำคัญ การเพิ่มจำนวนเซลล์ในห้องทดลองถือได้ว่าเป็นทางเลือกที่ เหมาะสม แต่เกิดปัญหาที่ชัดเจนจากปฏิบัติการดังกล่าว นั่นคือเซลล์แบ่งตัวได้น้อยลงและไม่สามารถ คงความเป็นเซลล์ต้นกำเนิดไว้ได้เมื่อผ่านการเพาะเลี้ยงหลาย ๆ ครั้ง จึงเป็นที่มาของงานวิจัยชิ้นนี้ ที่มุ่ง พัฒนาสภาวะสำหรับแยกเซลล์ต้นกำเนิดจากไขกระดูก เพาะเลี้ยงเซลล์ในหลอดทดลอง กระตุ้นเซลล์ ด้วยสารกระตุ้นการเจริญ (growth factor) ที่เหนี่ยวนำให้เกิดการแบ่งเซลล์และเปลี่ยนแปลงเป็นเซลล์ กระดูก (osteoblasts) ให้มากขึ้น ศึกษาการสร้างกระดูกใหม่ส่วนนอก (ectopic bone) ในสัตว์ทดลองที่ ได้รับการปลูกเซลล์ดังกล่าวลงไป และศึกษากลไกการเหนี่ยวนำการสร้างกระดูกใหม่ระดับโมเลกุลของ สารกระตุ้นการเจริญเหล่านั้น โดยมีเป้าหมายที่จะลดค่าใช้จ่ายในการเตรียมเซลล์ต้นกำเนิด และเพิ่ม ประสิทธิภาพของเทคนิควิศวกรรมเนื้อเยื่อกระดูกทางคลินิกให้สูงขึ้น

งานวิจัยชี้ให้เห็นว่า เทคนิคที่ใช้แยกเซลล์ต้นกำเนิดจากไขกระดูกมีประสิทธิภาพดี และง่ายหากจะนำไปใช้ในห้องปฏิบัติการทางคลินิก การกระตุ้นเซลล์ตามลำดับด้วย basic fibroblast growth factor (หรือ fibroblast growth factor 2; FGF2) ความเข้มข้น 2.5 ng/ml เสริมด้วยอินซูลิน ความเข้มข้น 60 ng/ml เป็นเวลา 1 วัน พักเซลล์เป็นเวลา 2 วัน กระตุ้นเซลล์ต่อด้วย Bone Morphogenetic Protein 2 (BMP2) ความเข้มข้น 10 ng/ml หรือ bone morphogenetic protein 7 (BMP7) ความเข้มข้น 10 ng/ml อีก 1 วัน ส่งผลเหนี่ยวนำให้เกิดการสร้างกระดูกใหม่ทั้งในหลอด ทดลองและในสัตว์ทดลอง การกระตุ้นเซลล์ช่วงแรกนอกจากจะส่งผลให้เซลล์แบ่งตัวเพิ่มขึ้นแล้ว ยัง สามารถชักนำเซลล์ต้นกำเนิดให้โน้มเอียงที่จะเปลี่ยนไปเป็นเซลล์ตัวอ่อนกระดูก (pre-osteoblast) เพิ่มขึ้นด้วย ส่วนการกระตุ้นเซลล์ช่วงหลังส่งผลให้เซลล์ต้นกำเนิดทั้งหมดเปลี่ยนไปเป็นเซลล์ตัวอ่อน กระดูกที่พร้อมจะสะสมแคลเซียมและฟอสฟอรัส (mineralization) และเปลี่ยนเป็นกระดูกในที่สุด

พบว่า การเพิ่มจำนวนเซลล์เกิดจากการกระตุ้นผ่านวิถีของ Wntless and Int1 (WNT pathway) ส่วนการเพิ่มแนวโน้มให้เซลล์เปลี่ยนเป็นเซลล์ตัวอ่อนกระดูก เกิดจากการที่เซลล์ สร้าง Runt-related transcription factor 2 (Runx2) เพิ่มขึ้นเมื่อถูกกระตุ้นด้วย FGF2

Runx2 เป็นโปรตีนหลักที่ทำหน้าที่ในการควบคุมการถอดรหัสของยีนที่เซลล์สร้างเพิ่มขึ้น และจะส่งผลต่อให้เซลล์สร้างโปรตีนที่เกี่ยวข้องกับการสร้างกระดูกเพิ่มขึ้นด้วย ได้แก่ BMP2 และ alkaline phosphatase (ALP) ปริมาณการสะสมแคลเซียมและฟอสฟอรัสสามารถตรวจสอบด้วยเทคนิคสีย้อมจำเพาะ Alizarin Red S กลไกกระตุ้นระดับเซลล์เกิดจาก Runx2 จับกับส่วนของดีเอ็นเอ *ap1* ที่อยู่เหนี่ยวยีน *runx2* แล้วส่งผลเชิงบวกให้เซลล์สร้าง Runx2 เพิ่มขึ้น ตามด้วยการสร้าง BMP2 และ ALP ที่เพิ่มขึ้น

เทคนิคการเพาะเลี้ยงเซลล์ต้นกำเนิดเพื่อใช้ในวิศวกรรมเนื้อเยื่อกระดูกที่พัฒนาขึ้นใหม่นี้เป็นวิธีที่ง่าย ปลอดภัย มีค่าใช้จ่ายที่เหมาะสม และสามารถนำไปใช้ได้จริงทางคลินิก

Thesis Title	Downstream Signaling Pathway in Bone Stromal Cells Induced with Basic Fibroblast Growth Factor (FGF2)
Author	Miss Paweena Wongwitwichot
Major Program	Pharmaceutical Sciences
Academic Year	2014

ABSTRACT

Bone tissue engineering using mesenchymal stromal cells (MSCs) becomes a promising technique for treatment of severe bone defect. Bone marrow is an easily accessible source of MSCs, which are autologous if own to the patient. Because of the rare population of MSCs (< 0.01%), this has been the major drawback of the repair technique as it requires large cell numbers. *In vitro* propagation is generally applied to increase the numbers of cells. However, the cells grow with reduced rate and have lowered differentiation potential during the expansion. Accordingly, this research is aimed to (1) improve techniques of MSC separation and cultivation with enhanced growth rate and preserved differentiation potential, by using suitable bone growth-related factors; (2) to determine the ability of the induced cells to form new bone *in vitro* and *in vivo*; and (3) to clarify the induction mechanisms by the used growth factors at molecular levels.

Results showed that the cell isolation method developed was efficient and could be applied in clinics. Improved *in vitro* and *in vivo* bone formation was apparent when the cells were sequentially induced by using 2.5 ng/ml basic fibroblast growth factor (or fibroblast growth factor 2; FGF2) plus 60 ng/ml insulin for 1 day (the 1st induction), followed by cell starvation for 2 days, and finally challenged by 10 ng/ml bone morphogenetic protein 2 (BMP2) or 10 ng/ml bone morphogenetic protein 7 (BMP7) for 1 day (the 2nd induction). The increase of cell growth and pre-osteoblastic commitment was achieved by the 1st induction phase, while the improvement of osteoblastic differentiation and mineralization processes was accomplished by the 2nd induction phase.

The effect on cell proliferation was found to involve in the Wingless and Int1 (WNT) pathway. Instead, the cells trended to produce Runt-related transcription

factor 2 (Runx2) after induced by FGF2, resulting in increased pre-osteoblastic commitment.

Since Runx2 was the principal transcription factor produced, it then positively regulated the synthesis of osteogenic proteins including BMP2 and alkaline phosphatase (ALP). The degree of mineralization was determined by Alizarin red s (ARS) staining. The proposed mechanism of Runx2 on accelerating new bone formation would be via the activation of *ap1* consensus sequence located up-stream of *runx2* gene by Runx2, resulting in increased production of BMP2 and ALP.

The newly developed method for cultivating MSCs isolated from bone marrow was simple, safe, cost-effective, and possible to be applied for bone tissue engineering in clinics.

CONTENTS

	Page
ABSTRACT (in Thai)	v
ABSTRACT (in English)	vii
ACKNOWLEDGEMENT	ix
CONTENTS	x
LIST OF TABLES	xv
LIST OF FIGURES	xvii
LIST OF ABBREVIATIONS AND SYMBOLS	xx
CHAPTER 1 INTRODUCTION	1
1.1 Background	1
1.1.1 Bone	1
1.1.2 Bone cells	2
1.1.3 Osteogenesis	4
1.1.3.1 Bone tissue formation process	4
1.1.3.2 Transcriptional regulation of osteogenesis	6
1.1.3.3 Major signaling pathways controlling bone formation	10
1.1.3.4 Signaling crosstalk in bone development	16
1.1.4 Bone defects and treatment	17
1.1.4.1 Defects of bone tissue	17
1.1.4.2 Bone fracture healing process	18
1.1.4.3 Treatments of lost bone tissue	19
1.1.5 Tissue engineering	20
1.1.5.1 The concept	20
1.1.5.2 Osteogenic cells	21
1.1.5.3 Scaffolds	22
1.1.5.4 Growth factors	23
1.2 Research rationale	23
1.3 Objectives	25

CONTENTS (continued)

	Page
CHAPTER 2 RESEARCH METHODOLOGY	26
2.1 Materials	26
2.1.1 General reagents	26
2.1.2 Reagents for cell isolation, culture, and characterization	26
2.1.3 Reagents for <i>in vitro</i> evaluation of induction conditions	27
2.1.4 Reagents for <i>in vivo</i> experiment	27
2.1.5 Reagents for plasmid construction	28
2.1.5.1 Plasmids	28
2.1.6 Reagents for transfection experiment	32
2.1.7 Laboratory animal	32
2.1.8 Primers and oligonucleotides	32
2.2 Experimental scheme	39
2.3 Methods	40
2.3.1 MSCs isolation and culture	40
2.3.1.1 Human bone marrow-derived MSCs (HBMSCs) isolation	40
2.3.1.2 Rat bone marrow-derived MSCs (RBMSCs) isolation	41
2.3.1.3 Cell culture technique	41
2.3.2 HBMSCs characterization and osteogenic induction	43
2.3.2.1 Flow cytometry	43
2.3.2.2 Induction of HBMSCs using FGF2 and BMP2	45
2.3.2.3 Determination of the gene expression levels by using real-time PCR (RT-PCR) technique	46
2.3.3 Induction for osteogenic differentiation of RBMSCs	48
2.3.4 Efficiency of the induction conditions developed	51
2.3.4.1 RT-PCR	51
2.3.4.2 Proliferation assay	52
2.3.4.3 Alkaline phosphatase (ALP) activity assay	53
2.3.4.4 Mineralization of monolayer cells culture	53
2.3.4.5 BMP2 immunoassay	54

CONTENTS (continued)

	Page
2.3.4.6 Determination of protein concentration for cell lysates	55
2.3.5 <i>In vivo</i> implantation	56
2.3.5.1 Preparation of the cell-seeded constructs	56
2.3.5.2 Implantation	56
2.3.5.3 Tissue processing	58
2.3.5.4 Histological staining	58
2.3.6 Plasmid construction	60
2.3.6.1 Cloning of the 5'-UTR of <i>runx2</i> gene into pGEM [®] -T easy vector	62
2.3.6.2 Construction of pGL3- <i>runx2</i> -N and pGL3- <i>runx2</i> -F reporter vector	70
2.3.6.3 Construction of plasmids containing tandem repeats of transcription factor binding site	78
2.3.7 Dual luciferase reporter assay	83
2.3.7.1 Preparation of the reporter vectors for transfection	83
2.3.7.2 Plasmid concentration determination	84
2.3.7.3 Transfection optimization	84
2.3.7.4 Transfection	85
2.3.7.5 Dual-luciferase measurement	87
2.4 Equipment	88
CHAPTER 3 RESULTS	90
3.1 Characterization of the isolated HBMSCs	90
3.1.1 Morphology	90
3.1.2 Cell surface markers	90
3.1.3 The expression of stem cell-specific genes	93
3.1.4 Changes in stem cells-gene expression of induced HBMSCs	94
3.2 Characterization of the isolated RBMSCs	96
3.3 Growth factors to be determined for the effects on bone regeneration	96

CONTENTS (continued)

	Page
3.3.1 Cell proliferation	97
3.3.2 mRNA expression of genes related to osteogenesis	97
3.3.2.1 The effects of FGF2 and insulin	98
3.3.2.2 The effects of BMP2 and BMP7	99
3.3.2.3 The effects of proliferation factors (FGF2 and insulin) and differentiation factors (BMP2 and BMP7)	100
3.3.3 Alkaline phosphatase (ALP) activity assay	103
3.3.4 Calcium deposition	103
3.3.5 BMP2 production	106
3.4 <i>In vivo</i> bone formation	107
3.5 Reporter vectors construction	111
3.5.1 Cloning of 5'-UTR of <i>runx2</i> gene	111
3.5.1.1 Cloning of 5'-UTR of <i>runx2</i> gene and construction of pGEM-U1557	111
3.5.1.2 Analysis of U1557-DNA sequence	113
3.5.2 Construction of reporter vectors containing <i>runx2</i> regulatory element	116
3.5.2.1 Cloning of 2 regions of <i>runx2</i> regulatory element	116
3.5.2.2 Construction of pGEM- <i>runx2</i> -N and pGEM- <i>runx2</i> -F	117
3.5.2.3 Construction of pGL3- <i>runx2</i> -N and pGL3- <i>runx2</i> -F reporter vector	118
3.5.3 Construction of reporter vectors containing tandem repeat of transcription factor binding site (pGL3-5X <i>ap1</i> and pGL3-5X <i>sry</i>)	122
3.6 Assay of the luciferase activity	125
3.6.1 Preparation of reporter vectors	125
3.6.2 Transfection optimization	127
3.6.3 Luciferase reporter assay	129
 CHAPTER 4 DISCUSSION	 131
4.1 Characteristics of HBMSCs	131

CONTENTS (continued)

	Page
4.2 Osteogenic induction of HBMSCs	133
4.3 Characteristics of RBMSCs	134
4.4 Bone-related growth factors for RBMSCs	135
4.5 Sequential induction of RBMSCs using proliferation factor(s) followed by differentiation factor(s)	138
4.6 <i>In vivo</i> bone formation	138
4.7 Analysis of the regulatory element of <i>runx2</i> gene in controlling osteogenesis	140
4.8 Intracellular signaling pathway of FGF2 and insulin induction	141
CHAPTER 5 CONCLUSION	142
REFERENCES	145
APPENDIX A PREPARATION OF SOLUTIONS AND BUFFERS	162
APPENDIX B ELECTROPHEROGRAMS AND DNA SEQUENCES	169
APPENDIX C SEQUENCE ALIGNMENT	185
APPENDIX D STATISTICAL ANALYSIS	192
VITAE	255

LIST OF TABLES

	Page
Table 2.1: Sequences of oligonucleotides and annealing temperatures.	33
Table 2.2: Real-time PCR primers.	35
Table 2.3: The synthesized oligonucleotides for the transcription factor binding site.	38
Table 2.4: Surface area of the culture vessel, the volumes of culture medium, and the volumes of trypsin used for trypsinization.	42
Table 2.5: The components for cDNA synthesis.	47
Table 2.6: The components for RT-PCR reaction (Bio-rad).	48
Table 2.7: The used growth factors and their concentrations.	49
Table 2.8: The components for RT-PCR reaction of RBMSCs.	52
Table 2.9: Protocols for deparaffinization and of tissue sections.	59
Table 2.10: The components for PCR reaction.	65
Table 2.11: Thermal cycle for 5'-UTR of <i>runx2</i> gene cloning.	65
Table 2.12: The concentration of agarose gel based on size of linear DNA to be separated.	66
Table 2.13: The components for ligation reaction.	67
Table 2.14: Components and conditions for <i>KpnI</i> , <i>BglII</i> , <i>NheI</i> , and <i>EcoRI</i> digestion.	69
Table 2.15: Components and conditions for <i>KpnI</i> and <i>NheI</i> double digestion.	70
Table 2.16: PCR components for <i>runx2</i> -N amplification.	73
Table 2.17: Thermal cycle for <i>runx2</i> -N amplification.	73
Table 2.18: PCR components for <i>runx2</i> -F amplification.	74
Table 2.19: Thermal cycle for <i>runx2</i> -N amplification.	74
Table 2.20: PCR components for pGL3- <i>runx2</i> -N and pGL3- <i>runx2</i> -F vector verification.	77
Table 2.21: Thermal cycle for pGL3- <i>runx2</i> -N and pGL3- <i>runx2</i> -F vector verification.	77
Table 2.22: The components for oligonucleotide annealing reaction.	79

LIST OF TABLES (continued)

	Page
Table 2.23: The components used for proving the success in cloning of pGL3-5Xap1.	81
Table 2.24: Thermal cycle used for proving the success in cloning of pGL3-5Xap1.	81
Table 2.25: The components used for proving the success in cloning of pGL3-5Xsry.	82
Table 2.26: Thermal cycle used for proving the success in cloning of pGL3-5Xsry.	82
Table 2.27: Optimization conditions for transfection.	85
Table 2.28: The components for transfection reactions. The ratio of transfection reagent to DNA was 6:1.	86
Table 3.1: Percentage of the cells expressing each specific surface marker.	93
Table 3.2: The relative mRNA expression levels of osteogenic markers for the RBMSCs initially induced by the proliferation factor(s) (2.5 ng/ml FGF2 and 60 ng/ml insulin) and followed by the differentiation factor(s) (10 ng/ml BMP2 and 10 ng/ml BMP7).	101
Table 3.3: The results of relative ALP activity and relative calcium deposition after proliferation induction.	104
Table 3.4: The results of relative ALP activity and relative calcium deposition of osteogenic induced RBMSCs using proliferation factor(s) (2.5 ng/ml FGF2 and 60 ng/ml insulin) and followed by differentiation factor(s) (10 ng/ml BMP2 and 10 ng/ml BMP7).	105
Table 3.5: Potential transcription factor binding sites identified on U1557 sequence.	115
Table 3.6: The recombinant plasmid purified by using QIAGEN plasmid midi kit, and their corresponding concentrations.	126
Table 3.7: The results for the optimization of transfection conditions.	128

LIST OF FIGURES

	Page
Figure 1.1: Structure and anatomy of long bone.	2
Figure 1.2: Four types of bone cells.	3
Figure 1.3: Skeleton tissue formation by endochondral and intramembranous ossification.	5
Figure 1.4: Transcriptional control of MSCs commitment.	6
Figure 1.5: Osteoblastic commitment of MSCs with some of the known transcription factors.	8
Figure 1.6: BMPs signal transduction pathway.	12
Figure 1.7: FGFs signaling cascade in osteoblasts.	13
Figure 1.8: Simplified view of insulin/IGFs signaling crosstalk.	14
Figure 1.9: Canonical WNT signaling pathway.	16
Figure 1.10: A four-stage model of fracture repair.	19
Figure 1.11: Concept of bone tissue engineering.	21
Figure 2.1: Circular map of pGEM [®] -T easy vector.	30
Figure 2.2: Circular map of pGL3-Promoter vector.	30
Figure 2.3: Circular map of pGL3-Control vector.	31
Figure 2.4: Circular map of pRL-SV40 vector.	31
Figure 2.5: Experimental workflow.	40
Figure 2.6: Schematic configuration of flow cytometer.	44
Figure 2.7: Induction scheme of HBMSCs.	45
Figure 2.8: The scheme for induction conditions of RBMSCs.	50
Figure 2.9: The hydrolysis reaction of pNPP as catalyzed by ALP producing a yellow color para-nitrophenol.	53
Figure 2.10: Timeline of RBMSCs induction and the measurement of BMP2 level in the medium supernatant.	55
Figure 2.11: Procedures for preparing cell-seeded scaffold implants.	57
Figure 2.12: The schematic representation of the implantation sites.	58
Figure 2.13: The construction procedures of luciferase reporter vectors.	61
Figure 2.14: Construction of pGEM-U1557 recombinant vector.	63

LIST OF FIGURES (continued)

	Page
Figure 2.15: Construction of pGEM- <i>runx2</i> -N and pGEM- <i>runx2</i> -F cloning vector.	72
Figure 2.16: Subcloning protocol for pGL3- <i>runx2</i> -N and pGL3- <i>runx2</i> -F vector construction.	76
Figure 2.17: Preparation of pGL3-5X <i>ap1</i> and pGL3-5X <i>sry</i> reporter vector.	80
Figure 2.18: The plan of transfection experiment and luciferase assay.	86
Figure 2.19: Bioluminescent reaction of firefly luciferase (a) and Renilla luciferase (b).	87
Figure 3.1: The morphology of HBMSCs (40x magnification).	91
Figure 3.2: Surface markers of HBMSCs, analyzed by flow cytometry.	92
Figure 3.3: The expression of stem cell-associated genes of HBMSCs in passage 2 and 5.	94
Figure 3.4: The mRNA expression of stem cell-associated and osteogenic genes of HBMSCs, after sequential induction with 2.5 ng/ml FGF2 and 10 ng/ml BMP2.	95
Figure 3.5: The morphology of RBMSCs (40x magnification).	96
Figure 3.6: The result of MTT assay.	97
Figure 3.7: Relative mRNA expression levels of osteogenic markers for the RBMSCs induced with 2.5 ng/ml FGF2, 60 ng/ml insulin, or FGF2 plus insulin for 1 day.	98
Figure 3.8: Relative gene expression levels of RBMSCs treated with 10 ng/ml BMP2, 10 ng/ml BMP7, or the combination for 1 day.	99
Figure 3.9: BMP2 levels produced by RBMSCs.	106
Figure 3.10: The implanted tissues at 8 weeks post-operation.	107
Figure 3.11: Tissue sections of 8-week after implantation, stained with H&E and ARS (40x magnification). The figures represented the groups of initially induced cells using FGF2.	108
Figure 3.12: Tissue sections of 8-week after implantation, stained with H&E and ARS (40x magnification). The figures represented the groups of initially induced cells using insulin.	109

LIST OF FIGURES (continued)

	Page
Figure 3.13: Tissue sections of 8-week after implantation, stained with H&E and ARS (40x magnification). The figures represented the groups of initially induced cells using FGF2 plus insulin.	110
Figure 3.14: The PCR product, called U1557, amplified by using <i>runx2</i> -U1557 and <i>runx2</i> -97 as the primers.	112
Figure 3.15: Screening of plasmids containing U1557 fragment by using <i>EcoRI</i> digestion.	113
Figure 3.16: The nucleotide sequence of U1557 and transcription factor binding sites.	114
Figure 3.17: The results of <i>runx2</i> -N and <i>runx2</i> -F amplification and purification.	117
Figure 3.18: Insertion analysis of pGEM- <i>runx2</i> -N and pGEM- <i>runx2</i> -F.	118
Figure 3.19: <i>KpnI</i> and <i>NheI</i> digestion of pGEM- <i>runx2</i> -N and pGEM- <i>runx2</i> -F.	120
Figure 3.20: Preparation of pGL3-Promoter vector.	121
Figure 3.21: Insertion analysis of pGL3- <i>runx2</i> -N and pGL3- <i>runx2</i> -F.	122
Figure 3.22: Preparation of pGL3-Promoter vector by sequential digestion with <i>KpnI</i> and <i>BglII</i> .	123
Figure 3.23: Screening and analysis of pGL3-5X <i>ap1</i> by PCR using LUC-F and LUC-R as the primers.	124
Figure 3.24: Screening and analysis of pGL3-5X <i>sry</i> by PCR using LUC-F and LUC-R as the primers.	124
Figure 3.25: An example for preparing of pGL3-5X <i>ap1</i> plasmid for transfection.	126
Figure 3.26: Relative luciferase activity of RBMSCs transfected with (a) pGL3- <i>runx2</i> -N, (b) pGL3- <i>runx2</i> -F, (c) pGL3-5X <i>ap1</i> , and (d) pGL3-5X <i>sry</i> .	130
Figure 5.1: The proposed mechanism of <i>runx2</i> gene regulation by FGF2, insulin, BMP2, and WNT signaling pathway.	143

LIST OF ABBREVIATIONS AND SYMBOLS

°C	Degree Celsius
α-MEM	Minimum essential medium α medium
β-GP	β-glycerophosphate
μg	micrograms
μl	microliter
5'-UTR	5'-untranslate region
AA	Ascorbic acid
ALP	Alkaline phosphatase
ANOVA	Analysis of variance
AP1	Activator protein 1
APC	Adenomatous polyposis coli
ARS	Alizarin red s
AXIN2	Axis inhibition protein 2
BMPR	Bone morphogenetic protein receptor
BMPs	Bone morphogenetic proteins
BMP2	Bone morphogenetic protein 2
BMP7	Bone morphogenetic protein 7
BSA	Bovine serum albumin
BSP	Bone sialoprotein
BST1	Bone marrow stromal cell antigen 1
C/EBP	CCAAT/enhancer binding protein
CBFA1	Core-binding factor alpha 1
CDD	Cleidocranial dysplasia
cDNA	Complementary DNA
Cdx	Caudal homeobox gene
CK-1	Casein kinase-1
COL-I	Type I collagen
COX-2	Cyclooxygenase-2
DKKs	Dickkopts
Dlx5	Distal-less homeobox 5

LIST OF ABBREVIATIONS AND SYMBOLS (continued)

DMEM/F-12	Dulbecco's modified eagle medium: nutrient mixture F-12
DNA	Deoxyribonucleic acid
DPBS	Dulbecco's phosphate buffer saline
DSH	Disheveled
<i>E. coli</i>	<i>Escherichia coli</i>
ERKs	Extracellular signal-regulated kinases
Evi-1	Ecotropic viral integration site 1
FBS	Fetal bovine serum
FGFR	Fibroblast growth factor receptor
FGFs	Fibroblast growth factors
FGF2	Fibroblast growth factor 2 or basic fibroblast growth factor
FGF4	Fibroblast growth factor 4
Fz	firzzled receptor
GAPDH	Glyceraldehyde 3-phosphate dehydrogenase
H&E	Hematoxylin-eosin
HA	Hydroxyapatite
HBMSCs	Human bone marrow-derived MSCs
IGFs	Insulin-like growth factors
IGF-1	Insulin-like growth factor-1
IGF-2	Insulin-like growth factor-2
Ihh	Indian hedgehog
Ik2	Ikaros 2
IL-1	Interleukins-1
<i>luc+</i>	<i>luciferase+</i> transcriptional unit
JNK	Jun N-terminal kinase
kb	Kilobase pair
kDa	Kilodalton
LRP5/6	Low-density lipoprotein receptor-related protein 5 or 6 co-receptor
M	Molar
MAP	Mitogen-activated protein

LIST OF ABBREVIATIONS AND SYMBOLS (continued)

MAPKs	Mitogen-activated protein kinases
MEF2	Myocyte-enhancer factor 2
mg	milligrams
ml	milliliter
Msx2	Msh homeobox 2
MTT	Mitochondrial toxicity test
mRNA	Messenger ribonucleic acid
MZF-1	Myeloid zinc finger
MSCs	Mesenchymal stromal cells
ng	nanograms
OCT1	Octamer-binding transcription factor 1
OCT4	Octamer-binding transcription factor 4
OC or OSC	Osteocalcin
OSE2	Osteoblastic-specific DNA-binding element
OSP	Osteopontin
OSX	Osterix
PCP	Planar cell polarity
PCR	Polymerase chain reaction
PDGF	Platelet-derived growth factor
PI3K	Phosphatidylinositol 3 kinase
PKA	Protein kinase A
PKC	Protein kinase C
PLB	Passive lysis buffer
PLC	Phospholipase C
pNPP	para-Nitrophenylphosphate
PPAR γ	Peroxisome proliferator-activated receptor γ
RBMSCs	Rat bone marrow-derived MSCs
REX1	RNA exonuclease 1
RLUs	Relative light units
RNA	Ribonucleic acid

LIST OF ABBREVIATIONS AND SYMBOLS (continued)

RT-PCR	Real-time PCR
Runx2	Runt-related transcription factor 2
sFRPs	Secreted frizzled-related proteins
SOX2	Sex determining region y (SRY)-related high mobility group (HMG) box 2
SRY	Sex determining region y
STAT1	Signal transducers and activators of transcription-1
TA	Triamcinolone acetone
TCF/LEF	T-cell factor/lymphoid enhancer factor
TCP	Tricalcium phosphate
TERT	Telomerase reverse transcriptase
TGF- β	Transforming growth factor- β
TNF- α	Tumor necrosis factor- α
Tsg	Twisted gastrulation
Tyr	Tyrosine
U	Units
USAG1	Uterine sensitization-associated gene 1
VEGF	Vascular endothelial growth factor
WNT	Wingless and Int1

CHAPTER 1

INTRODUCTION

1.1 Background

1.1.1 Bone

Skeleton tissue is a supporting structure of an organism. Bone is not only a primary site of blood cell synthesis, but it also regulates mineral metabolism (such as calcium and phosphate) [1]. Bone related problems such as age-related disease (e.g. osteoporosis), osteosarcoma, and bone fracture can cause a serious impact on personal life and social.

Bone tissue composes of cells and matrix of organic materials (collagen fiber, proteins, and lipids) and inorganic elements (calcium, fluoride, phosphorus, etc.) [2-4]. About 95% of bone matrix is type I collagen (COL-I) and calcium phosphate crystal, called hydroxyapatite (HA). Whereas HA governs bone hardness, collagen fiber is responsible for elasticity of the tissue [5].

Structure of mature bone comprises of two parts: cortical (or compact) bone and cancellous bone, also called spongy or trabecular bone (Figure 1.1). Cortical bone is a hard outer layer, while spongy bone is a porous network tissue located at the end of long bone or at the inner part of flat bone and vertebral body. Porosity of compact bone and spongy bone are 10% and 50-90%, respectively [6]. The spaces between the spongy meshwork and the hollow core of long bone are occupied by bone marrow.

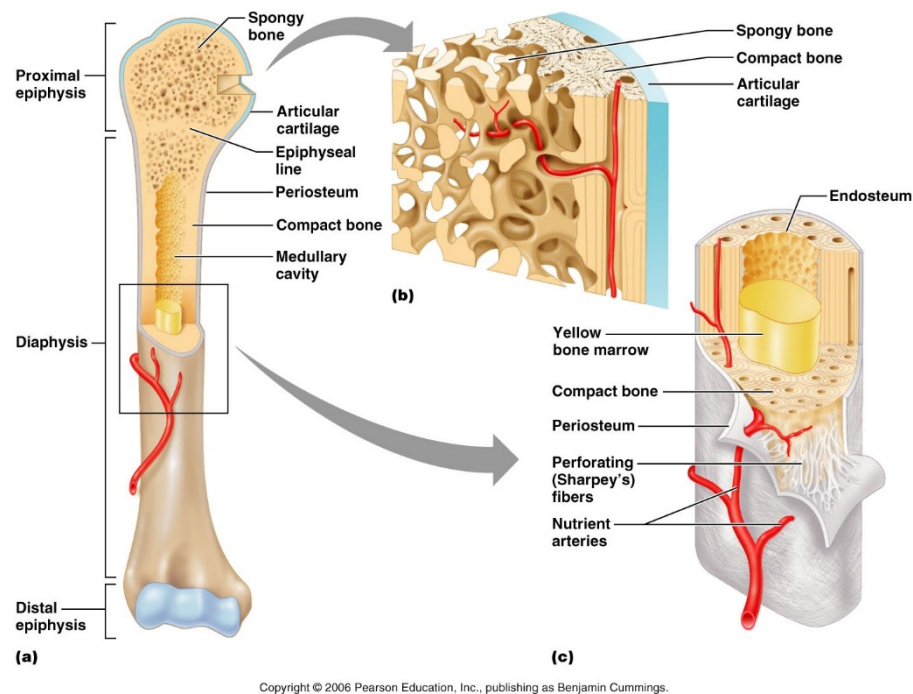


Figure 1.1: Structure and anatomy of long bone. The diagrams represent the structure of (a) long bone, (b) spongy bone, and (c) compact bone [7]. Diaphysis is a long tubular portion on bone consisted of cortical bone tissue. The end of long bone called epiphysis is filled with spongy bone. Articular cartilage covers the epiphysis where the joint between two bones occurs. The bone marrow is occupied in the cavity of long bone. The membranes covering outer and inner part of bone are periosteum and endosteum, respectively.

1.1.2 Bone cells

There are four cellular components of bone: osteoprogenitor cells, osteoblasts, osteocytes, and osteoclasts (Figure 1.2). Bone forming cells or osteoprogenitors are found in periosteum and endosteum, a connective tissue covered the outer and inner surface of bone, respectively (Figure 1.1). These cells have an osteogenic capability to develop to mature bone cells. Osteoblasts, the first cell type

developing from osteoprogenitors, are found at the boundaries of growing bone. They actively synthesize bone matrix components and enzymes to promote mineral deposition, such as alkaline phosphatase (ALP), bone sialoprotein (BSP), and COL-I. When these cells are entrapped in mineralized environment, osteoblasts become osteocytes. Another bone cell is osteoclasts. These multinucleated cells function for bone resorption. Osteoclasts dissolve bone matrix by acid secretion and specialized proteinase enzymes. Dynamic of bone growth and resorption are under the subtle coordination of these cells [8].

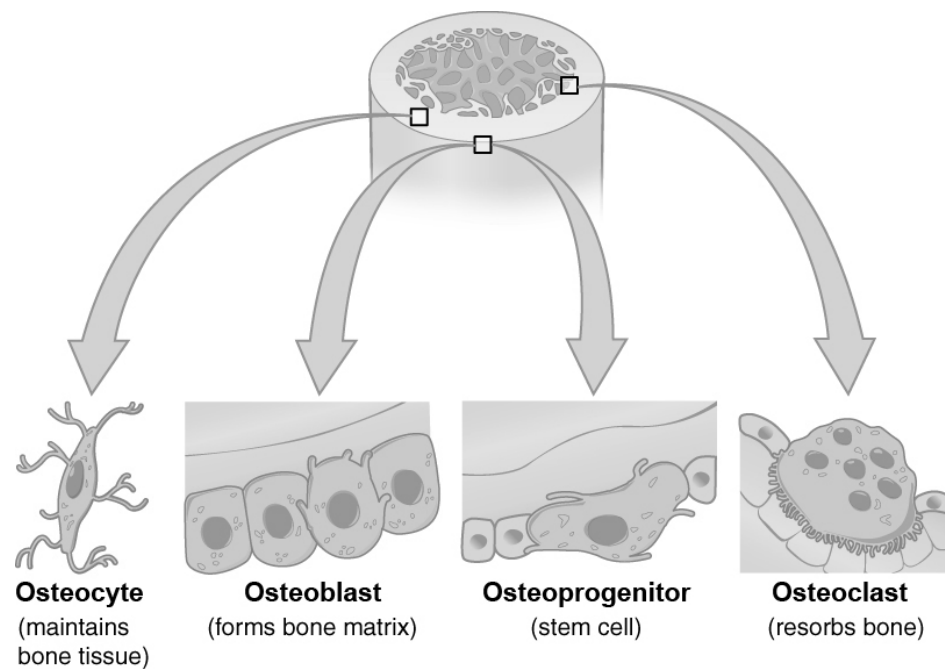


Figure 1.2: Four types of bone cells. Bone forming cells or osteoblasts are derived from osteoprogenitor cells. Osteocytes are mature bone cells trapped in mineralized matrix. Bone remodeling is controlled by bone resorption and bone replacement activity of osteoclasts and osteoblasts, respectively [9].

1.1.3 Osteogenesis

1.1.3.1 Bone tissue formation process

Osteogenesis or ossification initiates by a condensation of skeleton precursor cells or mesenchymal stromal cells (MSCs) to form a cartilaginous template (Figure 1.3). Cells in the center of template, then, become hypertrophy, when perichondrial cells differentiate to osteoblasts and construct bone collar. Mature hypertrophic chondrocytes produce mineralized matrix and undergo apoptosis, while blood vessel and osteoblast precursors invade to form a trabecular bone. Cortical bone is generated by osteoblasts at bone collar. Meanwhile, chondrocytes continuously proliferate to lengthen the bone. These processes are known as endochondral ossification which happen in long bone formation. For flat bone and skull, bone formation arises from intramembranous ossification process which osteoblast precursors directly condense and generate bone tissue termed woven bone. This bundle of erratically oriented collagen fiber and mineral, then, progressively remodels to mature lamellar bone.

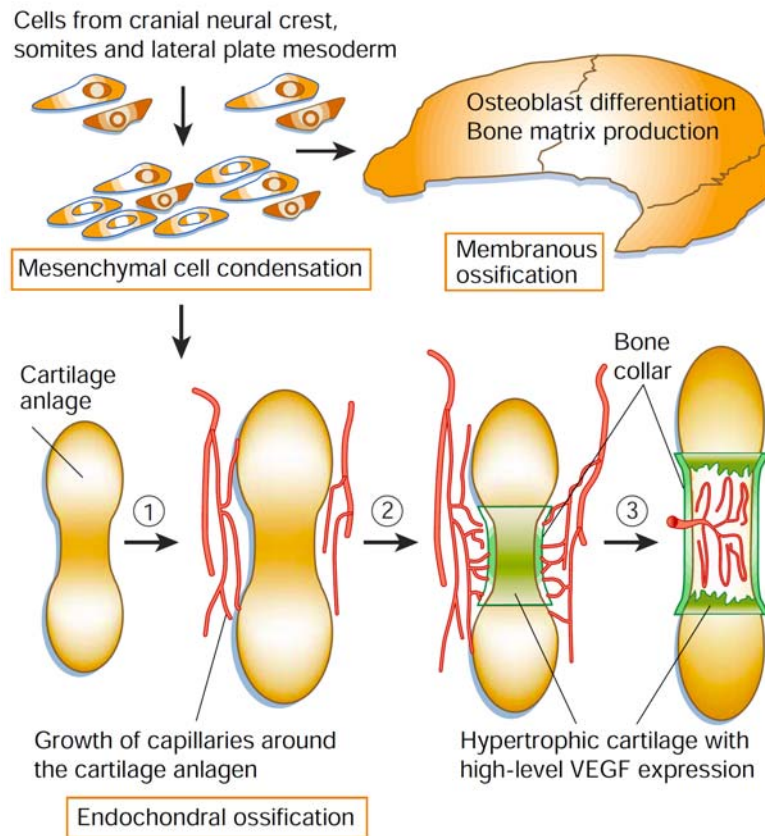


Figure 1.3: Skeleton tissue formation by endochondral and intramembranous ossification. MSCs accumulate and condense at the bone formation area. If intramembranous ossification occurs, stem cells directly turn into osteoblasts. In endochondral bone formation, cartilage model (anlagen) is formed first. After that, neovascular grows around the anlagen, while surrounding cells become osteoblasts and form bone collar. Chondrocytes in the bone collar mature to be hypertrophy. Finally, hypertrophic chondrocytes are replaced by bone [10].

1.1.3.2 Transcriptional regulation of osteogenesis

Differentiation of MSCs to a specific cell type is under the control of particular transcription factors (Figure 1.4). For osteogenic commitment, various bone specific molecules have been identified [11] such as runt-related transcription factor 2 (Runx2), osterix (OSX), and β -catenin. These DNA-binding proteins consequently activate their target genes for regulating cellular differentiation.

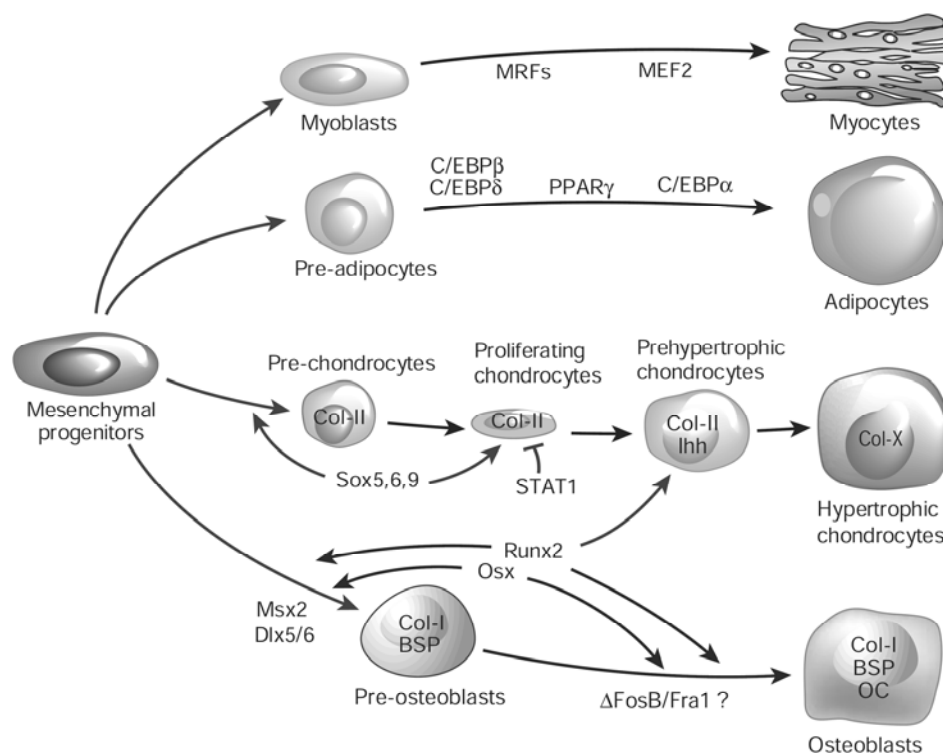


Figure 1.4: Transcriptional control of MSCs commitment. Each lineage requires gene activation signal from specific transcription factors. For example, chondrogenesis is directed by SOX proteins, while osteoblast differentiation needs the command from Runx2 and OSX [12].

1.1.3.2.1 Runt-related transcription factor 2 (Runx2)

Runx2/Cbfa1/Osf2/AML3 is recognized as a crucial regulator of osteoblastic commitment [13]. It is a skeleton cell specific protein, as it is found in only cells with osteo-chondroblastic phenotype. Runx2 belongs to Runt class of transcription factor that contains the DNA binding domain (128-amino acid domain) named Runt domain [14]. This protein binds to its binding site on DNA (sequence: PuACCPuCA [15, 16]) called osteoblastic-specific DNA-binding element (OSE2) which presents in the promoter region of osteogenic markers such as osteocalcin (OSC), osteopontin (OSP), BSP, and COL-I [17-20].

Human *runx2* gene locates on chromosome 6p21. Autosomal dominant of this gene is responsible for a congenital disorder named cleidocranial dysplasia (CDD) [21, 22]. This is a defective of endochondral and intramembranous ossification characterized by supernumerary teeth, underdeveloped or absent of clavicles, and open or delayed closure of calvarial sutures. *Runx2*^{-/-} mice have died after birth, and no bone or osteoblasts has been detected [23]. Runx2 also involves in chondrogenesis (Figure 1.4). Ectopically production of Runx2 has driven prematuration of chondroblasts, and chondrocyte terminal differentiation has been blocked in Runx2-null mice [24].

The expression of *runx2* gene is directed by auto-regulation manner [25]. Drissi *et al.* has found that there have been at least 3 Runx2 recognition sites on its promoter region which have been able to regulate itself by negative feedback loop. However, some research groups have also discovered that *runx2* expression has been under the function of other proteins such as bone morphogenetic proteins (BMPs) and Wingless and Int1 (WNT) proteins [26].

Transcriptional activity of Runx2 is governed by several co-activator and co-repressor. Histone deacetylase 7 [27] and Twist proteins [28] has been reported as an inhibitor of Runx2 (Figure 1.5). By physical interaction of histone deacetylase 7 and carboxy terminus of Runx2 or the binding of Twist box and Runt domain, DNA binding capability of Runx2 has been demolished. In contrast, Smad 1 and Smad 5 have been identified as an enhancer of Runx2 transcriptional activity [29].

Another researcher has revealed that Runt domain has been associated with core-binding factor β protein to enhance its DNA binding ability [30].

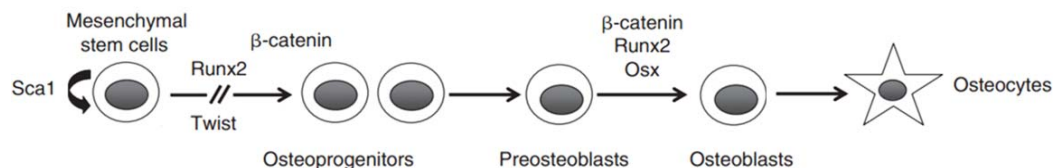


Figure 1.5: Osteoblastic commitment of MSCs with some of the known transcription factors. Runx2 and its downstream target, OSX, are the major transcription factor for osteoblastogenesis. β -catenin regulated by WNT proteins also plays role in osteogenic commitment of stem cells. The activity of Runx2 is inhibited by Twist protein [31].

1.1.3.2.2 Osterix (OSX)

OSX or Sp7 is a zinc finger-containing protein acting downstream of Runx2 in osteoblast differentiation process. Nishio et al. has cloned the OSX promoter and found that its 5'-upstream region has contained Runx2 binding site [32]. This study strongly supports the function of Runx2 over OSX for regulating of bone formation. Frameshift mutation of *osx* caused by deletion of alanine base at position 1,052 is involved in osteogenic imperfecta patient. This condition is described by low bone mass and high fragility of bone [33].

Osteogenic roles of OSX have been proved by various studies. For example, Fu and colleagues has found that osteogenic gene markers (*osc*, *osp*, and *alp*) have been increased in OSX overexpressing cells [34]. Deletion of this gene has resulted in completely lack of bone tissue, while cartilage formation has been normal [35]. OSX is essential for both embryonic bone development and postnatal bone homeostasis, since OSX postnatal-null mice have showed a low level of bone markers and new bone formation [36]. In addition, OSX is not only a potent mediator for osteoblastic commitment, but also an inhibitor of chondrogenesis [37].

1.1.3.2.3 Activator protein 1 (AP1)

AP1 is a dimeric transcription factor composed of Fos (c-Fos, FosB, Fra-1, Fra-2), Jun (c-Jun, JunB, JunD), and ATF protein families [38]. AP1 involves in variety of biological processes such as differentiation, proliferation, and apoptosis. Many studies have indicated that AP1 proteins are a regulator of skeletogenesis. For instance, Bozec and co-workers have reported the role of Fra-2 in bone development. They have found that, in Fra-2 deficient cells, the osteoblastic markers (COL-I and OSC) have been decreased leading to a deficient in osteoblastic differentiation [39]. Mice lacking of JunB have showed an osteopenia phenotype caused by the abnormality of osteoblasts and osteoclasts activities [40]. Moreover, c-fos overexpression has been able to alter bone marker expression patterns and to induce osteosarcoma formation [41].

1.1.3.2.4 Sox proteins

SOX is a protein in the sex-determining region Y (SRY)-related high mobility group (HMG) box family [42, 43]. SOX proteins are important for chondrogenesis, especially SOX9, L-SOX5, and SOX6. Akiyama and co-workers have found that osteo-chondroprogenitor cells have been originated from SOX9 expressing MSCs [44]. However, it has not been detected in hypertrophic chondrocytes and osteoblasts.

SOX9 is indispensable for the MSCs commitment to chondrocytes, since *sox9*^{-/-} cells did not express any chondrogenic markers [45]. Mutation of SOX9 gene is involved with Campomelic Dysplasia (CMDP), a skeleton malformation condition in human [46, 47]. Two other members of SOX protein, L-SOX5 and SOX6, also important for chondrocyte formation. These proteins cooperatively control the production of cartilage markers with SOX9 [48].

1.1.3.3 Major signaling pathways controlling bone formation

Osteoblastogenesis is regulated by various stimulating and inhibiting factors. To date, the control of osteogenic differentiation is partially known. Many studies have exhibited a potential use of growth factors, since self-repair property of bone cell together with stimulating molecules can increase the rate of tissue healing. Among them, BMPs signaling pathway, fibroblast growth factors (FGFs) signaling pathway, insulin and insulin-like growth factors (IGFs) signaling pathway, and WNT/ β -catenin signaling pathway are extensively investigated.

1.1.3.3.1 Transforming growth factor- β (TGF- β) and Bone morphogenetic proteins (BMPs) pathway

Transforming growth factor superfamily consists of more than 40 members including TGF- β isoforms, activins, and BMPs. These cytokines are crucial for various physiological process such as cell propagation, migration, differentiation, and extracellular matrix production [49].

TGF- β /BMPs proteins activate serine/threonine kinase receptor and transduce the signal through 2 distinct pathways, Smad dependent and independent pathway [50-52]. Phosphorylated Smad 2 and 3 are an effector of TGF- β , whereas Smad 1, 5, and 8 are stimulated by BMPs. These phosphorylated Smad proteins, then, bind with Smad 4 and translocate into nucleus. The complexes reveal a transcriptional activity by binding on their target DNA and stimulating gene expression (Figure 1.6). For Smad independent pathway, TGF- β transfers its signal via Jun N-terminal kinase (JNK), mitogen-activated protein kinases (MAPKs), and p38 pathway, while BMPs utilize TAK1 protein pathway as a signal transducer.

TGF- β is known as a chondrogenic differentiation factor [53]. Interestingly, the effect of this cytokine on bone formation seems to have conflict results. Mutation of this gene is responsible for Camurati-Engelmann disorder (CED), a genetic disorder associated with a heavily thickened bone [49]. Targeted disruption of *smad 3* gene in mice has developed an abnormal synovial joint and spine, while the amount of hypertrophic chondrocytes in growth plate and articular cartilage has been

increased in mutant mice. These results have suggested that lacking of Smad 3 has been able to stimulate terminal differentiation of chondrocytes [54]. However, Mohammad and colleagues have found that inhibition of TGF- β receptor has increased bone mass and bone quality [55]. TGF- β has blocked the later phase of cell differentiation and mineralization [56-58]. Hence, TGF- β supports bone formation by recruiting osteoprogenitor cells, promoting cell proliferation, and inducing the early phase of differentiation process.

BMPs function in a variety of cell developmental process. They are well known as a major chondro/osteoblastic inducer [59]. The highest osteogenic potency BMPs are BMP2, 4, 5, 6, 7, and 9 [60]. Many targets of BMPs are osteoblastic transcription factors such as Runx2, OSX, Dlx5, and Msx2. In addition, BMPs are able to up-regulate the production of OSC, collagens, and BSP. They also induce angiogenic factors synthesis such as vascular endothelial growth factor (VEGF) which can potentiate a new bone formation [61]. During bone fracture repair, exogenous BMP2 has stimulated both chondrogenesis and osteogenesis that have been found at the periosteum [62]. This phenomenon has implied that BMP2 has been able to regulate cell fate determination of periosteum stem cells. Mice lacking of Smad 1, 5, and 8 have a severe chondrodysplasia [63]. Therefore, BMP signaling is necessitated for endochondral bone formation.

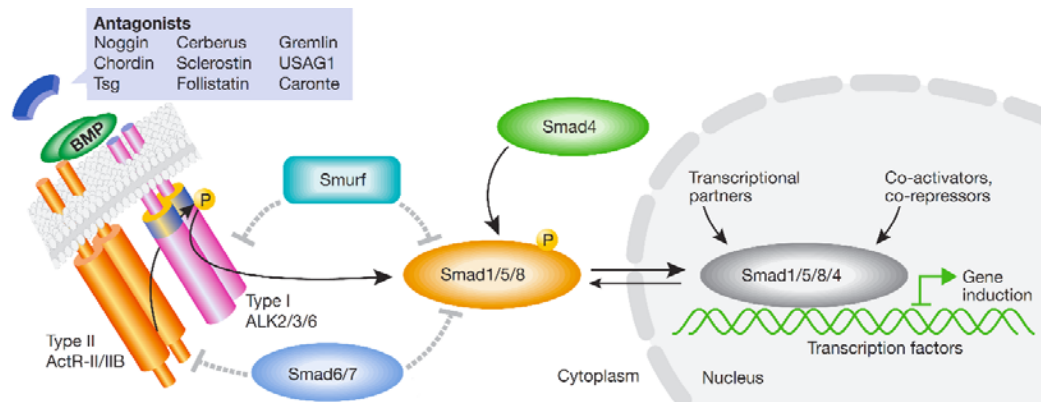


Figure 1.6: BMPs signal transduction pathway. BMPs bind a heterodimeric receptor and induce the intracellular signaling cascade. Group of phosphorylated Smad 1/5/8 and Smad 4 serves as a gene expression activator, whereas inhibitory Smads (Smad 6 and 7) and Smurf protein can block the intracellular signaling pathway. Receptor antagonists are listed in the figure [64].

1.1.3.3.2 Fibroblast growth factors (FGFs) pathway

The FGF family composes of 22 members that have amino acid identity about 30-70% and range in the size from 17 to 34 kilodalton (kDa) in vertebrate [65]. Among them, FGF2 or basic fibroblast growth factor (bFGF) is the most powerful factor for osteogenic cells. FGF2 regulates cell proliferation, tissue development, tissue repair, wound healing, and angiogenesis. FGF2 is known as a potent mitogen for stem cells. This growth factor has been able to maintain differentiation ability of bone marrow-derived MSCs and delay the senescence process of the cells [66, 67]. Many studies have proved that FGF2 has promoted distraction osteogenesis in rabbit model [68, 69]. Disruption of *fgf2* gene affects both bone mass and bone formation [70].

FGFs and FGF receptors (FGFRs) activate cell through protein kinase C (PKC), mitogen-activated protein (MAP), extracellular signal-regulated kinases (ERKs), and p38 MAP kinase [71]. These pathways are well known for

controlling osteoblast replication, osteoblastic gene expression, and cell survival (Figure 1.7). Abnormalities in FGFRs involve in several skeletal disorders. For example, activation mutation of FGFR3 causes achondroplasia or dwarfism. Mutation of an extracellular part of FGFR2 receptor involves in the defect bone formation or premature skull suture closure in Apert syndrome, Crouzon syndrome, Jackson-Weiss syndrome, and Pfeiffer syndrome [72].

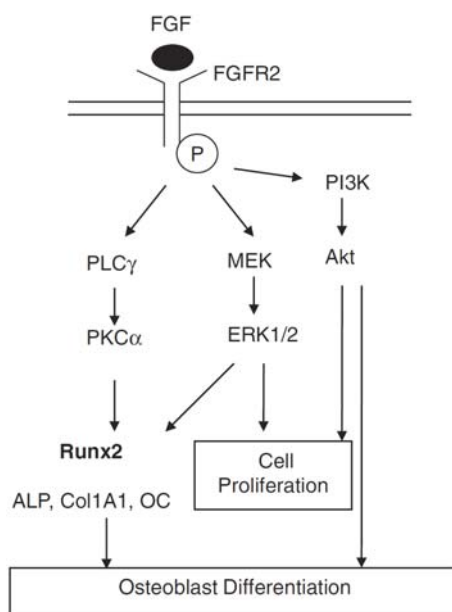


Figure 1.7: FGFs signaling cascade in osteoblasts. FGFs/FGFRs transduce signal via several pathways which responsible for cell proliferation and differentiation [71].

1.1.3.3.3 Insulin and insulin-like growth factors (IGFs) signaling pathway

Insulin and IGFs are actively associated with metabolism, growth, and development [73, 74]. Two IGFs have been identified including insulin-like growth factor-I (IGF-I) and insulin-like growth factor-II (IGF-II). In bone, IGF-II is the most abundant, but IGF-I has been found to be more potent. Intracellular signaling

pathways of insulin and IGFs serve overlapping functions through phosphatidylinositol 3 kinase (PI3K)/Akt and MAPK pathway (Figure 1.8).

A number of studies have reported that insulin has improved bone formation by decreasing Runx2 inhibitor and inducing the production of OSC [74, 75]. The effects of IGFs have also shown to promote osteoblast proliferation and calvarial bone defect healing in a rat model. Insulin or IGFs deficiency contribute to the adverse effects on bone quality, such as reduced bone mineral density and increased risk of bone fracture. In addition, loss of their receptors in osteoblasts also cause retardation of bone formation, mineralization, and bone volume.

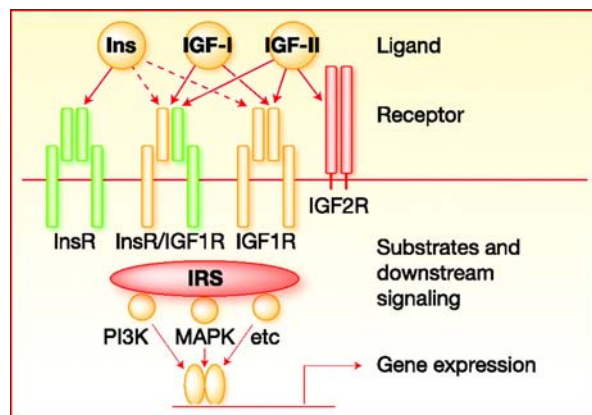


Figure 1.8 Simplified view of insulin/IGFs signaling crosstalk. Activation of insulin (InsR), IGFs (IGF1R and IGF2R), or hybrid (InsR/IGF1R) receptor tyrosine kinase subsequently phosphorylates Insulin receptor substrate (IRS) proteins creating signal transduction via effector molecules of PI3K/Akt and MAPK pathways. These signals stimulate variety downstream biological effects including gene expression, mitogenesis, and glucose metabolism [76].

1.1.3.3.4 Wingless and Int1 (WNT) pathway

The term of WNT is a combination of Wg and Int1, which stand for Wingless gene in *Drosophila* and gene from the integration site of mouse

mammary tumor virus, respectively. Secreted WNT proteins regulate many cellular processes, such as embryonic development and cell fate determination. WNT signaling is divided into 2 major pathways: canonical and non-canonical pathway [77].

β -catenin is a central effector of WNT canonical pathway (Figure 1.9). In a resting stage, β -catenin is destroyed via a destruction complex of glycogen synthase kinase 3 β (GSK3 β), axis inhibition protein 2 (AXIN2), casein kinase-1 (CK-1), and adenomatous polyposis coli (APC). This protein complex, then, phosphorylates β -catenin mediating proteasome digestion of β -catenin in cytoplasm. In the active stage, WNT proteins form a complex with frizzled (Fz) receptor and low-density lipoprotein receptor-related protein 5 or 6 (LRP5/6) co-receptor. Dishevelled (DSH), then, binds to Fz and induces a protein complex formation of DSH, AXIN, GSK3 β , and APC. Activation of WNT receptor prevents β -catenin degradation. Consequently, β -catenin can accumulate in nucleus and interacts with T-cell factor/lymphoid enhancer factor (TCF/LEF) to stimulate target gene synthesis [78].

Effect of β -catenin on osteogenic cell differentiation depends on the stage of target cells [79]. Canonical WNT signal triggers an osteogenic lineage commitment of MSCs, but terminal differentiation of mature osteoblasts is inhibited by WNT ligand. It is concluded that β -catenin acts as a molecular switch of MSCs, as it inactivates progenitor cells committed to chondrogenic lineage instead of osteoblasts [80]. Moreover, target deletion of β -catenin in mice has showed a reduction in both endochondral and intramembranous bone in embryo. Enhanced in osteogenic differentiation is a result of an up-regulation of osteoblastic transcription factors, Runx2 and OSX by WNT signal.

WNT pathway is controlled by several inhibitors such as sclerostin, dickkopts (DKKs), secreted frizzled-related proteins (sFRPs), and WNT inhibitory factors [81]. *Dkk1*-overexpressing cells have failed to express *runx2* [82]. Conversely, fracture healing process of *sFRP*^{-/-} mice has been accelerated [83].

For non-canonical WNT or β -catenin independent pathway, a signal transduction is due to calcium flux, planar cell polarity (PCP), and protein kinase A (PKA) pathway. The function of this pathway in bone formation, however, is still unclear [77].

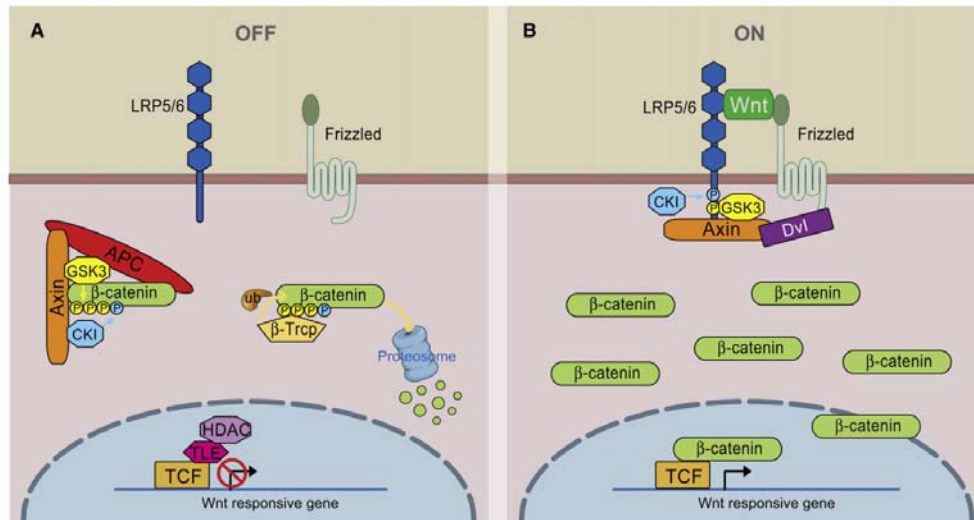


Figure 1.9: Canonical WNT signaling pathway. An activation of WNT/ β -catenin pathway by WNT proteins stabilizes β -catenin by blocking the ubiquitination degradation of β -catenin. Accumulated β -catenin and TCF/LEF complex, then, promotes target gene transcription [78].

1.1.3.4 Signaling crosstalk in bone development

The osteoblastic differentiation of stem cells is controlled by the action of transcription factors, cytokines, and hormones. By stimulating an intracellular signaling pathway, these molecules function in a precise time point, and their activation cascades appear in a complex system. There is a crosstalk among these signaling pathways. Here are some examples of relationships between the induction pathways which the whole picture still needs to be intensively studied.

BMP-induced osteoblastic differentiation has been inhibited by TGF- β . Moreover, addition of TGF- β to a confluent culture of rat calvarial cells has been able to block bone nodule formation, and down-regulate mRNA level of bone related gene, such as *bmp2*, *alp*, *osc*, and *col-1* [84].

β -catenin and BMP2 have synergistically promoted osteoblast differentiation. Mbalaviele and coworkers have reported that β -catenin has constitutively activated by BMP2 in murine MSCs [85]. The groups have revealed that ALP activity,

osc gene expression, and mineralization matrix have been increased in BMP2 treated cells, while adipogenicity of the cells has been reduced. They have suggested that β -catenin has improved osteogenic capacity of the uncommitted cells. Therefore, these cells have been fully responded to the stimulating signal from BMP2. Moreover, progenitor cells derived from BMP2 deficient mice had reduced level of OSX and proteins in WNT signaling pathway (i.e. AXIN2, WNT1, and Lrp5) [86].

Runx2 expression has been regulated by BMPs and WNT pathway. BMP2 has positively up-regulated *runx2* expression level [26], and it has influenced the activity of Runx2 [87]. BMP2 has accelerated Runx2 acetylation which protected Runx2 from ubiquitination and degradation. In addition, Gaur and colleges have found that WNT/ β -catenin signaling has controlled osteogenic lineage commitment by stimulating the expression of *runx2* gene [88].

FGFs signaling pathway also crosstalks with WNT and BMPs pathway. Marked reduction of β -catenin and WNT10b mRNA and protein expression have been observed in *fgf2*^{-/-} mice, while exogenous FGF2 has been able to restored nuclear β -catenin level [89]. Effect of BMP2 on ectopic bone development has enhanced by the presence of low dose FGF2 [90]. Furthermore, FGF2 has been found to modulate *bmp2* gene expression through the activation of Runx2 [91].

1.1.4 Bone defects and treatment

1.1.4.1 Defects of bone tissue

Bone lost caused by trauma, infection or cancer is a complicate medical condition. Some of bone defects are a result of severe injury which the surrounding muscles and vascular tissues are also injured. Treatment of this condition, still, is a challenging task for orthopedic surgeon. Even though bone tissue can heal itself spontaneously, large defect still needs a medical intervention for appropriately restoration [92].

1.1.4.2 Bone fracture healing process

Fracture healing is an intricate event involving in 4 overlapping phases as revealed by a histological observation of human and animal model (Figure 1.10) [93-96]. These are, in chronological order, initial inflammation, formation of soft callus, hard callus development, and bone remodeling. This process takes more than 3 months to complete the healing. Aim of ongoing research is to clarify the fracture healing process in both cellular and molecular level. The understanding of this event can lead to an advance and effective treatment for patient.

Normally, bone fracture is associated with the damage of nearby tissues and the interruption of vascular function. These events lead to an inflammation cascade. An extravasation at the fracture site develops into hematoma during the first few hours. Then, platelets, macrophages, and inflammatory cells (such as lymphocytes, monocytes, granulocytes, and polymorphonuclear cells) migrate to the defected area. These cells secrete cytokines and factors that facilitate a recruitment of inflammatory cells and MSCs from periosteum, bone marrow, blood circulation, and surrounding tissues. Major signaling molecules that play a crucial role in this primary phase are tumor necrosis factor- α (TNF- α), cyclooxygenase-2 (COX-2), interleukins-1 (IL-1), IL-6, platelet-derived growth factor (PDGF), insulin-like growth factor (IGF), FGFs, TGF- β , and BMPs. The second event of bone healing is soft callus or fibrocartilage formation. MSCs turn into chondrocytes which synthesize cartilaginous matrix and become cartilage, while fibroblasts replace a cartilage deficit region with fibrous tissue. In the final step of soft callus formation, chondrocytes become hypertrophy and mineralize before undergoing apoptosis. The proliferation and differentiation of fibroblast and chondrocytes are stimulated by many factors such as TGF- β , PDGF, FGF1, IGF, and BMPs family (BMP2, 4, 5, and 6). Angiogenesis also occurs in this step. The invasion of vascular endothelial cells into soft callus is controlled by VEGF, TGF- β , BMPs, FGF1, and FGF2. Hard callus or primary bone formation is the next stage of fracture healing. A soft callus is gradually removed, while osteoprogenitor cells invade to this area through the neovascular. Osteoprogenitors subsequently mature to osteoblasts and osteocytes and form mineralized bone matrix which is known as hard callus. This process is recognized as endochondral ossification. Besides, hard callus can be formed

will be used for small or large defects, respectively. Conventional therapy for severe bone injury is a surgical reconstruction which can be divided into 2 techniques: allografts and autografts. Allografts regularly use the tissue from other patients or cadaver. On the other hand, autografts utilize own tissue from another site of patient's body. Autografts may offer more advantages than allografts because it can reduce the risk of disease transmission and foreign graft rejection. Meanwhile, the successful of this method is hindered by the quality and amount of tissue supply. Autografts, however, can cause the donor site morbidity.

Since bone healing is a natural process, management of lost bone tissue is aimed to restore the scattered pieces of bone to their original position and maintain the correct pose along the intrinsic curative course. Bone healing takes about months to years depending on the severity of injury, associated vascular and tissue damage, method of treatment, and patients [97]. There are 6 million bone fracture patients reported each year in United States. However, approximately 5-10% of these do not heal properly [98, 99], and the rate of delayed or non-union fracture can be up to 40-100% for severe fracture.

1.1.5 Tissue engineering

1.1.5.1 The concept

In late 1980, Langer and Vacanti provided the concept of tissue engineering as "an interdisciplinary field that applies the principles of engineering and the life sciences toward the development of biological substitutes that restore, maintain, or improve tissue function" [100]. This strategy raises a great promise for lost bone tissue restoration. The principle of this technique for bone regeneration is the replacement of defected tissue using osteogenic cells controlled by osteoinductive factors and a proper material for creating suitable environment for the cells (Figure 1.11). Therefore, tissue engineering relies on 3 major components: osteoprogenitor cells, biomimetic/bioconductive scaffolds, and osteoinductive agents [101].

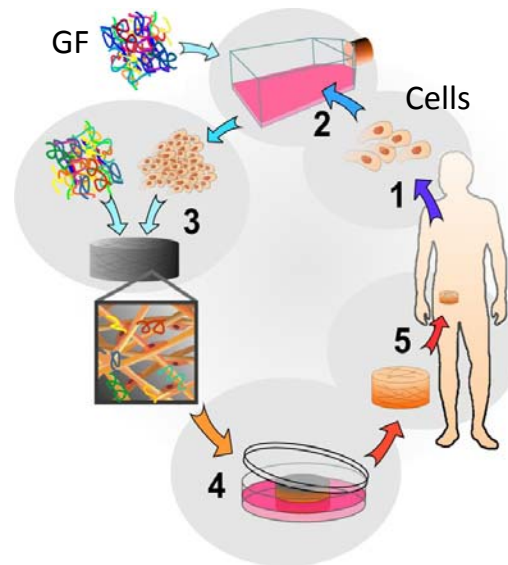


Figure 1.11: Concept of bone tissue engineering. Cells obtained from patient (1) are expanded (2) and seeded onto the scaffold (3). Growth factors (GF) are added in cell culture medium or the construct to enhance cell proliferation or induce osteogenic differentiation. Then, the construct (4) is implanted into the defect site (5) [102].

1.1.5.2 Osteogenic cells

One of the major components in bone tissue engineering is the osteogenic cells. However, methods used to prepare osteoblasts by either enzymatic digestion of bone tissue or explants culture are time consuming, and a yield is low [103, 104]. Besides, their proliferation potential is restricted. For these reasons, stem cells are more preferable. Mesenchymal stromal cells (MSCs) are an accessible source and have less ethical disagreement. They are non-hematopoietic multipotent stromal cells which can be obtained from many sources such as bone marrow, adipose tissue, and dental pulp. These cells exhibit the potential to become various cell sorts (Figure 1.4), including osteoblasts, chondroblasts, myoblasts, and adipocytes [105]. The quantity of MSCs, however, is very low. For example, stem cells comprise about 1 cell in 10^4 - 10^5 of bone marrow cell population [106-108]. They also lose their osteogenic capability

following culture and expansion [109]. Because MSCs are multipotent, culturing in a common condition may lead to a mixed cell phenotype. Moreover, glucocorticoid and ascorbic acid which are used as an inducer of osteogenesis are not specific for bone cells [110-112]. Hence, the method that can increase cell proliferation and maintain their osteogenic potential need to be investigated.

1.1.5.3 Scaffolds

Bone scaffold is developed under the concept of biocompatible and biodegradable. Ideal scaffold material should create an appropriate surrounding for bone cells and support capillary ingrowth (osteoconduction). It should favor cellular attachment and differentiation along the osteogenic lineage (osteinduction). To generate a new bone properly, there must be a suitable porosity inside a scaffold for nutrient supply, waste removal, and vascularization. Moreover, it must be resorbable for newly formed tissue replacement [113]. Numerous materials, including bioactive ceramics, natural polymers, synthetic polymers, and the composite, have been fabricated. Chemical composition of the most widely used ceramics, tricalcium phosphate (TCP) and HA, are like the mineral bone matrix. They show an osteoconductive and osteoinductive properties. Although, HA and TCP provide sufficient mechanical strength of non-load bearing, they remain unchanged after 5 years of implantation [114]. Natural polymers (such as collagen, fibrin, chitosan, etc.) provide an innate biological environment for bone cells, but they are poor in mechanical stability [115]. Synthetic polymers such as polylactide (PLA), polycaprolactone (PCL), and poly(lactide-co-glycolide) (PLGA) copolymers can easily be chemically modified and controlled a degradation rate [116]. Moreover, they exhibit reproducible and predictable mechanical and physical properties. Nevertheless, their harmful degradation products, especially acidic substances, affect cell growth and induce inflammatory response. Nowadays, composite scaffold materials are considerably developed. Combination of 2 or more types of materials gives advantageous properties and counteracts poor features of each substance.

1.1.5.4 Growth factors

Bone repair process is likely organized by numerous cytokines and growth factors, so the successfulness of bone reconstruction using tissue engineering strategy requires an earnest consideration of these osteoinductive molecules. As discussed above, multiple factors interact with many cell types during the healing process. Growth factors work cooperatively or antagonistically at distinct stages of bone development. For instant, VEGF and BMP4 synergistically enhance the recruitment of MSCs and augment cartilage formation and resorption [117]. Interestingly, simultaneous treatment of primary calvarial bone cells with recombinant human FGF2 and recombinant human BMP2 failed to develop mineralized nodules, but sequential treatment stimulated mineralization [118]. Thus, a comprehensive exploration on the osteogenic activity of these factors needs to be elucidated.

1.2 Research rationale

Bone tissue engineering is a promising tool for reconstruction of damaged skeleton tissue. This strategy integrates a number of knowledge on molecular biology, cell biology, biochemistry, tissue engineering, material science, and medical transplantation. However, the application of this multidisciplinary science in clinics have not proceeded due to several limitations relating to the key components of this technique, such as osteogenic cells, scaffolds, and growth factors [101]. This study was focused to overcome the restrictions on the acquirement of osteogenic cells by using bone growth factors that potentiate their osteogenicity.

MSCs and ordinary bone cells (osteoblasts) are essential for bone regeneration. In contrast to MSCs, osteoblasts have a limited proliferation potential when subcultured [103]. MSCs exhibit capability to give rise to diverse tissues, including bone, cartilage, adipose tissue, tendon and muscle [105]. However, there is a restricted numbers of MSCs in human body. On *in vitro* expansion, the cells strongly lose potential [107, 109]. Since conditions for culturing these cells have been varied among research groups, and being difficult to compare [119, 120], this study was thus aimed to increase proliferation

capacity while maintaining their osteogenic potential as long as possible upon subculturing.

The medium supplemented with glucocorticoid (such as dexamethasone), ascorbic acid (AA), and β -glycerophosphate (β -GP) has been widely used as an osteogenic culture medium [121]. This condition, however, is not specific for only osteogenic lineage, and the culture period can prolong to several weeks. The cell culture system using specific osteogenic induction factors is of interest. Since bone related growth factors are crucial in during MSCs to be differentiated into bone, it was necessary to choose the best one with an effective cost when applied clinically. Experimental evidences have shown that FGF2 has been critical for bone fracture healing [68, 69]. FGF2 has been reported to increase cell proliferation while maintaining the differentiation ability of bone marrow-derived MSCs [66, 67]. Nonetheless, economically limitation and incomplete activation pathway of FGF2 are major drawbacks of its clinical application. To improve an osteogenic culture system for MSCs, insulin becomes another induction factor, as its effects on osteo-chondroblastic cell proliferation and differentiation have been reported [75, 122]. It is postulated that cost of the treatment using insulin will be more economically-friendly than FGF2. In this study, the effects of FGF2, insulin, and their combination on stromal cell proliferation and osteogenic differentiation were compared. *In vitro* and *in vivo* experiments were carried out to evaluate the effectiveness of the developed conditions.

This study is also proposed to clarify the signal transduction pathways that control the differentiation of MSCs. Many publications strongly indicated that there is a complexity in cell signaling crosstalk between several pathways, and the coordination of these pathway is necessary to be well organized and balanced. To my knowledge, FGF2 and insulin pathway involve and are affected by others, as well. Whether FGF2 and insulin controls MSCs differentiation by activating *runx2* transcription and WNT pathway will be proven. To determine how these factors work, genetic approach and reporter gene assay will be applied. Identification of downstream FGF2 and insulin activation cascade may support the clinical use of these proteins in the future.

1.3 Objectives

The objectives of this work are

- 1) To establish the cost-effectiveness induction condition for MSCs osteogenic differentiation.
- 2) To explore the molecular mechanisms of FGF2 and insulin on bone formation.
- 3) To develop the potential therapeutic approach for the repair and regeneration of injured skeleton tissue.

CHAPTER 2

RESEARCH METHODOLOGY

2.1 Materials

2.1.1 General reagents

FGF2 was received from Merck (Darmstadt, Germany). Insulin was purchased from Novo Nordisk Pharmaceuticals Ltd. (Auckland, New Zealand). BMP2 and BMP7 were obtained from BioVision (Mountain View, CA, USA). Ascorbic acid (AA), triamcinolone acetonide (TA), β -glycerophosphate (β -GP), dimethyl sulfoxide (DMSO), Triton X-100, magnesium chloride ($MgCl_2$), ammonium acetate, and sodium dodecyl sulfate (SDS) were bought from Sigma-Aldrich (St. Louis, MO, USA). DNase/RNase free water, tris base, and dimethylformamide were purchased from Amresco (Solon, OH, USA). Sodium chloride (NaCl) was supplied from Lab-Scan Co., Ltd. (Bangkok, Thailand). Ethylenediamine tetra-acetic acid (EDTA) was received from Ajax Finechem Pty. Ltd. (Australia).

2.1.2 Reagents for cell isolation, culture, and characterization

Dulbecco's phosphate buffer saline (DPBS), Dulbecco's modified eagle medium: nutrient mixture F-12 (DMEM/F-12), minimum essential medium α medium (α -MEM), fetal bovine serum (FBS), 0.5% trypsin-EDTA (10x), and 100x antibiotic-antimycotic (10,000 units/mL of penicillin, 10,000 μ g/mL of streptomycin, and 25 μ g/mL of Fungizone[®]) solution were received from Gibco[™] Invitrogen Corporation (Grand Island, NY, USA). Heparin (5,000 i.u./u.i./ml) was supplied from LEO Pharmaceutical Products (Ballerup, Denmark). Ficoll-Paque Plus was bought from GE Healthcare Bio-Sciences (Uppsala, Sweden). Lymphoprep[™] solution was obtained from Axis-shield (Oslo, Norway). Fluorescence-conjugated antibodies targeted against HLA-DR, CD10,

CD13, CD14, CD29, CD34, CD44, CD45, CD73, and CD90 were purchased from BD Biosciences (San Jose, CA, USA).

2.1.3 Reagents for *in vitro* evaluation of induction conditions

MTT reagent and para-nitrophenyl phosphate (pNPP) were bought from Sigma-Aldrich (St. Louis, MO, USA). Tri Reagent[®] was supplied from Molecular Research Center, Inc. (Cincinnati, OH, USA). Qubit[™] dsDNA BR assay kits, SuperScript III first-strand synthesis, and SuperMix kit for two-step quantitative RT-PCR were received from Invitrogen (Carlsbad, CA, USA). RevoScript[™] RT premix (oligo (dT)15 Primer) was purchased from Intron Biotechnology (Gyeonggi-do, Korea). iScript Q PCR kit with SYBR Green was provided from Bio-Rad Laboratories (Hercules, CA, USA). Brilliant II SYBR[®] Green QPCR master mix was obtained from Agilent Technologies, Inc. (La Jolla, CA, USA). Complete protease inhibitor cocktail tablets was supplied from Roche (Mannheim, Germany). Pierce[®] BCA protein assay kit was purchased from Pierce (Rockford, IL, USA). Alizarin red s was bought from Sigma-Aldrich (St. Louis, MO, USA). Quantikine[®] BMP2 ELISA kit was provided from R&D Systems Inc. (Minneapolis, MN, USA).

2.1.4 Reagents for *in vivo* experiment

Xylazine (20 mg/ml) was received from Thai Nakorn Patana (Nonthaburi, Thailand). Zoletil[®] 100 (50 mg/ml Tiletamine and 50 mg/ml Zolazepam) was obtained from Virbac Pty Limited (Australia). Paraformaldehyde, sodium sulfate, alizarin red s, Meyer's hematoxylin solution, and eosin aqueous solution were bought from Sigma-Aldrich (St. Louis, MO, USA). Formic acid was supplied from Fisher Scientific UK (Leics, UK). Xylene, acetone, and sodium sulfate were purchased from RCI Labscan Limited (Bangkok, Thailand)

2.1.5 Reagents for plasmid construction

Taq DNA polymerase was purchased from Intron Biotechnology (Gyeonggi-do, Korea). X-gal was provided from Promega (Madison, WI, USA). Isopropyl β -D-1-thiogalactopyranoside (IPTG) was obtained from United States Biological, Inc. (Swampscott, MA, USA). HIT Competent Cells™ *E. coli* strain DH5 α was supplied from RBC Bioscience Corp. (New Taipei City, Taiwan). LB broth was received from Lab M Limited (Lancashire, UK). Bacteriological agar powder was provided from HiMedia Laboratories Pvt. Ltd. (Mumbai, India). Ampicillin sodium was purchased from Bio Basic Inc (Amherst, NY, USA). NucleoSpin® plasmid and NucleoSpin® extract II were bought from Macherey-Nagel (Duren, Germany). Novel juice (6X Loading Buffer) was purchased from GeneDireX (Las Vegas City, NV, USA). DNA molecular weight marker XIV 100–1500 base pair (bp) was bought from Roche (Mannheim, Germany). One kb DNA ladder was received from SibEnzyme Ltd. (West Roxbury, MA, USA). Proteinase K, *KpnI*, *BglII*, *NheI*, T4 DNA ligase, and 1 kb DNA ladder were obtained from New England Biolabs, Inc. (Ipswich, MA, USA). Plasmids were received from Promega (Madison, WI, USA).

2.1.5.1 Plasmids

2.1.5.1.1 pGEM®-T easy vector

pGEM®-T easy vector was utilized as a cloning vector because T-overhangs at the insertion site (Figure 2.1) afford the ligation of PCR product. It also contains ampicillin resistance gene (*Amp^r*) and coding sequence of β -galactosidase (*lacZ*) which will be disrupted by the insertion of target DNA. Therefore, blue/white colony and ampicillin agar selection are applicable for positive clone screening.

2.1.5.1.2 pGL3-Promoter vector

pGL3-Promoter vector was used as an experimental reporter vector. To evaluate the proficiency of gene regulatory element, DNA fragments of interest were inserted at the upstream of promoter-*luciferase*⁺ transcriptional unit (*luc*⁺) (Figure 2.2) where the transcription of firefly luciferase gene was under the control of DNA insert and SV40 promoter. With the present of ampicillin resistance gene, positive clone identification can be selected using ampicillin as a selection marker.

2.1.5.1.3 pGL3-Control vector

pGL3-Control vector (Figure 2.3) contains SV40 promoter, firefly luciferase gene transcriptional unit, and SV40 enhancer sequence which can influence the strong expression of luciferase enzyme. Thus, it is applicable for inspecting of transcriptional activity in transfected eukaryotic cells. In this study, pGL3-Control vector was utilized for transfection efficiency monitoring in the optimization process.

2.1.5.1.4 pRL-SV40 vector

The pRL-SV40 vector contains a cDNA encoding for *Renilla* luciferase (*Rluc*) (Figure 2.4) which was applied as an internal control of transfection experiment. In a co-transfection with pGL3 reporter vector, the expression of experimental firefly luciferase was normalized with *Renilla* luciferase to reduce the variations in transfection efficiency.

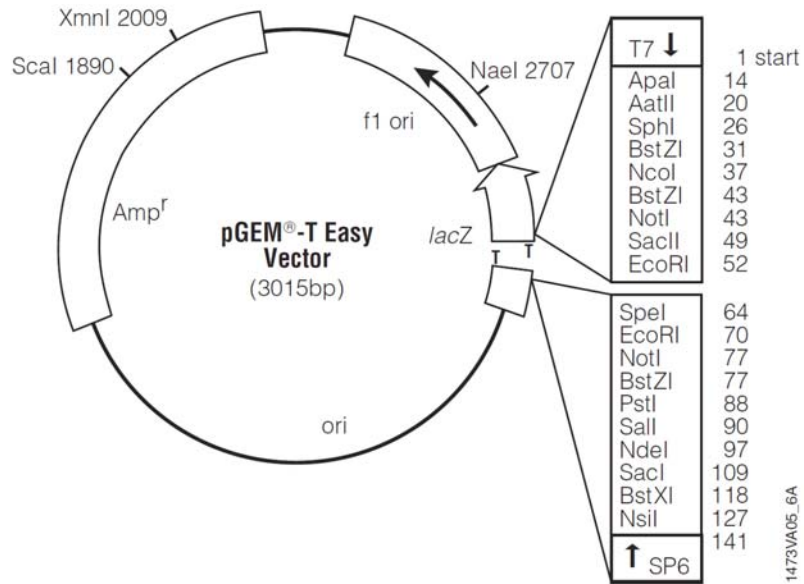


Figure 2.1: Circular map of pGEM[®]-T easy vector.

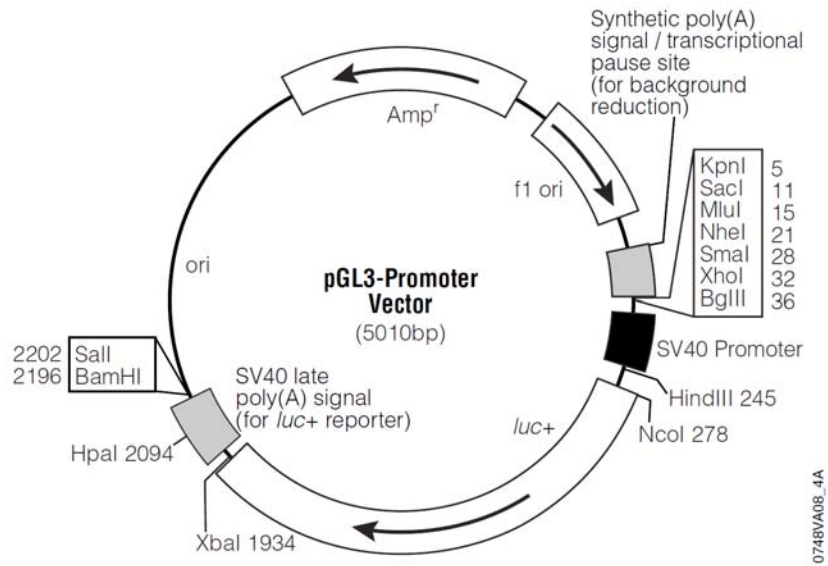


Figure 2.2: Circular map of pGL3-Promoter vector.

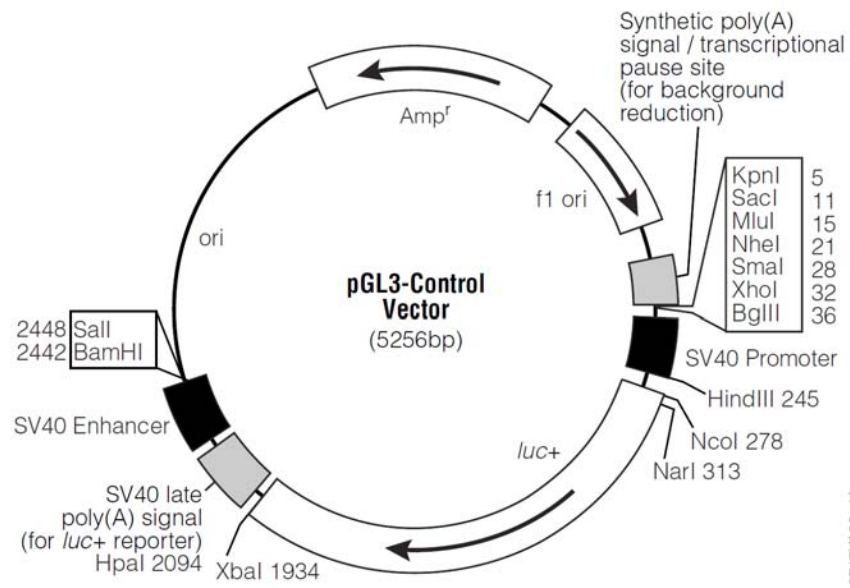


Figure 2.3: Circular map of pGL3-Control vector.

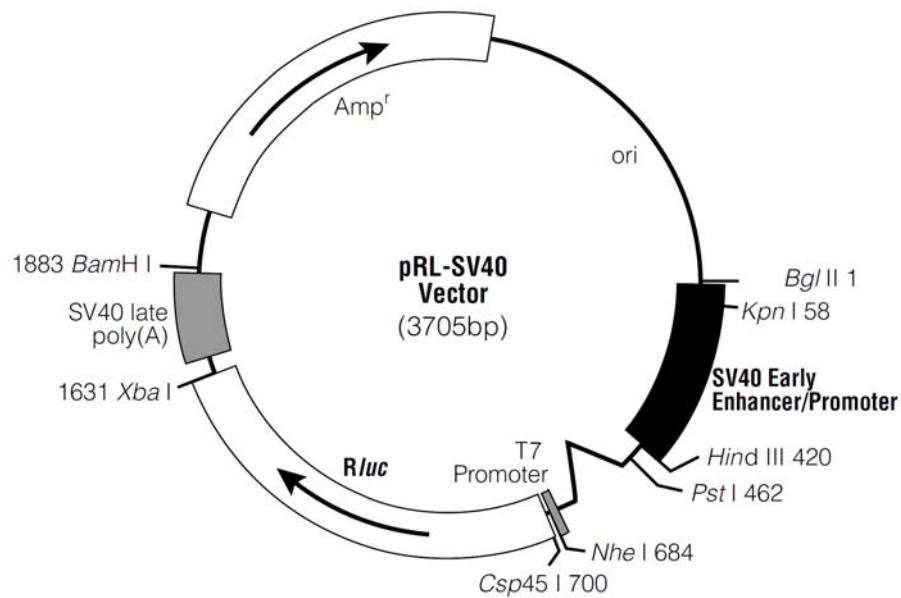


Figure 2.4: Circular map of pRL-SV40 vector.

2.1.6 Reagents for transfection experiment

QIAGEN plasmid midi and maxi kits was supplied from QIAGEN (Hilden, Germany). FuGENE® 6 transfection reagent was bought from Roche (Mannheim, Germany). Dual-Luciferase® reporter assay system was received from Promega (Madison, WI, USA).

2.1.7 Laboratory animal

Two-month-old male Wistar rats were used in this study. Rats were anesthetized by intramuscular injection using a mixture of 1: 1 volume ratio of xylazine (20 mg/ml) and Zoletil® (100 mg/ml) with a 0.2 ml per 250 gram body weight. When the experiment was completed, the animals were sacrificed by cervical dislocation. Care and use of laboratory animals was performed following the laboratory animal facility unit guideline of the Animal Ethic Committee, PSU.

2.1.8 Primers and oligonucleotides

The oligonucleotides used in this study were synthesized by Bio Basic Canada Inc. (Canada). Primers for DNA sequencing, *runx2* regulatory element cloning, real-time PCR, and tandem repeat of transcription factor binding site were summarized in the tables below.

Table 2.1: Sequences of oligonucleotides and annealing temperatures. The primers for *runx2* regulatory element were designed based on NCBI reference sequence database number NC_005108, and contain *KpnI* and *NheI* restriction sites (underlined).

Primers	Sequence (5' ---> 3')	Annealing temperature (°C)
<i>DNA sequencing primers</i>		
T7	TAA TAC gAC TCA CTA TAg gg	56
SP6	ATT TAg gTg ACA CTA TAg	48
U345-SEQ	gTg Agg CCT TCC Tgg CAT TCA	58
U1291-SEQ	ACA TAC TCT gTC TgC gTg CA	58
LUC-F	ACT gTT ggg AAg ggC gAT	56
LUC-R	Agg AAC CAg ggC gTA TCT C	56

Table 2.1 (Continued)

Primers	Sequence (5' ---> 3')	Annealing temperature (°C)
<i>Insertion analysis primers</i>		
<i>ap1</i> -LUC	gAT CTC TgA CTC ATg gTA C	48
<i>sry</i> -LUC	gTA CTT TTg TTT ggT AC	50
<i>Primers for runx2 regulatory element cloning</i>		
<i>runx2</i> -U1557	TCT gAg Tgg CgT ggA TAA ATg gC	57.5
<i>runx2</i> -97	Tgg CTg gTA gTg ACC TgC A	57.5
<i>runx2</i> -KPNI-U796	CgC <u>ggT ACC</u> TTA CAg TCA ATC CCg gCA Agg	64
<i>runx2</i> -NHEI-U73	gCC <u>gCT AgC</u> CAT gTg gTT TgT gAC CTC ACA g	64
<i>runx2</i> -KPNI-U1526	CgC <u>ggT ACC</u> Agg AAA TTg gTC TgC TCg CCT	58
<i>runx2</i> -NHEI-U630	gCC <u>gCT AgC</u> gTg ggT CAC ATC TTg ggA TTg	58

Table 2.2: Real-time PCR primers. F and R stand for forward and reverse primer, respectively.

Name of gene [reference]	Primer sequence (5' ---> 3')	NCBI Reference Sequence	Product size (bp)	Annealing temperature (°C)
Reference gene				
Human <i>gapdh</i> [123]	F TCC CTg AgC TgA ACg ggA Ag	NM_002046	218	60
	R ggA ggA gTg ggT gTC gCT gT			
Rat <i>gapdh</i> [124]	F ACC ACA gTC CAT gCC ATC AC	NM_017008	179	59
	R ACA Cgg AAg gCC ATg CCA gTg			
Stem cell-associated gene				
Human <i>fgf4</i> [125]	F gAT gAg TgC ACg TTC AAg gA	NM_002007	118	60
	R ggT TCC CCT TCT Tgg TCT TC			
Human <i>nanog</i> [126]	F CTg TGA TTT gTg ggC CTg AA	NM_024865	151	60
	R TgT TTg CCT TTg ggA CTg gT			
Human <i>oct4</i> [127]	F AAg gAT gTg gTC CgA gTg Tg	NM_002701	180	60
	R gAA gTg Agg gCT CCC ATA gC			
Human <i>sox2</i> [126, 127]	F TTA CCT CTT CCT CCC ACT CCA	NM_003106	132	60
	R ggT AgT gCT ggg ACA TgT gAA			

Table 2.2 (Continued)

Name of gene [reference]		Primer sequence (5' ---> 3')	NCBI Reference Sequence	Product size (bp)	Annealing temperature (°C)
Human <i>bst1</i> [127]	F	CgA TTA CCA ATC CTg CCC TA	NM_004334	154	60
	R	TTT gAT ggg ATA ggC TCC Tg			
Human <i>tert</i> [125]	F	AgA gTg TCT ggA gCA AgT TgC	NM_198253	183	60
	R	CgT AgT CCA TgT TCA CAA CCg			
Human <i>rex1</i> [126]	F	AAA ggT TTT CgA AgC Aag CTC	NM_174900	185	60
	R	CTg CgA gCT gTT TAg gAT CTg			
Osteogenic gene					
Human <i>runx2</i> [128]	F	gCA gTT CCC AAg CAT TTC ATC	NM_001024630	182	60
	R	CAC TCT ggC TTT ggg AAG Ag			
Human <i>osc</i>	F	gTg CAg AgT CCA gCA AAg gT	NM_199173	191	60
	R	CTg AAA gCC gAT gTg gTC Ag			
Human <i>osp</i>	F	CAC CTg TgC CAT ACC AgT TAA AC	NM_001040058	220	60
	R	ATC CAT gTg gTC ATg gCT TT			
Human <i>bsp</i>	F	ggg CAC CTC gAA gAC AAC AA	NM_004967	209	60
	R	CTC ggT AAT TgT CCC CAC gA			

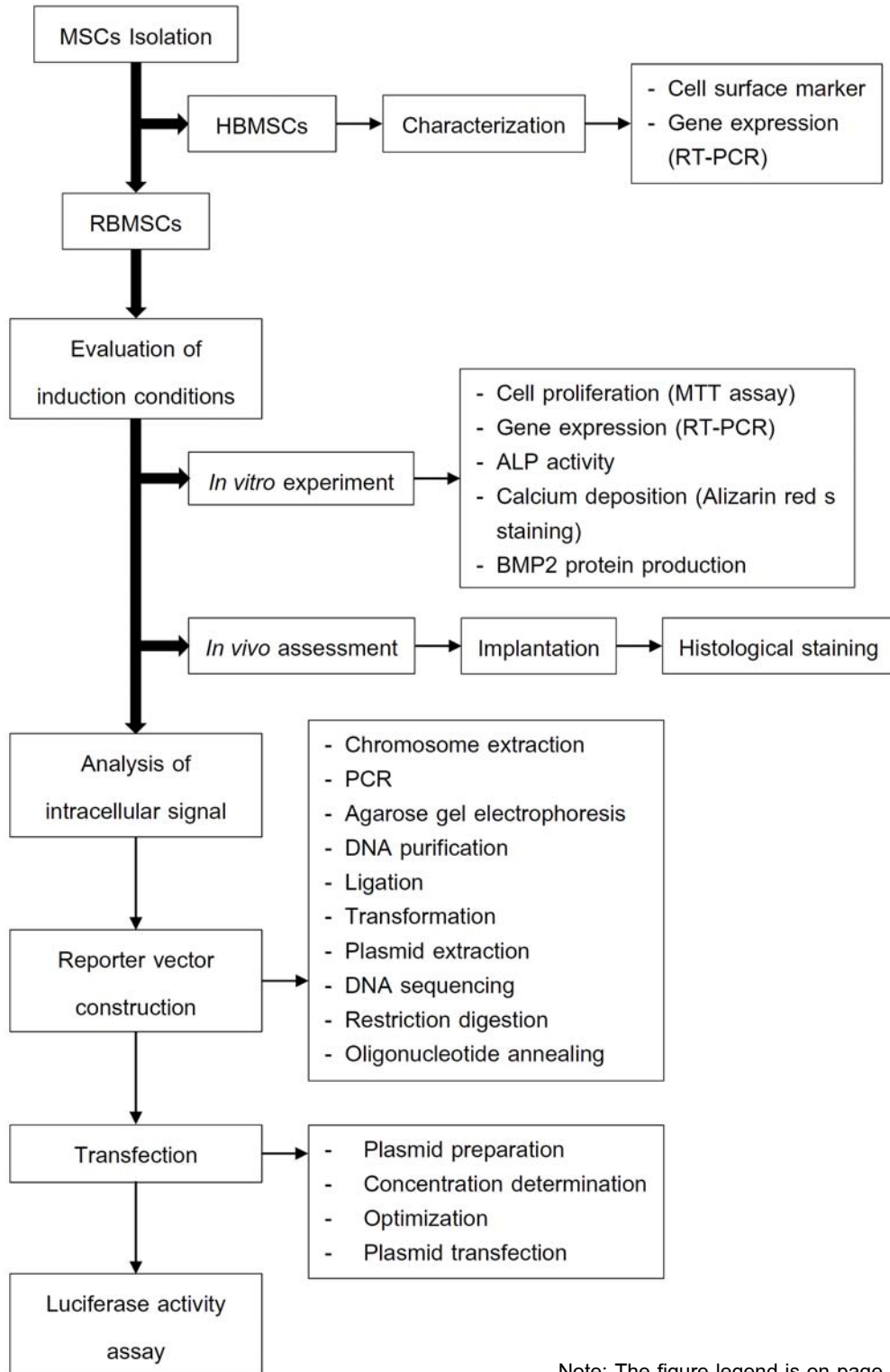
Table 2.2 (Continued)

Name of gene [reference]		Primer sequence (5' ---> 3')	NCBI Reference Sequence	Product size (bp)	Annealing temperature (°C)
Human <i>alp</i> [129]	F	gTA CTg gCg AgA CCA AgC gCA	NM_000478	200	60
	R	Agg ggA ACT TgT CCA TCT CC			
Rat <i>runx2</i>	F	ACA ACC ACA gAA CCA CAA g	NM_001278483	106	55
	R	TCT Cgg Tgg CTg gTA gTg A			
Rat <i>osx</i>	F	AAC Tgg CTT TTC TgT ggC A	NM_001037632	237	57
	R	Cgg CTg ATT ggC TTC TTC T			
Rat <i>bmp7</i>	F	gAC AgA TTA CAg ACT CCC ACA	XM_342591	215	54
	R	gTT gAT gAA gTg AAC CAg TgT			
Rat <i>axin2</i>	F	ACg AgT CAg CCg gCA CCA TC	NM_024355	165	57
	R	Tgg ggC TTT gAC ACC TCg gC			
Rat <i>dkk1</i>	F	gCT gCC CCg ggA ATT ACT gCA	NM_001106350	422	56
	R	gTg TCT CTg gCA ggT gTg gAg C			
Rat <i>β-catenin</i>	F	CgC CTT TgC ggg AAC Agg gT	NM_053357	121	57
	R	Cgg ACg CCC TCC ACg AAC Tg			

Table 2.3: The synthesized oligonucleotides for the transcription factor binding site. Sense and antisense strands were designed for perfect ligation. In the reverse strand, five tandem repeats of consensus binding site (5X CTgACTCAT and 5X TTTgTTT) were generated with a restriction enzyme overhangs. Overhangs of *Bgl*II at 5'-end and *Kpn*I at 3'-end were underlined.

Name of the oligonucleotide	Synthesized consensus binding site (Sequence 5' ---> 3')	Synthesized reverse strand (5X tandem repeats) (Sequence 5' ---> 3')
5Xap1	ATGAGTCAG	<u>gAT</u> <u>CTC</u> TgA CTC ATC TgA CTC ATC TgA CTC ATC TgA CTC ATC TgA CTC <u>ATg</u> <u>gTA</u> C
5Xsry	AAACAAA	<u>gAT</u> <u>CTT</u> TTg TTT TTT gTT TTT TgT TTT TTg TTT TTT gTT <u>Tgg</u> <u>TAC</u>

2.2 Experimental scheme



Note: The figure legend is on page 40.

Figure 2.5: Experimental workflow. Bone marrow-derived MSCs were applied as a cell model in this study. First of all, the isolation of stem cells from human (HBMSCs) and rat (RBMSCs) bone marrow aspirate were achieved. HBMSCs were then subjected for characterization, and the cells were used for preliminary evaluation of osteogenic induction. The cell surface marker and gene expression profile were studied. RBMSCs were grown in the experimental culture conditions. Both *in vitro* and *in vivo* assessment were carried out to appraise the effect of induction factors. Finally, intracellular signaling pathway of the growth factors was analyzed using luciferase reporter assay.

2.3 Methods

2.3.1 MSCs isolation and culture

Bone marrow-derived MSCs were used in this experiment. However, the major obstacles limiting the clinical use of MSCs are the lack of standardized protocols to separate the cells and their heterogeneous population which results in poor reproducibility of clinical outcome. Thus, monitoring of stem cell biomarkers will improve the understanding of their biology and lead to their application in regenerative medicine.

In this study, the density gradient technique was used to isolate the MSCs from bone marrow aspirate, and the cell surface markers were identified by flow cytometry. The isolated cells were cultured, expanded, and stored for further experiments using aseptic cell culture technique.

2.3.1.1 Human bone marrow-derived MSCs (HBMSCs) isolation

Remnant bone marrow samples were aspirated from patients who had hematological disorder without malignancy at Hematology Laboratory, Hospital Universiti Kebangsaan Malaysia. The patients were signed consent before their bone marrow samples were taken for the study. Bone marrow-derived MSCs were isolated

using ficoll solution by diluting the bone marrow with DPBS at a ratio of 1:1, and the mixture was layered over to the same volume of ficoll solution. After that, the samples was centrifuged at 2,000 rpm for 20 minutes at room temperature. The mononuclear cell layer at the liquid interface was collected and suspended in DPBS. The cells were precipitated by centrifugation at 6,000 rpm for 5 minutes. The aqueous layer was discarded and the cells were resuspended in DMEM/F-12 consisting of 10% FBS and 1% penicillin/streptomycin/amphotericin B. The cells were cultured in T-25 flask. Two days later, the medium was changed to remove the nonadherent cells. The culture condition was 37°C, 5% carbon dioxide, and 95% humidity.

2.3.1.2 Rat bone marrow-derived MSCs (RBMSCs) isolation

Bone marrow from femur and tibia bone of rats were aspirated and diluted with α -MEM containing heparin (10 units per 1 ml medium). MSCs were separated using density gradient technique. Equal volume of sample was layered over LymphoprepTM solution. Mononuclear cells at the interphase layer was collected after centrifugation at 800xg for 30 minutes at room temperature. Then, the cells were washed with DPBS and resuspended in α -MEM containing 10% FBS. The cells were cultured in T-25 flask. The nonadherent cells were removed on the next day by exchanging the culture medium. The culture condition was 37°C, 5% carbon dioxide, and 95% humidity.

2.3.1.3 Cell culture technique

2.3.1.3.1 Medium changing

The old medium was regularly replaced by the new one every 2-3 days. The procedures were in the following: supernatant was decanted from the flask. The cells were washed with DPBS prior to adding the new medium. Medium volume for each culture vessel was shown in Table 2.4.

Table 2.4: Surface area of the culture vessel, the volumes of culture medium, and the volumes of trypsin used for trypsinization.

Culture vessel	Surface area (cm²)	Culture medium (ml)	0.25x trypsin in DPBS (ml)
48-well plate	1	0.25-0.5	0.1
24-well plate	2	0.5	0.25
12-well plate	4	1	0.5
6-well plate	9.6	2	1
T-25 flask	25	3-5	2
T-75 flask	75	8-15	4

2.3.1.3.2 Subculture

When the adherent cells reached 80-90% confluence, they were subcultured using 0.25x trypsin solution in DPBS. Cell culture medium was aspirated. The cells were washed with DPBS and incubated with diluted trypsin solution at 37°C for 3-5 minutes (volume of trypsin solution per culture flask was described in Table 2.4). Trypsinization was terminated by adding 2-3 volumes of medium containing serum. Detached cells were gathered by centrifugation at 800xg for 5 minutes. The cells were washed again with DPBS before they were plated into a new culture vessel.

2.3.1.3.3 Cryopreservation

To preserve the cells, the adherent cells were trypsinized and prepared for cryostorage. They were resuspended in medium containing 20% FBS and 5% DMSO to a concentration of $1-2 \times 10^6$ cells per 1 ml per cryotube. The cells, then, were immediately frozen in liquid nitrogen tank for permanent storage.

2.3.1.3.4 Thawing and recovering of frozen stock

To recover the cells from cryostorage, cryotube was taken from liquid nitrogen tank and immediately immersed in a 37°C waterbath. After the stock was thawed, cell suspension was diluted with 10 ml of fresh medium. To remove DMSO, the suspension were centrifuged at 800xg for 5 minutes, and the cell pellet was collected. Finally, the cells were suspended in the medium and plated in a culture vessel.

2.3.2 HBMSCs characterization and osteogenic induction

To ensure the purity of the isolated HBMSCs, pattern of cell surface antigens were examined using flow cytometric analysis. The verified HBMSCs were then used for preliminary study of osteogenic induction. Since the sequential induction of 2.5 ng/ml FGF2 and 10 ng/ml BMP2 have shown to stimulate cell proliferation and osteogenic differentiation of rat MSCs within 7 days [130], the conditions were then used to investigate its impact on proliferation and differentiation of HBMSCs in this study. The acquired results would be an important information for osteogenic differentiation of stem cells from any sources in the future.

2.3.2.1 Flow cytometry

Flow cytometry is a laser-based biological technique employed for studying the information about each individual cell. By suspending the cells in a stream of fluid and force a single cell passes through a laser beam, the emerged light from each cell is captured (Figure 2.6). The data can be analyzed and reported as a cellular characteristic such as size, granularity, and phenotype. The general use of flow cytometry for determining cell property involves the use of fluorescent molecules. By using fluorescent-tagged antibody, cell surface antigen can be detected. The expression pattern of cell surface proteins is a useful information for cell type identification. For example, MSCs often express CD29, CD44, CD73, and CD90 and they do not present the hematopoietic markers such as CD14, CD34, and CD45 [131, 132].

Surface antigen characteristic of the isolated HBMSCs were identified in this study. Three colors flow cytometric detection was carried out using a BD FACSCalibur (Becton Dickinson, San Jose, CA, USA). Following CD markers were applied: phycoerythrin-conjugated (PE), peridinin chlorophyll protein-conjugated (PerCP), and fluorescence isothiocyanate-conjugated (FITC) antibodies targeted against HLA-DR, CD10, CD13, CD14, CD29, CD34, CD44, CD45, CD73, and CD90. Data analysis was evaluated by CellQuest™ Pro software (Becton Dickinson).

For sample preparation, the cells were resuspended in DPBS containing 1% FBS and divided to 5×10^5 cells per 50 μ l per 1 reaction tube. Each reaction, then, was incubated with 1 to 3 types of fluorescent-tagged antibody at room temperature for 30 minutes, protected from light. Unbound antibody was removed by washing with DPBS. After centrifugation at 800xg for 5 minutes, cells were resuspended in 1 ml of DPBS containing 1% FBS. Finally, they were analyzed by flow cytometer. Samples could be fixed with 4% paraformaldehyde for further analysis.

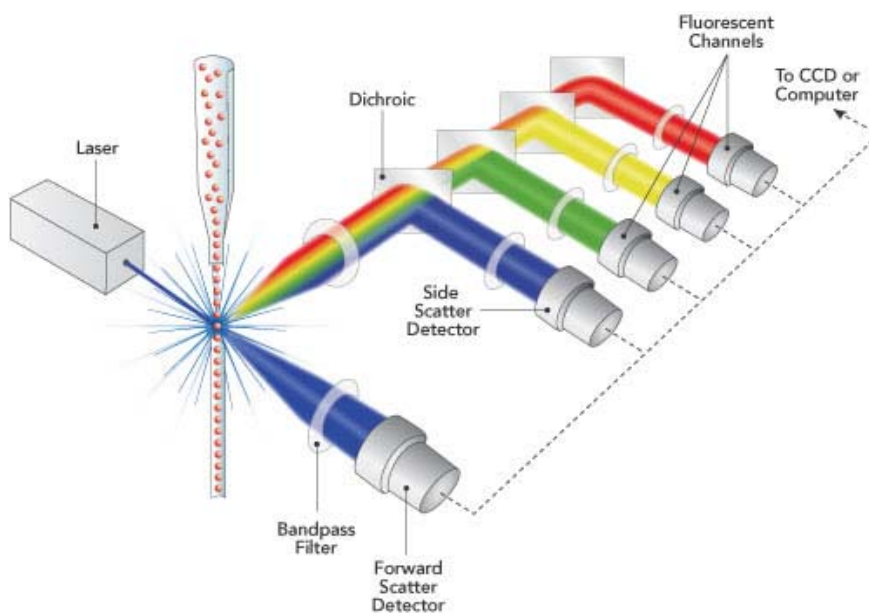


Figure 2.6: Schematic configuration of flow cytometer. The single cells flow through the flow chamber and pass the laser beam. Dichroic and filter gather and direct the emerged light to the specific light or fluorescent detectors. All signals are converted to digital data by computer system [133].

2.3.2.2 Induction of HBMSCs using FGF2 and BMP2

To evaluate the osteogenic differentiation of HBMSCs, sequential induction using FGF2 (2.5 ng/ml) and BMP2 (10 ng/ml) was used. HBMSCs were starved in DMEM/F12 supplemented with 2% FBS for 1 day, incubated with the medium containing FGF2 for 1 day, and starved again for 2 days. This was followed by the challenge with BMP2 for 1 day, and the expression of stem cell-specific genes and osteogenic genes were investigated. The schematic induction conditions and the time periods for measuring the gene expression was summarized in Figure 2.7.

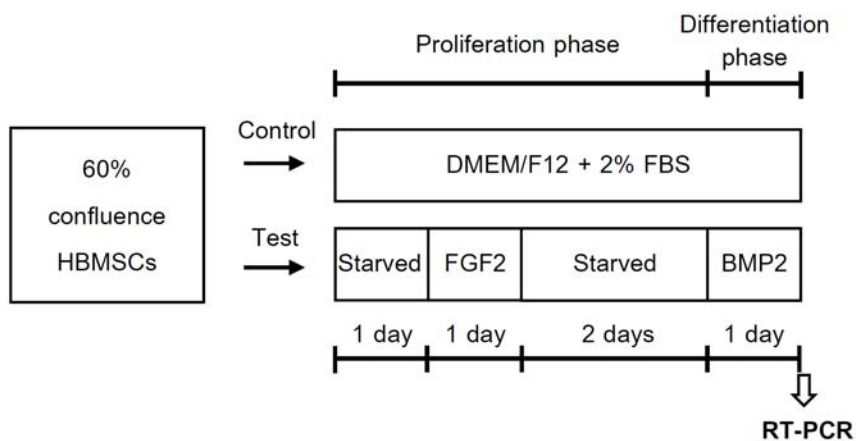


Figure 2.7: Induction scheme of HBMSCs. The cells of passage 2 at 60% confluence were starved in DMEM/F12 plus 2% FBS for 1 day, followed by the incubation with the medium containing FGF2 (2.5 ng/ml) for 1 day. The cells were starved for another 2 days and induced by 10 ng/ml BMP2 for 1 day. For the control, the cells were grown in DMEM/F12 supplemented with 2% FBS along the mentioned period. The expression level of stem cell-specific genes and that of osteogenic gene markers were determined and compared.

2.3.2.3 Determination of the gene expression levels using real-time PCR (RT-PCR) technique

Real-time PCR (RT-PCR) is a technique for quantification of transcription levels of the genes of interest. The method is based on recording the amount of PCR product in real time during the progression of PCR reaction using complementary DNA (cDNA) as a template. The expression level of the target genes was calculated as a fold change relative to that of an internal reference gene. Statistical analysis was performed by using one-way analysis of variance (ANOVA).

The pluripotency and self-renewal property of the stem cells have been reported to be controlled by many transcription factors and proteins. Since, octamer-binding transcription factor 4 (OCT4), SRY-related high mobility group (HMG) box 2 (SOX2), and Nanog have been indicated as a key transcriptional regulators of stem cells [134], it is important in this study to investigate these gene markers in HBMSCs. The cells of passage 2 and 5 were used for the test, and the results were evaluated during the cell expansion taking place.

To evaluate the osteogenic induction, HBMSCs of passage 2 were induced with FGF2 for 1 day followed by BMP2 for 1 day (Figure 2.7). The osteogenic markers were quantified by RT-PCR. The genes to be examined included *runx2*, *alp*, *osc*, *osp*, and *bsp* (Table 2.2).

2.3.2.3.1 Extraction of total RNA

Total RNA was separated from the cells of passage 2 and 5 grown in T-25 flask using Tri Reagent[®] according to the supplier's instruction. After the culture medium was aspirated, 2.5 ml of Tri Reagent[®] was directly added into the flask to lyse the cells. A 0.5 ml chloroform was added in the cell homogenate, mixed robustly for 15 seconds, incubated for 15 minutes at room temperature, and centrifuged at 12,000xg for 15 minutes at 4°C. Aqueous upper phase was collected and mixed with 1.25 ml isopropanol. After centrifugation at 12,000xg for 10 minutes at 4°C, total RNA was obtained. The RNA precipitate was washed with 75% ethanol by

centrifugation at 7,500xg for 5 minutes at 4°C. The RNA pellet was left for air-dry, dissolved with 20 µl of DNase/RNase free water, and converted to be cDNA.

2.3.2.3.2 cDNA synthesis

Total RNA was converted to be cDNA by using SuperScript III first-strand synthesis supermix kit (Invitrogen). It is a two-step quantitative RT-PCR kit. Components of which were shown in Table 2.5. The procedures were in according with the manufacturer. Briefly, the reaction of cDNA synthesis was conducted at 50°C for 30 minutes, but inactivated by heating at 85°C for 5 minutes. The synthesized product was kept at -20°C until use.

Table 2.5: The components for cDNA synthesis.

Components	Volume	Final concentration
SuperScript III reaction mixture (2x)	10 µl	1x
Reverse transcriptase enzyme mix (50 U/µl)	2 µl	5 U/µl
Template RNA (0.5 µg/µl)	5 µl	0.125 µg/µl
DNase/RNase free water	3 µl	-
Total volume	20 µl	

2.3.2.3.3 RT-PCR conditions of HBMSCs

The RNA expression levels were quantified using iScript Q PCR kit with SYBR Green (Bio-rad). Components of the reaction were shown in Table 2.6. The RT-PCR template was the cDNA converted from total RNA (experiment 2.3.2.3.2). The experiment was performed on MyiQ single-color real-time PCR detection system (Bio-rad), and the data were analyzed by iQ5 optical system software version 2.0 (Bio-rad). The thermal cycles consisted of 40 cycles of denaturation at 95°C for 10 seconds and annealing at 60°C for 30 seconds. Then,

melting pattern for a gene was detected. Its expression level was calculated and normalized by that of the reference gene (glyceraldehyde 3-phosphate dehydrogenase; *gapdh*). Statistical analysis was carried out by using one-way ANOVA.

Table 2.6: The components for RT-PCR reaction (Bio-rad).

Components	Volume	Final concentration
iScript Q PCR reaction mixture (2x)	10 μ l	1x
Forward primer (10 μ M)	1 μ l	0.5 μ M
Reverse primer (10 μ M)	1 μ l	0.5 μ M
cDNA (0.125 μ g/ μ l)	2 μ l	12.5 ng/ μ l
DNase/RNase free water	6 μ l	-
Total volume	20 μ l	

2.3.3 Induction for osteogenic differentiation of RBMSCs

Bone marrow-derived MSCs are an interesting cell source for bone tissue engineering, since they are multipotent and easily accessible. To date, there are numerous restrictions for their medical application, because specific inducers for the cells to become osteogenic lineage are still unclear. In addition, the yield of isolated MSCs is low, while long-term cultivation is not suitable, because the cells trends to lose their differentiation potential. Accordingly, it is necessary to maintain these properties during the expansion, while proper differentiation of the cells could be preserved in a robust conditions that developed.

In this part, the cells derived from rat bone marrow (RBMSCs) were used as the cell model. The reasons behind were that (1) human bone marrow from patient without hematological disorder was scarcely available and (2) large numbers of the cells were required for this study. To investigate and improve the osteogenic induction condition, the cells were challenged with bone-related growth factors. The induction protocol was separated into 2 phases: the proliferation phase and the differentiation

phase (Figure 2.8). Growth factors and their concentrations were summarized in Table 2.7. FGF2 and insulin were the growth factors used in the proliferation phase, while BMP2 and BMP7 were of the differentiation phase. It is hopeful to develop the cost-effective induction conditions for the MSCs. The osteogenic outcomes were examined using techniques such as RT-PCR, and the assay of bone-specific enzyme activity, mineralization, and bone-specific protein production.

Table 2.7: The used growth factors and their concentrations.

Induction phases	Growth factors	Concentration
Proliferation	FGF2	2.5 ng/ml
	Insulin	60 ng/ml
Differentiation	BMP2	10 ng/ml
	BMP7	10 ng/ml

The induction protocol was shown in Figure 2.8. The cells were starved in α -MEM supplemented with 2% FBS for 1 day, before inducing with 2.5 ng/ml FGF2, 60 ng/ml insulin, or FGF2 plus insulin for 1 day. The cells were starved again for 2 days followed by the addition of 10 ng/ml BMP2, 10 ng/ml BMP7, or BMP2 plus BMP7 for 1 day. After that, the cells were grown in the medium containing 10 mM β -GP for another 5 days. In the control group, the medium supplemented with 2% FBS was used in place of FGF2 or insulin, whereas TA (10 nM) plus AA (50 μ g/ml) were used instead of BMP2 and BMP7. Then, cell proliferation and differentiation were assessed.

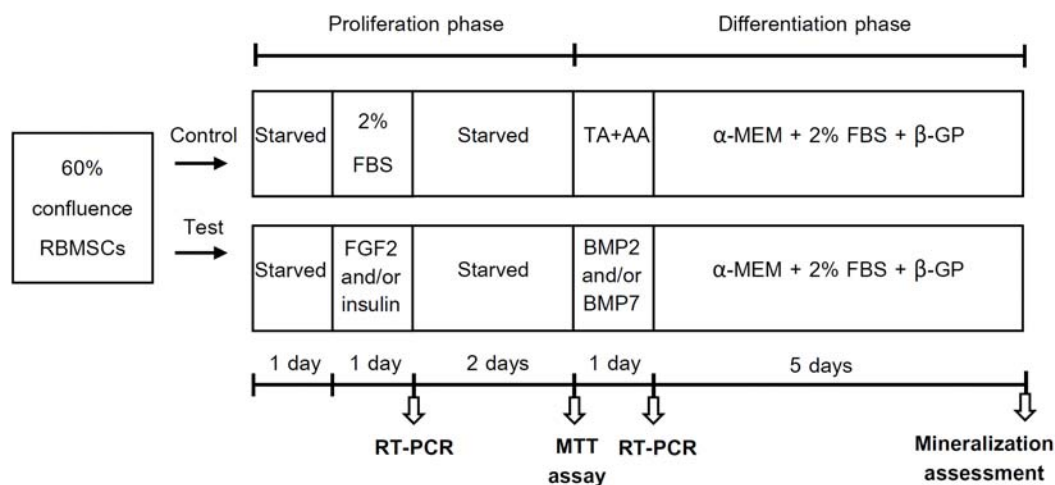


Figure 2.8: The scheme for induction conditions of RBMSCs. The cells were starved in α -MEM plus 2% FBS for 1 day. They were induced with 2.5 ng/ml FGF2, 60 ng/ml insulin, or their combination for 1 day. The cells were starved again for 2 days followed by differentiation induction using 10 ng/ml BMP2, 10 ng/ml BMP7, or their combination for 1 day. Next, the cells were allowed to grow in medium containing 2% FBS and 10 mM β -GP for 5 days. In the control group, α -MEM supplemented with 2% FBS was used instead of FGF2 or insulin, and 10 nM TA and 50 μ g/ml AA (TA+AA) were used in place of BMP2 or BMP7. Proliferation of the cells was analyzed by MTT assay. Changes in gene expression were evaluated by RT-PCR. Bone formation was assessed at the end of the treatment by alkaline phosphatase (ALP) activity assay and calcium deposition measurement.

2.3.4 Efficiency of the induction conditions developed

2.3.4.1 RT-PCR

Changes in gene expression in response to the growth factors were measured by using RT-PCR. Target genes consisted of osteogenic transcription factors (*runx2* and *osx*), *bmp7*, and the genes translated to proteins in WNT signaling pathway (*axin2*, β -*catenin*, and *dkk1*).

2.3.4.1.1 Extraction of total RNA

Total RNA was separated from the cells of passage 4 grown in T-25 flask using Tri Reagent[®] according to the supplier's instruction. The RNA extraction protocol was previously described (topic 2.3.2.3.1).

2.3.4.1.2 cDNA synthesis

Total RNA was converted to be cDNA by using RevoScript[™] RT premix (oligo (dT)15 Primer) (Intron Biotechnology). The procedures were in according to the manufacturer's instruction. RNA template and DNase/RNase free water was mixed into the tube containing RT premix to make a reaction volume of 20 μ l. The reaction of cDNA synthesis was performed at 50°C for 60 minutes followed by reverse transcriptase enzyme inactivation at 95°C for 5 minutes. The cDNA product was stored at -20°C until use.

2.3.4.1.3 RT-PCR conditions

Osteogenic gene expression of RBMSCs was measured by using Brilliant II SYBR[®] Green QPCR master mix (Agilent Technologies), and performed on LightCycler[®] nano (Roche) using LightCycler[®] nano SW1.0 software (Roche). The template of RT-PCR reaction was the cDNA converted from the total RNA. Components of the reaction were shown in Table 2.8. The reaction volume was

25 μ l with a 40-thermal cycle of denaturation at 95°C for 15 seconds, annealing at the specified temperature (Table 2.2) for 15 seconds, and extension at 72°C for 20 seconds. The melting curve was achieved at the end of the thermal cycle. The gene expression level was calculated and normalized by that of the reference gene (*gapdh*). Statistical analysis was performed by using one-way ANOVA.

Table 2.8: The components for RT-PCR reaction of RBMSCs.

Components	Volume	Final concentration
Brilliant II SYBR [®] Green QPCR reaction mixture (2x)	12.5 μ l	1x
Forward primer (10 μ M)	1 μ l	0.4 μ M
Reverse primer (10 μ M)	1 μ l	0.4 μ M
cDNA (0.125 μ g/ μ l)	2 μ l	10 ng/ μ l
DNase/RNase free water	8.5 μ l	-
Total volume	25 μ l	

2.3.4.2 Proliferation assay

Mitochondrial toxicity test (MTT) is a colorimetric method for quantifying viable cells. By incubating with cells in cultures, the yellowish MTT substrate is reduced to formazan by the active cells. The amounts of formazan product are proportional to the viable cell numbers.

The proliferative effect of FGF2, insulin, and their combination was compared after 1-day of the proliferation induction. Following the cultured medium was withdrawn, the adherent cells were incubated with 5 mg/ml MTT in DPBS in a CO₂ incubator for 4 hours. Then, MTT solution was aspirated, and the developed formazan crystal was dissolved in DMSO. The optical density at a wavelength of 570 nm was measured. The experiment was performed in triplicate. Statistical analysis was carried out by using one-way ANOVA.

2.3.4.3 Alkaline phosphatase (ALP) activity assay

Since ALP is an early marker for the progression of osteogenesis [135], increasing in the enzyme activity is a prominent indicator for successful osteogenic differentiation of the induced cells. ALP assists the conversion of colorless pNPP to yellowish para-nitrophenol and phosphate (Figure 2.9). The color intensity is directly proportional to the enzymatic activity. After the induction was completed, monolayer cells were wash with DPBS and lyzed with cell lysis buffer (containing 150 mM NaCl, 50 mM Tris pH 8.0, 1% triton X-100, and protease inhibitor). The cell lysate was centrifuged at 10,000xg at 4°C for 15 minutes to remove cell debris. ALP reaction consisted of 75 µl of the ALP reaction buffer (10 mM PNPP, 10 mM MgCl₂, 0.25 M Tris; pH 9.0) and 25 µl of the lysate. After incubation at 37°C for 1 hour, the reaction was terminated by adding 20 µl of 2 N NaOH. The absorbance at 405 nm was measured using a spectrophotometer. Data were normalized with the corresponding protein concentration before reporting. All experiments were done in triplicate. Statistical analysis was performed by using one-way ANOVA.

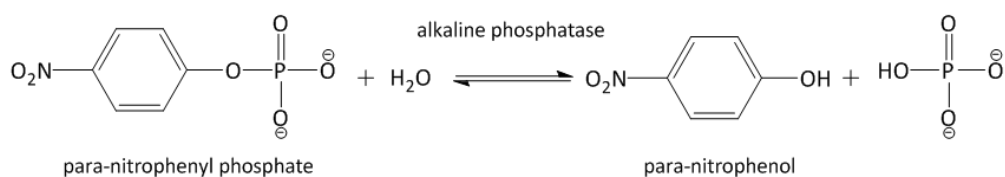


Figure 2.9: The hydrolysis reaction of pNPP as catalyzed by ALP producing a yellow color para-nitrophenol.

2.3.4.4 Mineralization of monolayer cells culture

In general, the progress in bone matrix production is related to the activity of osteoblasts, in which mineralization is a marker of osteogenesis. In this work, calcium deposition was evaluated by alizarin red s (ARS) staining method. The dye can form a chelation complex with calcium in cultured monolayer cells, resulting in a brick red stain.

The induced cells were washed with DPBS and fixed with 4% paraformaldehyde in DPBS for 15 minutes. Once washing with excess distilled water, the cells were incubated in 2% ARS solution (pH 4.2) for 20 minutes at room temperature. The excess dye was removed, and the cells were left for air-dry. The cell images were acquired by a microscope with Cell P Software (Olympus). The amount of calcium deposition was assessed by colorimetric technique. The stained dye was extracted by using the mixture of 10% acetic acid and 20% methanol in distilled water. After agitation for 20 minutes, the supernatant was collected, and the absorbance at 450 nm was measured. The OD value was proportional to the amount of the extracted ARS dye from the complex. All experiments were done in triplicate. Statistical analysis was performed by using one-way ANOVA.

2.3.4.5 BMP2 immunoassay

BMPs are identified as the key protein regulators of cartilage and bone formation, and the level of BMPs correlates with osteogenesis process. In this study, BMP2 concentration secreted by the cells into the cultured medium was measured using Quantikine[®] BMP2 ELISA kit (R&D Systems). To evaluate the effect of FGF2 and insulin on osteogenic lineage commitment, the level of BMP2 was measured after the cells were induced with these growth factors.

The culture supernatants were collected on day 1 and 3 after the proliferation induction (Figure 2.10). The cells were lysed with lysis buffer (150 mM NaCl, 50 mM Tris pH 8.0, 1% triton X-100, and protease inhibitor), and the cell debris was removed by centrifugation at 12,000xg for 10 minutes. The supernatant was drawn out and incubated for 2 hours in BMP2 antibody pre-coated in the Quantikine[®] microplate (R&D Systems). The solution in the well was aspirated, and the well was rinsed 4 times with the washing buffer. Bound BMP2 was identified by incubating with horseradish peroxidase-conjugated BMP2 antibody for 2 hours. After several time washes, tetramethylbenzidine substrate was added, and the reaction was left for 30 minutes before stopping by adding the stop solution. The absorbance at 450 nm was quantified. The amount of BMP2 in the samples was extrapolated from a standard

curve of known concentrations of recombinant BMP2. The BMP2 level was normalized by protein concentration of the cell lysate before reporting. All experiments were done in triplicate. Statistical analysis was carried out by using one-way ANOVA.

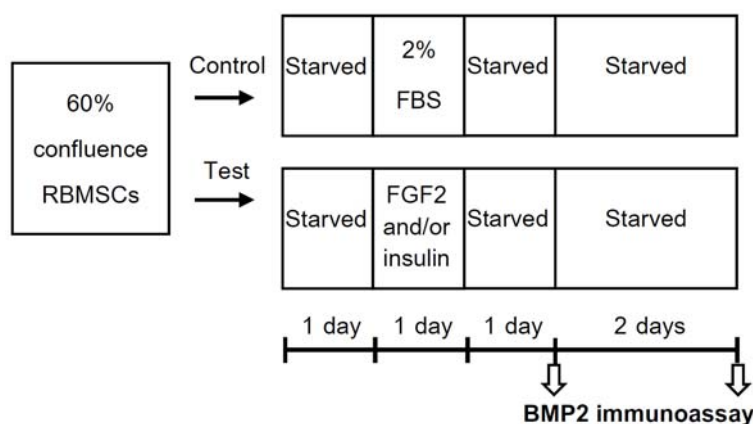


Figure 2.10: Timeline of RBMSCs induction and the measurement of BMP2 level in the medium supernatant. The starved cells were induced with 2.5 ng/ml FGF2, 60 ng/ml insulin, or FGF2 plus insulin for 1 day. BMP2 concentrations were measured at day 1 and day 3 after withdrawing the growth factors.

2.3.4.6 Determination of protein concentration for cell lysates

The concentration of proteins in cell homogenate was assessed by Pierce[®] BCA Protein Assay Kit (Pierce), according to the manufacturer instruction. The assay relies on the reduction of Cu^{2+} to Cu^{+} by any reducing proteins. Two molecules of bicinchoninic acid (BCA) chelate with 1 molecule of Cu^{+} ion, creating a purple-colored product. This complex is water-soluble and strongly absorbs light at wavelength of 570 nm.

Clear cell lysate was mixed with BCA working reagent at a 1:8 volume ratio. The color reaction was developed at 37°C for 30 minutes. The absorbance of purple-colored product was measured at 570 nm. The protein

concentration was determined by extrapolating with the standard curve of bovine serum albumin (BSA).

2.3.5 *In vivo* implantation

2.3.5.1 Preparation of the cell-seeded constructs

Osteogenic differentiation and bone tissue formation were studied *in vivo*. As this study aimed to develop the technique for clinical use, the effects of the growth factors in living organisms need to be considered. Wistar rats were used as the animal model. Hydroxyapatite (HA) scaffolds were seeded with RBMSCs of passage 4 at a density of 1×10^4 cells per scaffold and placed in a well-plate. After seeding, the cells were allowed to attach the scaffold for 1 hours before the culture medium was added in the culture plate. The seeded scaffolds were treated according to Figure 2.11. For the control group, cell-free scaffolds were immersed in α -MEM containing 2% FBS throughout the induction period.

2.3.5.2 Implantation

The rats were anesthetized with a combination of Zoletil® (40 mg/kg body weight) and xylazine (8 mg/kg body weight) before the operation. The cell-treated scaffolds were implanted subcutaneously on the back of the rat (Figure 2.12). Suture closure of the skin incision was performed, and antibiotic ointment was applied on the wounds. Following surgery, post-operative monitoring was carried out. The observation included the animal activity and the wound healing. The animals were sacrificed at 8 weeks after the operation. Implanted tissues were processed for histological analysis. By using 2 histological staining techniques, bone tissue formation can be determined.

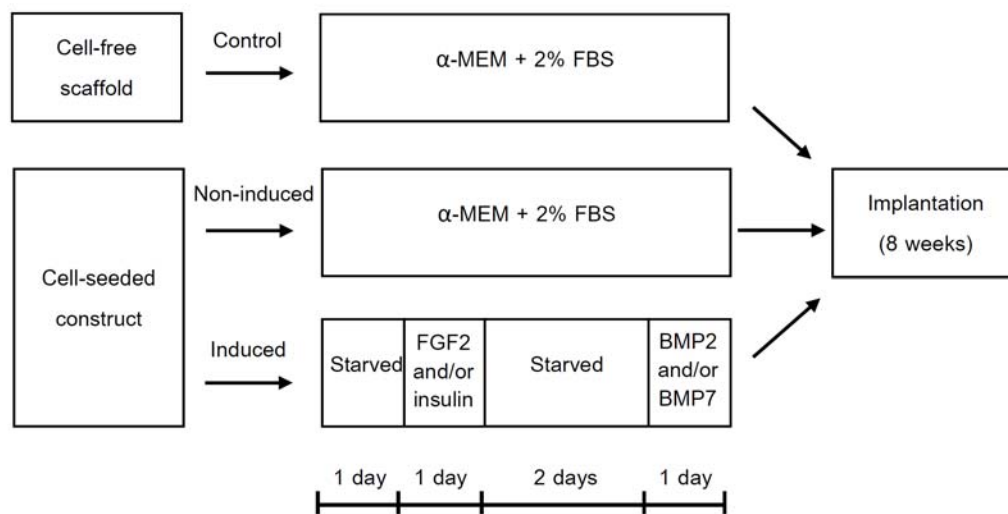


Figure 2.11: Procedures for preparing cell-seeded scaffold implants. The implants were divided into 3 groups including cell-free scaffolds, non-induced cell-seeded scaffolds, and induced cell-seeded scaffolds. RBMSCs seeded on scaffolds were induced with 2.5 ng/ml FGF2, 60 ng/ml insulin, or FGF2 plus insulin for 1 day followed by starvation for 2 days and induction with 10 ng/ml BMP2, 10 ng/ml BMP7, or BMP2 plus BMP7 for 1 day. For non-induced cell group, the cells were cultured in α -MEM plus 2% FBS. The control were the scaffolds being incubated with medium plus 2% FBS during the induction. The prepared constructs were implanted on the back of the rat (Figure 2.12). Bone formation was observed at 8 weeks post-implantation.

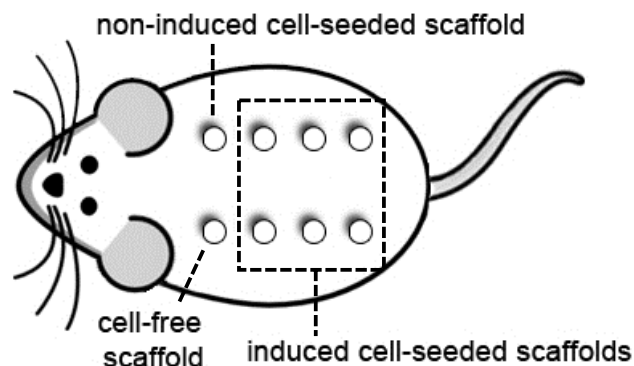


Figure 2.12: The schematic representation of the implantation sites. Eight constructs including one of cell-free scaffold, one of non-induced cell-seeded scaffolds, and six of induced cell-seeded scaffolds were subcutaneously implanted onto the dorsal part of Wistar rats.

2.3.5.3 Tissue processing

After 8 weeks post-implantation, the implants were removed and processed for histological analysis as follows. The implants were fixed by immersing in 4% Paraformaldehyde in DPBS for 24 hours. After several washes with distilled water, the fixed samples were decalcified in 10% formic acid (EDTA saturated) solution until soften, neutralized in 5% sodium sulfate solution for 24 hours, and embedded in paraffin block. The paraffin blocks were sectioned with thickness of 3-5 μM using microtome and placed on glass slide.

2.3.5.4 Histological staining

The tissue sections were dewaxed using xylene and ethanol series and rehydrated in distilled water before staining. The protocol for dewaxing was shown in Table 2.9. Two techniques of hematoxylin-eosin (H&E) and ARS staining were performed as generally noted [136]. The overall tissue morphology was revealed by H&E staining. The nucleus of the cells were stained by hematoxylin in which the color was purple-blue. The cytoplasm was colored by eosin as bright pink color. Since ARS

is specific for calcium deposit in tissues, ARS staining was used to identify the site of mineralization resulting in orange-red color.

Table 2.9: Protocols for deparaffinization of tissue sections.

Reagents	Incubation time (minutes)
Xylene I	3
Xylene II	3
Absolute ethanol I	3
Absolute ethanol II	3
95% ethanol	3
70 % ethanol	3
Distilled water	5

2.3.5.4.1 Hematoxylin and eosin (H&E) staining

The rehydrated section was incubated in Mayer's hematoxylin solution (1 g/L, Sigma-Aldrich) for 8 minutes, washed with running water for 10 minutes, and dipped in 95% ethanol. The sample was then stained with eosin solution (0.5% (w/v) in water, Sigma-Aldrich) for 30 seconds to 1 minute. After washing in 95% ethanol and absolute ethanol for 5 minutes, the slide was soaked in xylene and left for air dry. The resulting sample was inspected under a light microscope. Tissue images were acquired by Cell P Software (Olympus).

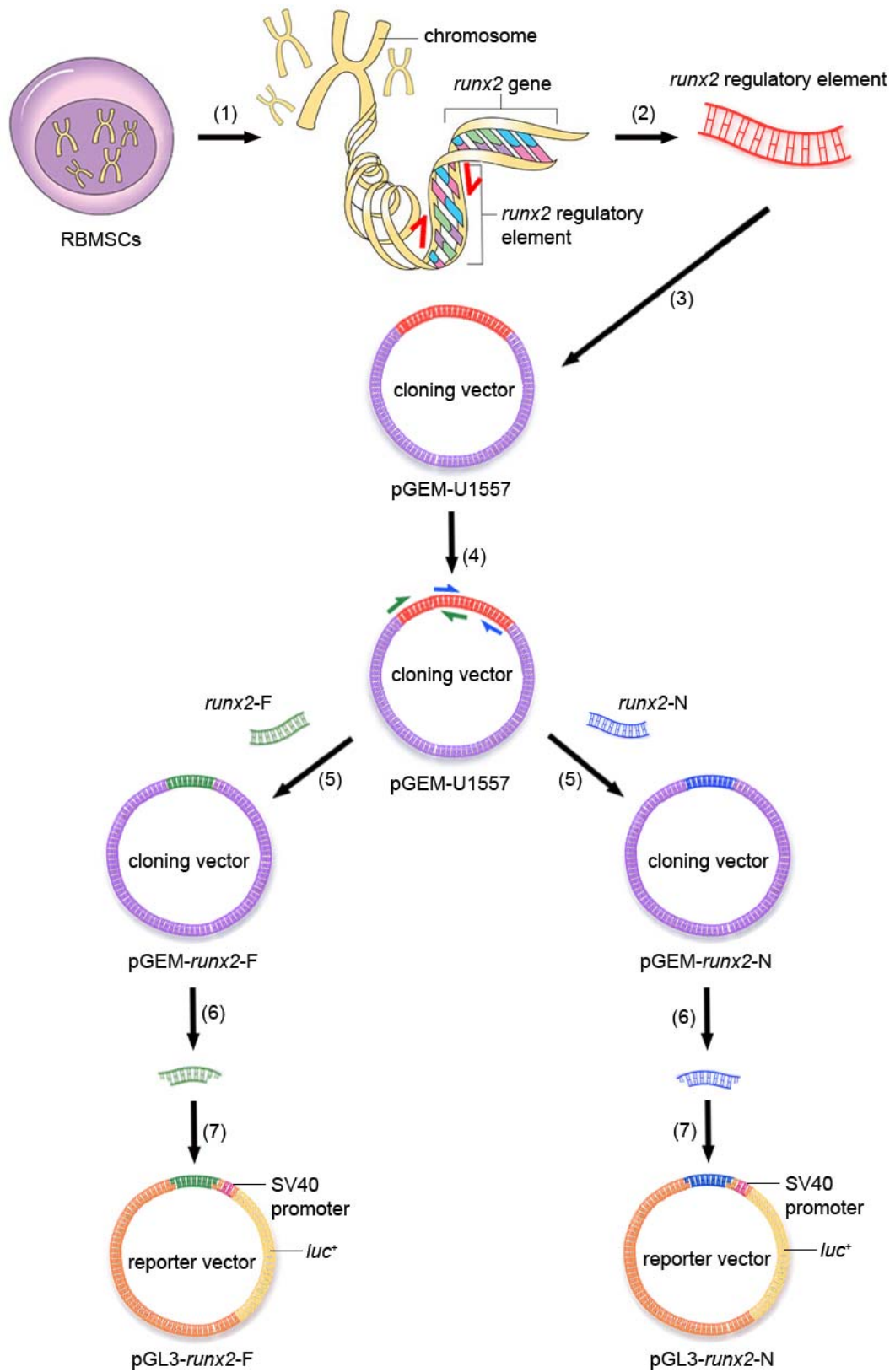
2.3.5.4.2 Alizarin Red S (ARS) Staining

The rehydrated sample was immersed in 2% w/v ARS solution (pH 4.1) for 30 seconds to 5 minutes. Excess dye was removed by dipping the slides in acetone. The section was then dehydrated in xylene and left for air

dry. The prepared sample was checked microscopically under a light microscope. Tissue images were acquired by Cell P Software (Olympus).

2.3.6 Plasmid construction

To support the results acquired from *in vitro* and *in vivo* experiments, cellular cascade induced by FGF2 and insulin affecting on osteogenic differentiation was investigated. The technology of luciferase reporter assay was used to study gene regulation and intracellular signaling pathways that may involve. Since Runx2 acts as a molecular hub among pathways, the study was aimed to explore the influence of these growth factors on *runx2* expression as follows. Firstly, the regulatory element of *runx2* gene at 5'-untranslate region (5'-UTR) was cloned into *KpnI* and *NheI* restriction sites of the luciferase reporter vector (Figure 2.13). Secondly, the potential transcription factor binding sites on *runx2* promoter were synthesized and introduced into *KpnI* and *BglII* restriction sites of the reporter vector. These response elements were identified by analysis of the obtained 5'-UTR sequence using a transcription factor binding site search tool. The constructed reporter vectors were then transfected into RBMSCs. After the induction, the expression of luciferase reporter gene was measured.



Note: The figure legend is on page 62.

Figure 2.13: The construction procedures of luciferase reporter vectors. (1) The chromosome of RBMSCs was extracted; (2) the regulatory element of *runx2* gene was amplified using RBMSCs chromosome as a template in which the specific primers of 5'-UTR of *runx2* were shown in red color; (3) the purified PCR product (U1557) was ligated into pGEM-T[®] easy vector (Figure 2.1), resulting in pGEM-U1557 cloning vector. The sequence of the inserted DNA was verified by DNA sequencing technique; (4) to construct the reporter vectors, *runx2* element was prepared into two consecutive fragments, *runx2*-F and *runx2*-N. The specific primers for *runx2*-F and *runx2*-N were represented in green and blue color, respectively; (5) PCR amplicon of each fragments was inserted into pGEM-T[®] easy vector, resulting in pGEM-*runx2*-F and pGEM-*runx2*-N cloning vector, respectively. The inserted DNA was (6) digested with *Kpn*I and *Bgl*II from the cloning vector and then ligated into pGL3-promoter vector that contains SV40 promoter *luc*⁺ transcription unit (7). The pGL3-*runx2*-N and pGL3-*runx2*-F vectors were subjected to sequencing analysis and used for transfection experiment.

2.3.6.1 Cloning of the 5'-UTR of *runx2* gene into pGEM[®]-T easy vector

The 5'-UTR was amplified by polymerase chain reaction (PCR) using RBMSCs chromosome as a template. The expected product called U1557 with a size of 1.7 kilobase pair (kb) was inserted into pGEM[®]-T easy vector. The recombinant plasmid (called pGEM-U1557) was multiplied and sequenced. Various molecular techniques, including agarose gel electrophoresis, DNA purification, ligation, transformation, and plasmid extraction and digestion with restriction enzyme, had been performed for constructing the pGEM-U1557 cloning vector (Figure 2.14).

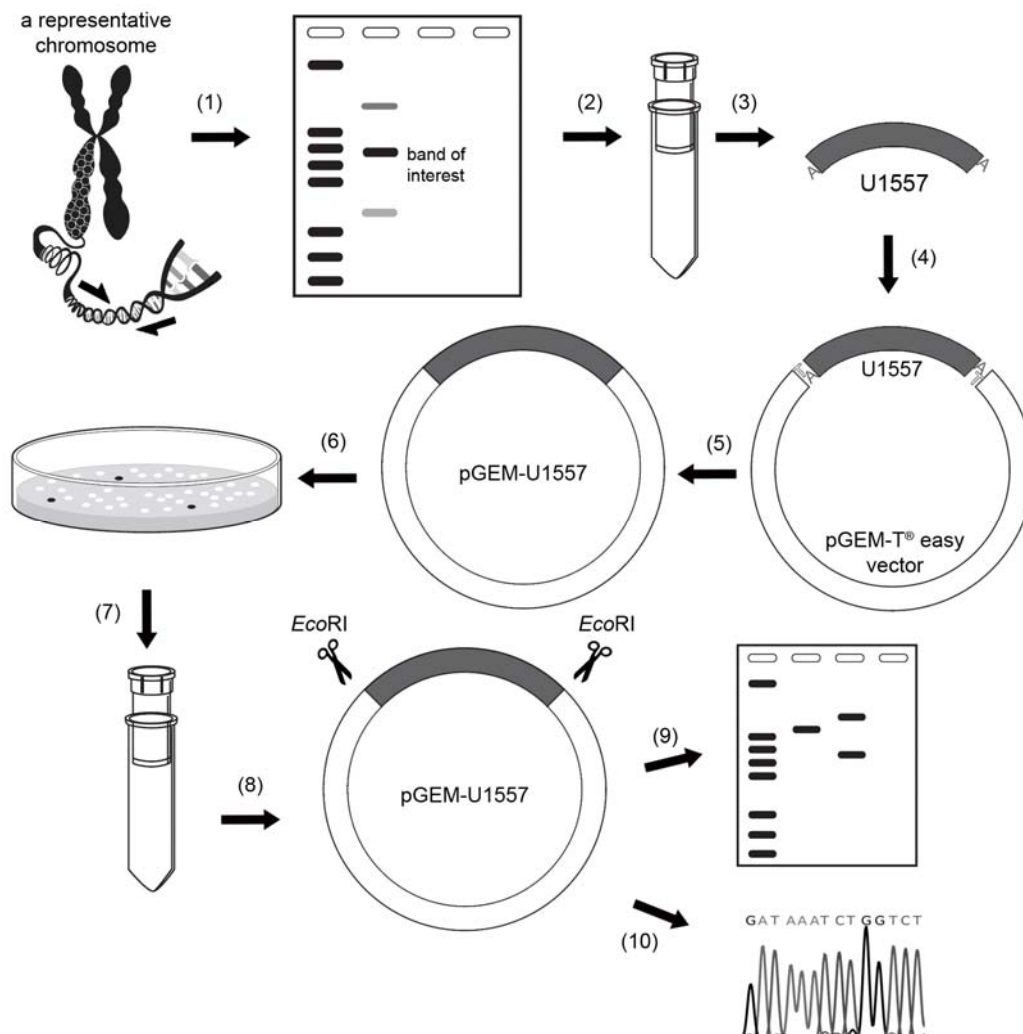


Figure 2.14: Construction of pGEM-U1557 recombinant vector. (1) 5'-UTR of *runx2* gene was amplified from RBMSCs chromosome. (2) The PCR products were separated on 0.7% agarose gel. (3) The selected band (called U1557) was purified using Nucleospin[®] extract II column and (4-5) ligated into pGEM-T[®] easy vector. The recombinant plasmid (called pGEM-U1557) was (6) transformed into *E. coli* strain DH5 α . (7) White colonies were selected, and (8) extracted for the recombinant plasmid by using Nucleospin[®] plasmid column. (9) The extracted DNA was digested with *Eco*RI and examined for the inserted DNA by agarose gel electrophoresis. (10) Sequence of the insert was determined by DNA sequencing technique.

2.3.6.1.1 Chromosome extraction

The genomic DNA of RBMSCs (passage 4) was extracted by phase separation technique (Figure 2.13, step 1). The cells were grown in α -MEM supplemented with 10% FBS until 90% confluence. The monolayer cells were trypsinized and collected by centrifugation at 700xg for 5 minutes. The cell pellet was digested in buffer containing 100 mM NaCl, 10 mM Tris-Cl (pH 8), 25 mM EDTA (pH 8), 0.5% SDS, and 0.1 mg/ml proteinase K (1 ml of digestion buffer per T-75 flask) at 50°C with gentle agitation for 15-17 hours. The cell homogenate was extensively mixed with an equal volume of phenol/chloroform/isoamyl alcohol solution. After centrifugation at 1700xg for 10 minutes, aqueous layer was collected. Two volume of absolute ethanol and half volume of 7.5 M ammonium acetate (calculated from the original amount of top layer) were added to precipitate the chromosome, and collected by centrifugation at 1700xg for 5 minutes. After washing with 70% ethanol, the precipitated DNA was left for air-dry and redissolved in DNase/RNase free water. Genomic DNA was preserved at 4°C until use.

2.3.6.1.2 Polymerase chain reaction (PCR)

PCR is used to generate a specific DNA fragment. The reaction required a DNA template and site-specific primers complementing to the corresponding end of the fragment. The components of PCR reaction were listed in Table 2.10. To amplify the 5'-UTR of *runx2*, the extracted chromosome was used as a template (Figure 2.14, step 1). *Runx2*-U1557 and *runx2*-97 (Table 2.2) were used as forward and reverse primers, respectively. Thermal cycle was indicated in Table 2.11. The PCR product was separated on 0.7% agarose gel electrophoresis (Figure 2.14, step 2). The band of interest with a sized of 1.7 kb (called U1557) was then purified by using gel purification technique.

Table 2.10: The components for PCR reaction.

Components	Volume	Final concentration
MgCl ₂ free PCR Buffer (10x)	5 µl	1x
MgCl ₂ (50 mM)	2.5 µl	2.5 mM
dNTP mix (10 mM)	2.5 µl	0.5 mM
<i>runx2</i> -U1557 (forward primer; 10 µM)	3 µl	0.6 µM
<i>runx2</i> -97 (reverse primer; 10 µM)	3 µl	0.6 µM
Tag DNA polymerase (5 U/µl)	0.5 µl	0.05 U/µl
DNA template (2.5 µg/µl)	2 µl	0.1 µg/µl
DNAse/RNAse free water	31.5 µl	-
Total volume	50 µl	

Table 2.11: Thermal cycle for 5'-UTR of *runx2* gene cloning.

Step	Temperature	Time	Number of cycles
Initial denaturation	95°C	5 minutes	1 cycle
Denaturation	95°C	30 seconds	} 35 cycles
Annealing	57.5°C	30 seconds	
Extension	72°C	90 seconds	
Final extension	72°C	10 minutes	1 cycle
Hold	4°C	∞	

2.3.6.1.3 Agarose gel electrophoresis

Agarose gel electrophoresis was used to separate DNA based on sizes. The concentrations of the gel were according to Table 2.12. Running buffer was Tris Acetate EDTA (TAE) buffer (40 mM Tris, 20 mM acetic acid, and 1 mM EDTA). To prepare electrophoresis sample, 1 μ l of Novel Juice (6X Loading Buffer) was combined with 5 μ l of DNA sample. Electrophoresis was performed at 90-100 mA at room temperature. DNA marker (0.5-1 μ g/lane) was run in parallel. The separated DNA bands were photographed using UV transilluminator equipped with a digital camera (Kodak EasyShare P880).

Table 2.12: The concentration of agarose gel based on size of linear DNA to be separated.

% agarose gel	Optimum resolution for linear DNA
0.5	1,000–30,000 bp
0.7	800–12,000 bp
1.0	500–10,000 bp
1.2	400–7,000 bp
1.5	200–3,000 bp
2.0	50–2,000 bp

2.3.6.1.4 DNA extraction from agarose gel

A specific band on agarose gel (at 1.7 kb) was excised and extracted from the gel (Figure 2.14, step 3) by using NucleoSpin[®] extract II (Macherey-Nagel) as followed. The band was dissolved in buffer NT (200 μ l for 100 mg of gel) at 50°C, loaded into the NucleoSpin[®] extract II column, and centrifuged at 11,000xg for 1 minute. Bound DNA was washed with 700 μ l of wash buffer (buffer NT3)

and eluted with DNase/RNase free water. The purified DNA called U1557 was verified by agarose gel electrophoresis and kept at -20°C until use.

2.3.6.1.5 Ligation

Ligation between the prepared DNA fragment (U1557) and the pGEM-T[®] easy vector was achieved by using T4 DNA ligase enzyme. The components of ligation reaction were shown in Table 2.13, and carried out at 4°C overnight (Figure 2.14, step 4-5).

Table 2.13: The components for ligation reaction.

Components	Volume	Final concentration
Ligation buffer (10x)	1 µl	1x
T4 DNA ligase (20 U/µl)	1 µl	2 U/µl
Vector (50 ng/µl)	0.5 µl	2.5 ng/µl
Purified insert DNA (0.5 µg/µl)	2 µl	0.1 µg/µl
DNase/RNase free water	5.5 µl	-
Total volume	10 µl	

2.3.6.1.6 Transformation

Transformation of the recombinant plasmid into HIT Competent Cells[™] *E. coli* strain DH5 α (RBC Bioscience Corp.) was performed according to the manufacturer's protocol. The frozen bacterial cells were thawed, and the ligation mixture with a volume of less than 10% of the cell volume was added. The mixed DNA-cell was vortexed for 1 second and incubated on ice for 1-10 minutes. Finally, the mixture was spread on LB agar (containing 0.8 mg X-gal, 0.8 mg IPTG, and 100 µg/ml ampicillin) and incubated at 37°C for 15-17 hours (Figure 2.14, step 6). The

positive clone of recombinant pGEM-T[®] easy vector was selected by blue/white colony screening based on an interruption of *β-galactosidase* gene by the DNA insert. The recombinant plasmid failed to express this gene and could not form blue colonies on X-gal agar plate.

2.3.6.1.7 Plasmid extraction

White colonies were selected and separately grown in LB liquid medium containing 100 µg/ml ampicillin at 37°C for 15-17 hours (Figure 2.14, step 7). Recombinant plasmid namely pGEM-U1557 was extracted (Figure 2.14, step 8) from transformed *E. coli* using NucleoSpin[®] Plasmid (Macherey-Nagel) as followed. Bacterial cells from 5 ml of saturated *E. coli* culture were collected. The cell pellet was resuspended in 250 µl buffer A1 (containing RNase), lysed in 250 µl buffer A2 by upturning the tube 6-8 times, incubated for 5 minutes, and neutralized with 300 µl buffer A3. The mixture was thoroughly mixed by flipping the tube 6-8 times and centrifuged at 11,000xg for 2 minutes. Clear lysate was loaded into DNA binding column, washed with 600 µl buffer A4, and eluted with DNase/RNase free water. The purified plasmid was verified by agarose gel electrophoresis and kept at -20°C until use.

2.3.6.1.8 Digestion with specified restriction enzyme

Digestion with restriction enzyme was used for screening of the recombinant plasmid and was carried out to generate compatible ends, able to be ligated into a selected plasmid. Components and conditions for a desired enzyme were explained in Table 2.14 and 2.15.

Table 2.14: Components and conditions for *KpnI*, *BglII*, *NheI*, and *EcoRI* digestion.

Components	<i>KpnI</i> reaction	<i>BglII</i> reaction	<i>NheI</i> reaction	<i>EcoRI</i> reaction	Final concentration
NEBuffer (10x)	1 μ l (Buffer 1)	1 μ l (Buffer 3)	1 μ l (Buffer 1)	1 μ l (<i>EcoRI</i> Buffer)	1x
BSA (10 mg/ml)			1 μ l		1 mg/ml
Enzyme (10 U/ μ l)			1 μ l		1 U/ μ l
Plasmid (0.5 μ g/ μ l)			1 μ l		50 ng/ μ l
DNAse/RNAse free water			6 μ l		-
Total volume			10 μ l		
Incubation temperature	37°C	37°C	37°C	37°C	
Incubation time	6-8 hours	6-8 hours	6-8 hours	overnight	

Table 2.15: Components and conditions for *KpnI* and *NheI* double digestion.

Components	<i>KpnI</i> and <i>NheI</i> reaction	Final concentration
NEBuffer 1 (10x)	1 μ l	1x
BSA (10 mg/ml)	1 μ l	1 mg/ml
<i>KpnI</i> (10 U/ μ l)	0.5 μ l	0.5 U/ μ l
<i>NheI</i> (10 U/ μ l)	0.5 μ l	0.5 U/ μ l
Plasmid (0.5 μ g/ μ l)	1 μ l	50 ng/ μ l
DNAse/RNAse free water	6 μ l	-
Total volume	10 μ l	
Incubation temperature	37°C	
Incubation time	6-8 hours	

2.3.6.1.9 DNA sequencing

The sequences of all constructed plasmid were verified by ABI3730XL Platform using specific primers shown in Table 2.1. Electropherograms were analyzed by Sequencing Analysis Software (BioEdit version 7.0.8.0 and FinchTV version 1.4). The sequence of U1557 was aligned with those deposited in NCBI database using Clustal Omega, a Multiple Sequence Alignment tool.

2.3.6.2 Construction of pGL3-*runx2*-N and pGL3-*runx2*-F reporter vector

One of the gene regulation mechanism is the control of gene transcription by enhancer or repressor molecules. These regulatory proteins usually bind their specific DNA sequence located at upstream or downstream region of the promoter. In this study, the mechanism of *runx2* regulation through the upstream regulatory element of the gene was performed using luciferase reporter gene assay. By

constructing the DNA fragment of interest into the upstream of luciferase gene, the reporter vector was able to evaluate the influence of the insert DNA on reporter gene expression.

To investigate the influence of FGF2 and insulin on *runx2* expression, 5'-UTR of *runx2* (U1557) was the DNA of interest for constructing the reporter vector. Because the expression of *runx2* has been shown to be regulated by several factors [26, 88], it was hypothesized that a shorter sequence of U1557 would provide more precise mechanism in controlling the gene regulation. Moreover, the length of PCR products has been limited by fidelity. Therefore, the U1557 sequence was divided into two consecutive fragments for easier amplification and improving fidelity. Two halves of the *runx2* regulatory element, called *runx2-N* and *runx2-F*, were generated by PCR technique (Figure 2.13, step 4), and each fragment was separately cloned into the reporter vector. The cloning vectors containing these DNA were created before the DNA inserts were subcloned into the reporter vectors (Figure 2.13, step 5 to 7). Then, the recombinant plasmids were proven by sequencing and utilized as the reporter vectors for gene regulation analysis.

2.3.6.2.1 Cloning of *runx2-N* and *runx2-F* into pGEM[®]-T easy vector

pGEM-U1557 was used as a template for amplification of *runx2-N* and *runx2-F*. The primers were designed to have the restriction site for *KpnI* or *NheI* digestion (Table 2.2). PCR components and condition were described in Table 2.16 to 2.19. The PCR products were separated on 0.7% agarose gel. The obtained DNA at 723 bp (*runx2-N*) and 896 bp (*runx2-F*) were purified by using NucleoSpin[®] extract II. The purified *runx2-N* and *runx2-F* were ligated with pGEM-T[®] easy vector resulting in pGEM-*runx2-N* and pGEM-*runx2-F* cloning vector. The recombinant plasmids were separately propagated in *E. coli* strain DH5 α , extracted from bacterial culture by using NucleoSpin[®] plasmid, and verified by *KpnI* and *NheI* digestion (Figure 2.15).

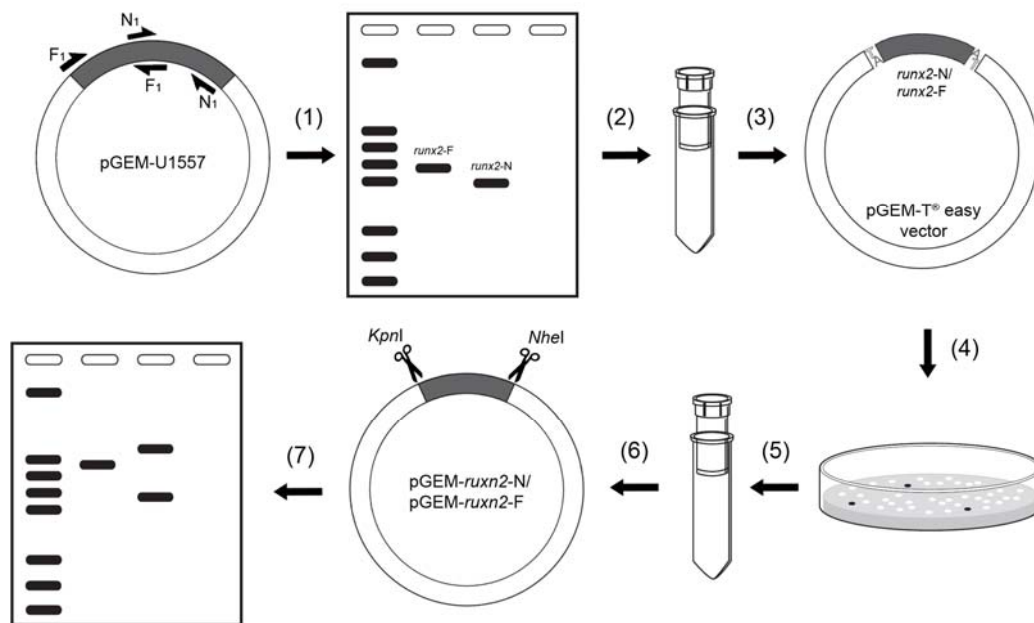


Figure 2.15: Construction of pGEM-*runx2-N* and pGEM-*runx2-F* cloning vector. The fragments of *runx2* regulatory element, *runx2-F* and *runx2-N*, were amplified using pGEM-U1557 as a template. The specific primers for each fragment were labeled as F₁ and N₁. These primers were designed to contain the restriction site for *KpnI* or *NheI* digestion. The PCR product was (1) separated on agarose gel, and (2) the specific bands were purified by Nucleospin® extract II column. (3) The PCR products were ligated with pGEM-T® easy cloning vector and (4) transformed into *E. coli* strain DH5α. (5-6) The recombinant plasmids were extracted from bacterial culture of the selected white colony and (7) examined by *KpnI* and *NheI* digestion.

Table 2.16: PCR components for *runx2*-N amplification.

Components	Volume	Final concentration
MgCl ₂ free PCR Buffer (10x)	5 µl	1x
MgCl ₂ (50 mM)	1.5 µl	1.5 mM
dNTP mix (10 mM)	2.5 µl	0.5 mM
<i>runx2</i> -KPNI-U796 (forward primer; 10 µM)	3 µl	0.6 µM
<i>runx2</i> -NHEI-U73 (reverse primer; 10 µM)	3 µl	0.6 µM
Tag DNA polymerase (5 U/µl)	0.5 µl	0.05 U/µl
pGEM-U1557 (0.5 µg/µl)	2 µl	20 ng/µl
DNAse/RNAse free water	32.5 µl	-
Total volume	50 µl	

Table 2.17: Thermal cycle for *runx2*-N amplification.

Step	Temperature	Time	Number of cycles
Initial denaturation	94°C	5 minutes	1 cycle
Denaturation	94°C	30 seconds	} 35 cycles
Annealing	64°C	30 seconds	
Extension	72°C	40 seconds	
Final extension	72°C	10 minutes	1 cycle
Hold	4°C	∞	

Table 2.18: PCR components for *runx2*-F amplification.

Components	Volume	Final concentration
MgCl ₂ free PCR Buffer (10x)	5 µl	1x
MgCl ₂ (50 mM)	1.5 µl	1.5 mM
dNTP mix (10 mM)	2.5 µl	0.5 mM
<i>runx2</i> -KPNI-U1526 (forward primer; 10 µM)	3 µl	0.6 µM
<i>runx2</i> -NHEI-U630 (reverse primer; 10 µM)	3 µl	0.6 µM
Tag DNA polymerase (5 U/µl)	0.5 µl	0.05 U/µl
pGEM-U1557 (0.5 µg/µl)	2 µl	20 ng/µl
DNase/RNase free water	32.5 µl	-
Total volume	50 µl	

Table 2.19: Thermal cycle for *runx2*-N amplification.

Step	Temperature	Time	Number of cycles
Initial denaturation	94°C	5 minutes	1 cycle
Denaturation	94°C	30 seconds	} 35 cycles
Annealing	58°C	30 seconds	
Extension	72°C	45 seconds	
Final extension	72°C	10 minutes	1 cycle
Hold	4°C	∞	

2.3.6.2.2 Subcloning of *runx2-N* and *runx2-F* into pGL3-Promoter vector.

runx2-N and *runx2-F* were subcloned into pGL3-Promoter vector (Figure 2.16). These fragments were isolated from pGEM-*runx2-N* and pGEM-*runx2-F* by *KpnI* and *NheI* digestion and gel electrophoresis. The digested DNA was then purified from agarose gel by using NucleoSpin[®] extract II. The obtained *runx2-N* and *runx2-F* were ligated with pGL3-Promoter vector and transformed into *E. coli* strain DH5 α . The recombinant plasmids called pGL3-*runx2-N* and pGL3-*runx2-F* were multiplied and inspected for the DNA insert by *KpnI* and *NheI* digestion and by PCR technique using specific primers (LUC-F and LUC-R). The obtained PCR product at 800-900 bp was verified by agarose gel electrophoresis. The components and condition of PCR analysis was shown in Table 2.20 and 2.21.

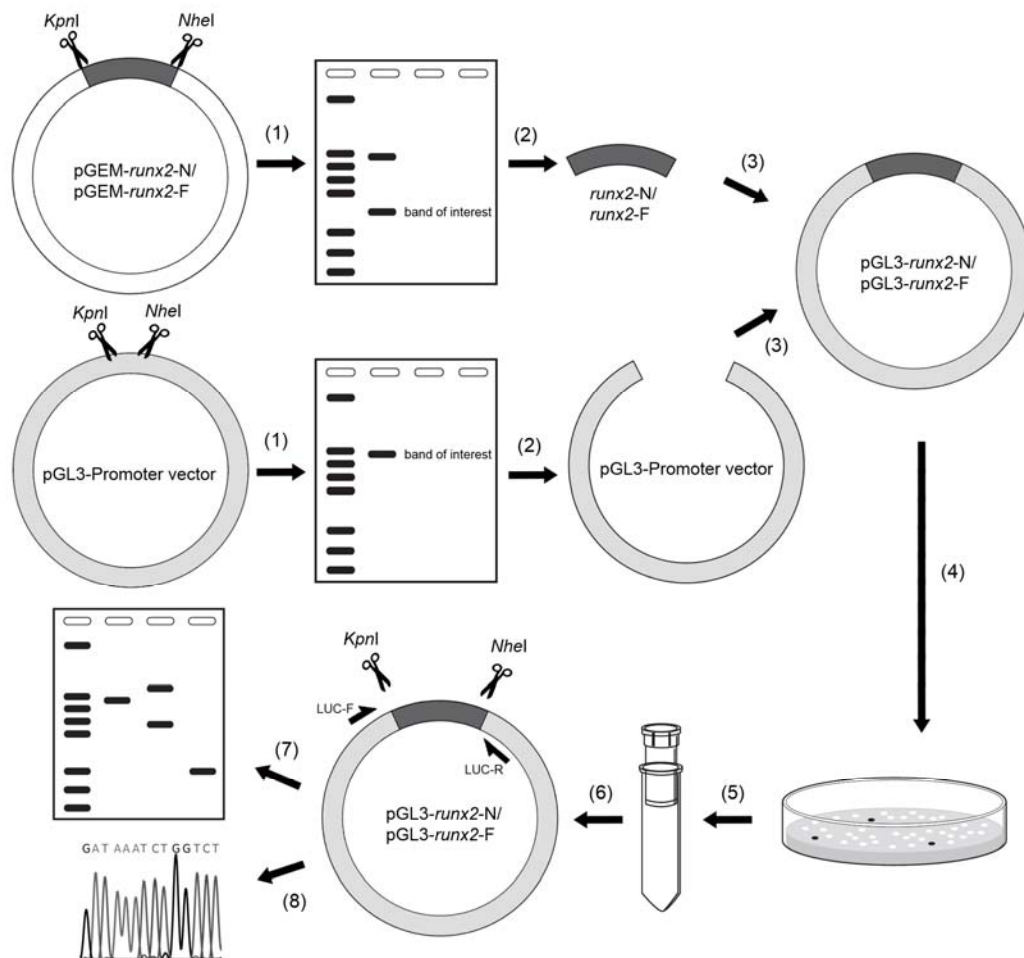


Figure 2.16: Subcloning protocol for pGL3-runx2-N and pGL3-runx2-F vector construction. (1) pGEM-runx2-N plasmid, pGEM-runx2-F plasmid, and pGL3-Promoter vector were separately digested with *KpnI* and *NheI*. (2) The desired bands on agarose gel were extracted. The digested pGL3-Promoter vector and the purified runx2-N and runx2-F fragments were (3) ligated and (4) transformed into *E. coli* strain DH5 α . (5) The positive clones were selected and (6) extracted for the recombinant plasmid which were then double digested with *KpnI* and *NheI*. (7) Products determined by using LUC-F and LUC-R primers were examined on 0.7% agarose gel electrophoresis. (8) The recombinant plasmids were subjected to DNA sequencing.

Table 2.20: PCR components for pGL3-*runx2*-N and pGL3-*runx2*-F vector verification.

Components	Volume	Final concentration
MgCl ₂ free PCR Buffer (10x)	5 μ l	1x
MgCl ₂ (50 mM)	1.5 μ l	1.5 mM
dNTP mix (10 mM)	2.5 μ l	0.5 mM
LUC-F (forward primer; 10 μ M)	3 μ l	0.6 μ M
LUC-R (reverse primer; 10 μ M)	3 μ l	0.6 μ M
Tag DNA polymerase (5 U/ μ l)	0.5 μ l	0.05 U/ μ l
Plasmid DNA template (0.5 μ g/ μ l)	2 μ l	20 ng/ μ l
DNase/RNase free water	31.5 μ l	-
Total volume	50 μ l	

Table 2.21: Thermal cycle for pGL3-*runx2*-N and pGL3-*runx2*-F vector verification.

Step	Temperature	Time	Number of cycles
Initial denaturation	94°C	5 minutes	1 cycle
Denaturation	94°C	30 seconds	} 35 cycles
Annealing	57°C	30 seconds	
Extension	72°C	30 seconds	
Final extension	72°C	10 minutes	1 cycle
Hold	4°C	∞	

2.3.6.3 Construction of plasmids containing tandem repeats of transcription factor binding site

This experiment was aimed to study the specific targets of FGF2 and insulin signaling cascade on *runx2* promoter. The DNA binding sites of the particular transcription factors on U1557 sequence were identified, and the selected response elements were commercially synthesized as five tandem repeats. These oligonucleotides were ligated with reporter vector which the recombinant reporter plasmids were used for studying the signaling pathway in the cells. It was proposed that the growth factors were able to activate the cells through the elements of interest which the repetitive binding site intensified the reporter gene expression.

2.3.6.3.1 Transcription factor binding site

Transcription factor is a protein that controls the gene transcription. It recognizes a specific sequence on DNA called a consensus sequence. In this study, the possible transcription factor binding sites on the obtained *runx2* promoter (U1557) were characterized by using the TFSEARCH database, a consensus binding site of transcription factor search tool [137]. The remarkable consensus sequences with the threshold score above 90.0 were selected concerning on the regulation of bone formation. Among these *ap1* and *sry* were chosen. Sense or coding strand and its complementary or antisense strands of five tandem repeats of *ap1* and *sry* consensus binding site were commercially synthesized (called 5X*ap1* and 5X*sry*, respectively). A strand of oligonucleotide was designed to contain 5'-*KpnI* and 3'-*BglII* restriction sites, both were the overhang ends (Table 2.3).

2.3.6.3.2 Preparation of double stranded oligonucleotides

Sense and antisense strands of 5X*ap1* and 5X*sry* binding site (Table 2.3) were mixed in buffer containing 50 mM NaCl, 10 mM Tris, and 1 mM EDTA (pH 8.0) and incubated at above 95°C for 5 minute. The heat-treated

mixture was gradually cooled to room temperature (more than 1 hour) in which annealing of two complementary strands could occur. The reaction components were described in Table 2.22.

Table 2.22: The components for oligonucleotide annealing reaction.

Components	Volume	Final concentration
Annealing buffer (10x)	2 μ l	1X
Sense strand (100 μ M)	15 μ l	75 μ M
Antisense strand (100 μ M)	3 μ l	15 μ M
Total volume	20 μ l	-

2.3.6.3.3 Preparation of reporter vector

According to Figure 2.17, pGL3-Promoter vector was digested with *Kpn*I and *Bgl*II (Table 2.14), purified by gel purification column, and ligated with 5Xap1 or 5Xsry at 4°C overnight. The recombinant plasmids were separately transformed into *E. coli* strain DH5 α and cultured on LB agar plate containing ampicillin at 37°C for 16 hours. The positive clones were selected and further expanded for plasmid extraction. The recombinant plasmids were verified by PCR (Table 2.23 to 2.26), agarose gel electrophoresis, and DNA sequencing, resulting in pGL3-5Xap1 and pGL3-5Xsry.

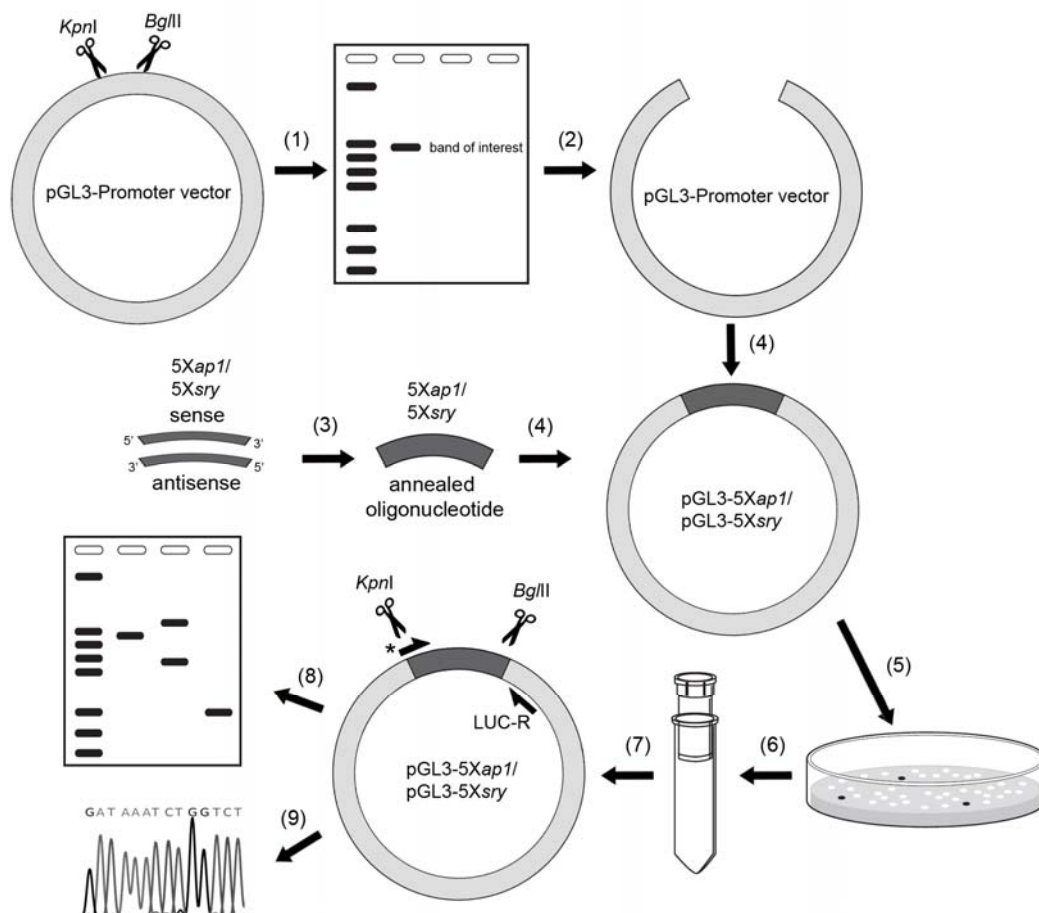


Figure 2.17: Preparation of pGL3-5Xap1 and pGL3-5Xsry reporter vector. (1-2) The pGL3-Promoter vector was digested with *KpnI* and *BglII*, separated, and purified by Nucleospin[®] extract II column. (3) 5Xap1 and 5Xsry sense and antisense strand were annealed to generate the double-stranded inserts and (4) ligated with pGL3-Promoter vector. (5) The plasmids were transformed into *E. coli* strain DH5 α . (6-7) The recombinant plasmids were extracted from the selected colonies. The isolated pGL3-5Xap1 and pGL3-5Xsry were proved by *KpnI* and *BglII* digestion and PCR analysis using LUC-F and specific primer* (ap1-LUC or sry-LUC) as forward primer and reverse primer, respectively. (8) The digestion and PCR reaction were inspected on 0.7% agarose gel electrophoresis. (9) The proven plasmids were subjected to DNA sequencing.

Table 2.23: The components used for proving the success in cloning of pGL3-5Xap1.

Components	Volume	Final concentration
MgCl ₂ free PCR Buffer (10x)	5 µl	1x
MgCl ₂ (50 mM)	1.5 µl	1.5 mM
dNTP mix (10 mM)	2.5 µl	0.5 mM
LUC-F (forward primer; 10 µM)	3 µl	0.6 µM
ap1-LUC (reverse primer; 10 µM)	3 µl	0.6 µM
Tag DNA polymerase (5 U/µl)	0.5 µl	0.05 U/µl
pGL3-5Xap1 (0.5 µg/µl)	2 µl	20 ng/µl
DNAse/RNAse free water	31.5 µl	-
Total volume	50 µl	

Table 2.24: Thermal cycle used for proving the success in cloning of pGL3-5Xap1.

Step	Temperature	Time	Number of cycles
Initial denaturation	94°C	5 minutes	1 cycle
Denaturation	94°C	25 seconds	} 35 cycles
Annealing	50°C	25 seconds	
Extension	72°C	25 seconds	
Final extension	72°C	7 minutes	1 cycle
Hold	4°C	∞	

Table 2.25: The components used for proving the success in cloning of pGL3-5Xsry.

Components	Volume	Final concentration
MgCl ₂ free PCR Buffer (10x)	5 µl	1x
MgCl ₂ (50 mM)	1.5 µl	1.5 mM
dNTP mix (10 mM)	2.5 µl	0.5 mM
LUC-F (forward primer; 10 µM)	3 µl	0.6 µM
sry-LUC (reverse primer; 10 µM)	3 µl	0.6 µM
Tag DNA polymerase (5 U/µl)	0.5 µl	0.05 U/µl
pGL3-5Xsry (0.5 µg/µl)	2 µl	20 ng/µl
DNAse/RNAse free water	31.5 µl	-
Total volume	50 µl	

Table 2.26: Thermal cycle used for proving the success in cloning of pGL3-5Xsry.

Step	Temperature	Time	Number of cycles
Initial denaturation	94°C	5 minutes	1 cycle
Denaturation	94°C	25 seconds	} 35 cycles
Annealing	48°C	25 seconds	
Extension	72°C	25 seconds	
Final extension	72°C	7 minutes	1 cycle
Hold	4°C	∞	

2.3.7 Dual luciferase reporter assay

Dual luciferase reporter assay is a system used for analysis of gene regulation at a transcriptional level. This system utilizes two types of vector including the experimental vector and the internal control vector. The experimental vector carries a firefly luciferase as a reporter gene, while the control vector contains a *Renilla* luciferase. The experimental vector is prepared by insertion of the DNA fragment of interest at the upstream of firefly luciferase gene in which the activity of firefly luciferase depends on the transcriptional potential of the inserted DNA fragment.

To investigate the effect of FGF2 and insulin on *runx2* gene regulation and their activation target on the gene promoter, two sets of the recombinant reporter plasmids namely pGL3-*runx2*-N and pGL3-*runx2*-F which utilized for the study of *runx2* regulation, and pGL3-5X*ap1* and pGL3-5X*sry* which used to specify the signaling cascade of the growth factor induction were separately transfected into RBMSCs. The cells were induced with 2.5 ng/ml FGF2, 60 ng/ml insulin, or FGF2 plus insulin for 1 day. The luciferase activity produced by the reporter vector was evaluated by dual luciferase reporter assay technique. The plasmids used in this study needed to be aplenty prepared, and the transfection needed to be optimized before starting the experiment.

2.3.7.1 Preparation of the reporter vectors for transfection

For transfection experiment, the reporter vectors including pGL3-Control vector, pGL3-Promoter vector, pGL3-*runx2*-N, pGL3-*runx2*-F, pGL3-5X*ap1*, pGL3-5X*sry*, and pRL-SV40 were isolated from its corresponding recombinant *E. coli* by using QIAGEN Plasmid Midi and Maxi Kits (QIAGEN) as followed. The bacteria was harvested from 50 ml culture by centrifugation at 6,000xg for 15 minutes at 4°C. The cells were resuspended in 4 ml of buffer P1 containing RNase, lysed in 4 ml of buffer P2, and neutralized in 4 ml of buffer P3. The mixture was combined immediately by robustly inverting 4-6 times, placed on ice for 15 minutes, and centrifuged at 20,000xg for 30 minutes at 4°C. Clear supernatant was filled into QIAGEN-tip in which the DNA

was captured by the resin. The column was rinsed twice using 10 ml of buffer QC to remove all contaminants. The bound plasmid was then eluted by using 5 ml of elution buffer (buffer QF). The eluted DNA was precipitated by adding 0.7 volumes of isopropanol and centrifuged immediately at 15,000xg, 15 minutes, 4°C. The precipitate was rinsed with 70% ethanol and centrifuged again at 15,000xg for 15 minutes at 4°C. The DNA was left for air-dry, and redissolved in a suitable volume of DNase/RNase free water. The purified DNA was examined on 0.7% agarose gel electrophoresis and kept at -20°C until use.

2.3.7.2 Plasmid concentration determination

The plasmid concentration was quantified by using Qubit™ dsDNA BR Assay Kits (Invitrogen) and performed on using Qubit® 2.0 Fluorometer (Invitrogen). After mixing 1-20 µl of sample with Qubit™ working solution to a final volume of 200 µl, the reaction was incubated at room temperature for 2 minutes. Then, the fluorescence signal was recorded, and the plasmid concentration was calculated.

2.3.7.3 Transfection optimization

Optimization for transfection conditions is critical for the reporter assay, as the luciferase signal is limited by the delivery method for DNA to mammalian cells which depends on several factors [138]. This experiment was aimed to balance between the maximal DNA uptake (which then express as much protein as possible) and the minimal impact on cell viability.

The condition for transfection was optimized using pGL3-Control vector as an experimental vector and pRL-SV40 vector as an internal control. The ratio of FuGENE® 6 transfection reagent to the experimental vector were varied from 3:1 to 6:1. The amounts of the experimental vector were of 0.2 µg or 0.4 µg, and the ratio of this vector to the control vector were of 50:1 and 200:1. The transfection efficiency was considered from firefly and *Renilla* luciferase activities and protein concentration of the

cell lysate which referred to viability. The most efficient condition was used for gene regulation analysis. The optimization conditions were described in Table 2.27.

Table 2.27: Optimization conditions for transfection.

Conditions	Ratio of transfection reagent and DNA (volume; μ l/weight; μ g)	Amount of DNA	Ratio of experimental vector and internal control
1	3:1	0.2 μ g	50:1
2			200:1
3		0.4 μ g	50:1
4			200:1
5	6:1	0.2 μ g	50:1
6			200:1
7		0.4 μ g	50:1
8			200:1
9	Non-transfection control		

2.3.7.4 Transfection

RBMSCs of passage 4 at a density of 60% confluence in 24-well plates were transfected by using FuGENE[®] 6 Transfection Reagent. As shown in Table 2.28, FuGENE[®] 6 was diluted in α -MEM (without serum) and incubated for 5 minutes at room temperature. The experimental vectors (including pGL3-*runx2*-N, pGL3-*runx2*-F, pGL3-5X*ap1*, pGL3-5X*sry*, and pRL-SV40) and control vector (pRL-SV40 vector) were added into the mixture and incubated for 15 minutes at room temperature. The complex was slowly dropped on to the cells cultured in a well and incubated for 4 hours in a CO₂ incubator. After that, the culture supernatant was removed and replaced by α -MEM supplemented with 2% FBS. After 24 hours of incubation, the cells were induced

with 2.5 ng/ml FGF2, 60 ng/ml insulin, or FGF2 plus insulin for 24 hours. The reporter assay was performed after 24 hours of incubation in 2% FBS medium (Figure 2.18).

Table 2.28: The components for transfection reactions. The ratio of transfection reagent to DNA was 6:1.

Components	Volume	Final concentration
Serum free medium	95.35 μ l	-
FuGENE [®] 6 reagent	2.4 μ l	-
Experimental vector (0.2 μ g/ μ l)	2 μ l	4 ng/ μ l
pRL-SV40 vector (8 ng/ μ l)	0.25 μ l	0.02 ng/ μ l
Total volume	100 μ l	

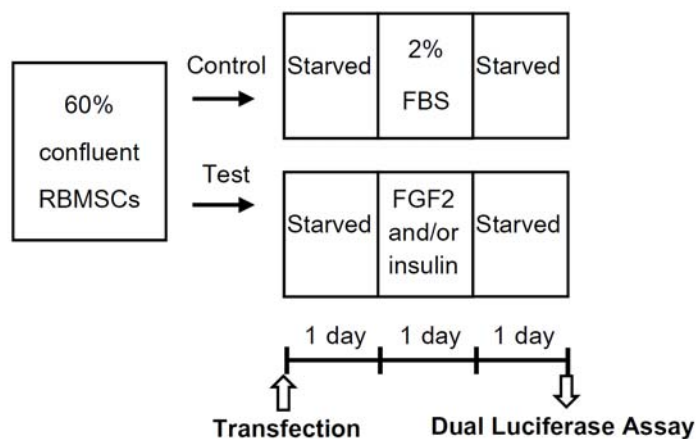


Figure 2.18: The plan of transfection experiment and luciferase assay. The cells were transfected with the experimental vectors (including pGL3-*runx2*-N, pGL3-*runx2*-F, pGL3-5X*ap1*, pGL3-5X*sry*, and pRL-SV40) and pRL-SV40 control vector and starved for 1 day post-transfection. The old medium was replaced by growth factor containing medium (2.5 ng/ml FGF2, 60 ng/ml insulin, or FGF2 plus insulin) for 1 day. After starvation for 1 day, the luciferase activity was measured.

2.3.7.5 Dual-luciferase measurement

Luciferase activity was quantified by using Dual-Luciferase[®] reporter assay kit (Promega) and performed on GloMax[®] 20/20 Luminometer (Promega). The luminescent signal of firefly luciferase was firstly determined followed by the signal of *Renilla* luciferase. Luciferin and coelenterazine were the substrate of firefly and *Renilla* luciferase, respectively (Figure 2.19). The cells were induced by FGF2 and insulin, by which related transcription factors were presumed to be activated and bound to the inserted DNA fragment on the reporter vector, resulting in increased luciferase production.

To measure the dual-luciferase activity, the cells were lysed in Passive Lysis Buffer (PLB) with gently rocking for 15 minutes at room temperature (200 μ l of PLB per well of 24-well plate). One hundred microliter of Luciferase Assay Reagent II was pre-dispensed into the reaction tubes and mixed with 20 μ l of PLB lysate by pipetting. The firefly luciferase activity of the experimental vector was recorded. Afterwards, 100 μ l of Stop & Glo[®] Reagent was added and mixed by vortexing. The *Renilla* luciferase activity was then measured. Data was reported as a ratio of firefly luciferase activity and *Renilla* luciferase activity. Statistical analysis was performed by using one-way ANOVA.

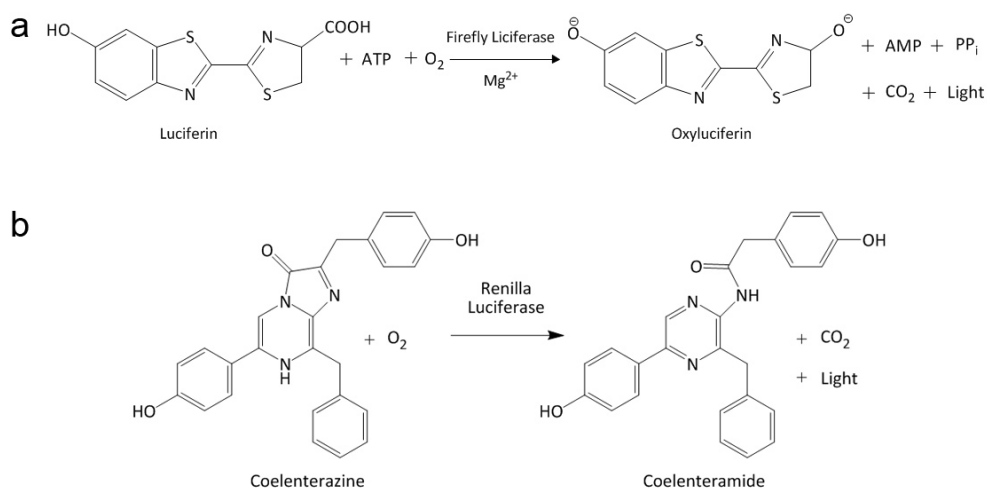


Figure 2.19: Bioluminescent reaction of firefly luciferase (a) and *Renilla* luciferase (b).

2.4 Equipment

Equipment	Model
Aspirator	Flask-trap Aspirator FTA-1, Biosan (Latvia)
Autoclave	SA-300VF-F-A500, Sturdy (Taiwan)
Balances	300A (max 350 g, min 0.01 g), Precisa (Switzerland); T-203 (max 200 g, min 0.001 g), Denver Instrument (Germany)
Centrifuge	Allerga [®] X-15R, Beckman Coulter (CA, USA); Z383K, Hermle (Germany); Universal 16R, Hettich Lab Technology (Germany); VS-15000N, Vision (Korea); Centrifuge CF-5, Daihan Scientific (Korea)
CO ₂ incubator	2323-2, Shel Lab (OR, USA); 3111, ThermoScientific (MA, USA)
DNA electrophoresis	i-MyRun, Cosmo Bio CO., LTD (Japan); MJ-105, Major Science (CA, USA)
DNA sequencer	Applied Biosystems 3730XL, Life Technologies Corporation (CA, USA)
Flowcytometer	BD FACSCalibur, BD Biosciences (CA, USA)
Fluorescent Microscope	BX61 Motorized System Microscope, Olympus (Japan)
Fluorometer	Qubit [®] Fluorometer, Life Technologies Corporation (CA, USA)
Hot air oven	Schutzart DIN 40050-IP20, Mommert (Germany)
Hot plate and stirrer	C-MAG HS7, IKA [®] (Malaysia)
Laminar air flow cabinet	Ultrasafe 48, Faster S.r.l (Italy); Aristream class II BSC, Esco Technologies, Inc (PA, USA)
Light Microscope	CK2, Olympus (Japan)
Luminometer	Glomax [™] 20/20 Luminometer, Promega (WI, USA)

Equipment	Model
Macropipette	Acura [®] Manual 835 1-10 ml, Socorex (Switzerland)
Micropipettes	Labnet: 0.1-2.5 μ l, and 0.5-10 μ l (NY, USA); Biohit: 0.5-10 μ l, 5-50 μ l, and 10-100 μ l (Finland); Pipet-Lite XLS 100-1,000 μ l, Rainin (OH, USA)
Microplate reader	DTX 880 Multimode Detector, Beckman Coulter (Austria)
Microwave oven	NN-NX21WX, Panasonic (Thailand)
Orbital shaker	Mini Shaker PSU-2T, Biosan (Latvia)
pH meter	Mettler Toledo (Switzerland)
Pipette Motorized Controller	PipetteBoy Pro, Integra (Switzerland); Pipet-aid, Drummond (PA, USA)
Power supply	EC 105 LVD, E-C Apparatus Corporation (CT, USA)
Real-time PCR Machine	MyiQ Single-color Real-time PCR Detection System, Bio-rad (CA, USA); LightCycler [®] Nano, Roche (Germany);
Refrigerator	Tiara (4°C and -20°C), Mitsubishi (Thailand); Low Temperature Freezer (-40°C), Haier (Thailand); SCL510 Scanlaf UTL Freezer (-80°C), Labogene (Denmark)
Shaker	Rocker platform, Bellco Biotechnology (NJ, USA)
Shaking incubator	VS-8480S, Vision Scientific CO., LTD (Korea)
Spectrophotometer	Diode Array Spectrophotometer 8452A, Hewlett Packard (CA, USA)
Thermal cycler	G-Strom GS00482, Gene Technology LTD (England)
UV transilluminator	TCX-26.M, Vilber Lourmat (France); Benchtop UV transilluminator M-15E, UVP (CA, USA) equipped with camera (Kodak EasyShare P880)
Vortex	Vortex-Genie 2 G-560E, Scientific Industries (NY, USA)

CHAPTER 3

RESULTS

3.1 Characterization of the isolated HBMSCs

3.1.1 Morphology

HBMSCs isolated from human bone marrow (passage 0) were apparent as fibroblast-like cells (Figure 3.1a). Their size was gradually increased up on culturing. The mononuclear cells adhered and reached confluence after 2 weeks. The cells in passage 2 to 3 were used for the induction experiment. Beyond the passage 5 of culturing, the cells took longer time periods to reach confluence, while changes in cell morphology was observed (Figure 3.1d).

Osteogenic differentiation was induced by the addition of 2.5 ng/ml FGF2 in DMEM/F12 for 24 hours followed by starvation with the medium supplemented with 2% FBS. Then, 10 ng/ml BMP2 was added into the medium for 24 hours before the induced cells were taken for use (Figure 2.7). The cells had more spindle-like morphology in FGF2 containing medium, whereas BMP2 might cause size enlargement of the cells. By the sequential induction, the cells produced extracellular matrix as could be determined under a microscope (Figure 3.1b and 3.1c).

3.1.2 Cell surface markers

To investigate specific characteristics of the isolated HBMSCs, surface antigens for the cells of passage 2 were identified using fluorochrome-labeled antibody against such the surface markers and analyzed by flow cytometry (Figure 3.2). As shown in Table 3.1, the majority of the cells in monolayer exhibited the surface antigen pattern of MSCs. These markers included CD13, CD29, CD44, CD73, and CD90, revealed by 76-100% of cell population. However, one of the hematopoietic cell

markers, such as CD45, was also detected. About 62% of the HBMSCs were CD45 positive. Other markers such as CD14, CD34, and HLA-DR were identified in less than 30% of the cell population.

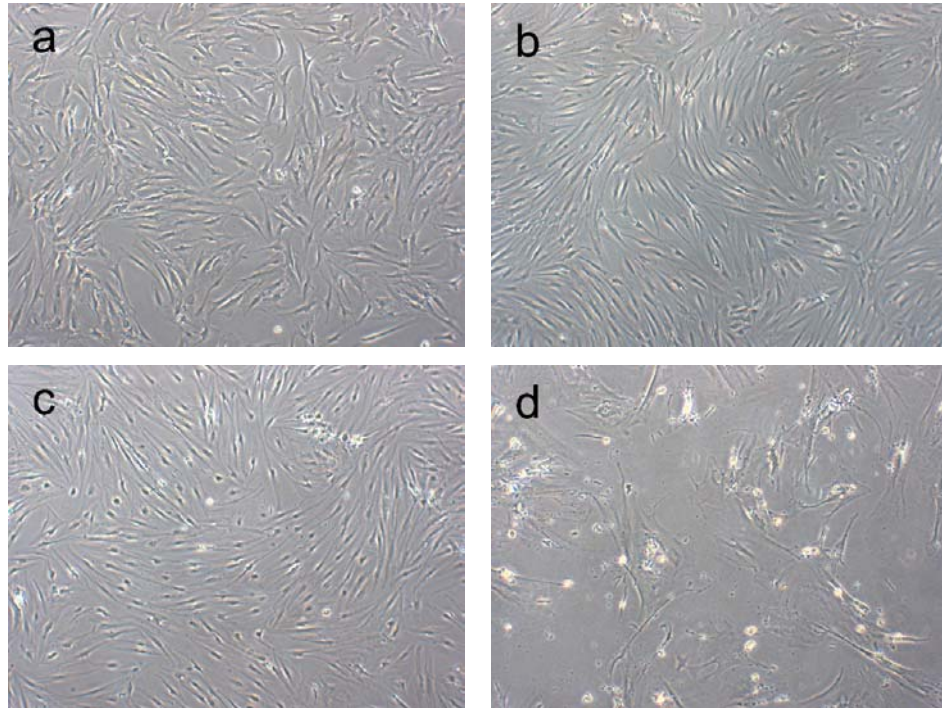


Figure 3.1: The morphology of HBMSCs (40x magnification). (a) The cells of passage 2 grown in normal medium (10% FBS in DMEM/F12). Osteo-induction for the cells were conducted using (b) 2.5 ng/ml FGF2 for 24 hours followed by (c) 10 ng/ml BMP2 for 24 hours. (d) Dramatic changes in cell morphology were observed in the cells of passage 5.

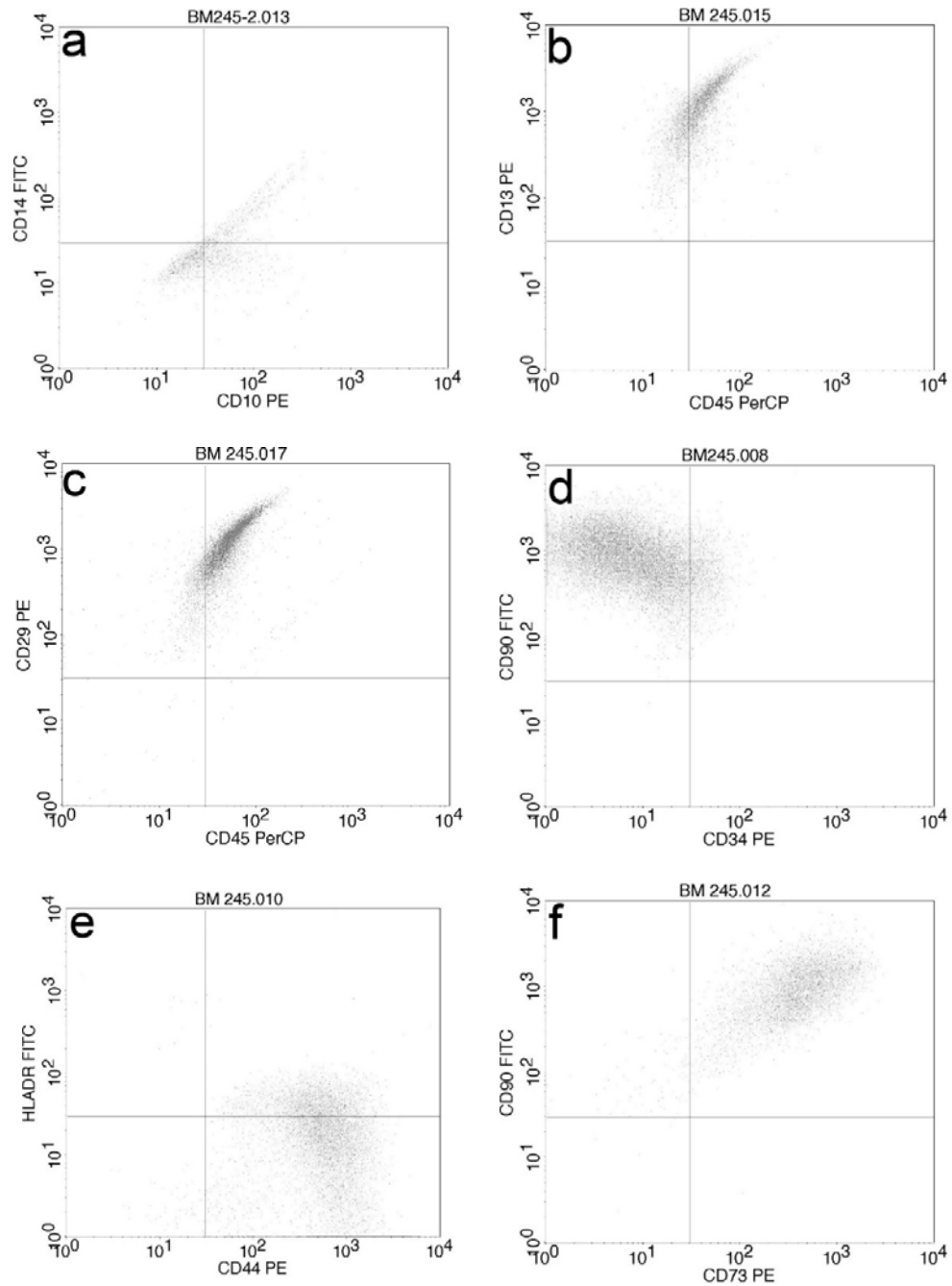


Figure 3.2: Surface markers of HBMSCs, analyzed by flow cytometry. The scatter plots of 2 markers: (a) CD10 and CD14, (b) CD45 and CD13, (c) CD45 and CD29, (d) CD34 and CD90, (e) CD44 and HLA-DR, and (f) CD73 and CD90.

Table 3.1: Percentage of the cells expressing each specific surface marker.

Surface Marker	Expression	% Positive
CD10	+	76.28
CD13	+	100
CD29	+	99.64
CD44	+	99.34
CD73	+	98.11
CD90	+	99.86
CD14	-	26.01
CD34	-	7.7
CD45	-	62.36
HLA-DR	-	19.63

3.1.3 The expression of stem cell-specific genes

MSCs in bone marrow cell population have been estimated to be 1 cell in 10^4 - 10^5 cells [106-108]. These cells can be expanded by serial subculture to a desired number. For clinical application of tissue engineering, large amounts of the cells are needed. Therefore, the subculture step is very important. This manipulation should not be to disturb the self-renewal and differentiation potentials of the cells. Numerous factors that control the cells proliferation and maintain their multipotency have long been studied. However, little is known for the mechanism at molecular levels. Among these factors, OCT4, SOX2, Nanog, FGF4, REX1, BST1, and TERT have been reported and proven to be specific for the stem cells [139-144].

To investigate the expandability of HBMSCs, the stem cell-associated genes were serially followed up by using RT-PCR technique. The quantitative changes in the stem cell gene expressions for the cells of passage 2 and 5 were compared. The stem cell-associated genes to be tested included *oct4*, *sox2*, *nanog*, *fgf4*, *rex1*, *bst1*, and *tert*. These genes were found to express in the isolated HBMSCs. In comparison, the genes of *oct4*, *sox2*, *nanog*, and *fgf4* were significantly lowered for the cells of

passage 5. The difference in *rex1* expression for these two passages was not significant, while the expression levels of *tert* and *bst1* were enhanced (Figure 3.3).

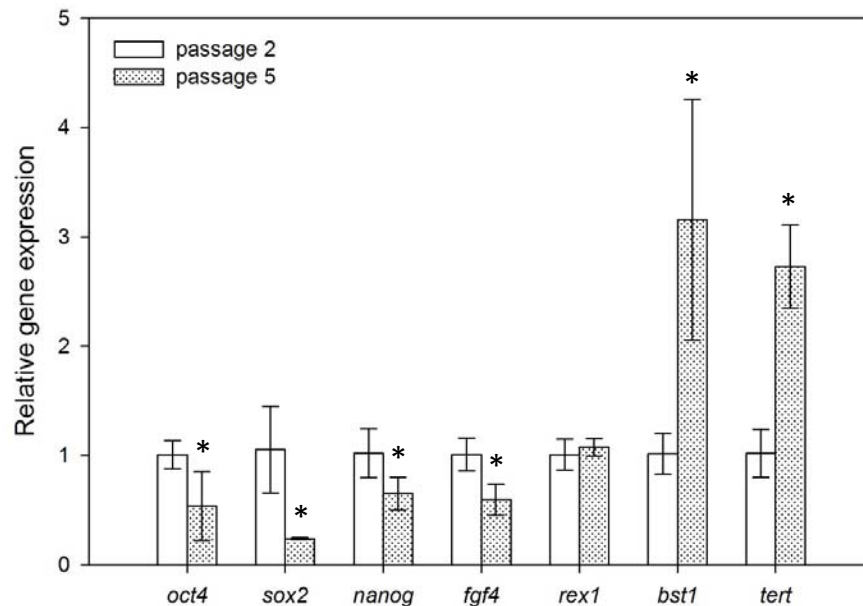


Figure 3.3: The expression of stem cell-associated genes of HBMSCs in passage 2 and 5. Decreased expression of the core transcription factors such as *oct4*, *sox2*, *nanog*, and *fgf4* were identified. Almost 3-fold increase of *tert* and *bst1* genes were observed. * indicates significant differences ($p < 0.05$) as calculated by t-test.

3.1.4 Changes in stem cells-gene expression of induced HBMSCs

Based on the previous study, the induction effects of FGF2 and BMP2 for improving bone regeneration were further examined using another cell source. The robustness of culturing protocols that might influence the stem cell properties after this induction was verified. HBMSCs were firstly induced by 2.5 ng/ml FGF2 for 1 day, followed by 10 ng/ml BMP2 for 1 day (Figure 2.7) before the determination of osteogenic gene markers were carried out. These important markers included *runx2*,

alp, *osc*, *opn*, and *bsp* which involves in either differentiation or mineralization process of bone regeneration.

After induction, increase in *fgf4*, *sox2*, and *bst1* mRNA levels by almost 2.5-folds was detected. The levels of *opn*, and *bsp* were significantly increased by 2.5 and 3.5-fold, respectively. However, the expression of *nanog*, *rex1*, and *runx2* were not changed. The levels of *tert*, *oct4*, *osc*, and *alp* were decreased significantly. (Figure 3.4).

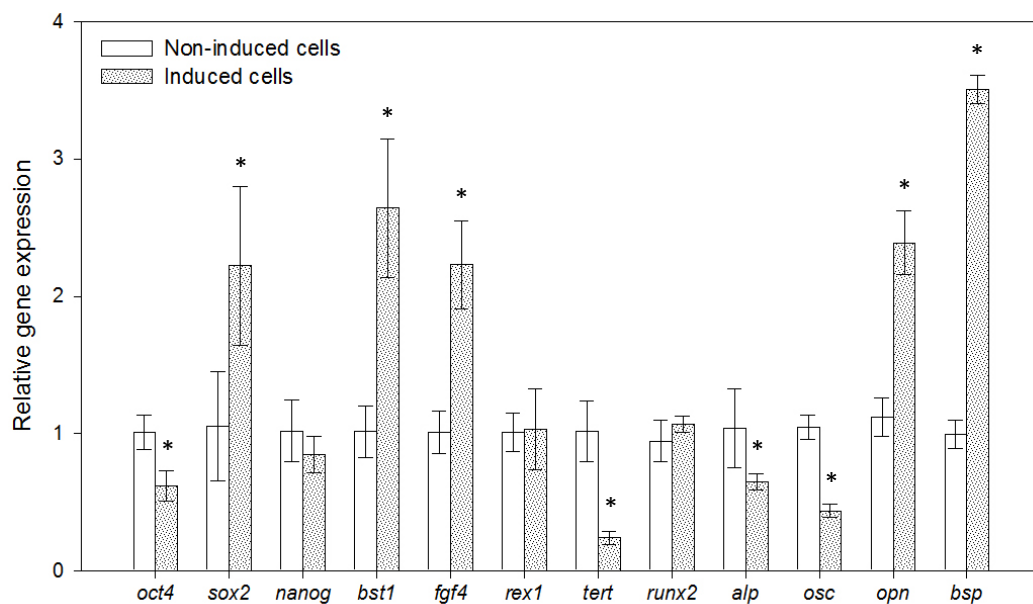


Figure 3.4: The mRNA expression of stem cell-associated and osteogenic genes of HBMSCs, after sequential induction with 2.5 ng/ml FGF2 and 10 ng/ml BMP2. The expression of *sox2*, *bst1*, *fgf4*, *opn*, and *bsp* were increased, while *oct4*, *tert*, *alp*, and *osc* were decreased. The level of *nanog*, *rex1*, and *runx2* were not affected by the induction. * indicates significant differences ($p < 0.05$) as calculated by t-test compared to the gene levels of the non-induced cells.

3.2 Characterization of the isolated RBMSCs

The isolated RBMSCs showed a spindle-like shape. After isolation, the cells reached confluence within 2 weeks. The rate of proliferation was decreased when subculturing to passage 8, and the cell morphology was changed to be a flattened epithelial shape (Figure 3.5).

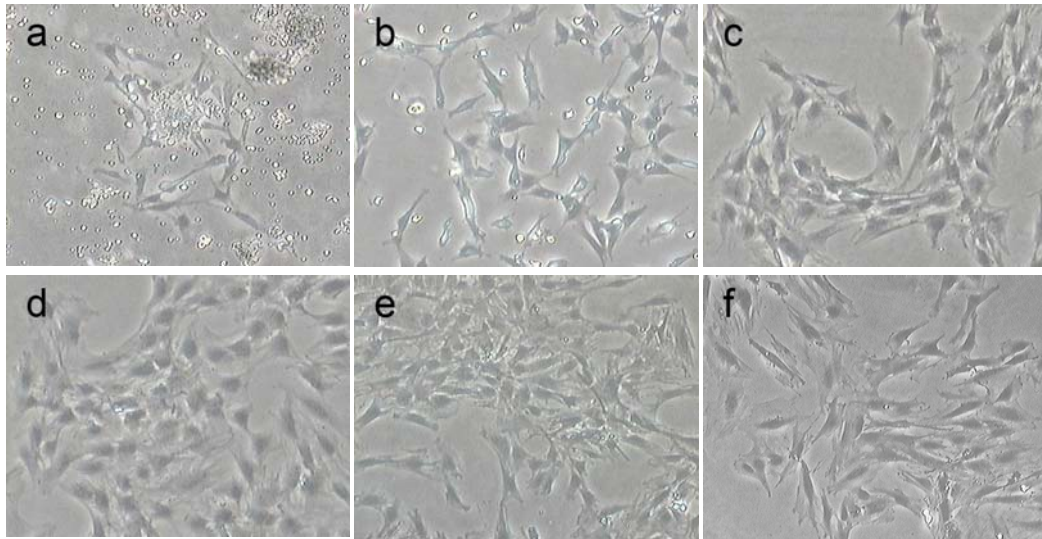


Figure 3.5: The morphology of RBMSCs (40x magnification). The cells of passage 0 at (a) day 1 and (b) day 3 post-isolation. A colony of adherent cells could be detected at the first day. The size of the cells at (c) passage 2, (d) passage 4, (e) passage 8, and (f) passage 8 gradually increased upon culturing.

3.3 Growth factors to be determined for the effects on bone regeneration

The induction by growth factors were divided into two subsequent phase: proliferation and differentiation phases, respectively. The growth factors for the former phase included FGF2 and insulin, while for the later phase these were BMP2 and BMP7. In the control group, the cells were treated with 10 nM TA and 50 μ g/ml AA

(TA+AA) in addition to 2% FBS. The summation of the used growth factors and their concentration was shown in Table 2.7 (Page 49).

3.3.1 Cell proliferation

In the proliferation phase, improved growth was not revealed by FGF2 induction (Figure 3.6). In contrast, the number of cells was increased by 1.2- to 1.3-fold when insulin was used as an inducer.

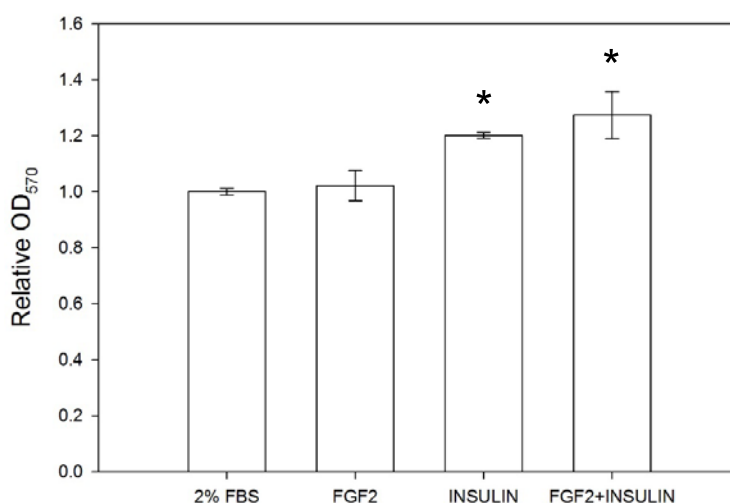


Figure 3.6: The result of MTT assay. Relative cell viability of RBMSCs after incubation with 2.5 ng/ml FGF2, 60 ng/ml insulin, or FGF2 plus insulin for 24 hours. The cells cultured in α -MEM plus 2% FBS were of the control. * indicates significant differences ($p < 0.05$) as calculated by t-test.

3.3.2 mRNA expression of genes related to osteogenesis

In this experiment, the expression levels of genes related to osteogenesis were measured. The tested genes were divided into 3 groups including the genes of osteogenic transcription factors, *runx2* and *osx*; the gene of osteogenic protein, *bmp7*; and the genes of WNT pathway proteins, *axin2*, *β -catenin*, and *dkk1*.

3.3.2.1 The effects of FGF2 and insulin

The cells of passage 4 were challenged with 2.5 ng/ml FGF2, 60 ng/ml insulin, or FGF2 plus insulin for 24 hours. Results showed that the expression levels of *runx2*, *osx*, *bmp7*, *axin2*, β -*catenin*, and *dkk1* were significantly increased by the co-treatment. In contrast, FGF2 decreased the expression levels of all genes under investigated. The level of *bmp7* mRNA was up-regulated by insulin, while it did not influence the remaining genes (Figure 3.7).

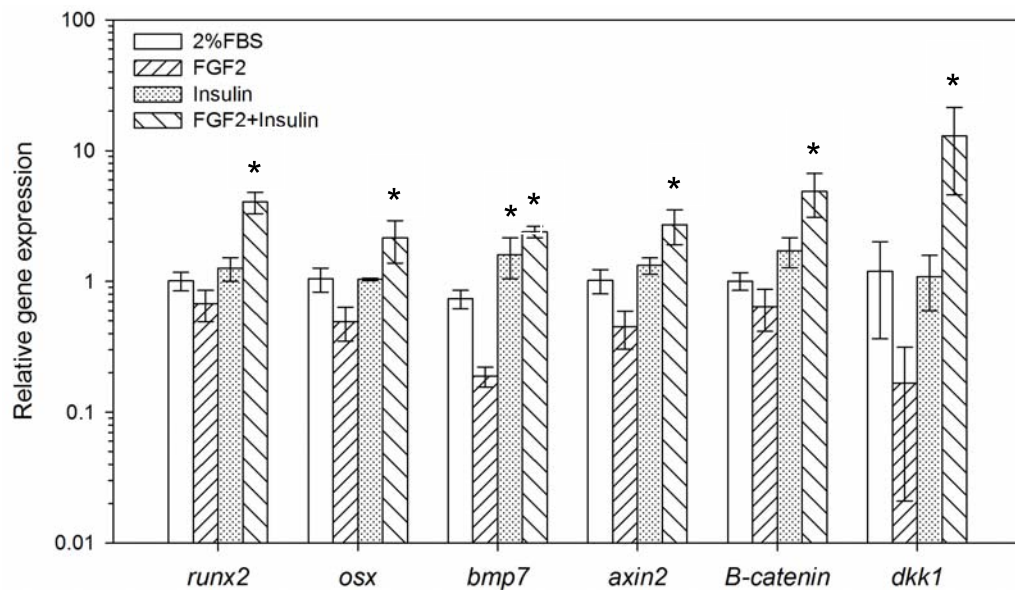


Figure 3.7: Relative mRNA expression levels of osteogenic markers for the RBMSCs induced with 2.5 ng/ml FGF2, 60 ng/ml insulin, or FGF2 plus insulin for 1 day. The control group was the cells cultured by α -MEM plus 2% FBS. * indicates significant differences ($p < 0.05$) as calculated by t-test.

3.3.2.2 The effects of BMP2 and BMP7

The cells of passage 4 were challenged by 10 ng/ml BMP2, 10 ng/ml BMP7, or BMP2 plus BMP7. Those cultured in the medium containing 10 nM TA and 50 μ g/ml AA (TA+AA) were of the control group. The levels of *runx2* and *osx* mRNA were increased by 2- to 3-fold when induced with BMP7, whereas BMP2 lowered these genes (Figure 3.8). Both BMPs inhibited *bmp7* gene expression. The levels of *axin2* and β -*catenin*, were enhanced by BMP7, but blocked by BMP2. The expression of *dkk1* was inhibited by BMP2 and BMP7. Especially, BMP7 strongly suppressed *dkk1* mRNA expression, by 25 folds.

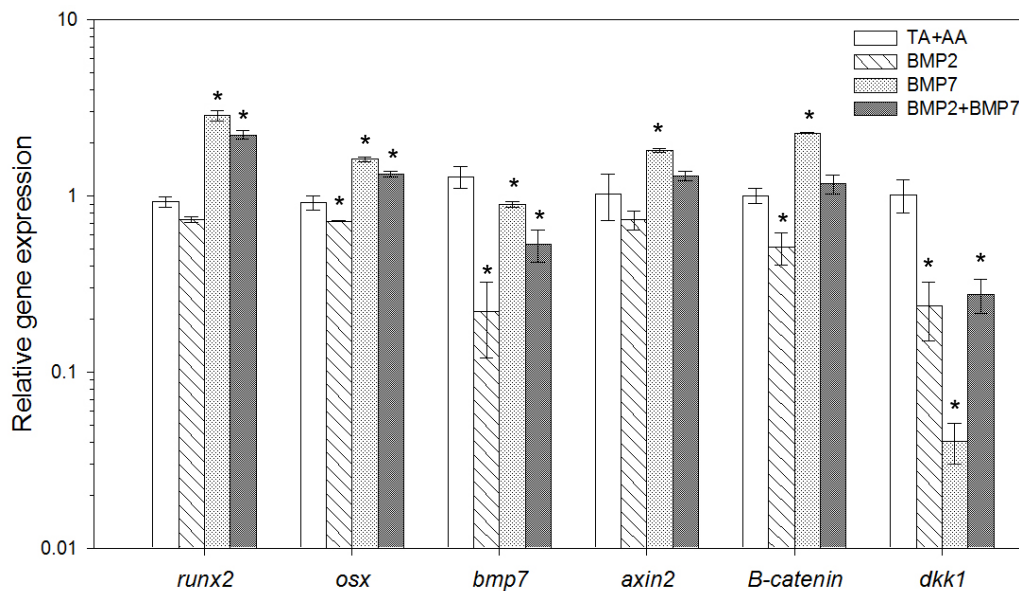


Figure 3.8: Relative gene expression levels of RBMSCs treated with 10 ng/ml BMP2, 10 ng/ml BMP7, or their combination for 1 day. The cells cultured in TA (10 nM) and AA (50 μ g/ml) containing medium were of the control group. * indicates significant differences ($p < 0.05$) as calculated by t-test.

3.3.2.3 The effects of proliferation factors (FGF2 and insulin) and differentiation factors (BMP2 and BMP7)

The cells of passage 4 were induced by the proliferation factor(s) for 1 day followed by starvation in medium plus 2% FBS for 2 days and stimulation with the differentiation factor(s) for 1 day before the expression of osteogenic markers were investigated (Table 3.2).

The results showed that *runx2* expression of FGF2 pre-treatment group was significantly down-regulated by TA+AA, BMP2, and BMP7, but not in the BMPs combination treatment. For insulin induction followed by BMP2, *runx2* mRNA was decreased by 0.6-fold. When the combination of the proliferation factors was used, the expression of *runx2* was also lowered by these differentiation factors. The expression level of *osx* was up-regulated by TA+AA or BMP7 in the insulin pre-induction group, while the combination of BMP2 and BMP7 promoted *osx* mRNA level in FGF2 and the combination of FGF2 and insulin pre-treatment. *Osx* expression was decreased by BMP2 in all of the pre-induction groups. For *bmp7* gene, the expression level was increased by 2-fold in insulin followed by TA+AA group. In the remaining groups, down-regulation of *bmp7* expression was observed. The level of *bmp7* was lowered by 0.07-fold in FGF2 followed by TA+AA group.

For the genes in WNT pathway, the expression of *axin2* was not affected by any induction conditions. The expression of *β-catenin* was increased by BMP7 when the cells were pre-treated with insulin. However, the opposite result was observed in FGF2 pre-treatment followed by BMP7 that the level of *β-catenin* was decreased by 0.56-fold. The presence of BMP2 improved *β-catenin* expression in FGF2 and insulin combination group. In FGF2 followed by TA+AA, *β-catenin* mRNA was significantly down-regulated by 0.4-fold. The down-regulation of *dkk1* expression was observed in almost all treatment group, excepted for the group treated with insulin followed by TA+AA.

Table 3.2: The relative mRNA expression levels of osteogenic markers for the RBMSCs initially induced by the proliferation factor(s) (2.5 ng/ml FGF2 and 60 ng/ml insulin) and followed by the differentiation factor(s) (10 ng/ml BMP2 and 10 ng/ml BMP7). The cells treated by the condition A1 were of the control group. * indicates significant differences ($p<0.05$) as calculated by one-way ANOVA.

Proliferation induction	Differentiation induction	Relative expression level (\pm SD)					
		<i>runx2</i>	<i>osx</i>	<i>bmp7</i>	<i>axin2</i>	<i>β-catenin</i>	<i>dkk1</i>
A 2% FBS	1 TA+AA	0.93 \pm 0.06	0.92 \pm 0.09	1.29 \pm 0.18	1.03 \pm 0.31	1.00 \pm 0.10	1.02 \pm 0.22
	2 BMP2	0.74 \pm 0.03*	0.72 \pm 0.01*	0.22 \pm 0.10*	0.73 \pm 0.09	0.51 \pm 0.11*	0.24 \pm 0.09*
	3 BMP7	2.87 \pm 0.20*	1.62 \pm 0.05*	0.90 \pm 0.03*	1.81 \pm 0.05	2.28 \pm 0.02*	0.04 \pm 0.01*
	4 BMP2+BMP7	2.22 \pm 0.13*	1.34 \pm 0.05*	0.53 \pm 0.11*	1.30 \pm 0.08	1.17 \pm 0.14	0.28 \pm 0.06*
B FGF2	1 TA+AA	0.28 \pm 0.04*	0.48 \pm 0.03*	0.07 \pm 0.02*	0.65 \pm 0.06	0.40 \pm 0.04*	0.15 \pm 0.08*
	2 BMP2	0.74 \pm 0.01*	0.59 \pm 0.07*	0.26 \pm 0.07*	1.13 \pm 0.02	0.77 \pm 0.09	0.11 \pm 0.01*
	3 BMP7	0.56 \pm 0.02*	0.66 \pm 0.01*	0.20 \pm 0.03*	0.83 \pm 0.03	0.56 \pm 0.02*	0.23 \pm 0.01*
	4 BMP2+BMP7	1.19 \pm 0.00	1.22 \pm 0.07*	0.66 \pm 0.03	1.44 \pm 0.24	1.27 \pm 0.22	0.32 \pm 0.15*

Table 3.2 (Continued)

Proliferation induction	Differentiation induction	Relative expression level (\pm SD)					
		<i>runx2</i>	<i>osx</i>	<i>bmp7</i>	<i>axin2</i>	<i>β-catenin</i>	<i>dkk1</i>
C Insulin	1 TA+AA	1.13 \pm 0.19	1.33 \pm 0.06*	2.29 \pm 0.58*	1.47 \pm 0.21	1.22 \pm 0.12	1.23 \pm 0.21
	2 BMP2	0.61 \pm 0.01*	0.85 \pm 0.10	0.22 \pm 0.03*	0.89 \pm 0.14	0.75 \pm 0.05	0.13 \pm 0.03*
	3 BMP7	1.24 \pm 0.20	1.29 \pm 0.15*	0.20 \pm 0.12*	1.44 \pm 0.78	1.83 \pm 0.05*	0.77 \pm 0.46
	4 BMP2+BMP7	1.30 \pm 0.19	1.03 \pm 0.06	1.08 \pm 0.39	1.21 \pm 0.13	1.21 \pm 0.16	0.06 \pm 0.00*
D FGF2+Insulin	1 TA+AA	1.19 \pm 0.07	0.65 \pm 0.09*	0.70 \pm 0.36	1.89 \pm 0.83	1.09 \pm 0.24	0.39 \pm 0.09*
	2 BMP2	0.90 \pm 0.02*	0.89 \pm 0.10	0.70 \pm 0.21	1.47 \pm 0.37	1.38 \pm 0.18*	0.47 \pm 0.36*
	3 BMP7	0.68 \pm 0.06*	0.98 \pm 0.07	0.15 \pm 0.06*	1.34 \pm 0.54	0.85 \pm 0.07	0.41 \pm 0.34*
	4 BMP2+BMP7	0.66 \pm 0.02*	1.41 \pm 0.06*	0.31 \pm 0.13*	1.20 \pm 0.03	1.51 \pm 0.23*	0.76 \pm 0.23

3.3.3 Alkaline phosphatase (ALP) activity assay

For the cells treated with the proliferation factor(s), ALP activity was raised by either FGF2 or insulin, but significantly decreased when the combined growth factors were used (Table 3.3). The effect of insulin on ALP activity was stronger than FGF2.

The sequential effects of the proliferation factor(s) and the differentiation factor(s) on ALP activity were also investigated (Table 3.4). The enzyme activity was slightly promoted by FGF2 or insulin. Followed by BMP2, BMP7, or BMP2 plus BMP7 induction, the enzyme activity was significantly increased (1.18 to 1.36-fold increment). Enhanced ALP activity was only found for the cells treated with FGF2 plus insulin, followed by BMP2 plus BMP7 (1.05-fold), while the remaining treatment groups were not affected by these growth factors.

3.3.4 Calcium deposition

In table 3.3, slight increment of calcium deposition was determined for the cells treated with the used proliferative growth factors, compared to the control group. The degree of calcium deposition was not different among these treatment groups, but significantly higher than that of the control. When the cells were subsequently induced by the differentiation growth factors (BMP2 and/or BMP7), improved calcium deposition was detected (Table 3.4). However, the higher degree of calcium deposition was found for the cells previously cultured in 2% FBS and subsequently induced by either BMP2 or BMP7.

Table 3.3: The results of relative ALP activity and relative calcium deposition after proliferation induction. RBMSCs were cultured in medium supplemented with 2.5 ng/ml FGF2, 60 ng/ml insulin, or the combination for 1 day. The control group was the cells cultured by α -MEM plus 2% FBS. Calcium deposition was estimated from the OD values at 450 nm by which ARS dye forms complexes with Ca^{2+} , generating brick-red color. * indicates significant differences ($p < 0.05$) as calculated by one-way ANOVA.

Proliferation induction	Relative ALP activity (\pmSD)	Relative Calcium deposition (\pmSD)
2% FBS	1.00 \pm 0.06	1.00 \pm 0.03
FGF2	1.11 \pm 0.01*	1.90 \pm 0.09*
Insulin	1.17 \pm 0.02*	2.01 \pm 0.15*
FGF2+Insulin	0.95 \pm 0.01*	1.92 \pm 0.05*

Table 3.4: The results of relative ALP activity and relative calcium deposition of osteogenic induced RBMSCs using proliferation factor(s) (2.5 ng/ml FGF2 and 60 ng/ml insulin) and followed by differentiation factor(s) (10 ng/ml BMP2 and 10 ng/ml BMP7). The cells treated by the condition A1 were of the control group. Calcium deposition was estimated from the OD values at 450 nm by which ARS dye forms complexe with Ca^{2+} , generating brick-red color. * indicates significant differences ($p < 0.05$) as calculated by one-way ANOVA.

	Proliferation induction	Differentiation induction	Relative ALP activity (\pmSD)	Relative Calcium deposition (\pmSD)
A	2% FBS	1 TA+AA	1.00 \pm 0.01	1.00 \pm 0.05
		2 BMP2	1.06 \pm 0.06*	2.54 \pm 0.19*
		3 BMP7	1.10 \pm 0.03*	2.48 \pm 0.06*
		4 BMP2+BMP7	1.09 \pm 0.00*	2.10 \pm 0.31*
B	FGF2	1 TA+AA	1.27 \pm 0.01*	1.65 \pm 0.05*
		2 BMP2	1.18 \pm 0.01*	1.90 \pm 0.12*
		3 BMP7	1.36 \pm 0.01*	1.82 \pm 0.16*
		4 BMP2+BMP7	1.27 \pm 0.01*	1.78 \pm 0.29*
C	Insulin	1 TA+AA	1.10 \pm 0.00*	1.72 \pm 0.03*
		2 BMP2	1.25 \pm 0.02*	2.01 \pm 0.22*
		3 BMP7	1.31 \pm 0.01*	2.18 \pm 0.02*
		4 BMP2+BMP7	1.23 \pm 0.03*	2.00 \pm 0.20*
D	FGF2+Insulin	1 TA+AA	0.87 \pm 0.01*	1.71 \pm 0.03*
		2 BMP2	1.00 \pm 0.01	1.92 \pm 0.08*
		3 BMP7	1.00 \pm 0.00	1.88 \pm 0.21*
		4 BMP2+BMP7	1.05 \pm 0.01*	1.55 \pm 0.07*

3.3.5 BMP2 production

Following the induction with FGF2, insulin, or FGF2 plus insulin for 1 day, the production of BMP2 by the induced cells was quantified. In Figure 3.9, the levels of BMP2 was increased within the 24 hours post-induction, which significantly affected by insulin. However, the protein levels were decreased when determined at 72 hours post-induction.

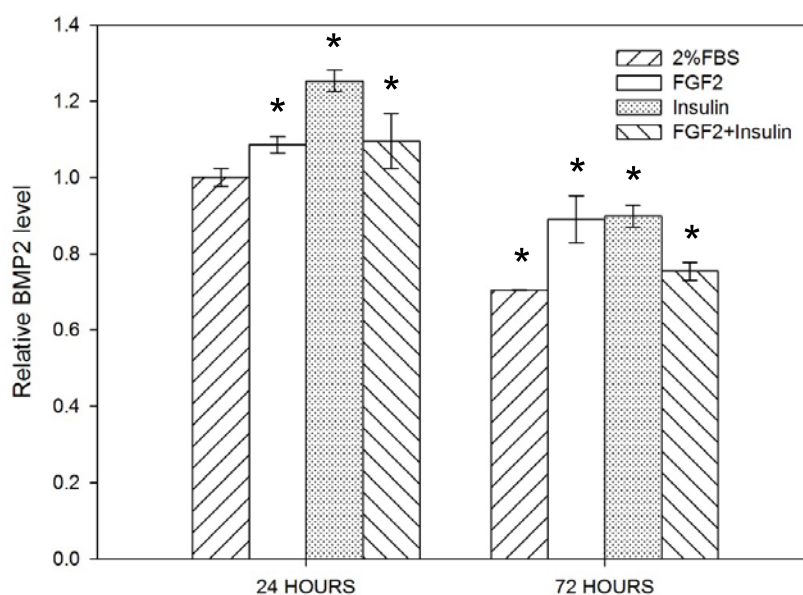


Figure 3.9: BMP2 levels produced by RBMSCs. The cells were induced with 2.5 ng/ml FGF2, 60 ng/ml insulin, or FGF2 plus insulin for 24 hours, and the level of BMP2 was detected after 24 and 72 hours post-induction. The cells grown in 2% FBS containing medium were used as the control. * indicates significant differences ($p < 0.05$) as calculated by one-way ANOVA.

3.4 *In vivo* bone formation

RBMSCs at a density of 10^4 cells/scaffold were seeded onto scaffold samples and cultured in the induction conditions previously studied (Experiment 2.3.5, Figure 2.11). The cell-seeded constructs cultured in 2% FBS containing medium were used as the control. The prepared constructs were implanted subcutaneously on the back of the rats for the study of ectopic bone formation (Figure 2.12). The implants were removed after 8 weeks post-operation and proceeded for histological analysis. The staining dyes including H&E and ARS were utilized for microscopic investigation.

After 8 weeks of implantation, the scaffolds were remained undegraded (Figure 3.10). For the scaffolds without cells and with non-induced cells, fibrous tissue was found to cover the implant surfaces. The newly formed bone was detected inside the implants, previously induced with FGF2, followed by BMP2 or BMP7 (Figure 3.11). In contrast, the new bony tissue was not apparent for insulin treated samples (Figure 3.12). The bone tissue was formed inside the constructs treated with the combination of the proliferation and differentiation factors (Figure 3.13).



Figure 3.10: The implanted tissues at 8 weeks post-operation. The constructs were subcutaneously implanted into the dorsal part of 2-month-old Wistar rats and harvested after 8 weeks of implantation. All samples were persisted at the implantation site.

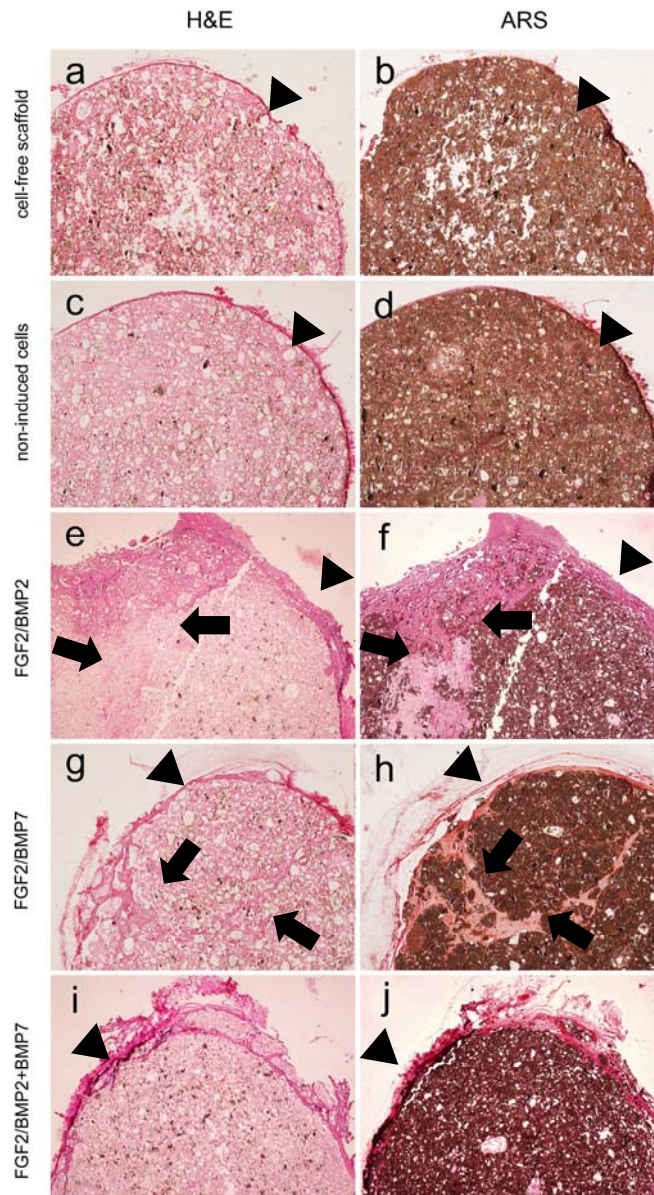


Figure 3.11: Tissue sections of 8-week after implantation, stained with H&E and ARS (40x magnification). The figures represented the groups of initially induced cells using FGF2 followed by differentiation induction using BMP2 (e and f), BMP7 (g and h), and the combination (i and j). The cell-free scaffolds (a and b) and cell-seeded constructs cultured in 2% FBS containing medium (c and d) were used as the control. Symbols: (➡) newly formed bone tissue and (▲) fibrous tissue.

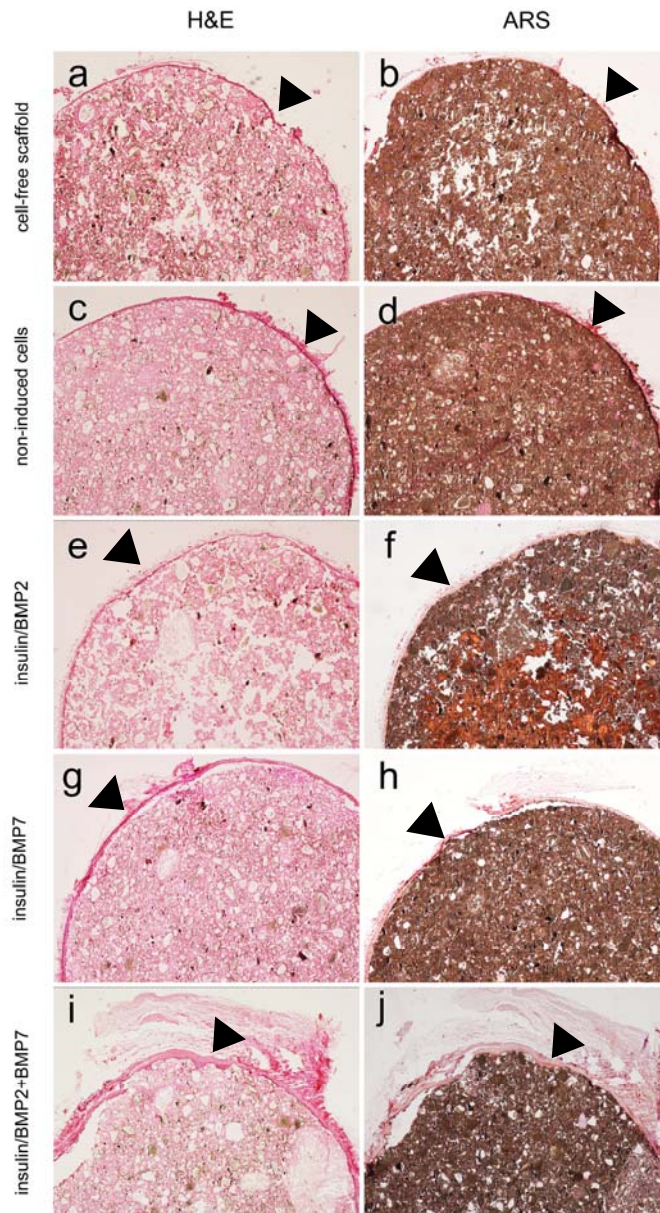


Figure 3.12: Tissue sections of 8-week after implantation, stained with H&E and ARS (40x magnification). The figures represented the groups of initially induced cells using insulin followed by differentiation induction using BMP2 (e and f), BMP7 (g and h), and the combination (i and j). The cell-free scaffolds (a and b) and cell-seeded constructs cultured in 2% FBS containing medium (c and d) were used as the control. Symbols: (➡) newly formed bone tissue and (▲) fibrous tissue.

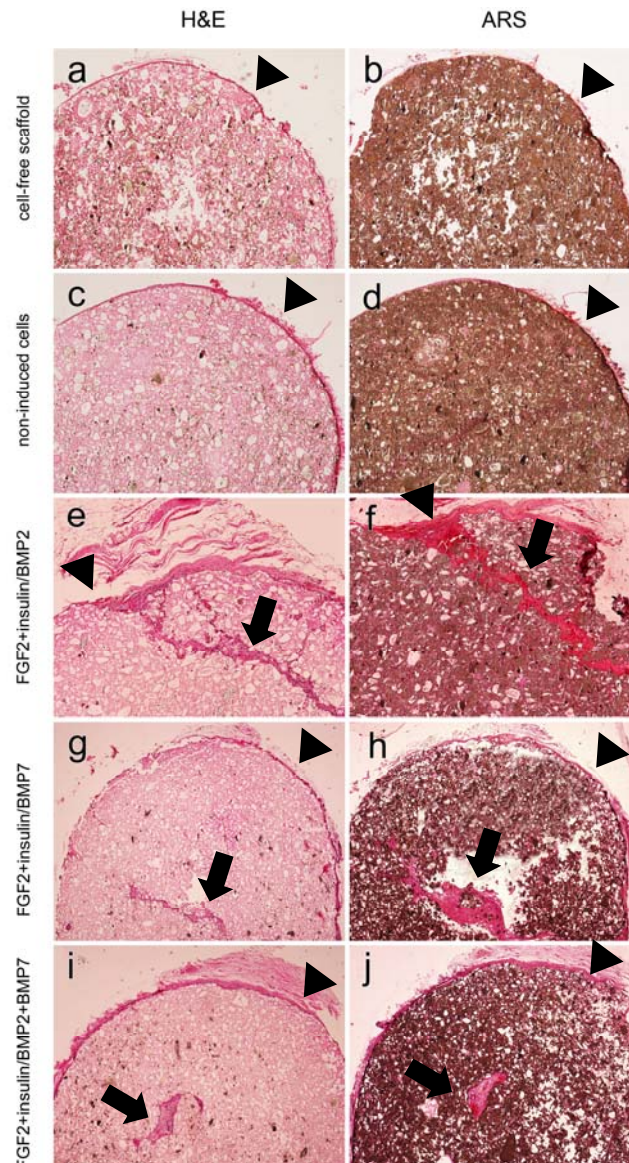


Figure 3.13: Tissue sections of 8-week after implantation, stained with H&E and ARS (40x magnification). The figures represented the groups of initially induced cells using FGF2 plus insulin, followed by differentiation induction using BMP2 (e and f), BMP7 (g and h), and the combination (i and j). The cell-free scaffolds (a and b) and cell-seeded constructs cultured in 2% FBS containing medium (c and d) were used as the control. Symbols: (➡) newly formed bone tissue and (▲) fibrous tissue.

3.5 Reporter vectors construction

As *runx2* expression was up-regulated by FGF2 and insulin induction, the mechanisms at molecular levels of this transcription factor on osteogenesis need to be clarified. Luciferase reporter gene assay was performed for such the objective.

The 5'-UTR of *runx2* (-1557 to +97, namely U1557) was amplified using the genomic DNA isolated from RBMSCs as a template by PCR and cloned into pGEM-T[®] easy vector (the cloning vector). After extraction and purification from transformed *E. coli*, the recombinant plasmid was used as a template using two pairs of primers to amplify two consecutive fragments of *runx2*-5'-UTR. These two fragments were cloned into the cloning vector and subcloned into pGL3-Promoter vector (the reporter vector). Two different clones, namely pGL3-*runx2*-N and pGL3-*runx2*-F, were then obtained. The sequence of *runx2*-N and *runx2*-F were presumed as targets of particular transcription factors.

In addition, by aligning with database using TFSEARCH program, consensus sequence, namely *ap1* and *sry*, were identified. Five repeats of each consensus sequence were designed, chemically synthesized, and prepared for cloning into pGL3-Promoter vector. Luciferase gene is located 3'-downstream of the repeat sequence. Increased luciferase activity could be detected if any transcription factors bound specifically to the repeat.

3.5.1 Cloning of 5'-UTR of *runx2* gene

3.5.1.1 Cloning of 5'-UTR of *runx2* gene and construction of pGEM-U1557

Genomic DNA isolated from RBMSCs of passage 4 was utilized as a template for PCR reaction using *runx2*-U1557 forward primer and *runx2*-97 reverse primer to amplify the U1557 fragment (Figure 2.14, step 1). The expected PCR product was located about 1.7 kb band (Figure 3.14a). The selected band was purified by gel

purification column (Figure 2.14, step 2 to 3) and analyzed again on 0.7% agarose gel (Figure 3.14b). The verified band was used for the next cloning after gel purification.

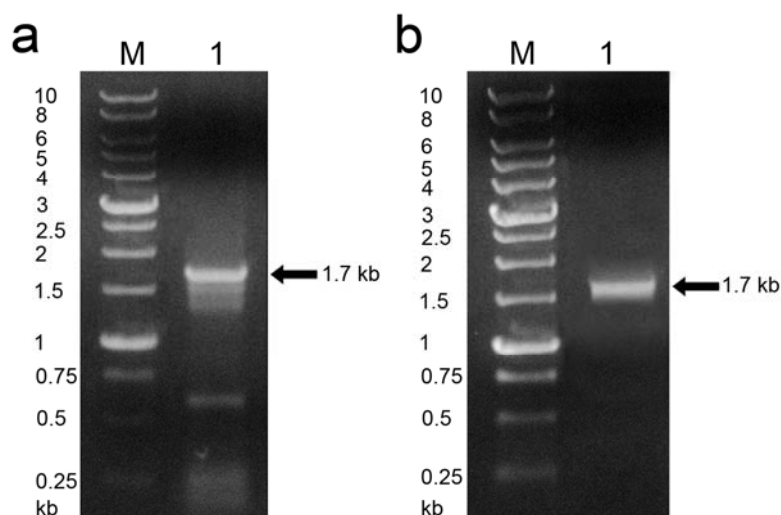


Figure 3.14: The PCR product, called U1557, amplified by using *runx2*-U1557 and *runx2*-97 as the primers (a, lane 1). The corresponding band after gel purification using Nucleospin[®] extract II column (b, lane 1). M: 1 kb DNA marker.

The purified U1557 was cloned into pGEM-T[®] easy vector (Figure 2.14, step 4) and transformed into competent *E. coli* strain DH5 α (Figure 2.14, step 6). The white single colony was picked and separately cultured overnight in LB liquid medium supplemented with 100 μ g/ml ampicillin after which the recombinant plasmid was isolated. The isolated plasmid was digested with *Eco*RI and subjected to 0.7% agarose gel electrophoresis (Figure 2.14, step 7 to 9). Two DNA bands located at 3 kb and 1.7 kb were found (Figure 3.15, lane 4). The purified plasmid was subjected to DNA sequencing to acquire the sequence of DNA insert.

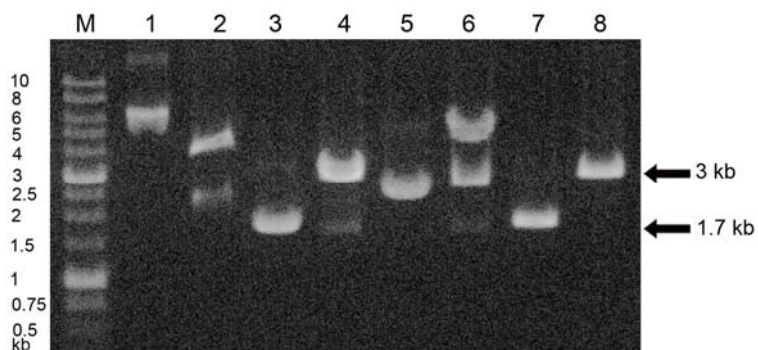


Figure 3.15: Screening of plasmids containing U1557 fragment by using *Eco*RI digestion. Undigested plasmids (odd lanes) and *Eco*RI digested plasmids (even lanes). In lane 4, a 3 kb band represents a linearized pGEM-T[®] easy vector and a 1.7 kb band denotes an insert DNA fragment. M: 1 kb DNA marker.

3.5.1.2 Analysis of U1557-DNA sequence

The U1557 inserted fragment was sequenced. On aligning the U1557 sequence with the sequence 2,000 bases 5'-upstream of *runx2* gene, the result revealed that these sequences were of 99% similarity (Appendix C). There were 7 mismatch points (at positions +1, -204, -603, -768, -989, -1104, and -1327) and 1 insertion mutation (at a position -980) found in the amplified fragment of U1557. This recombinant clone was used as the template for the next cloning.

Possible transcription factor binding sites were determined for the U1557 sequence (Figure 3.16). Each consensus sequence and its proposed functions were listed in Table 3.5. Among these sequences, *ap1* and *sry* were selected for further analysis because of their association with osteo-chondrogenesis [145-147].

-1558 GAGTGGCGTGGATAAATGGCAAGAAATGCCTAGGAAATGGTCTGCTCGCCTTTATAATGTTTGTGAAAAATCCTCCATC
 RUNX2-KPNI-U1526

-1477 GCTCCCAACTGATGAAAACAGGAAGCTCTATTATAAATGTGAAATTCAGTGCCTATGATATATAATCATCCTAATAAGAA
 c-Ets

-1396 AATGAGCTCTAGACATACATGTCCAAGAGGGCAAAAGAAGAGATAGTTTCCCAAAGATGGTTTCAATTCTCTTCTGAATCA
 1 AP1

-1315 GAATTAGCAAATCGAGACGACTAACATACTCTGTCTGCGTGCATTATTCCCTTACTACACACAGCATTGTAATTTATTTCC
 C/EBP-β

-1234 AAAGCTTCCATTATAAACAAAAAATACAGTTTCTGTTAACCCACTCTATTCTGAACTATGGAACTACTGAATATCTCAT
 1 SRY SRY

-1153 TATATATGCAGAGCTGAAGCCCAAAGTCTGTACAGTCACTTCCAAGTGGACTAAAGAATCATACAAAACGTTTCTTTTA
 Nkx-2

-1072 GAGATAAAATCCAGTCATGCAGAAAATTAACACTATTCCAACAACCTGTATCCTGCAGGTCTTGACATTTGTTTTTTGG
 5 SRY

-991 GTTTTTTTTTCGTTTGTGTTTGTGTTTAAAGATCTTCAAAGTAACCAAGGGATGATGGTAAAAATAAATAAATGATAC
 2 3 4 SRY SRY SRY CdxA

-910 TAATTACATTTAATCTTTATTGTAAGAGCTACCACCTAATAAAAAAATCAACTACACAGTCATGATTTAGTATTTGTAAAG
 S8 6 SRY C/EBP

-829 GAATCCCAGGCTAACACTTTTGTGACAGCCAATTACAGTCAATCCCGCAAGGAGTTTGCAGAGCAGACCTTTGGAAAGGT
 C/EBP
 RUNX2-KPNI-U796

-748 AAAGTGTTTTACAATGAGTTACAGATCTACAAGCTTAGGAAGACAAGCAGGAAAGAAGCAGCCACCTGGGAAATCCGAAG
 Ik2

-667 CAGCCCTGAAAGTGATACAATCCCAAGATGTGACCCACTGCGAAGCAGCAGTTGTTTCAGAAGCTGCCTCACTTGAACA
 RUNX2-NHEI-U630

-586 GTTTTGCTCACTTTTCCATAGACATAATAATGAAGGAAAGAGAGGGGTAGAGAAAAGAGAAGAAAGAGCAGACGAGGG
 Oct-1 Evi-1

-505 AAGGAGGGAAGGGGGAGTAGGGAGGTGAGAAAGAAACCCTTAGTGCAGAGTTCTGCTCTCCAAGTGCTTAACCTT
 MZF1 Cbfa1 Nkx-2

-424 ACAGGAGTGTGGCTCCTTCAGCATTGTATTCTATCCAAATCCTCATGAGTCACAAAAATAAAAAGCTATAACCTTCTG
 2 AP1

-343 AATGCCAGGAAGGCCTCACCACAAGCCTTTTGTGAGAGAGGGAGAAAGGGGGAGGAAGGGAGAGAGAGGAAGGGA
 MZF1

-262 GGAAGGGAGAGAGAGCACCATAAGTAAAGAGACAGAAGGAAGGAAGGGAGAGGACAACAGAAGAGAAAAGGGAGGGGA
 MZF1

-181 GGGGAGAAGGAAAAGATTGAGAAAAGAGGGAGGGAGAGAGAAAAGGGGAAGCCACAGTGGTAGGCAGTCCCCTTTACTT
 C/EBP-β MZF1 Cbfa1

-100 TGAGTACTGTGAGGTCAAAACCACATGATTCTGTCTCTCCAGTAATAGTGCTTGCAAAAAATAGGAGTTTTAAAGCTTTT
 TATA
 RUNX2-NHEI-U73

-19 GCTTTTTTGATTGTGTGATGTGCTTCATTTCGCCTCACAAACAACCACAGAACCACAAGTGGGTGCAAACTTTCTCCAGGA
 Transcription start site

+63 GGACAGCAAGGAGGCCCTGGTGTTTAAATGGTTAATCTCTGCAGGTCCTACCAGCCA

Figure 3.16: The nucleotide sequence of U1557 and transcription factor binding sites. The broken line depicts the consensus binding sites for known transcription factors. +1 states the transcription start site. The single-

headed arrows represent the annealing site of forward and reverse primers for the amplification of 2 consecutive regions of *runx2* regulatory element.

Table 3.5: Potential transcription factor binding sites identified on U1557 sequence. The consensus sequence and the functional role of each regulatory element were presented.

Transcription factor	Response element (5' ---> 3')	Functional role	Reference
c-Ets	RCCGGAWGY	Cell proliferation, differentiation, and oncogenesis	[148]
AP1	TGASTCAG	Osteoblast Differentiation	[146, 147]
C/EBP	NTKTGGWNANN	Adipocyte differentiation	[146]
C/EBP- β	NRTKNNGMAAKNN	Regulation of adipocytic and osteoblastic genes	[146]
SRY and SOX	WWCAAW	Control of cell developmental processes, such as sex determination, neurogenesis, and skeletogenesis	[145]
Nkx-2	TYAAGTG	Cardiogenic differentiation	[149]
CdxA	MTTATR	Development of intestinal epithelium	[150]
Ik2	NNTTGGGAWNNC	Development of lymphoid lineage	[151]

Table 3.5 (Continued)

Transcription factor	Response element (5' ---> 3')	Functional role	Reference
Oct-1	WNAWTKWSATRYN	Transcriptional control of various genes	[152]
Evi-1	GAYAAGATAA	Cell development and organogenesis	[153]
MZF-1	AGTGGGGA and CCGNGAGGGGGAA	Myeloid differentiation	[154, 155]
Cbfa1	TGYGGT	Osteoblast Differentiation and Bone Development	[156]
Nucleotide codes			
W: A or T	B: C, G, or T		
S: C or G	D: A, G, or T		
R: A or G	H: A, C, or T		
Y: C or T	V: A, C, or G		
K: G or T	N: A, C, G, or T		
M: A or C			

3.5.2 Construction of reporter vectors containing *runx2* regulatory element

3.5.2.1 Cloning of 2 regions of *runx2* regulatory element

The fragment of 5'-UTR of *runx2* gene (called U1557) were successfully cloned. It was used for studying signaling pathway related to *runx2* transcription. To decrease errors on PCR amplification, the U1557 fragment was divided into two consecutive parts called *runx2*-N and *runx2*-F. The primers for *runx2*-F amplification consisted of *runx2*-KPNI-U796 (forward primer) and *runx2*-NHEI-U73 (reverse primer), while the primers for *runx2*-N amplification included *runx2*-KPNI-U1526 (forward primer) and *runx2*-NHEI-U630 (reverse primer) (Figure 2.15, step 1).

The single sharp bands of *runx2-N* and *runx2-F* were located at 0.7 and 0.9 kb, respectively (Figure 3.17a). To decontaminate any impurities, the PCR products were purified by gel purification (Figure 3.17b).

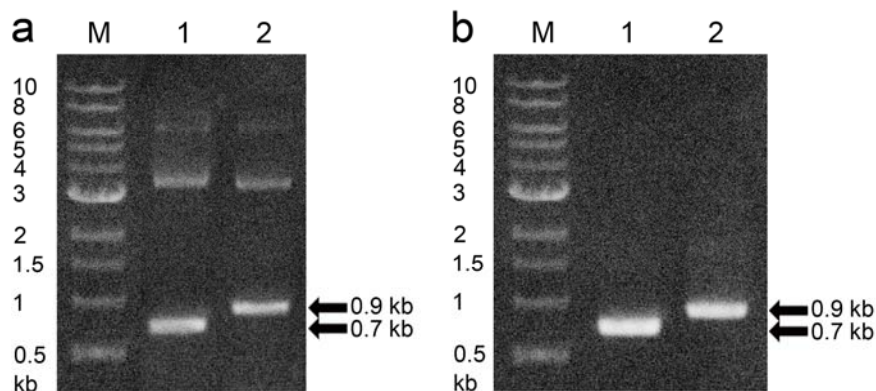


Figure 3.17: The results of *runx2-N* and *runx2-F* amplification and purification. (a) Amplification of 2 regions of *runx2* regulatory element using pGEM-U1557 as a template. Two sets of primers were used, and 2 PCR products, *runx2-N* (lane 1) and *runx2-F* (lane 2), were obtained. (b) The purified *runx2-N* and *runx2-F* bands in lane 1 and lane 2, respectively. M: 1 kb DNA marker.

3.5.2.2 Construction of pGEM-*runx2-N* and pGEM-*runx2-F*

The purified *runx2-N* and *runx2-F* were ligated with pGEM-T[®] easy cloning vector to result in the recombinant plasmids named pGEM-*runx2-N* and pGEM-*runx2-F*, respectively (Figure 2.15, step 3). These recombinant plasmids were separately transformed into *E. coli* strain DH5 α , multiplied, and extracted by using Nucleospin[®] Plasmid column, and analyzed for DNA insertion by restriction enzyme digestion (Figure 2.15, step 4 to 7). The purified plasmids were digested with *Kpn*I and *Nhe*I and separated on 0.7% agarose gel (Figure 3.18). Linearized pGEM-T[®] easy vector was obtained at 3 kb, while the DNA inserts of *runx2-N* and *runx2-F* were located at 0.7 kb and 0.9 kb, respectively.

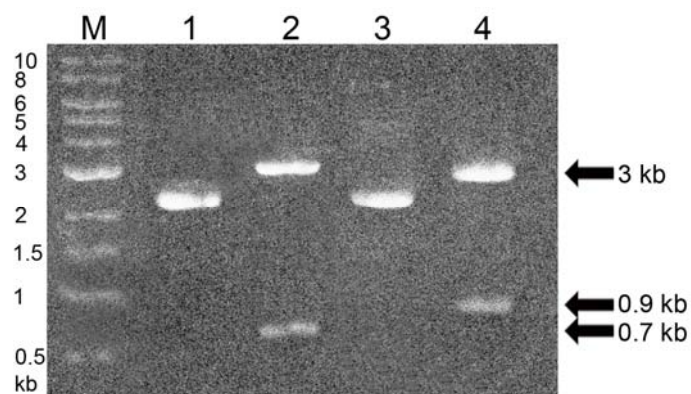


Figure 3.18: Insertion analysis of pGEM-*runx2-N* and pGEM-*runx2-F*. The *KpnI* and *NheI* digestion resulted in a fully cut of the pGEM-*runx2-N* (lane 2) and pGEM-*runx2-F* (lane 4) compared to the undigested plasmids (lane 1 and 3). M: 1 kb DNA marker.

3.5.2.3 Construction of pGL3-*runx2-N* and pGL3-*runx2-F* reporter vector

runx2-N and *runx2-F* fragments from the cloning vector were subcloned into the reporter vector (pGL3-Promoter vector). These DNA fragments were previously digested with *KpnI* and *NheI*, separated on 0.7% agarose gel, and purified by gel purification column (Figure 2.16, step 1 and 2). Figure 3.19 revealed the bands of *KpnI* and *NheI* digested pGEM-*runx2-N* (Figure 3.19a) and that of pGEM-*runx2-F* (Figure 3.19b) at 0.7 kb and 0.9 kb, respectively. Single bands of *runx2-N* and *runx2-F* were obtained by gel purification (Figure 3.19c).

To generate compatible ends for efficient ligation, the pGL3-Promoter vector was digested with *KpnI* and *NheI* as well. The digestion reaction was separated on 0.7% agarose gel, and the selected bands were cut and purified (Figure 2.16, step 1 and 2). The size of *KpnI* and *NheI* treated pGL3-Promoter vector was 5 kb (Figure 3.20a). After purification, the digested vector were examined by gel electrophoresis (Figure 3.20b, lane 2). PCR analysis of the vector was performed using LUC-F and LUC-R primer. These primers were designed to annealed at the upstream

and downstream of multi-cloning site of the vector which the amplification covered the digested region. The resulted PCR product of undigested pGL3-Promoter vector was 0.7 kb (Figure 3.20b, lane 3), while the product of the digested vector was not obtained (Figure 3.20b, lane 4).

runx2-N and *runx2-F* fragments were then ligated with pGL3-Promoter vector, transformed into *E. coli* strain DH5 α , isolated from bacterial transformants, and examined by *KpnI* and *NheI* digestion and PCR analysis (Figure 2.16, step 3 to 7). The digestion of recombinant plasmids called pGL3-*runx2-N* and pGL3-*runx2-F* revealed the insert bands at 0.7 kbp (Figure 3.21, lane 2) and 0.9 kbp (Figure 3.21, lane 4), respectively. On analyzing by PCR using LUC-F and LUC-R as the primers, different sizes of PCR products were obtained. For the pGL3-Promoter vector, the product was located at 0.7 kb (Figure 3.21, lane 5). For pGL3-*runx2-N* and pGL3-*runx2-F*, the product sizes were of 1.4 kb and 1.6 kb, respectively (Figure 3.21, lane 6 and lane 7). The sequences of *runx2-N* and *runx2-F* inserts were verified by DNA sequencing (Figure 2.16, step 8). By performing sequence alignment, a 100% similarity between U1557 and the DNA inserts was demonstrated (Appendix C). The nucleotide sequence of *runx2-N* was correspond to the position of -796 to -73 from *runx2* transcription start site, and that of *runx2-F* was identical at the position of -1526 to -630 from the start site. These reporter vectors were successfully cloned and used for further transfection experiment.

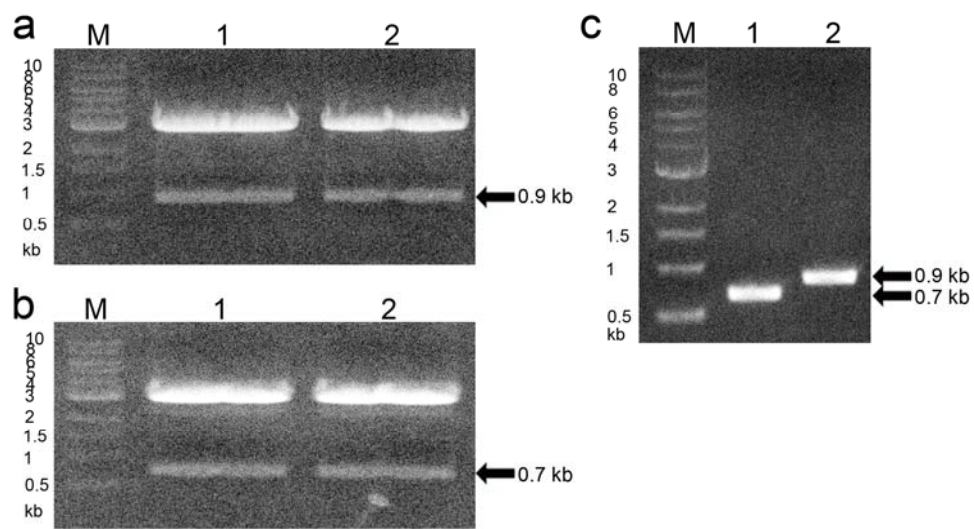


Figure 3.19: *KpnI* and *NheI* digestion of pGEM-*runx2-N* and pGEM-*runx2-F*. The digestion products of pGEM-*runx2-N* (a) and pGEM-*runx2-F* (b). Bands of interest were purified bands using NucleoSpin[®] Extract II column. The purified *runx2-N* (c, lane 1) and *runx2-F* (c, lane 2). M: 1 kb DNA marker.

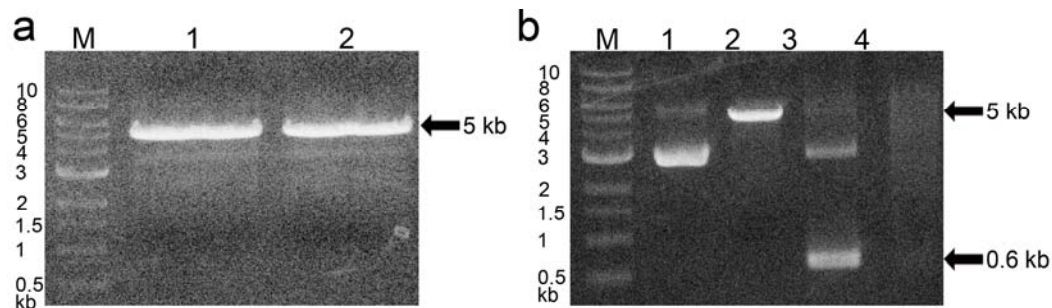


Figure 3.20: Preparation of pGL3-Promoter vector. (a) The pGL3-Promoter vector was digested with *KpnI* and *NheI* resulting in a linearized vector at the size of 5 kb. The uncut pGL3-Promoter vector (b, lane 1), the digested vector (b, lane 2), and the PCR analysis of undigested and digested vector (b, lane 3 and 4). The PCR reaction using LUC-F and LUC-R primers and the uncut pGL3-Promoter vector as a template resulted in 0.7 kb PCR product, but the digested vector did not provide any product. M: 1 kb DNA marker.

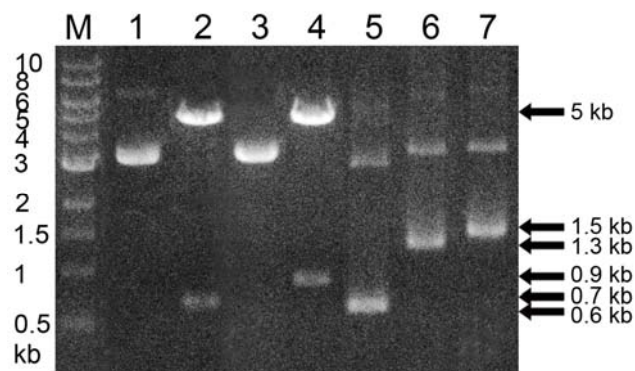


Figure 3.21: Insertion analysis of pGL3-*runx2*-N and pGL3-*runx2*-F. Lane 1 and 3 were the extracted pGL3-*runx2*-N and pGL3-*runx2*-F, respectively. Lane 2 and 4 were *KpnI* and *NheI* digested product of these plasmids. Lane 5-7 were the bands from PCR using pGL3-Promoter vector, pGL3-*runx2*-N, and pGL3-*runx2*-F as a template, respectively. LUC-F and LUC-R primers were used as a forward and reverse primer, respectively. Insertion of *runx2*-N and *runx2*-F in the vector resulted in an increase of the product size, compared to the reaction using pGL3-Promoter vector without DNA insert. M: 1 kb DNA marker.

3.5.3 Construction of reporter vectors containing tandem repeat of transcription factor binding site (pGL3-5X*ap1* and pGL3-5X*sry*)

The pGL3-Promoter vector was firstly digested with *KpnI* and *BglII* and purified by gel purification technique (Figure 2.17, step 1 and 2). The resulted products were about 5 kb (Figure 3.22c). The synthesized double-strand oligonucleotides of tandem repeat for *ap1* (called 5X*ap1*) and for *sry* (called *sryX5*) were ligated with the prepared pGL3-Promoter vector, transformed into *E. coli* strain DH5 α , multiplied, and extracted from transformants by using Nucleospin[®] Plamid column (Figure 2.17, step 4 to 6).

The positive colony was selected by PCR-based screening using LUC-F and LUC-R as the primers. In Figure 3.23a, lane 3 and Figure 3.24a, lane 3, the length of PCR product was increased. After that, these recombinant plasmids were further analyzed by *KpnI* and *BglII* digestion aiming to obtain a product of 5 kb. For PCR analysis, specific reverse primers for pGL3-5X*ap1* (named *ap1*-LUC) and pGL3-5X*sry* (named *sry*-LUC) and the LUC-F forward primer were used, and the PCR products were obtained at 0.5 kb (Figure 3.23b and Figure 3.24b). Finally, the pGL3-5X*ap1* and pGL3-5X*sry* were proved by DNA sequencing.

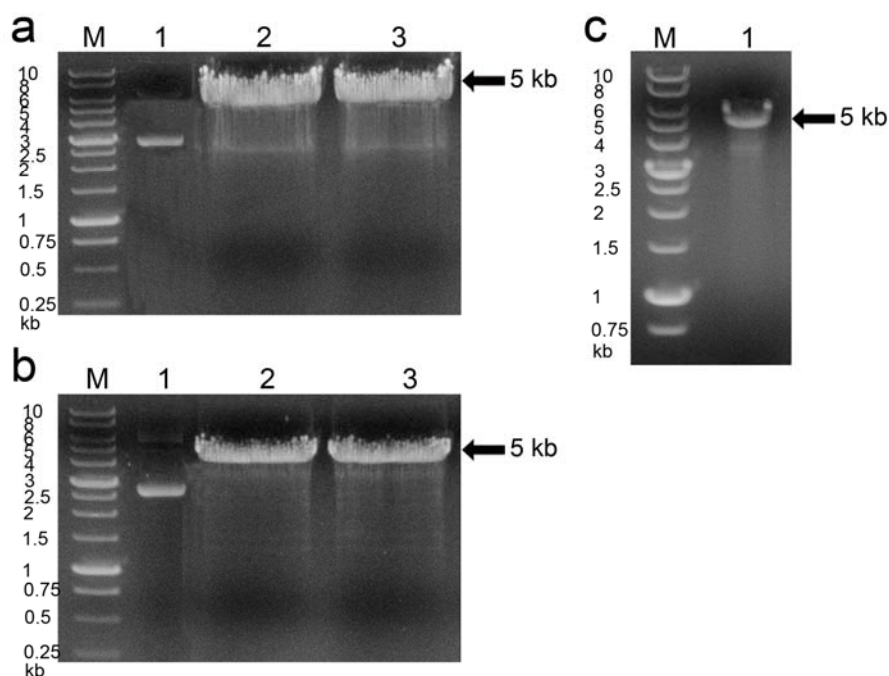


Figure 3.22: Preparation of pGL3-Promoter vector by sequential digestion with *KpnI* and *BglII*. (a) pGL3-Promoter vector in lane 1 and *KpnI* single cut plasmid in lane 2 and 3. (b) Purified *KpnI*-cut vector in lane 1 and *KpnI* and *BglII* digested product in lane 2 and 3. (c) Purified pGL3-Promoter vector containing *KpnI* and *BglII* overhang. M: 1 kb DNA marker.

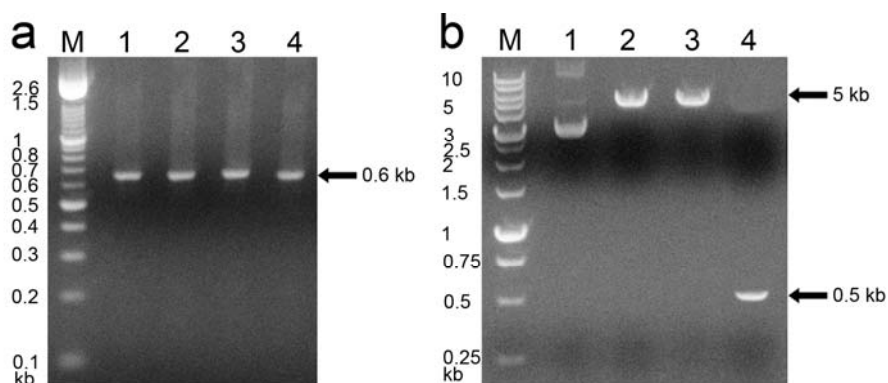


Figure 3.23: Screening and analysis of pGL3-5Xap1 by PCR using LUC-F and LUC-R as the primers. PCR screening of pGL3-Promoter vector (a, lane 1) and the extracted pGL3-5Xap1 plasmids from different clones (a, lane 2-4). The *KpnI* digestion (b, lane 2), *BglII* digestion (b, lane 3), and PCR using LUC-F forward primer and *ap1*-LUC reverse primer (b, lane 4) of the pGL3-5Xap1 plasmid from a selected clone. M: 1 kb DNA marker.

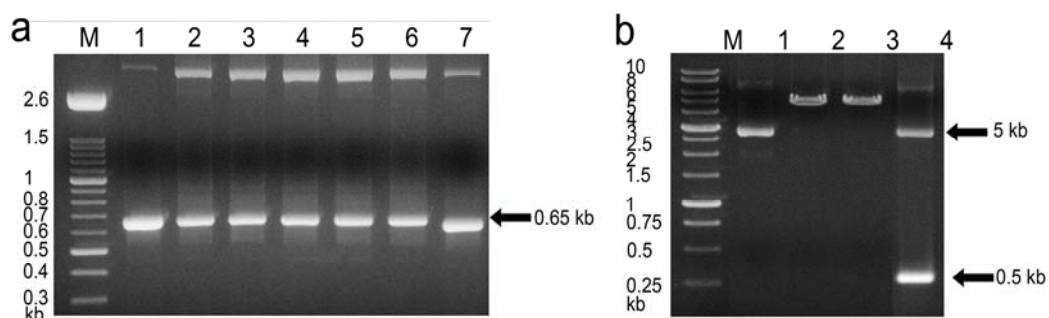


Figure 3.24: Screening and analysis of pGL3-5Xsry by PCR using LUC-F and LUC-R as the primers. PCR screening using pGL3-Promoter vector (lane 1 and 7) and the extracted pGL3-5Xsry plasmids from different clones (lane 2-6) as a template. Further analysis of the selected clone by *KpnI* digestion (b, lane 2), *BglII* digestion (b, lane 3), and PCR using LUC-F forward primer and *sry*-LUC reverse primer (b, lane 4). M: 1 kb DNA marker.

3.6 Assay of the luciferase activity

The effects of FGF2 and insulin on *runx2* gene expression were determined by using luciferase reporter assay. RBMSCs of passage 4 were co-transfected with the experimental vector (pGL3-*runx2*-N, pGL3-*runx2*-F, pGL3-5X*ap1*, or pGL3-5X*sry*) and the internal control plasmid (pRL-SV40 vector). After that, the transfected cells were treated with FGF2, insulin, or FGF2 plus insulin for 1 day followed by starvation in medium plus 2% FBS for 1 day. The cells were lysed in PLB. In the same sample, the firefly luciferase activity of the experimental vector was firstly detected and quenched before the *Renilla* luciferase activity of the control vector was measured.

3.6.1 Preparation of reporter vectors

To prepare the reporter vectors including pGL3-Control vector, pGL3-Promoter vector, pGL3-*runx2*-N, pGL3-*runx2*-F, pGL3-5X*ap1*, pGL3-5X*sry*, and pRL-SV40, midi scale plasmid extraction using QIAGEN plasmid midi kits was performed (Experiment 2.3.7.1). The plasmid DNA was extracted from transformed *E. coli* strain DH5 α using procedures as recommended by the manufacturer (QIAGEN). The isolated plasmids were analyzed by *KpnI* digestion, and the plasmid concentration was determined. The results were shown in Table 3.6.

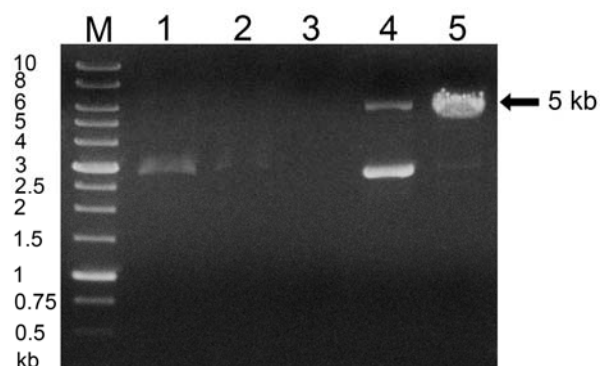


Figure 3.25: An example for preparing of pGL3-5Xap1 plasmid for transfection. The plasmid was extracted from transformed *E. coli* strain DH5 α using QIAGEN plasmid midi kit. Lane 1-3 show the appearances from the cleared cell lysate, the flow-through fraction, and the wash fraction from QIAGEN-tip, respectively, on 0.7% agarose gel. The eluted plasmid and the *Kpn*I digested plasmid are in lane 4 and 5. M: 1 kb DNA marker.

Table 3.6: The recombinant plasmid purified by using QIAGEN plasmid midi kit, and their corresponding concentrations.

Plasmid	Concentration ($\mu\text{g}/\mu\text{l}$)
pRL-SV40 vector	1.8
pGL3-Control vector	1.2
pGL3-Promoter vector	1.45
pGL3- <i>runx2</i> -N	0.92
pGL3- <i>runx2</i> -F	0.97
pGL3-5Xap1	1.36
pGL3-5Xsry	1.5

3.6.2 Transfection optimization

To optimize transfection condition, the pGL3-Control vector and pRL-SV40 vector were used as the experimental vector and the internal control vector, respectively. The ratio of FuGENE[®] 6 transfection reagent to DNA and of the experimental vector to the control vector were varied. After transfection, the cells were cultured in the medium supplemented with 2% FBS for 1 day, and the activities of firefly and *Renilla* luciferase were measured and expressed as the relative light units (RLUs). Which condition is suited was judged by balancing between transfection efficiency and cytotoxicity. Transfection efficiency was evaluated from these luciferase activities, while the cell viability was estimated from the total protein content of the cell lysate. The results of this optimization were shown in Table 3.5. The highest transfection efficiency were obtained by the condition 7. The ratio between the experimental vector and the control vector was set at 50:1. When the amount of the former vector was 0.4 µg, the amount of the later vector was calculated to be of 8 ng. In consequence, the transfecting reagent to be added to the mixture was 2.4 µl. By using this condition, the cell viability was not strongly affected, because the lysate samples of transfected and non-transfected cells contained similar protein concentration (Table 3.7). Thus, this condition was used for further experiment.

Table 3.7: The results for the optimization of transfection conditions. The optimal condition gave the highest firefly and *Renilla* luciferase activities with no impact on cell viability (highlighted in bold).

Optimization conditions						
Conditions	Reagent to DNA ratio	Amount of experimental vector (μg)	Experimental vector to control vector ratio	RLUs (firefly luciferase)	RLUs (<i>Renilla</i> luciferase)	Protein concentration ($\mu\text{g/ml}$)
1	3:1	0.2 μg	50:1	64	189	27.80
2			200:1	111	191	55.76
3		0.4 μg	50:1	4641	488	47.11
4			200:1	75555	811	41.06
5	6:1	0.2 μg	50:1	6450	131	25.21
6			200:1	15422	225	27.80
7		0.4 μg	50:1	215607	14768	39.04
8			200:1	74	175	43.94
9	Non-transfection control			73	172	37.60

3.6.3 Luciferase reporter assay

Luciferase reporter assay is one of the tools for studying gene expression. The DNA fragment of interest is inserted upstream of luciferase gene in which the expression is controlled by the target sequence. In this study, the role of FGF2 and insulin on *runx2* gene transcription was evaluated by cloning two consecutive regulatory elements of *runx2* into pGL3-Promoter vector. Two plasmids were obtained, namely pGL3-*runx2*-N and pGL3-*runx2*-F. To specify the intracellular signaling pathway induced by FGF2 and insulin, another two vectors containing five repeats of *ap1* and *sry* binding motif were constructed. The resulting plasmids called pGL3-5X*ap1* and pGL3-5X*sry* were acquired. There were four reporter plasmids (pGL3-*runx2*-N, pGL3-*runx2*-F, pGL3-5X*ap1*, and pGL3-5X*sry*) to be used in transfection experiment as the experimental vectors, while pRL-SV40 vector was used as the internal control vector. A pair of the experimental vector and the control vector was co-transfected into RBMSCs of passage 4. The transfected cells were induced with 2.5 ng/ml FGF2, 60 ng/ml insulin, or FGF2 plus insulin for 1 day before the activities of firefly and *Renilla* luciferase were measured and reported as RLU.

In pGL3-*runx2*-N transfected cells, the RLUs were increased by 4 and 3.5 folds when the cells were respectively induced by insulin and FGF2 plus insulin (Figure 3.26a). The lower RLUs (1.5-2.5 folds) were found for the cells transfected with pGL3-*runx2*-F regardless of the used inducers (Figure 3.26b). By transfected with pGL3-5X*ap1*, the RLUs were increased by 2 folds after induced by FGF2 plus insulin (Figure 3.26c). In contrast, the RLUs were reduced for the cells transfected with pGL3-5X*sry* following challenged by FGF2 (Figure 3.26d).

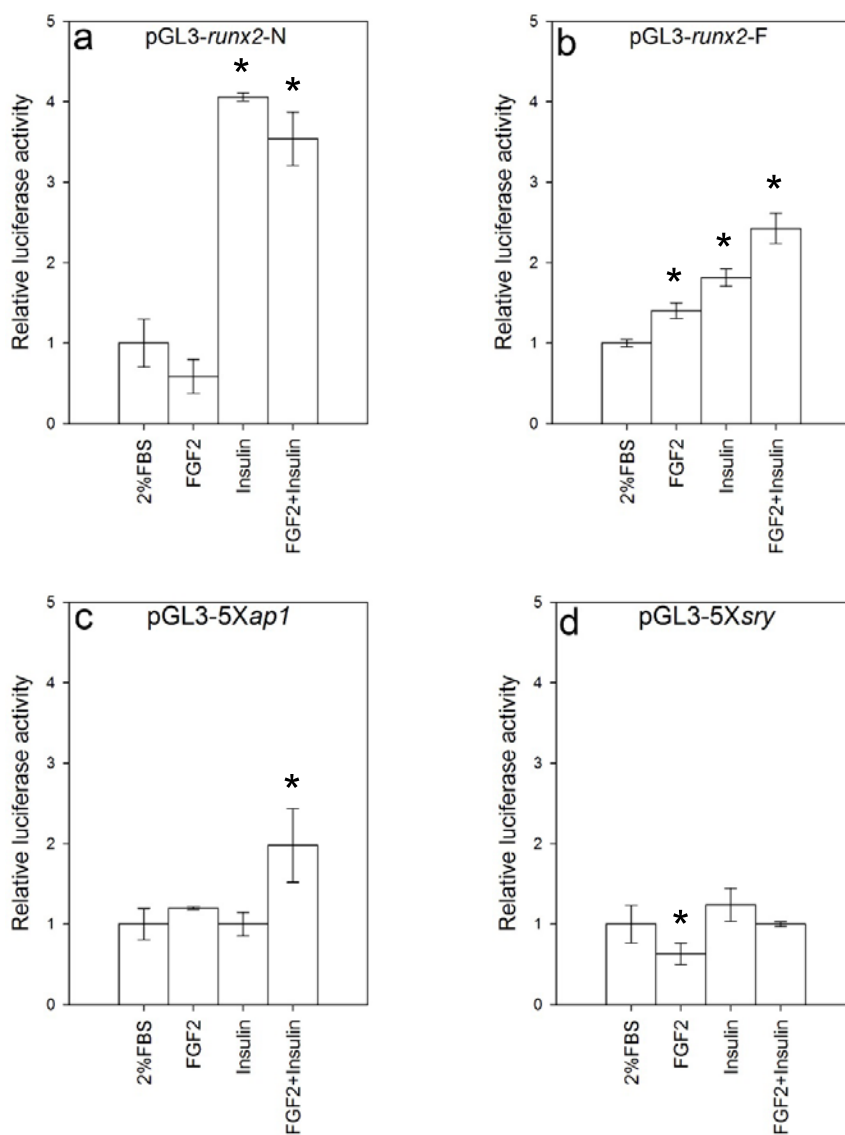


Figure 3.26: Relative luciferase activity of RBMSCs transfected with (a) pGL3-*runx2*-N, (b) pGL3-*runx2*-F, (c) pGL3-5X*ap1*, and (d) pGL3-5X*sry*. The transfected cells were induced with 2.5 ng/ml, 60 ng/ml insulin, or FGF2 plus insulin for 1 day followed by starvation for 1 day using medium plus 2% FBS. The cells grown in 2% FBS containing medium were used as the control. Luciferase activity assay was carried out for the induced cells after 1 day of starvation in the medium supplemented with 2% FBS. * indicates significant differences ($p < 0.05$).

CHAPTER 4

DISCUSSION

4.1 Characteristics of HBMSCs

In the 1960s, Friedenstein and colleagues have discovered multipotent progenitor cells or MSCs in bone marrow. The adherent cell fraction expanded and established the colonies initiated from a single cell which were defined as colony-forming unit fibroblasts [157-159]. The investigators have found that these cells differentiated under appropriate conditions to various types of connective tissue including bone, cartilage, adipose tissue, and muscle, which appeared to be a promising tool for experimental and clinical study. However, worldwide use of MSCs in regenerative medicine is hindered by their characteristics which are inconsistent among the research groups. Several methods have been developed for cell isolation from adult tissues resulting in heterogeneous population of the cells. In addition, differences in animal strain or cell culture condition also affect the cell properties [119, 120]. Variation in these laboratory techniques lead to a question of whether the isolated cells can be compared with other reports. Therefore, cautious characterizations of the cells are very important.

In this study, mononuclear cell fraction from human marrow aspirate was isolated by using density gradient centrifugation. The separation is based on the differences in cell density. After centrifugation, erythrocytes and granulocytes were sedimented through the density centrifugation medium, while the mononuclear cells were accumulated between the layer of plasma and density centrifugation medium. The cells in this interphase layer was collected and cultured in a plastic culture flask. The non-adherent cells were removed simultaneously with discarding the culture medium. The adherent cells (or HBMSCs) showed fibroblastic-like shape (Figure 3.1). This cell morphology was maintained at early stages of cultures. After continuously subcultured, the cells trended to lose their phenotype, as revealed that the cells of passage 5 changed from the spindle shape to be large polygonal or cuboidal cells (Figure 3.1d). In

addition, the growth rate was shown to be altered. These findings were in an agreement with the previous reports [160, 161]. The long term culture of MSCs would result in cell aging for which morphological deterioration and reduced proliferation and differentiation capacity were observed.

The keys advantages of MSCs are self-renewal and multipotency. However, the properties have been controlled by several factors. For example, OCT4, SOX2, and Nanog have been determined as the core transcriptional factors that regulate the differentiation potency of stem cells [134, 140]. FGF4 and REX1 have been reported as a multipotent marker of stem cells. These factors have been proven to be a target of OCT4 transcriptional activation [139, 144]. The self-renewal property of stem cells has been controlled by the activity of TERT in a prevention of telomere shortening [143]. Moreover, BST1 found in bone marrow stromal cells has been described to be involved with hematopoietic progenitor cell proliferation [141-142]. In this study, the expression of stem cell-associated genes including *oct4*, *sox2*, *nanog*, *fgf4*, *rex1*, *bst1*, and *tert* were measured upon the subculturing. The RT-PCR results revealed that the expression of *oct4*, *sox2*, *nanog* and, *fgf4* were decreased in HBMSCs of passage 5 (Figure 3.3). Changes in the gene expression of the major transcription factors denoted the reduction of the undifferentiated stage of stem cells in the later passage [162-164]. However, increased expressions for *tert* and *bst1* gene were observed. The impact of *tert* expression has been reported to be positive on cell proliferation and telomere length [165], resulting in cancer development [166]. Thus, the abnormal cell morphology for HBMSCs of passage 5 might be relative to the higher level of *tert* mRNA. The loss of stem cell properties in this study might also contribute by the nature of the cells, in which the bone marrow samples were obtained from hematological disorder patients. As a result, HBMSCs should be grown by subculturing for less than 5 passages.

The surface antigen markers of HBMSCs of passage 2 was examined by flow cytometry technique. About 76-100% of the isolated HBMSCs population expressed CD10, CD13, CD29, CD44, CD73, and CD90 (Figure 3.2 and Table 3.1). Twenty six percent of the cell population showed CD14, CD34, and HLA-DR, but 60% of the cell population had CD45. The expression of CD29, CD44, CD73, and CD90 by MSCs has been reported [167], whereas CD14, CD34, and CD45, which are the hematopoietic markers, have been undetected. Thus, the isolated HBMSCs had a surface antigen pattern of stem cells, although the hematopoietic markers were also detected. This

might be due to the isolation method in that all of mononuclear cells were collected. Since the mononuclear cells in bone marrow consist of the cells in hematopoietic lineage [168] (such as lymphoid progenitors and monocytic progenitors), these cells were in accompany with other mononuclear cells during isolation. This finding was consistent with the previous study [169], indicating that the isolated MSC from rat bone marrow has been a mixture of cells expressing CD45 up to 75% of the cell population. To improve the homogeneity of the cells isolated, antibody-based isolation methods such as immunodepletion and fluorescence-activated cell sorting (FACS) might be suggested.

4.2 Osteogenic induction of HBMSCs

MSCs in bone marrow cell population have been estimated to be less than 0.01% [106-108]. These cells can be expanded by serial subculture to a desired number. For clinical application of bone tissue engineering, large amounts of the cells are needed. Although, MSCs are multipotent, that be able to differentiate into various lineages, the specific differentiation strictly depends on culture conditions. Therefore, the cell culture step is very important. This manipulation should not be to disturb the self-renewal and differentiation potential of the cells. Many studies have exhibited a potential use of growth factors to enhance the osteogenic differentiation of MSCs [170, 171]. At different stage of osteogenesis, it is orchestral governed by several factors. The combination or subsequent induction by growth factors have been developed to imitate the natural process [130].

HBMSCs were treated with FGF2 followed by BMP2 (Figure 2.7), and the expression level of stem cell-associated genes and osteogenic genes were measured. The mRNA levels of *fgf4*, *sox2*, and *bst1* were significantly elevated, while *oct4* and *tert* were decreased after the activation (Figure 3.4). Numerous factors that control the cells proliferation and maintain their multipotency have long been studied. However, little is known for their mechanisms at molecular levels. Among these factors, OCT4, SOX2, Nanog, FGF4, REX1, BST1, and TERT have been proven to be specific for the stem cells [139-144]. The reduction of *oct4* expression has been suggested to be an indicator of somatic differentiation of MSCs [164]. The results indicated that FGF2 and BMP2

affected the undifferentiated stage of stem cells by inducing differentiation. For osteogenic gene expressions, mRNA level of *runx2* was not changed (Figure 3.4). The up-regulation of *opn* and *bsp* were significantly detected, but the levels of *osc* and *alp* mRNAs were down-regulated. ALP is known as an early marker of osteoblastic differentiation [135], and OSC which is a non-collagenous protein in mineralized bone matrix, is secreted by osteoblasts [172]. OPN and BSP are normally found in the differentiated osteoblasts, involving in calcium phosphate crystal formation and osteoblast adhesion to the formed matrix [173, 174]. A decrease in *alp* expression might reflect a terminal differentiation stage of osteoblastic lineage, in agreement with the previous study [175]. These gene expression patterns might be the induction signal of FGF2 and BMP2 that following activated the osteogenic differentiation of HBMSCs. The sequential induction using FGF2 and BMP2 has been explored using MSCs derived from rat [130], suggesting the improvement of osteogenic differentiation by increasing the expression of *runx2*, *bmp2*, *alp*, and *bsp* genes. The expression of *runx2* and *alp* were incomparable between human and rat MSCs, so different cell source might influence the responses of the cells to the growth factors.

4.3 Characteristics of RBMSCs

Since the availability of human bone marrow aspirates from healthy donors have not been sustained. MSCs derived from rat bone marrow (RBMSCs) was used as the cell model for the next investigations. These cells were separated from granulocytes and red blood cells by using density gradient centrifugation technique and cultured in plastic culture vessel. After the medium was discarded, the non-adherent cells were removed remaining the spindle-like cells attached to the flask. These cells proliferated and grew to form colonies (Figure 3.5). During continuous passaging, the cells morphology was enlarged, while the growth rate was significantly decreased, in consistent with that of the HBMSCs culture (Figure 3.1d). It was suggested that the cells of higher passage was differentiated or aged. The changes in cell properties might be consequences of prolong culturing and the effect of serum supplemented in the culture medium. Therefore, the method for stem cell culture that can sustain the cell properties needs to be developed. It might be that for properly used, the cells should

not be grown exceeding the 7th passage. Accordingly, RBMSCs of passages between 2 and 4 were used for all experiments.

4.4 Bone-related growth factors for RBMSCs

Bone marrow-derived MSCs are an easily accessible cell source. Due to their multipotential property, these cells is beneficial for bone tissue engineering. Unfortunately, they are found in a very rare number among the cells of bone marrow. To be applicable in tissue engineering technique, it is needed to increase the cell numbers and maintain their osteogenic differentiation potential. In the previous study, the sequential induction condition using FGF2 followed BMP2 has been developed [130]. The strategy has based on using FGF2 to initiate cell proliferation and osteogenic commitment. The full induction to obtain osteogenic differentiation has been achieved by using BMP2. Since very low concentrations of these growth factors have been inoculated, the method has provided interesting results on improving bone formation *in vivo*. However, the cost of treatment has been still high. Finding a new inducing factor with comparable or improved osteoinduction property is thus interesting. Many studies have reported the impacts of insulin on bone development. For example, localized insulin treatment had promoted diabetic fracture healing in rat model [176]. Thus, insulin became a candidate for proliferation induction in this study. If it be effective, the treatment cost using insulin is much lower than using FGF2. FGF2, insulin, and their combination were determined for proliferative effect and directing MSCs to be cells ready to become osteoblast. The supportive property of FGF2 and insulin on proliferation and osteoblastic commitment was determined by measuring the numbers of growing cells, the expression levels of osteoblastic genes, and BMP2 protein, ALP activity, and mineralization. BMP2, BMP7, and their combination were tested for differentiation induction effect in the second phase, and the markers for osteoblastic differentiation including the expression levels of osteoblastic genes, ALP activity, and mineralization were determined.

After the cells were treated with FGF2 (2.5 ng/ml for 1 day), the numbers of growing cells were comparable with the control group. Even though the proliferative and angiogenic effects of FGF2 were expected, these require very high dose of FGF2 [177].

The mRNA levels of osteogenic transcription factors (including *runx2* and *osx*), osteogenic protein (*bmp7*), and WNT pathway-related proteins (consisted of *axin2*, β -*catenin*, and *dkk1*) were slightly decreased by FGF2 induction (Figure 3.7). These results were not consistent with the previous study [130], because *runx2* expression has been increased by FGF2. The inconsistency might be due to the different cell type and cell stage. However, BMP2 protein, ALP activity and calcium deposition were evaluated by FGF2 induction (Figure 3.9 and Table 3.3). These parameters donated the osteogenic differentiation of the treated cells. In summation, FGF2 (2.5 ng/ml) was able to direct RBMSCs to be osteoblasts, although its proliferative effect was scant.

For insulin treatment (60 ng/ml for 1 day), significantly improved cell propagation was observed, indicating the effect on RBMSCs. However, all of tested genes were not affected by insulin, excepted for *bmp7* that be enhanced (Figure 3.7). Interestingly, insulin had positive effect on BMP2 synthesis at 24-hours post-induction (Figure 3.9). It might be that insulin mediated osteogenic commitment via BMPs. In addition, the ALP activity and calcium deposition were increased by insulin (Table 3.3). Therefore, insulin functioned as a mitogen and osteoblastic inducer on RBMSCs.

In the presence of FGF2 and insulin, the cell numbers were significantly increased compared to those treated with FGF2 alone. All of tested genes were significantly up-regulated (Figure 3.7). The increase of *runx2* and *osx* transcription was demonstrated. This activation would be via WNT signaling affecting on cell growth. Since β -catenin and insulin have been shown to increase *runx2* and *osx* expression [88, 178]. The up-regulation of *bmp7* gene and BMP2 protein level by FGF2 plus insulin suggested the mechanisms regulating osteogenic differentiation by both BMP2-dependent and BMP2-independent manners [179]. FGF2 and insulin might cooperatively stimulate cell proliferation via WNT pathway because of the up-regulation of β -*catenin* [80]. The negative feedback loop for balancing the activation of β -catenin was assumed to occur due to the stimulated expression of WNT inhibitors, *axin2* and *dkk1*. These results were consistent with the previous studies [180, 181]. These finding confirmed the presence of multi-molecular network for controlling osteogenesis. However, ALP activity was lowered by this treatment, whereas mineralization was increased (Table 3.3). Indeed, a low but functional level of ALP activity has been found to support mineralization of pre-osteoblasts [182]. The decreased ALP activity could be defined for the termination of

osteoblastic differentiation in agreement with the previous report [175]. Taken together, used of FGF2 in combined with insulin was able to induce cell growth and sensitize RBMSCs to be osteoblasts.

The property on inducing RBMSCs differentiation of BMP2 and BMP7 were determined. The expression levels of *runx2* and *osx* were not enhanced by BMP2 (10 ng/ml for 1 day; Figure 3.8). This result was in contrast to the previous reports, indicating the stimulated expression of the genes by BMP2 [183, 184]. The expression of *bmp7* was also suppressed by BMP2. The effect was supposed to be via the negative feedback loop of BMP signaling pathway, as suggested by Heldin, *et al* [185]. β -*catenin* and *dkk1* mRNA were reduced by BMP2 that was not in agreement with the previous study [186]. It might be influenced by the cell stage difference, which responses to BMP2 in different ways.

By treated with BMP7 (10 ng/ml for 1 day), the expression levels of *runx2* and *osx* were increased (Figure 3.8), indicating an effective osteogenic factor of BMP7 on RBMSCs. The reduction of *bmp7* gene expression was apparent. This might involve in controlling *bmp7* expression via the auto-regulation loop of BMPs [185]. The expression levels of *axin2* and β -*catenin* were up-regulated, while *dkk1* level was strongly suppressed. This could be explained by that BMP7 has had a direct effect on WNT pathway by interfering the production of WNT inhibitor but stimulating other transcription mediators [187].

When BMP2 and BMP7 were combined, the up-regulation of *runx2* and *osx* was observed (Figure 3.8). Similarly, *bmp7* gene expression was down-regulated. The expression of *dkk1*, while the level of β -*catenin* was not changed. It could be that the effect of BMP7 on WNT pathway was hindered by BMP2, since the level of β -*catenin* using the combination growth factors was lower than that of using BMP7 alone. Although, ALP activity and calcium content were enhanced by treated with BMP2 and BMP7 (Table 3.4, group A), the results were lower than those of using BMP2 or BMP7 alone. Thus, cautions should be made when applying the BMPs combination to osteogenic culture system.

4.5 Sequential induction of RBMSCs using proliferation factor(s) followed by differentiation factor(s)

By inducing RBMSCs with proliferation factors (FGF2 and insulin) followed by differentiation factors (BMP2 and BMP7) according to Figure 2.8, the expression of *runx2* was increased by the treatment of FGF2 or insulin followed by BMP7 (Table 3.2). In contrast, the level of *runx2* was reduced by FGF2 plus insulin followed by BMP7. It might be that the expression of *runx2* reached the peak level before the detection date, suggesting the accelerating effect for osteoblastic commitment of insulin. For *osx*, the gene expression was enhanced by FGF2 or FGF2 plus insulin followed by BMP2 plus BMP7. The synergistic effect of BMP2 and BMP7 has been due to the activity of heterodimeric BMP2/BMP7 which is higher than the homodimeric form, e.g. BMP2/BMP2 and BMP7/BMP7 [188]. *Bmp7* gene expression was down-regulated in all treated conditions suggesting to trigger the negative feedback loop by BMPs addition. By these treatments, the expression level of *axin2* was not affected (Table 3.2). The expression of β -*catenin* gene was enhanced by insulin followed by BMP7. In contrast, the level of β -*catenin* mRNA was elevated by FGF2 plus insulin, followed by BMP2. Thus, the activity of BMPs was influenced by the proliferation condition. The expression level of *dkk1* was down-regulated by all treatment conditions, suggesting to be controlled by WNT pathway via the reduction of WNT inhibitor. The highest level of ALP activity was determined for FGF2 or insulin followed by BMP7 (Table 3.4). The degree of calcium deposition was comparable in all tested groups.

4.6 *In vivo* bone formation

To evaluate the effectiveness of the induction conditions in developed biological environment, an ectopic bone formation in rat model was carried out. A scaffold was seeded by RBMSCs at a density of 1×10^4 cells. The seeded construct was induced with each induction condition developed previously (Figure 2.11). Then, eight constructs were subcutaneously implanted into the dorsal part of Wistar rats (Figure 2.12). After 8 weeks post-implantation, new bone formation was estimated by histological techniques.

All constructs remained undegraded within the period of implantation (8 weeks) (Figure 3.10). Fibrous tissue was observed around the scaffold surface of all groups. This might be an immunological response of the rat against the scaffolds, in which host fibroblasts were accumulated to cover the foreign material. Bone tissue was not detected in the cell-free scaffolds and non-induced cell-seeded scaffolds (Figure 3.11 to 3.13). A considerable new bone tissue and mineralization was observed when treated the seeded cells with FGF2 followed by BMP2 or BMP7 (Figure 3.11) and those treated with FGF2 plus insulin followed by BMP2 and/or BMP7 (Figure 3.13). No major change in forming new bone occurred in the insulin pre-treated groups (Figure 3.12). The results indicated that insulin could accelerate the activity of FGF2 on bone tissue formation *in vivo*. In addition, blood vessels were identified for cell-seeded constructs formerly induced with FGF2 plus insulin. It was suggested that insulin could preserve the angiogenic effect of low dose FGF2. For insulin pre-induction, the results of *in vitro* experiments were contrast to those acquired from the *in vivo* test. Since native mechanisms that regulate osteogenic differentiation are highly complicated, it might be that numerous intervening factors in the animal contributed to this variation. The synergistic effect of BMP2 and BMP7 was not clearly demonstrated. Therefore, either BMP2 or BMP7 was sufficient for use as the bone differentiation growth factor. In summary, the most efficient *in vivo* osteoinduction condition would be of FGF2 plus insulin pre-treatment, followed by BMP2 or BMP7.

FGF2 has been reported to promote the expression of bone morphogenetic protein receptor-1B and pSmad 1 mRNA and protein [90], resulting in increased bone formation. Therefore, pre-treatment the cells with FGF2 might improve the cellular response to the secondary induction phase by increasing the BMPs receptor and the intracellular mediator. As revealed previously, FGF2 stimulated in bone formation that might be mediated by Runx2 transcription factor (Figure 3.7). Tou and co-workers [189] have also reported the up-regulation of *runx2* in response to BMP7 induction. Accordingly, increased expression of *runx2* might be contributed by FGF2 and BMP7 (Figure 3.8). Instead, the activation of WNT signaling pathway by insulin could enhance the rate of cell proliferation and differentiation. It was suggested that, for fully osteogenic response, both FGF2 and insulin should be used as a combination for pre-sensitizing the cells, regardless of whether the later inducer was.

4.7 Analysis of the regulatory element of *runx2* gene in controlling osteogenesis

Runx2 is a master regulator of osteogenesis, acting as a molecular hub of several osteogenic signaling pathways. The results showed that *runx2* expression level was increased by the induction of FGF2 plus insulin (Figure 3.7), resulting in increased amount of calcium deposition (Table 3.3 and 3.4) and the *in vivo* bone formation (Figure 3.13). In accordance, FGF2 and insulin action on stimulating bone formation might involve *runx2*.

To prove this hypothesis, the promoter region at positions -1557 to +97 from the transcription start site of *runx2* gene was cloned (namely U1557, Figure 3.14) using the chromosomal DNA as the template. The sequence of U1557 was verified and aligned with NCBI database sequences of rat *runx2* promoter. The alignment result revealed a 99% similarity. On identification using TFSEARCH tool for possible transcription factor binding sites [137], several potential transcription factor binding sites were recognized (Figure 3.16). Each binding motif and its functional role was summarized in Table 3.3. Two AP1 binding regions were identified, and the SRY motif were presented of at least 5 consensus. Two conserved region of CBFA1 recognition motifs were demonstrated. Drissi and co-workers [25] have indicated that there are at least 3 CBFA1 binding sites on murine *runx2* promoter. These consensus are responsible for negative feedback of *runx2* expression, and they are known as a target of BMP2 signaling pathway [190]. Other response elements of adipogenic, cardiogenic, and others lineage specific transcription factors were located, such as C/EBP (an adipocyte differentiation factors binding site)

Interestingly, due to that *sry* motif shares the same core binding site with SOX proteins, although these transcription factor are responsible for chondrogenesis [145], possible roles of this binding site in osteogenic cells lineage is thus interesting to be proven. In addition, function of AP1 transcription factor on osteoblastic differentiation has been reported [146-147], suggesting the contribution of *ap1* motif in FGF2 and insulin induction pathway.

4.8 Intracellular signaling pathway of FGF2 and insulin induction

For the cells transfected with pGL3-*runx2-N* vector, the activity of the reporter vector were significantly increased in compared to those of pGL3-*runx2-F*. The *runx2-N* DNA (-73 and -796 fragment of 5' upstream of *runx2* gene) consisted of one C/EBP β consensus (at position -155), one AP1 binding site (at position -369), and two CBFA1 motifs (at positions -199 and -475), while the *runx2-F* DNA (-630 and -1526 fragment of 5' upstream of *runx2* gene) contained three binding sites of C/EBP β (at position -749, -828, and -1239), six SRY/SOX motifs (at positions -860, -965, -973, -999, -1166, and -1214), and one AP1 binding site (at position -1315). The impact of C/EBP β was suggested to be insignificant because the binding consensus was found on both DNA fragments. It had been reported that CBFA1 site was a target of TGF β and BMP2 signaling pathway [190]. Therefore, the binding site of CBFA1 might contribute to an increasing of pGL3-*runx2-N* activity. The presence of SRY/SOX motifs had a negative effect on the reporter gene expression (Figure 3.26d), since the RLUs of cells transfected with five repeats of this binding site were markedly reduced. In addition, FGF2 inhibited the activity of *sry*-dependent luciferase activity. This binding site has been reported as the target of SOX9 in reducing *runx2* expression [191]. The repression of pGL3-5X*sry* reporter activity might indicate the preference of FGF2 for the cells of osteogenic by indirectly reducing the activity of *sry* site. For the cells transfected with five repeats of AP1 binding motif, the luciferase activity was dramatically improved by the co-treatment using FGF2 plus insulin (Figure 3.26c). The co-induction was also induced the activity of pGL3-*runx2-N* and pGL3-*runx2-F* reporter vectors which was in an agreement with the *runx2* gene expression (Figure 3.7). It was concluded that the FGF2 and insulin corporately promoted *runx2* transcription by the activation of the gene promoter. Furthermore, it was expected that FGF2 and insulin co-activated their intracellular signaling pathway, at least in part, through the *ap1* site, in agreement with the previous study [38].

CHAPTER 5

CONCLUSION

Bone tissue engineering is a technique for regeneration of extensive bone loss. Cell-based approach using MSCs is currently developed to engineer the ideal bone graft. However, a major drawback of this approach is that the MSCs is very rare population. In addition, to be successful in bone repair, sufficient cell numbers with osteogenic capacity are needed. In this study, bone marrow-derived MSCs from human (HBMSCs) and rat (RBMSCs) were used as cell models. The identifications of stem cell characteristic for HBMSCs were carried out. The cells were isolated from bone marrow aspirate by using density gradient centrifugation. The selected cells showed stem cell specific surface antigens and expressed many stem cell-associated genes. After challenged by 2.5 ng/ml FGF2 followed by 10 ng/ml BMP2, the cells were activated to be osteogenic cells. Due to being high cost of the treatment, insulin was an alternative for substituting or combining with FGF2 for the induction. RBMSCs were used instead of HBMSCs because of freely available. Insulin was an efficient mitogen compared to FGF2. It also increased ALP activity. However, in combining with FGF2, increased proliferation was also achieved. Many bone related genes were strongly activated. The genes of WNT pathway as well as mineralization were enhanced. In addition, FGF2 and insulin were able to stimulate BMP2 production. Thus, using these combination growth factors, RBMSCs were accelerated to commit into osteoblasts. BMP7 was an effective osteogenic factor for RBMSCs, as the expression of *runx2* and *osx* were significantly increased. Its activity on WNT signaling pathway was observed by the increase of β -*catenin* expression. ALP activity and mineralization were also enhanced by BMP7. The patterns of gene expressions were varied when the cells were treated with the proliferation factor(s) followed by the differentiation factor(s). Calcium deposition was comparable among the treatment. ALP activity was not enhanced by the BMP2 or BMP7, after pre-treated with FGF2 plus insulin. In contrast, the other remaining treatment groups were able to promote the enzyme activity. Indeed, the activity of

BMP2 and BMP7 was influenced by FGF2 and insulin pre-treatment. The effect of these growth factors on an ectopic bone formation was evaluated. Improved bone tissue formation was observed by induced with FGF2 and insulin followed by BMP2 and/or BMP7.

The expression level of *runx2* was strongly increased by FGF2 plus insulin suggesting that Runx2 might be a primary mediator for this induction. By using the reporter gene assay, FGF2 and insulin were found to regulate *runx2* transcription. AP1 was proposed as a transcription factor in signaling cascade of *runx2* expression (Figure 5.1). This expression has been reported to directly regulate by BMPs-Smad signaling pathway and WNT/ β -catenin signaling pathway in which cross-talks between these signals have occurred in nucleus. The level of β -catenin was up-regulated by BMP7, suggesting that BMPs signaling pathway might accelerate WNT/ β -catenin signaling.

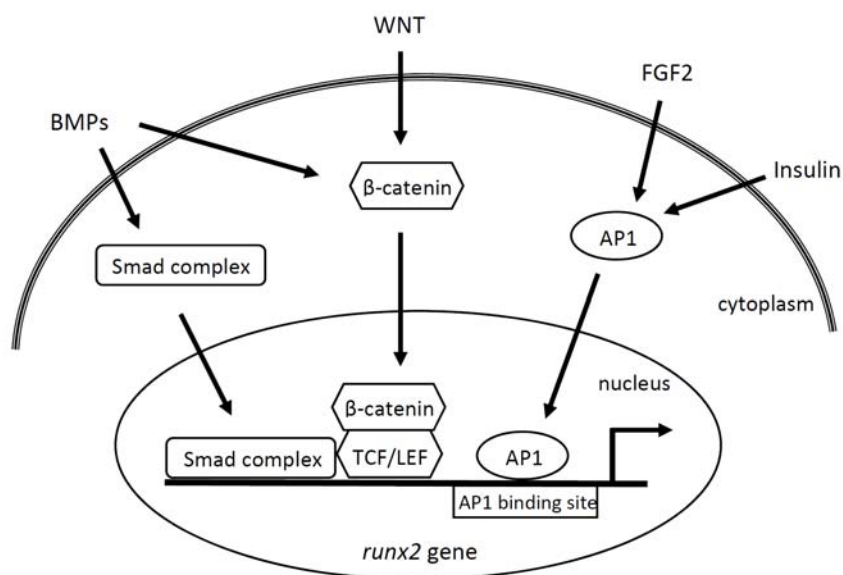


Figure 5.1: The proposed mechanism of *runx2* gene regulation by FGF2, insulin, BMP2, and WNT signaling pathway. BMPs and WNT signaling pathway directly control the *runx2* expression via Smad protein complex and β -catenin, respectively. The common cross-talk of BMPs and WNT signaling pathway occurs in the nucleus. AP1 transcription factor is proven to be one of the mediator of FGF2-insulin co-induction.

The *in vitro* and *in vivo* results indicated the combined effect of FGF2 and insulin on stimulating cell proliferation, mineralization, BMP2 protein production, and new bone formation. Therefore, this use could encourage RBMSCs proliferation along with osteogenic commitment providing the potential induction condition for MSCs. The induced condition would be advantageous in developing of cost-effectiveness condition for preparing cells to be used in bone tissue engineering in the future.

In summary, by comprehensively performing the research to achieve the expected aims, there are points that can be made conclusions as follow

- 1) Insulin could be used in combination with FGF2 as a cost-effectiveness induction condition for MSCs osteogenic differentiation.
- 2) Either BMP2 or BMP7 was sufficient for directing osteogenesis.
- 3) The molecular mechanisms of FGF2 and insulin on bone formation was likely governed by diverse signaling pathway.
- 4) The combination of FGF2 and insulin promoted *runx2* gene expression by activating the intracellular signal through AP1 binding motif on 5'-upstream of *runx2* gene.

REFERENCES

1. Hing KA. Bone repair in the twenty-first century: biology, chemistry or engineering? *Phil Trans R Soc Lond A* 2004;362:2821-50.
2. Hollinger JO, Einhorn TA, Doll BA, Sfeir C, editors. *Bone tissue engineering*. 1st ed. New York: CRC Press; 2004.
3. Cowin SC, editor. *Bone mechanics handbook*. 2nd ed. New York: CRC Press; 2001.
4. Bilezikian JP, Martin TJ, Raisz LG, editors. *Principles of bone biology*. 3rd ed. New York: Academic Press. Inc; 2008.
5. Ritchie RO, Buehler MJ, Hansma P. Plasticity and toughness in bone. *Phys Today*. 2009;62(6):41-7.
6. Buckwalter J, Glimcher M, Cooper R, Recker R. Bone biology. *J Bone Joint Surg Am*. 1995;77(8):1256-75.
7. Martini FH. *Fundamentals of anatomy & physiology*. 6 th ed. San Francisco: Pearson; 2004.
8. Sims NA, Gooi JH. Bone remodeling: Multiple cellular interactions required for coupling of bone formation and resorption. *Semin Cell Dev Biol* 2008;19(5):444-51.
9. College O. Bone structure. OpenStax_CNX; 2013; Available from: <http://cnx.org/content/m46281/latest/?collection=col11496/latest>.
10. Zelzer E, Olsen BR. The genetic basis for skeletal diseases. *Nature* 2003;423(6937):343-8.
11. Karsenty G. Transcriptional control of skeletogenesis. *Annu Rev Genomics Hum Genet*. 2008;9:183-96.
12. Harada S-i, Rodan GA. Control of osteoblast function and regulation of bone mass. *Nature*. 2003;423(6937):349-55.
13. Sudhakar S, Li Y, Katz MS, Elango N. Translational regulation is a control point in RUNX2/Cbfa1 gene expression. *Biochem Bioph Res Co*. 2001;289(2):616-22.
14. Wheeler JC, Shigesada K, Peter Gergen J, Ito Y. Mechanisms of transcriptional regulation by Runt domain proteins. *Semin Cell Dev Biol*. 2000;11(5):369-75.

15. Otto F, Lübbert M, Stock M. Upstream and downstream targets of RUNX proteins. *J Cell Biochem.* 2003;89(1):9-18.
16. Kamachi Y, Ogawa E, Asano M, Ishida S, Murakami Y, Satake M, et al. Purification of a mouse nuclear factor that binds to both the A and B cores of the polyomavirus enhancer. *J Virol.* 1990;64(10):4808-19.
17. Schinke T, Karsenty G. Characterization of *osf1*, an osteoblast-specific transcription factor binding to a critical cis-acting element in the mouse osteocalcin promoters. *J Biol Chem.* 1999;274(42):30182-9.
18. Roca H, Phimpilai M, Gopalakrishnan R, Xiao G, Franceschi RT. Cooperative interactions between RUNX2 and homeodomain protein-binding sites are critical for the osteoblast-specific expression of the bone sialoprotein gene. *J Biol Chem.* 2005;280(35):30845-55.
19. Kern B, Shen J, Starbuck M, Karsenty G. *Cbfa1* contributes to the osteoblast-specific expression of type I collagen genes. *J Biol Chem.* 2001;276(10):7101-7.
20. Ducy P, Zhang R, Geoffroy Vr, Ridall AL, Karsenty Gr. *Osf2/Cbfa1*: a transcriptional activator of osteoblast differentiation. *Cell.* 1997;89(5):747-54.
21. Otto F, Kanegane H, Mundlos S. Mutations in the RUNX2 gene in patients with cleidocranial dysplasia. *Hum Mutat.* 2002;19(3):209-16.
22. Mundlos S, Otto F, Mundlos C, Mulliken JB, Aylsworth AS, Albright S, et al. Mutations involving the transcription factor *cbfa1* cause cleidocranial dysplasia. *Cell.* 1997;89(5):773-9.
23. Yoshida CA, Furuichi T, Fujita T, Fukuyama R, Kanatani N, Kobayashi S, et al. Core-binding factor β interacts with Runx2 and is required for skeletal development. *Nat Genet.* 2002;32(4):633-8.
24. Hecht J, Seitz V, Urban M, Wagner F, Robinson P, Stiege A, et al. Detection of novel skeletogenesis target genes by comprehensive analysis of a *Runx2*^{-/-} mouse model. *Gene Expr Patterns.* 2007;7(1):102-12.
25. Drissi H, Luc Q, Shakoori R, Chuva De Sousa Lopes S, Choi J-Y, Terry A, et al. Transcriptional autoregulation of the bone related CBFA1/RUNX2 gene. *J Cell Physiol.* 2000;184(3):341-50.

26. Jensen ED, Gopalakrishnan R, Westendorf JJ. Bone morphogenic protein 2 activates protein kinase d to regulate histone deacetylase 7 localization and repression of Runx2. *J Biol Chem*. 2009;284(4):2225-34.
27. Jensen ED, Schroeder TM, Bailey J, Gopalakrishnan R, Westendorf JJ. Histone deacetylase 7 associates with Runx2 and represses its activity during osteoblast maturation in a deacetylation-independent manner. *J Bone Miner Res*. 2008;23(3):361-72.
28. Bialek P, Kern B, Yang X, Schrock M, Sosic D, Hong N, et al. A twist code determines the onset of osteoblast differentiation. *Dev Cell*. 2004;6(3):423-35.
29. Komori T. Regulation of skeletal development by the Runx family of transcription factors. *J Cell Biochem*. 2005;95(3):445-53.
30. Backstrom S, Wolf-Watz M, Grundstrom C, Hard T, Grundstrom T, Sauer UH. The RUNX1 Runt domain at 1.25a resolution: a structural switch and specifically bound chloride ions modulate DNA binding. *J Mol Biol*. 2002;322(2):259-72.
31. Aubin JE. Chapter 4 - Mesenchymal stem cells and osteoblast differentiation. In: Bilezikian J, Raisz L, Martin TJ, editors. *Principles of Bone Biology (Third Edition)*. San Diego: Academic Press; 2008. p. 85-107.
32. Nishio Y, Dong Y, Paris M, O'Keefe RJ, Schwarz EM, Drissi H. Runx2-mediated regulation of the zinc finger Osterix/Sp7 gene. *Gene*. 2006;372(0):62-70.
33. Lapunzina P, Aglan M, Temtamy S, Caparros-Martin JA, Valencia M, Leton R, et al. Identification of a frameshift mutation in osterix in a patient with recessive osteogenesis imperfecta. *Am J Hum Gen*. 2010;87(1):110-4.
34. Fu H, Doll B, McNelis T, Hollinger JO. Osteoblast differentiation in vitro and in vivo promoted by Osterix. *J Biomed Mater Res A*. 2007;83A(3):770-8.
35. Nakashima K, Zhou X, Kunkel G, Zhang Z, Deng JM, Behringer RR, et al. The novel zinc finger-containing transcription factor osterix is required for osteoblast differentiation and bone formation. *Cell*. 2002;108(1):17-29.
36. Zhou X, Zhang Z, Feng JQ, Dusevich VM, Sinha K, Zhang H, et al. Multiple functions of osterix are required for bone growth and homeostasis in postnatal mice. *Proc Natl Acad Sci USA*. 2010;107(29):12919-24.
37. Kaback LA, Soung DY, Naik A, Smith N, Schwarz EM, O'Keefe RJ, et al. Osterix/Sp7 regulates mesenchymal stem cell mediated endochondral ossification. *J Cell Physiol*. 2008;214(1):173-82.

38. Wagner E. Functions of AP1 (Fos/Jun) in bone development. *Ann Rheum Dis.* 2002;61(suppl 2):ii40-ii2.
39. Bozec A, Bakiri L, Jimenez M, Schinke T, Amling M, Wagner EF. Fra-2/AP-1 controls bone formation by regulating osteoblast differentiation and collagen production. *J Cell Biol.* 2010;190(6):1093-106.
40. Kenner L, Hoebertz A, Beil FT, Keon N, Karreth F, Eferl R, et al. Mice lacking JunB are osteopenic due to cell-autonomous osteoblast and osteoclast defects. *J Cell Biol.* 2004;164(4):613-23.
41. Grigoriadis A, Schellander K, Wang Z, Wagner E. Osteoblasts are target cells for transformation in c-fos transgenic mice. *J Cell Biol.* 1993;122(3):685-701.
42. Hattori T, Müller C, Gebhard S, Bauer E, Pausch F, Schlund B, et al. SOX9 is a major negative regulator of cartilage vascularization, bone marrow formation and endochondral ossification. *Development.* 2010;137(6):901-11.
43. Kamachi Y, Kondoh H. Sox proteins: regulators of cell fate specification and differentiation. *Development.* 2013;140(20):4129-44.
44. Akiyama H, Kim JE, Nakashima K, Balmes G, Iwai N, Deng JM, et al. Osteochondroprogenitor cells are derived from Sox9 expressing precursors. *Proc Natl Acad Sci USA.* 2005;102(41):14665-70.
45. Bi W, Deng JM, Zhang Z, Behringer RR, de Crombrughe B. Sox9 is required for cartilage formation. *Nat Genet.* 1999;22(1):85-9.
46. Wagner T, Wirth J, Meyer J, Zabel B, Held M, Zimmer Jr, et al. Autosomal sex reversal and campomelic dysplasia are caused by mutations in and around the SRY-related gene SOX9. *Cell.* 1994;79(6):1111-20.
47. Cameron FJ, Hageman RM, Cooke-Yarborough C, Kwok C, Goodwin LL, Silience DO, et al. A novel germ line mutation in SOX9 causes familial campomelic dysplasia and sex reversal. *Hum Mol Genet.* 1996;5(10):1625-30.
48. Han Y, Lefebvre V. L-Sox5 and Sox6 drive expression of the aggrecan gene in cartilage by securing binding of Sox9 to a far-upstream enhancer. *Mol Cell Biol.* 2008;28(16):4999-5013.
49. Dallas SL, Alliston T, Bonewald LF, John PB, Lawrence GR, T. John Martin A2 - John P. Bilezikian LGR, et al. Chapter 53 - Transforming growth factor- β . In: *Principles of Bone Biology (Third Edition)*. San Diego: Academic Press; 2008. p. 1145-66.

50. Massagué J, Chen Y-G. Controlling TGF- β signaling. *Gene Dev.* 2000;14(6):627-44.
51. Chen G, Deng C, Li YP. TGF- β and BMP signaling in osteoblast differentiation and bone formation. *Int J Biol Sci.* 2012;8(2):272-88.
52. Zhang YE. Non-smad pathways in TGF- β signaling. *Cell Res.* 2009;19(1):128-39.
53. Joyce ME, Roberts AB, Sporn MB, Bolander ME. Transforming growth factor- β and the initiation of chondrogenesis and osteogenesis in the rat femur. *J Cell Biol.* 1990;110(6):2195-207.
54. Yang X, Chen L, Xu X, Li C, Huang C, Deng C-X. TGF- β /Smad3 signals repress chondrocyte hypertrophic differentiation and are required for maintaining articular cartilage. *J Cell Biol.* 2001;153(1):35-46.
55. Mohammad KS, Chen CG, Balooch G, Stebbins E, McKenna CR, Davis H, et al. Pharmacologic inhibition of the TGF- β type I receptor kinase has anabolic and anti-catabolic effects on bone. *PLoS ONE.* 2009;4(4):e5275.
56. Alliston T, Choy L, Ducky P, Karsenty G, Derynck R. TGF- β -induced repression of CBFA1 by Smad3 decreases cbfa1 and osteocalcin expression and inhibits osteoblast differentiation. *EMBO J.* 2001;20(9):2254-72.
57. Maeda S, Hayashi M, Komiya S, Imamura T, Miyazono K. Endogenous TGF- β signaling suppresses maturation of osteoblastic mesenchymal cells. *EMBO J.* 2004;23(3):552-63.
58. Tang Y, Wu X, Lei W, Pang L, Wan C, Shi Z, et al. TGF- β 1-induced migration of bone mesenchymal stem cells couples bone resorption with formation. *Nat Med.* 2009;15(7):757-65.
59. Kang Q, Song WX, Luo Q, Tang N, Luo J, Luo X, et al. A comprehensive analysis of the dual roles of BMPs in regulating adipogenic and osteogenic differentiation of mesenchymal progenitor cells. *Stem Cells Dev.* 2009 May;18(4):545-59.
60. Xiao Y-T, Xiang L-X, Shao J-Z. Bone morphogenetic protein. *Biochem Bioph Res Co.* 2007;362(3):550-3.
61. Ten Dijke P, Fu J, Schaap P, Roelen BA. Signal transduction of bone morphogenetic proteins in osteoblast differentiation. *J Bone Joint Surg.* 2003;85(suppl_3):34-8.

62. Yu YY, Lieu S, Lu C, Colnot C. Bone morphogenetic protein 2 stimulates endochondral ossification by regulating periosteal cell fate during bone repair. *Bone*. 2010;47(1):65-73.
63. Retting KN, Song B, Yoon BS, Lyons KM. BMP canonical Smad signaling through Smad1 and Smad5 is required for endochondral bone formation. *Development*. 2009;136(7):1093-104.
64. Simic P, Vukicevic S. Bone morphogenetic proteins: from developmental signals to tissue regeneration. *EMBO rep*. 2007;8(4):327-31.
65. Itoh N, Ornitz DM. Functional evolutionary history of the mouse Fgf gene family. *Dev Dyn*. 2008;237(1):18-27.
66. Bikfalvi A, Klein S, Pintucci G, Rifkin DB. Biological roles of fibroblast growth factor-2. *Endocr Rev*. 1997;18(1):26-45.
67. Bianchi G, Banfi A, Mastrogiacomo M, Notaro R, Luzzatto L, Cancedda R, et al. Ex vivo enrichment of mesenchymal cell progenitors by fibroblast growth factor 2. *Exp Cell Res*. 2003;287(1):98-105.
68. Abbaspour A, Takata S, Sairyo K, Katoh S, Yukata K, Yasui N. Continuous local infusion of fibroblast growth factor-2 enhances consolidation of the bone segment lengthened by distraction osteogenesis in rabbit experiment. *Bone*. 2008;42(1):98-106.
69. Jiang X, Zou S, Ye B, Zhu S, Liu Y, Hu J. bFGF-Modified BMMSCs enhance bone regeneration following distraction osteogenesis in rabbits. *Bone*. 2010;46(4):1156-61.
70. Montero A, Okada Y, Tomita M, Ito M, Tsurukami H, Nakamura T, et al. Disruption of the fibroblast growth factor-2 gene results in decreased bone mass and bone formation. *J Clin Invest*. 2000;105(8):1085-93.
71. Marie PJ. Fibroblast growth factor signaling controlling bone formation: an update. *Gene*. 2012;498(1):1-4.
72. Ornitz DM. FGF signaling in the developing endochondral skeleton. *Cytokine Growth F R*. 2005;16(2):205-13.
73. Lieberman JR, Daluiski A, Einhorn TA. The role of growth factors in the repair of bone biology and clinical applications. *J Bone Joint Surg*. 2002;84(6):1032-44.

74. Zhang W, Shen X, Wan C, Zhao Q, Zhang L, Zhou Q, et al. Effects of insulin and insulin-like growth factor 1 on osteoblast proliferation and differentiation: differential signalling via Akt and ERK. *Cell Biochem Funct.* 2012;30(4):297-302.
75. Fulzele K, Riddle RC, DiGirolamo DJ, Cao X, Wan C, Chen D, et al. Insulin receptor signaling in osteoblasts regulates postnatal bone acquisition and body composition. *Cell.* 2010;142(2):309-19.
76. Yee D. How to train your biomarker. *Clin Cancer Res.* 2010;16(12):3091-3.
77. Chen Y, Alman BA. Wnt pathway, an essential role in bone regeneration. *J Cell Biochem.* 2009;106(3):353-62.
78. MacDonald BT, Tamai K, He X. Wnt/ β -catenin signaling: components, mechanisms, and diseases. *Dev Cell.* 2009;17(1):9-26.
79. Ling L, Nurcombe V, Cool SM. Wnt signaling controls the fate of mesenchymal stem cells. *Gene.* 2009;433(1-2):1-7.
80. Day TF, Guo X, Garrett-Beal L, Yang Y. Wnt/ β -catenin signaling in mesenchymal progenitors controls osteoblast and chondrocyte differentiation during vertebrate skeletogenesis. *Dev Cell.* 2005;8(5):739-50.
81. Galli C, Passeri G, Macaluso G. Osteocytes and WNT: the mechanical control of bone formation. *J Dent Res.* 2010;89(4):331-43.
82. Kim J-B, Leucht P, Lam K, Luppen C, Ten Berge D, Nusse R, et al. Bone regeneration is regulated by wnt signaling. *J Bone Miner Res.* 2007;22(12):1913-23.
83. Gaur T, Wixted JJ, Hussain S, O'Connell SL, Morgan EF, Ayers DC, et al. Secreted frizzled related protein 1 is a target to improve fracture healing. *J Cell Physiol.* 2009;220(1):174-81.
84. Harris S, Bonewald L, Harris M, Sabatini M, Dallas S, Feng J, et al. Effects of transforming growth factor β on bone nodule formation and expression of bone morphogenetic protein 2, osteocalcin, osteopontin, alkaline phosphatase, and type I collagen mRNA in long-term cultures of fetal rat calvarial osteoblasts. *J Bone Miner Res.* 1994;9(6):855-63.
85. Mbalaviele G, Sheikh S, Stains JP, Salazar VS, Cheng SL, Chen D, et al. β -Catenin and BMP-2 synergize to promote osteoblast differentiation and new bone formation. *J Cell Biochem.* 2005;94(2):403-18.

86. Rosen V. BMP2 signaling in bone development and repair. *Cytokine Growth F R*. 2009;20(5-6):475-80.
87. Jeon E-J, Lee K-Y, Choi N-S, Lee M-H, Kim H-N, Jin Y-H, et al. Bone morphogenetic protein-2 stimulates Runx2 acetylation. *J Biol Chem*. 2006;281(24):16502-11.
88. Gaur T, Lengner CJ, Hovhannisyan H, Bhat RA, Bodine PVN, Komm BS, et al. Canonical WNT signaling promotes osteogenesis by directly stimulating Runx2 gene expression. *J Biol Chem*. 2005;280(39):33132-40.
89. Fei Y, Xiao L, Doetschman T, Coffin DJ, Hurley MM. Fibroblast Growth factor 2 stimulation of osteoblast differentiation and bone formation is mediated by modulation of the WNT signaling pathway. *J Biol Chem*. 2011;286(47):40575-83.
90. Nakamura Y, Tensho K, Nakaya H, Nawata M, Okabe T, Wakitani S. Low dose fibroblast growth factor-2 (FGF-2) enhances bone morphogenetic protein-2 (BMP-2)-induced ectopic bone formation in mice. *Bone*. 2005;36(3):399-407.
91. Choi KY, Kim HJ, Lee MH, Kwon TG, Nah HD, Furuichi T, et al. Runx2 regulates FGF2-induced Bmp2 expression during cranial bone development. *Dev Dyn*. 2005;233(1):115-21.
92. Gersbach CA, Phillips JE, Garcia AJ. Genetic engineering for skeletal regenerative medicine. *Annu Rev Biomed Eng*. 2007;9(1):87-119.
93. Schindeler A, McDonald MM, Bokko P, Little DG. Bone remodeling during fracture repair: The cellular picture. *Semin Cell Dev Biol*. 2008;19(5):459-66.
94. Barnes GL, Kostenuik PJ, Gerstenfeld LC, Einhorn TA. Growth factor regulation of fracture repair. *J Bone Miner Res*. 1999;14(11):1805-15.
95. Dimitriou R, Tsiridis E, Giannoudis PV. Current concepts of molecular aspects of bone healing. *Injury*. 2005;36(12):1392-404.
96. Bronner F, Farach-Carson MC, Mikos AG, Gerstenfeld L, Edgar C, Kakar S, et al. Osteogenic growth factors and cytokines and their role in bone repair. In: Bronner F, Farach-Carson MC, editors. *Engineering of Functional Skeletal Tissues*: Springer London; 2007. p. 17-45.
97. LaStayo PC, Winters KM, Hardy M. Fracture healing: Bone healing, fracture management, and current concepts related to the hand. *J Hand Ther*. 2003;16(2):81-93.

98. Zimmermann G, Moghaddam A. Trauma: non-union: new trends. In: European Instructional Lectures: Springer; 2010. p. 15-9.
99. Phillips JE, Gersbach CA, Garcia AJ. Virus-based gene therapy strategies for bone regeneration. *Biomaterials*. 2007;28(2):211-29.
100. Langer R, Vacanti J. Tissue engineering. *Science*. 1993 May 14;260(5110):920-6.
101. Ikada Y. Challenges in tissue engineering. *J R Soc Interface*. 2006;3(10):589-601.
102. George JHS. Engineering of fibrous scaffolds for use in regenerative medicine: Imperial College London; 2009.
103. Marie P, Lomri A, Sabbagh A, Basle M. Culture and behavior of osteoblastic cells isolated from normal trabecular bone surfaces. *In Vitro Cell Dev-PL*. 1989;25(4):373-80.
104. Declercq H, Van den Vreken N, De Maeyer E, Verbeeck R, Schacht E, De Ridder L, et al. Isolation, proliferation and differentiation of osteoblastic cells to study cell/biomaterial interactions: comparison of different isolation techniques and source. *Biomaterials*. 2004;25(5):757-68.
105. Caplan AI, Bruder SP. Mesenchymal stem cells: building blocks for molecular medicine in the 21st century. *Trends Mol Med*. 2001;7(6):259-64.
106. Lin GL, Hankenson KD. Integration of BMP, Wnt, and notch signaling pathways in osteoblast differentiation. *J Cell Biochem*. 2011;112(12):3491-501.
107. Hipp J, Atala A. Sources of stem cells for regenerative medicine. *Stem Cell Rev*. 2008;4(1):3-11.
108. Dawson JI, Oreffo ROC. Bridging the regeneration gap: Stem cells, biomaterials and clinical translation in bone tissue engineering. *Arch Biochem Biophys*. 2008;473(2):124-31.
109. Bonab M, Alimoghaddam K, Talebian F, Ghaffari S, Ghavamzadeh A, Nikbin B. Aging of mesenchymal stem cell in vitro. *BMC Cell Biol*. 2006;7(1):14.
110. Grigoriadis AE, Heersche JN, Aubin JE. Differentiation of muscle, fat, cartilage, and bone from progenitor cells present in a bone-derived clonal cell population: effect of dexamethasone. *J Cell Biol*. 1988;106(6):2139-51.
111. Franceschi RT. The Role of ascorbic acid in mesenchymal differentiation. *Nutr Rev*. 1992;50(3):65-70.

112. Oshina H, Sotome S, Yoshii T, Torigoe I, Sugata Y, Maehara H, et al. Effects of continuous dexamethasone treatment on differentiation capabilities of bone marrow-derived mesenchymal cells. *Bone*. 2007;41:575-83.
113. Schieker M, Seitz H, Drosse I, Seitz S, Mutschler W. Biomaterials as scaffold for bone tissue engineering. *Eur J Trauma*. 2006;32(2):114-24.
114. Mastrogiacomo M, Muraglia A, Komlev V, Peyrin F, Rustichelli F, Crovace A, et al. Tissue engineering of bone: search for a better scaffold. *Orthod Craniofacial Res*. 2005;8(4):277-84.
115. Stevens MM. Biomaterials for bone tissue engineering. *Mater Today*. 2008;11(5):18-25.
116. Hollinger JO, Battistone GC. Biodegradable bone repair materials synthetic polymers and ceramics. *Clin Orthop Relat R*. 1986;207:290-306.
117. Peng H, Wright V, Usas A, Gearhart B, Shen H-C, Cummins J, et al. Synergistic enhancement of bone formation and healing by stem cells expressed VEGF and bone morphogenetic protein-4. *J Clin Invest*. 2002;110(6):751-9.
118. Fakhry A, Ratisoontorn C, Vedhachalam C, Salhab I, Koyama E, Leboy P, et al. Effects of FGF-2/-9 in calvarial bone cell cultures: differentiation stage-dependent mitogenic effect, inverse regulation of BMP-2 and noggin, and enhancement of osteogenic potential. *Bone*. 2005;36(2):254-66.
119. Peister A, Mellad JA, Larson BL, Hall BM, Gibson LF, Prockop DJ. Adult stem cells from bone marrow (MSCs) isolated from different strains of inbred mice vary in surface epitopes, rates of proliferation, and differentiation potential. *Blood*. 2004;103(5):1662-8.
120. Shahdadfar A, Frønsdal K, Haug T, Reinholt FP, Brinchmann JE. In vitro expansion of human mesenchymal stem cells: choice of serum is a determinant of cell proliferation, differentiation, gene expression, and transcriptome stability. *Stem cells*. 2005;23(9):1357-66.
121. Vater C, Kasten P, Stiehler M. Culture media for the differentiation of mesenchymal stromal cells. *Acta Biomater*. 2011;7(2):463-77.
122. Quarto R, Campanile G, Cancedda R, Dozin B. Modulation of commitment, proliferation, and differentiation of chondrogenic cells in defined culture medium. *Endocrinology*. 1997;138(11):4966-76.

123. Ruszymah B, Lokman B, Asma A, Munirah S, Chua K, Mazlyzam A, et al. Pediatric auricular chondrocytes gene expression analysis in monolayer culture and engineered elastic cartilage. *Int J Pediatr Otorhi.* 2007;71(8):1225-34.
124. Ma Xi, Liu Zp, Ma Jx, Han C, Zang Jc. Dynamic expression of Runx2, Osterix and AJ18 in the femoral head of steroid-induced osteonecrosis in rats. *Orthop Surg.* 2010;2(4):278-84.
125. Fariha MMN, Chua KH, Tan GC, Lim YH, Hayati AR. Endogenous and induced angiogenic characteristics of human chorion-derived stem cells. *Cell Biol Int.* 2012;36(12):1145-53.
126. Harun MHN, Sepian SN, Chua K-H, Ropilah AR, Ghafar NA, Che-Hamzah J, et al. Human forniceal region is the stem cell-rich zone of the conjunctival epithelium. *Hum Cell.* 2013;26(1):35-40.
127. Ishak M, Chua K, Asma A, Saim L, Aminuddin B, Ruszymah B, et al. Stem cell genes are poorly expressed in chondrocytes from microtic cartilage. *Int J Pediatr Otorhi.* 2011;75(6):835-40.
128. Tingart M, Beckmann J, Opolka A, Matsuura M, Wiech O, Grifka J, et al. Influence of factors regulating bone formation and remodeling on bone quality in osteonecrosis of the femoral head. *Calcified Tissue Int.* 2008;82(4):300-8.
129. Choong P, Mok P, Cheong S, Leong C, Then K. Generating neuron-like cells from BM-derived mesenchymal stromal cells in vitro. *Cytotherapy.* 2007;9(2):170-83.
130. Kaewsrichan J, Wongwitwichot P, Chandarajoti K, Chua K, Ruszymah B. Sequential induction of marrow stromal cells by FGF2 and BMP2 improves their growth and differentiation potential in vivo. *Arch Oral Biol.* 2011;56(1):90-101.
131. Baksh D, Song L, Tuan RS. Adult mesenchymal stem cells: characterization, differentiation, and application in cell and gene therapy. *J Cell Mol Med.* 2004;8:301-16.
132. Pountos I, Corscadden D, Emery P, Giannoudis PV. Mesenchymal stem cell tissue engineering: Techniques for isolation, expansion and application. *Injury.* 2007;38(Supplement 4):S23-S33.
133. Semrock. Filters for flow cytometry. Available from: <http://www.semrock.com/flow-cytometry.aspx>.

134. Young Richard A. Control of the embryonic stem cell state. *Cell*. 2011;144(6):940-54.
135. Stein GS, Lian JB, Owen TA. Relationship of cell growth to the regulation of tissue-specific gene expression during osteoblast differentiation. *FASEB J*. 1990;4(13):3111-23.
136. An YH, Martin KL. *Handbook of histology methods for bone and cartilage*: Springer; 2003.
137. Akiyama Y. TFSEARCH: Searching transcription factor binding sites. Available from: <http://www.cbrc.jp/research/db/TFSEARCH.html>.
138. Schagat T, Kopish K. *Optimize transfection of cultured cells*. Promega Corporation; 2010; Available from: <http://worldwide.promega.com/resources/pubhub/optimize-transfection-of-cultured-cells>.
139. Yuan H, Corbi N, Basilico C, Dailey L. Developmental-specific activity of the FGF-4 enhancer requires the synergistic action of Sox2 and Oct-3. *Gene Dev*. 1995;9(21):2635-45.
140. Shenghui H, Nakada D, Morrison SJ. Mechanisms of Stem Cell Self-Renewal. *Annu Rev Cell Dev Bi*. 2009;25(1):377-406.
141. Podestà M, Benvenuto F, Pitto A, Figari O, Bacigalupo A, Bruzzone S, et al. Concentrative uptake of cyclic ADP-ribose generated by BST-1+ stroma stimulates proliferation of human hematopoietic progenitors. *J Biol Chem*. 2005;280(7):5343-9.
142. Kaisho T, Ishikawa J, Oritani K, Inazawa J, Tomizawa H, Muraoka O, et al. BST-1, a surface molecule of bone marrow stromal cell lines that facilitates pre-B-cell growth. *Proc Natl Acad Sci USA*. 1994;91(12):5325-9.
143. Flores I, Benetti R, Blasco MA. Telomerase regulation and stem cell behaviour. *Curr Opin Cell Biol*. 2006;18(3):254-60.
144. Ben-Shushan E, Thompson JR, Gudas LJ, Bergman Y. Rex-1, a gene encoding a transcription factor expressed in the early embryo, is regulated via Oct-3/4 and Oct-6 binding to an octamer site and a novel protein, Rox-1, binding to an adjacent site. *Mol Cell Biol*. 1998;18(4):1866-78.

145. Lefebvre V, Dumitriu B, Penzo-Méndez A, Han Y, Pallavi B. Control of cell fate and differentiation by Sry-related high-mobility-group box (Sox) transcription factors. *Int J Biochem Cell B.* 2007;39(12):2195-214.
146. Marie PJ. Transcription factors controlling osteoblastogenesis. *Arch Biochem Biophys.* 2008;473(2):98-105.
147. Long F. Building strong bones: molecular regulation of the osteoblast lineage. *Nat Rev Mol Cell Biol.* 2011;13(1):27-38.
148. Nye JA, Petersen JM, Gunther CV, Jonsen MD, Graves BJ. Interaction of murine ets-1 with GGA-binding sites establishes the ETS domain as a new DNA-binding motif. *Gene Dev.* 1992;6(6):975-90.
149. Sepulveda JL, Belaguli N, Nigam V, Chen C-Y, Nemer M, Schwartz RJ. GATA-4 and Nkx-2.5 coactivate Nkx-2 DNA binding targets: role for regulating early cardiac gene expression. *Mol Cell Biol.* 1998;18(6):3405-15.
150. Suh E, Chen L, Taylor J, Traber PG. A homeodomain protein related to caudal regulates intestine-specific gene transcription. *Mol Cell Biol.* 1994;14(11):7340-51.
151. Molnár A, Georgopoulos K. The Ikaros gene encodes a family of functionally diverse zinc finger DNA-binding proteins. *Mol Cell Biol.* 1994;14(12):8292-303.
152. Herr W, Sturm R, Clerc R, Corcoran L, Baltimore D, Sharp P, et al. The POU domain: a large conserved region in the mammalian pit-1, Oct-1, Oct-2 and *Caenorhabditis elegans* unc-86 gene products. *Gene Dev.* 1988;2:1513-6.
153. Hirai H. The transcription factor Evi-1. *Int J Biochem Cell B.* 1999;31(12):1367-71.
154. Morris JF, Hromas R, Rauscher FJ. Characterization of the DNA-binding properties of the myeloid zinc finger protein MZF1: two independent DNA-binding domains recognize two DNA consensus sequences with a common G-rich core. *Mol Cell Biol.* 1994;14(3):1786-95.
155. Hromas R, Morris J, Cornetta K, Berebitsky D, Davidson A, Sha M, et al. Aberrant expression of the myeloid zinc finger gene, MZF-1, is oncogenic. *Cancer Res.* 1995;55(16):3610-4.
156. Otto F, Thornell AP, Crompton T, Denzel A, Gilmour KC, Rosewell IR, et al. Cbfa1, a candidate gene for cleidocranial dysplasia syndrome, is essential for osteoblast differentiation and bone development. *Cell.* 1997;89(5):765-71.
157. Deans RJ, Moseley AB. Mesenchymal stem cells: Biology and potential clinical uses. *Exp Hematol.* 2000;28(8):875-84.

158. Friedenstein A, Chailakhjan R, Lalykina K. The development of fibroblast colonies in monolayer cultures of guinea-pig bone marrow and spleen cells. *Cell Proliferat.* 1970;3(4):393-403.
159. Friedenstein AJ, Petrakova KV, Kurolesova AL, Frolova GP. Heterotopic transplants of bone marrow. *Transplantation.* 1968;6(2):230-47.
160. Fehrer C, Lepperdinger G. Mesenchymal stem cell aging. *Exp Gerontol.* 2005;40(12):926-30.
161. Liu L, Rando TA. Manifestations and mechanisms of stem cell aging. *J Cell Biol.* 2011;193(2):257-66.
162. Hyslop L, Stojkovic M, Armstrong L, Walter T, Stojkovic P, Przyborski S, et al. Downregulation of NANOG induces differentiation of human embryonic stem cells to extraembryonic lineages. *Stem Cells.* 2005;23(8):1035-43.
163. Xiang R, Liao D, Cheng T, Zhou H, Shi Q, Chuang TS, et al. Downregulation of transcription factor SOX2 in cancer stem cells suppresses growth and metastasis of lung cancer. *Br J Cancer.* 2011;104(9):1410-7.
164. Pesce M, Schöler HR. Oct-4: Gatekeeper in the beginnings of mammalian development. *Stem Cells.* 2001;19(4):271-8.
165. Yang C, Przyborski S, Cooke MJ, Zhang X, Stewart R, Anyfantis G, et al. A key role for telomerase reverse transcriptase unit in modulating human embryonic stem cell proliferation, cell cycle dynamics, and in vitro differentiation. *Stem Cells.* 2008;26(4):850-63.
166. Artandi SE, Alson S, Tietze MK, Sharpless NE, Ye S, Greenberg RA, et al. Constitutive telomerase expression promotes mammary carcinomas in aging mice. *Proc Natl Acad Sci USA.* 2002;99(12):8191-6.
167. Dominici M, Le Blanc K, Mueller I, Slaper-Cortenbach I, Marini F, Krause D, et al. Minimal criteria for defining multipotent mesenchymal stromal cells. The International Society for Cellular Therapy position statement. *Cytotherapy.* 2006;8(4):315-7.
168. Phinney DG, Kopen G, Isaacson RL, Prockop DJ. Plastic adherent stromal cells from the bone marrow of commonly used strains of inbred mice: Variations in yield, growth, and differentiation. *J Cell Biochem.* 1999;72(4):570-85.

169. Harting MT, Jimenez F, Pati S, Baumgartner J, Cox Jr CS. Immunophenotype characterization of rat mesenchymal stromal cells. *Cytotherapy*. 2008;10(3):243-53.
170. Gerstenfeld LC, Edgar CM, Kakar S, Jacobsen KA, Einhorn TA. Osteogenic growth factors and cytokines and their role in bone repair. *Engineering of functional skeletal tissues*: Springer; 2007. p. 17-45.
171. Lieberman JR, Daluiski A, Einhorn TA. The role of growth factors in the repair of bone biology and clinical applications. *J Bone Joint Surg*. 2002;84(6):1032-44.
172. Nefussi JR, Brami G, Modrowski D, Obcuf M, Forest N. Sequential expression of bone matrix proteins during rat calvaria osteoblast differentiation and bone nodule formation in vitro. *J Histochem Cytochem*. 1997;45(4):493-503.
173. Bernards MT, Qin C, Ratner BD, Jiang S. Adhesion of MC3T3-E1 cells to bone sialoprotein and bone osteopontin specifically bound to collagen I. *J Biomed Mater Res A*. 2008;86(3):779-87.
174. Yang Y, Cui Q, Sahai N. How does bone sialoprotein promote the nucleation of hydroxyapatite? A molecular dynamics study using model peptides of different conformations. *Langmuir*. 2010;26(12):9848-59.
175. Jaiswal N, Haynesworth SE, Caplan AI, Bruder SP. Osteogenic differentiation of purified, culture-expanded human mesenchymal stem cells in vitro. *J Cell Biochem*. 1997;64(2):295-312.
176. Gandhi A, Beam HA, O'Connor JP, Parsons JR, Lin SS. The effects of local insulin delivery on diabetic fracture healing. *Bone*. 2005;37(4):482-90.
177. Kottakis F, Polytarchou C, Foltopoulou P, Sanidas I, Kampranis SC, Tsihchlis PN. FGF-2 regulates cell proliferation, migration, and angiogenesis through an NDY1/KDM2B-miR-101-EZH2 pathway. *Mol Cell*. 2011;43(2):285-98.
178. Yang J, Zhang X, Wang W, Liu J. Insulin stimulates osteoblast proliferation and differentiation through ERK and PI3K in MG-63 cells. *Cell Biochem Funct*. 2010;28(4):334-41.
179. Hie M, Iitsuka N, Otsuka T, Tsukamoto I. Insulin-dependent diabetes mellitus decreases osteoblastogenesis associated with the inhibition of Wnt signaling through increased expression of Sost and Dkk1 and inhibition of Akt activation. *Int J Mol Cell Med*. 2011;28(3):455-62.

180. Jho E-h, Zhang T, Domon C, Joo C-K, Freund J-N, Costantini F. Wnt/ β -catenin/Tcf signaling induces the transcription of axin2, a negative regulator of the signaling pathway. *Mol Cell Biol.* 2002;22(4):1172-83.
181. Niida A, Hiroko T, Kasai M, Furukawa Y, Nakamura Y, Suzuki Y, et al. DKK1, a negative regulator of Wnt signaling, is a target of the β -catenin//TCF pathway. *Oncogene.* 2004;23(52):8520-6.
182. Beck GR, Sullivan EC, Moran E, Zerler B. Relationship between alkaline phosphatase levels, osteopontin expression, and mineralization in differentiating MC3T3-E1 osteoblasts. *J Cell Biochem.* 1998;68(2):269-80.
183. Lee M-H, Kim Y-J, Kim H-J, Park H-D, Kang A-R, Kyung H-M, et al. BMP-2-induced Runx2 expression is mediated by Dlx5, and TGF- β 1 opposes the BMP-2-induced osteoblast differentiation by suppression of Dlx5 expression. *J Biol Chem.* 2003;278(36):34387-94.
184. Lee M-H, Kwon T-G, Park H-S, Wozney JM, Ryoo H-M. BMP-2-induced Osterix expression is mediated by Dlx5 but is independent of Runx2. *Biochem Bioph Res Co.* 2003;309(3):689-94.
185. Heldin C-H, Miyazono K, ten Dijke P. TGF- signalling from cell membrane to nucleus through SMAD proteins. *Nature.* 1997;390(6659):465-71.
186. Chen Y, Whetstone HC, Youn A, Nadesan P, Chow EC, Lin AC, et al. β -catenin signaling pathway is crucial for bone morphogenetic protein 2 to induce new bone formation. *J Biol Chem.* 2007;282(1):526-33.
187. Kamiya N. The role of BMPs in bone anabolism and their potential targets SOST and DKK1. *Curr Mol Pharmacol.* 2012;5(2):153-63.
188. Zheng Y, Wu G, Zhao J, Wang L, Sun P, Gu Z. rhBMP2/7 heterodimer: an osteoblastogenesis inducer of not higher potency but lower effective concentration compared with rhBMP2 and rhBMP7 homodimers. *Tissue Eng Pt A.* 2010;16(3):879-87.
189. Tou L, Quibria N, Alexander JM. Transcriptional regulation of the human Runx2/Cbfa1 gene promoter by bone morphogenetic protein-7. *Mol Cell Endocrinol.* 2003;205(1):121-9.

190. Lee K-S, Kim H-J, Li Q-L, Chi X-Z, Ueta C, Komori T, et al. Runx2 is a common target of transforming growth factor β 1 and bone morphogenetic protein 2, and cooperation between Runx2 and Smad5 induces osteoblast-specific gene expression in the pluripotent mesenchymal precursor cell line C2C12. *Mol Cell Biol.* 2000;20(23):8783-92.
191. Yamashita S, Andoh M, Ueno-Kudoh H, Sato T, Miyaki S, Asahara H. Sox9 directly promotes Bapx1 gene expression to repress Runx2 in chondrocytes. *Exp Cell Res.* 2009;315(13):2231-40.

APPENDIX A

PREPARATION OF SOLUTIONS AND BUFFERS

Cell culture medium and reagents

- DMEM/F12
- 1) Dissolve powdered media and 2.438 g sodium bicarbonate with 800-900 ml of Milli-Q water.
 - 2) Stir until dissolved.
 - 3) Add 10 ml of 100x antibiotic-antimycotic solution.
 - 4) Adjust pH to 7.1-7.2 using 1 N HCl or 1 N NaOH.
 - 5) Add additional Milli-Q water to bring the solution to final volume of 1000 ml.
 - 6) Sterilize immediately by filtration using 0.22 microns membrane filter. Store at 4°C.
- α -MEM
1. Dissolve powdered media and 2.2 g sodium bicarbonate with 800-900 ml of Milli-Q water.
 2. Stir until dissolved.
 3. Add 10 ml of 100x antibiotic-antimycotic solution.
 4. Adjust pH to 7.1-7.2 using 1 N HCl or 1 N NaOH.
 5. Adjust the volume to 1000 ml.
 6. Sterilize immediately by filtration through 0.22 microns membrane filter. Store at 4°C.
- DPBS
- 1) Dissolve powdered media with 800-900 ml of Milli-Q water and stir until dissolved.
 - 2) Adjust pH to 7.1-7.2 using 1 N HCl or 1 N NaOH.
 - 3) Bring the final volume to 1000 ml.
 - 4) Sterilize immediately by filtration through 0.22 microns membrane filter. Store at 4°C.
- 0.25x trypsin
- 0.25x trypsin solution was diluted from 10x trypsin-EDTA solution using sterilized DPBS.
- 1 μ M Triamcinolone Acetonide (TA)
- 1) Dissolve 8.69 mg triamcinolone acetonide in 1 ml of absolute ethanol. (A)
 - 2) Dilute (A) 200:1 with Milli-Q water. (B)
 - 3) Dilute (B) 100:1 with Milli-Q water.
 - 4) Sterilize by filtration using 0.22 microns membrane filter.
 - 5) Store at 4°C. Protect from light

Cell culture medium and reagents (Continued)

- | | |
|--|--|
| Ascorbic acid
stock solution
(5 mg/ml) | <ol style="list-style-type: none"> 1) Dissolve 50 mg ascorbic acid in 5 ml of Milli-Q water. 2) Sterilize using 0.22 microns membrane filter. 3) Store at 4°C. Protect from light. |
| 1 M β -glycerophosphate | <ol style="list-style-type: none"> 1) Dissolve 1.53 g β-glycerophosphate in 5 ml of Milli-Q water. 2) Sterilize by filtration through 0.22 microns membrane filter. 3) Store at 4°C. Protect from light. |

Assay buffers

- | | |
|-------------------------|---|
| Cell lysis buffer | <ol style="list-style-type: none"> 1) Dissolve 8.766 g Tris base in 800 ml of distilled water. 2) Add 10 ml Triton X-100 and 50 ml of 1 M Tris-HCl (pH 8.0) 3) Adjust pH to 8.0 using HCl or NaOH solution. 4) Add additional distilled water to bring the solution to final volume of 1000 ml. 5) Aliquot and store at -20°C. 6) Add 1 tablet of cocktail protease inhibitor per 10 ml buffer before use. This solution can be store at 4°C. |
| MTT solution (50 mg/ml) | <p>Dissolve 0.5 g MTT in 10 ml of DPBS.</p> <p><i>The solution needs to be prepared freshly each time.</i></p> |
| 1 M Tris-HCl, pH 9.0 | <ol style="list-style-type: none"> 1) Dissolve 121.1 g Tris base in 800 ml distilled water. 2) Adjust the pH 9.0 with concentrated HCl. 3) Adjust the volume to 1000 ml with distilled water. 4) Store at room temperature. |
| 0.1 M PNPP | <p>Dissolve 37.112 g PNPP in 1000 ml of distilled water.</p> <p>Store at room temperature.</p> |

Assay buffers (Continued)

0.1 M MgCl ₂	Dissolve 9.521 g MgCl ₂ in 1000 ml of distilled water. Store at room temperature.
2 N NaOH	Dissolve 80 g NaOH in 1000 ml of distilled water. Store at room temperature.
2% w/v Alizarin red s solution, pH 4.1-4.2	<ol style="list-style-type: none"> 1) Dissolve 2 g alizarin red s in 100 ml of distilled water. 2) Adjust pH to 4.1-4.3 using 0.5% ammonium hydroxide 3) Store at room temperature. Protect from light.
0.5% Ammonium hydroxide	Dissolve 0.5 g ammonium hydroxide in 100 ml of distilled water. Store at room temperature.
10% Acetic acid and 20% Methanol	Mix 10 ml of glacial acetic acid and 20 ml of methanol with 70 ml distilled water. Store at room temperature.

Anesthetic drug

Mixture of Zoletil [®] and xylazine at 1:1 volume ratio	<ol style="list-style-type: none"> 1) Aseptically mix 1 volume of Zoletil[®] 100 with 1 volume of xylazine (20 mg/ml). 2) Store at 4°C and protect from light. <p><i>The mixture needs to be prepared freshly each time.</i></p>
---	---

Reagents for tissue processing and staining

4% Paraformaldehyde in DPBS	<ol style="list-style-type: none"> 1) Dissolve 4 g Paraformaldehyde in 100 ml of DPBS. 2) Heat the solution to 70°C. 3) Add NaOH solution until the mixture is clear. 4) Check pH with pH stripe (should be 7.2-7.4). 5) Aliquot and store at -20°C. Thawed solution should be kept at 4°C and used within a week.
--------------------------------	---

Reagents for tissue processing and staining (Continued)

- | | |
|------------------------------------|--|
| 10% Formic acid,
EDTA saturated | <ol style="list-style-type: none">1) Mix 10 ml of formic acid with 90 ml of distilled water.2) Add EDTA until saturate.3) Store at room temperature. Protect from light. |
| 5% Sodium sulfate | Dissolve 5 g sodium sulfate in 100 ml of distilled water. Store at room temperature. |

Bacterial culture mediums and reagents

- | | |
|--------------------|--|
| LB liquid media | <ol style="list-style-type: none">1) Dissolve 6.25 g LB broth in 250 ml of distilled water.2) Sterilized by autoclave.3) Allow the agar solution to cool to 50-60°C.4) Add antibiotic stock solution (if desire).5) Store at 4°C. |
| LB agar | <ol style="list-style-type: none">1) Dissolve 6.25 g LB broth in 250 ml of distilled water.2) Add 3.75 g bacteriological agar.3) Sterilized by autoclave.4) Allow the agar solution to cool to 50-60°C.5) Add antibiotic stock solution (if desire).6) Pour 20-25 ml of LB agar per 10 cm polystyrene Petri dish.7) Allow the agar to solidified before inverting the plate and Leave at room temperature for several hours8) Store at 4°C. |
| X-gal/IPTG LB agar | <ol style="list-style-type: none">1) Incubate the LB agar plate at 37°C for 2 hours.2) Add 40 µl of X-gal stock solution, 4 µl of IPTG stock solution, and 50 µl of LB liquid media on the top of agar.3) Spread the solution over the agar.4) Incubate the plate at 37°C for few hours before use. |

Bacterial culture mediums and reagents (Continued)

- | | |
|--|---|
| Ampicillin stock solution
(100 mg/ml) | <ol style="list-style-type: none">1) Dissolve 1 g of ampicillin sodium in 10 ml of distilled water.2) Sterilize by filtering3) Aliquot and stored at -20°C. Protect from light. |
| X-gal stock solution
(20 mg/ml) | <ol style="list-style-type: none">1) Dissolve 0.1 g of X-gal in 5 ml of dimethylformamide.2) Aliquot and store at -20°C. Protect from light. |
| IPTG stock solution
(200 mg/ml) | <ol style="list-style-type: none">1) Dissolve 1 g of IPTG in 5 ml of distilled water.2) Filter through 0.22 µm membrane to sterilize.3) Aliquot and store at -20°C. Protect from light. |

Buffers and reagents for plasmid construction

- | | |
|---------------------------------------|--|
| 50x Tris acetate EDTA
(TAE) buffer | <ol style="list-style-type: none">1) Dissolve 242 g Tris base in distilled water2) Add 57.1 ml of glacial acetic acid and 100 ml of 0.5 M EDTA (pH 8.0) solution.3) Adjust volume to 1 L.4) Store at room temperature. <p><i>Dilute this stock solution with distilled water to make a 1x working solution.</i></p> |
| 0.5 M EDTA, pH 8.0 | <ol style="list-style-type: none">1) Stir 186.1g EDTA into 800 ml of distilled water.2) Add NaOH pellets while stirring to bring the pH to 8.03) Dilute the solution to 1 L with distilled water.4) Sterilize in an autoclave.5) Store at room temperature. |
| 1 M Tris-HCl, pH 8.0 | <ol style="list-style-type: none">1) Dissolve 121.1 g Tris base in 800 ml of distilled water.2) Adjust the pH 8.0 with concentrated HCl.3) Adjust the volume to 1000 ml with distilled water.4) Store at room temperature. |

Buffers and reagents for plasmid construction (Continued)

Digestion buffer for chromosome extraction	<ol style="list-style-type: none">1) Dissolve 58.44 g NaCl in distilled water.2) Add 10 ml of 1 M Tris-HCl (pH 8.0), 50 ml of 0.5 M EDTA (pH 8.0), and 50 ml of 10% SDS.3) Add additional distilled water to bring the solution to final volume of 1000 ml.4) Store at room temperature.5) Add 5 μl of 20 mg/ml Proteinase K per 1 ml digestion buffer before use.
10% SDS	Dissolve 10 g SDS in 100 ml of distilled water. Heat to 60°C if necessary. Store at room temperature.
7.5 M Ammonium acetate	Dissolve 578.1 g Ammonium acetate in 1000 ml distilled water. Store at room temperature.
10x Annealing buffer	<ol style="list-style-type: none">1) Dissolve 12.11 g Tris base, 3.72 g EDTA, and 29.22 g NaCl in 800 ml distilled water.2) Adjust pH to 8.0 using HCl or NaOH solution.3) Bring the solution to final volume of 1000 ml.4) Store at room temperature.

APPENDIX B

ELECTROPHEROGRAMS AND DNA SEQUENCES

1. pGEM-U1557

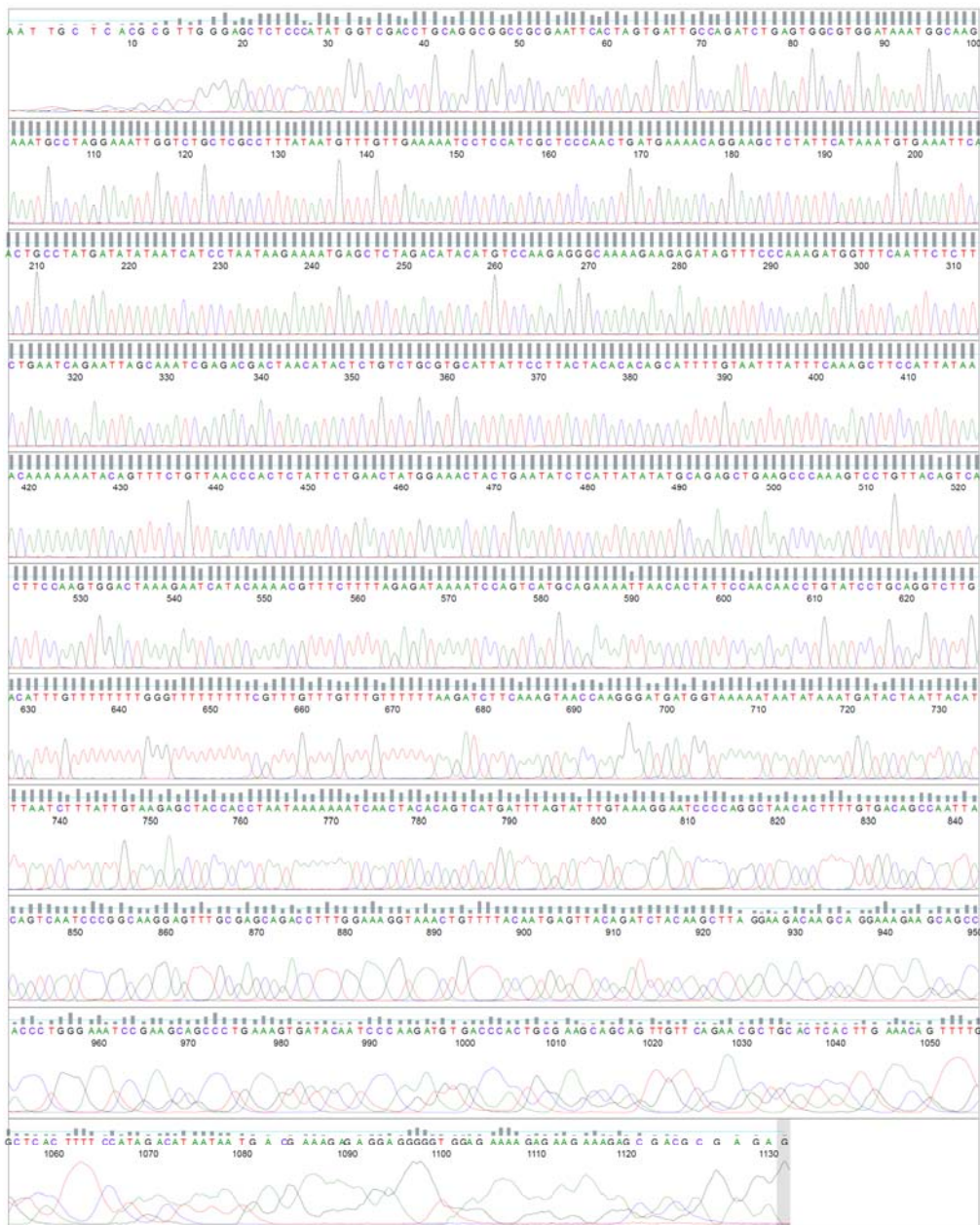
1.1. Electropherogram of pGEM-U1557 sense strand sequenced with SP6 primer

File: ZB02250604(pGEM-U1557)SP6_H02.ab1

Geospiza
www.geospiza.com

Sample Name: ZB02250604(pGEM-U1557)SP6
Mobility: KB_3730_POP7_BDTv3.mob
Spacing: 16.5095
Comment: n/a

Signal Strengths: A = 1849, C = 1459, G = 1185, T = 2058
Lane/Cap#: 2
Matrix: n/a
Direction: Native

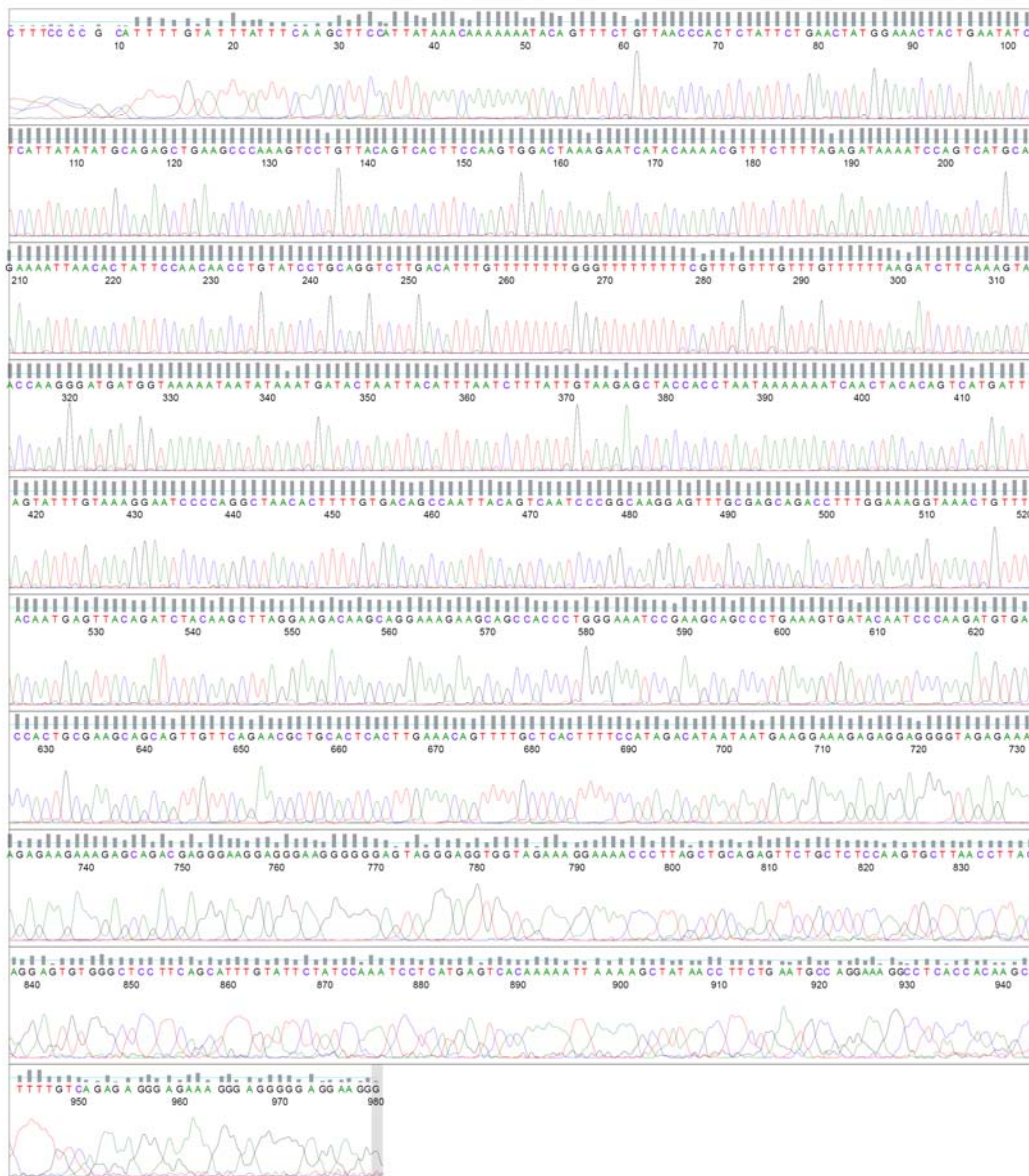


1.2. Electropherogram of pGEM-U1557 sense strand sequenced with SEQ_U1291 primer

File: ZB02250606(pGEM-U1557)SEQ_U1291(Tm=58)_B03.ab1

Geospiza
www.geospiza.com

Sample Name: ZB02250606(pGEM-U1557)SEQ_U1291(Tm=58) Signal Strengths: A = 937, C = 726, G = 681, T = 1065
 Mobility: KB_3730_POP7_BDTv3.mob Lane/Cap#: 29
 Spacing: 16.5077 Matrix: n/a
 Comment: n/a Direction: Native



1.3. Electropherogram of pGEM-U1557 antisense strand sequenced with T7 primer

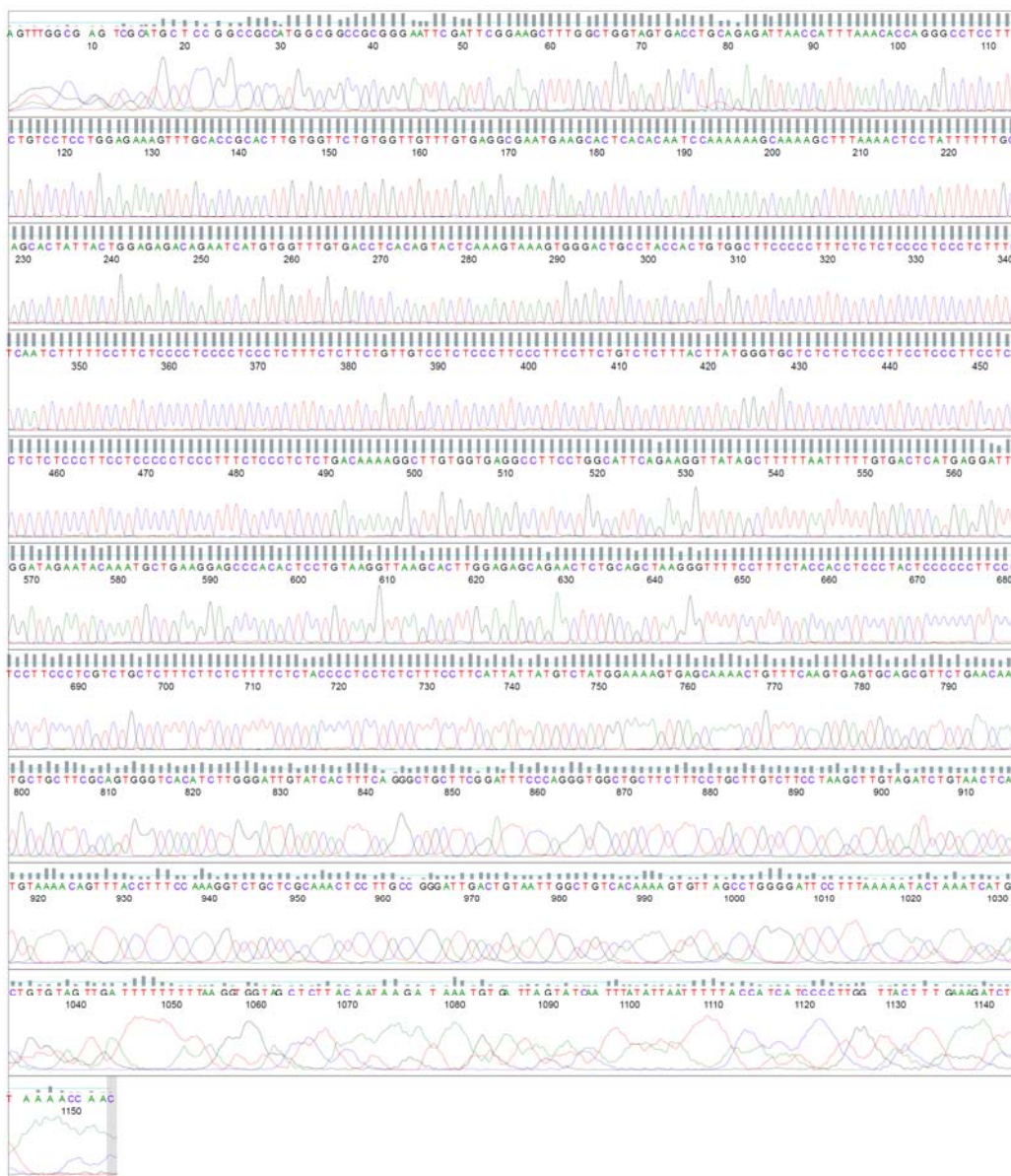
File: ZB02250603(pGEM-U1557)T7_G02.ab1



www.geospiza.com

Sample Name: ZB02250603(pGEM-U1557)T7
 Mobility: KB_3730_POP7_BDTv3.mob
 Spacing: 16.4435
 Comment: n/a

Signal Strengths: A = 478, C = 591, G = 481, T = 699
 Lane/Cap#: 4
 Matrix: n/a
 Direction: Native

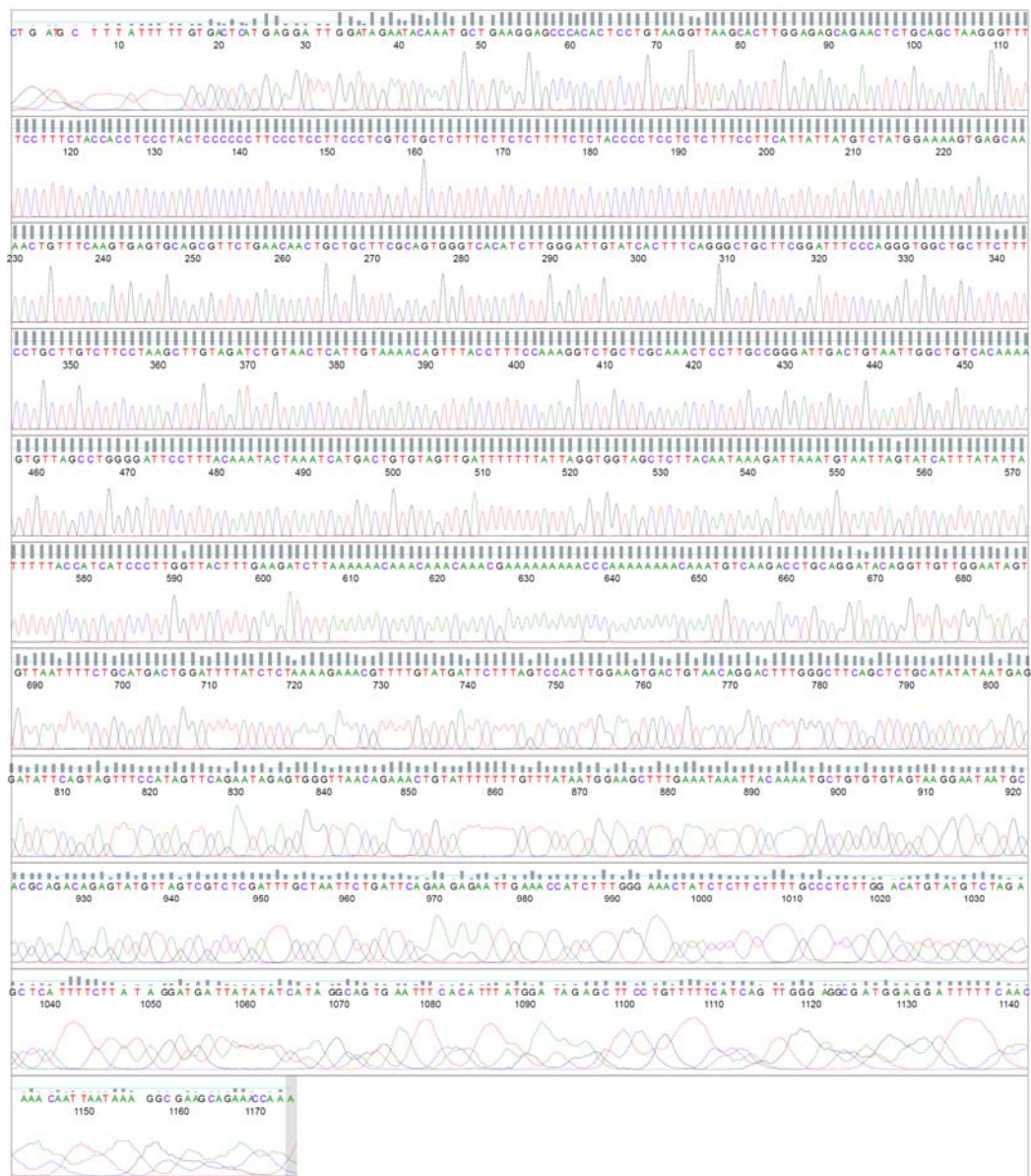


1.4. Electropherogram of pGEM-U1557 antisense strand sequenced with SEQ_U345 primer

File: ZB02250605(pGEM-U1557)SEQ_U345(Tm=58)_A03.ab1



Sample Name: ZB02250605(pGEM-U1557)SEQ_U345(Tm=58) Signal Strengths: A = 1335, C = 1433, G = 1079, T = 1960
 Mobility: KB_3730_POP7_BDTv3.mob Lane/Cap#: 31
 Spacing: 16.4969 Matrix: n/a
 Comment: n/a Direction: Native



1.5. U1557 sequence

U1557

1678 bp

```

1 GAGTGGCGTG GATAAATGGC AAGAAATGCC TAGGAAATTG GTCTGCTCGC CTTTATAATG
61 TTTGTTGAAA AATCCTCCAT CGCTCCCAAC TGATGAAAAC AGGAAGCTCT ATTCATAAAT
121 GTGAAATTCA CTGCCTATGA TATATAATCA TCCTAATAAG AAAATGAGCT CTAGACATAC
181 ATGTCCAAGA GGGCAAAAGA AGAGATAGTT TCCCAAAGAT GGTTC AATT CTCTTCTGAA
241 TCAGAATTAG CAAATCGAGA CGACTAACAT ACTCTGTCTG CGTGCATTAT TCCTTACTAC
301 ACACAGCATT TTGTAATTTA TTTCAAAGCT TCCATTATAA ACAAAAAAAT ACAGTTTCTG
361 TTAACCCACT CTATTCTGAA CTATGGAAAC TACTGAATAT CTCATTATAT ATGCAGAGCT
421 GAAGCCCAA GTCTGTGTTAC AGTCACTTCC AAGTGGACTA AAGAATCATA CAAAACGTTT
481 CTTTTAGAGA TAAAATCCAG TCATGCAGAA AATTAACACT ATTCCAACAA CCTGTATCCT
541 GCAGGTCTTG ACATTTGTTT TTTTTGGGTT TTTTTTTCGT TTGTTTGTGTT GTTTTTTAAG
601 ATCTTCAAAG TAACCAAGGG ATGATGGTAA AAATAATATA AATGATACTA ATTACATTTA
661 ATCTTTATTG TAAGAGCTAC CACCTAATAA AAAAATCAAC TACACAGTCA TGATTTAGTA
721 TTTGTAAAGG AATCCCCAGG CTAACACTTT TGTGACAGCC AATTACAGTC AATCCCGGCA
781 AGGAGTTTGC GAGCAGACCT TTGGAAAGGT AAAGTGTGTTT ACAATGAGTT ACAGATCTAC
841 AAGCTTAGGA AGACAAGCAG GAAAGAAGCA GCCACCCTGG GAAATCCGAA GCAGCCCTGA
901 AAGTGATACA ATCCAAGAT GTGACCCACT GCGAAGCAGC AGTTGTTTCAG AACGTGCAC
961 TCACTTGAAA CAGTTTTGCT CACTTTTCCA TAGACATAAT AATGAAGGAA AGAGAGGAGG
1021 GGTAGAGAAA AGAGAAGAAA GAGCAGACGA GGAAGGAGG GAAGGGGGGA GTAGGGAGGT
1081 GGTAGAAAGG AAAACCCTTA GCTGCAGAGT TCTGCTCTCC AAGTGCTTAA CCTTACAGGA
1141 GTGTGGGCTC CTTCAGCATT TGTATTCTAT CCAAATCCTC ATGAGTCACA AAAATTAAAA
1201 AGCTATAACC TTCTGAATGC CAGGAAGGCC TCACCACAAG CCTTTTGTCA GAGAGGGAGA
1261 AAGGGAGGGG GAGGAAGGGA GAGAGAGAGG AAGGGAGGAA GGGAGAGAGA GCACCCATAA
1321 GTAAAGAGAC AGAAGGAAGG GAAGGGAGAG GACAACAGAA GAGAAAGAGG GAGGGGAGGG
1381 GAGAAGGAAA AAGATTGAGA AAGAGGGAGG GGAGAGAGAA AGGGGAAGC CACAGTGGTA
1441 GGCAGTCCCA CTTTACTTTG AGTACTGTGA GGTCACAAAC CACATGATTC TGTCTCTCCA
1501 GTAATAGTGC TTGCAAAAAA TAGGAGTTTT AAAGCTTTTG CTTTTTTGGA TTGTGTGAGT
1561 GCTTCATTCG CCTCACAAC AACACAGAA CCACAAGTGC GGTGCAAACT TTCTCCAGGA
1621 GGACAGCAAG GAGGCCCTGG TGTTTAAATG GTTAATCTCT GCAGGTCACT ACCAGCCA

```


2.3. *runx2*-N sequence

*runx2*_N

724 bp

```
1 TTACAGTCAA TCCCGGCAAG GAGTTTGC GA GACACCTTT GGAAAGGTAA ACTGTTTTAC
61 AATGAGTTAC AGATCTACAA GCTTAGGAAG ACAAGCAGGA AAGAAGCAGC CACCCTGGGA
121 AATCCGAAGC AGCCCTGAAA GTGATACAAT CCCAAGATGT GACCCACTGC GAAGCAGCAG
181 TTGTTTCAGAA CGCTGCACTC ACTTGAAACA GTTTTGCTCA CTTTTCATA GACATAATAA
241 TGAAGGAAAAG AGAGGAGGGG TAGAGAAAAG AGAAGAAAGA GCAGACGAGG GAAGGAGGGA
301 AGGGGGGAGT AGGGAGGTGG TAGAAAGGAA AACCCTTAGC TGCAGAGTTC TGCTCTCCAA
361 GTGCTTAACC TTACAGGAGT GTGGGCTCCT TCAGCATTG TATTCTATCC AAATCCTCAT
421 GAGTCACAAA AATTAAAAAG CTATAACCTT CTGAATGCCA GGAAGGCCTC ACCACAAGCC
481 TTTTGTTCAGA GAGGGAGAAA GGGAGGGGGA GGAAGGGAGA GAGAGAGGAA GGGAGGAAGG
541 GAGAGAGAGC ACCCATAAGT AAAGAGACAG AAGGAAGGGA AGGGAGAGGA CAACAGAAGA
601 GAAAGAGGGA GGGGAGGGGA GAAGGAAAAA GATTGAGAAA GAGGGAGGGG AGAGAGAAAG
661 GGGGAAGCCA CAGTGGTAGG CAGTCCCACT TTA CTTT GAG TACTGTGAGG TCACAAACCA
721 TG
```

3. pGL3-*runx2*-F

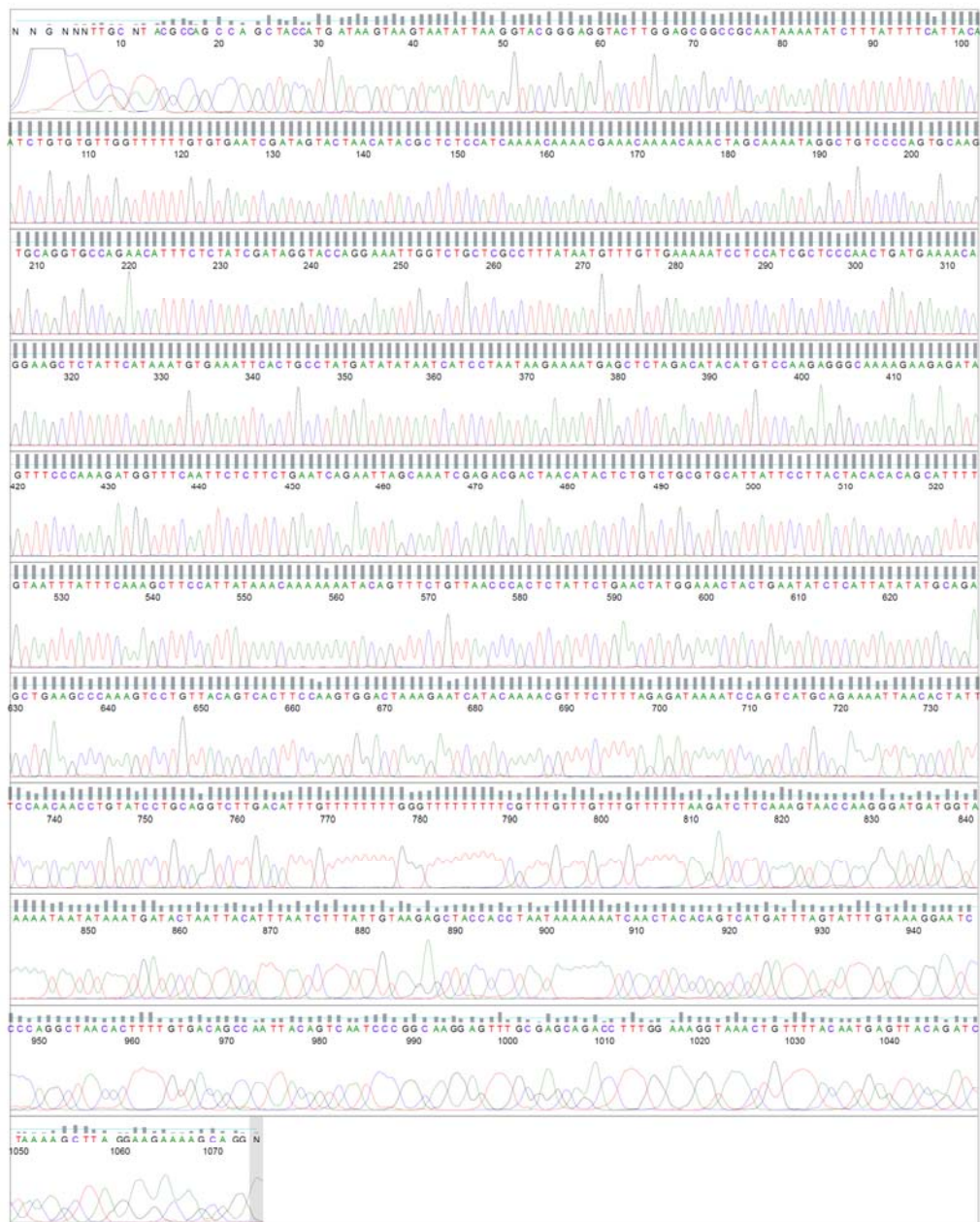
3.1. Electropherogram of pGL3-*runx2*-F sense strand sequenced with LUC_R primer

File: pGL3-RUNX2-F5-LUC-F_A12.ab1

Geospiza
www.geospiza.com

Sample Name: pGL3-RUNX2-F5-LUC-F
Mobility: KB_3730_POP7_BDTV3.mob
Spacing: 17.2164
Comment: n/a

Signal Strengths: A = 1188, C = 1123, G = 1001, T = 1473
Lane/Cap#: 96
Matrix: n/a
Direction: Native



3.3. *runx2-F* sequence

runx2_F 830 bp

```
1 AGGAAATTGG TCTGCTCGCC TTTATAATGT TTGTTGAAAA ATCCTCCATC GCTCCCAACT
61 GATGAAAACA GGAAGCTCTA TTCATAAATG TGAAATTCAC TGCCTATGAT ATATAATCAT
121 CCTAATAAGA AAATGAGCTC TAGACATACA TGTCCAAGAG GCAAAAGAA GAGATAGTTT
181 CCCAAAGATG GTTTC AATTC TCTTCTGAAT CAGAATTAGC AAATCGAGAC GACTAACATA
241 CTCTGTCTGC GTGCATTATT CCTTACTACA CACAGCATTT TGTAATTTAT TTCAAAGCTT
301 CCATTATAAA CAAAAAATA CAGTTTCTGT TAACCCACTC TATTCTGAAC TATGGAAACT
361 ACTGAATATC TCATTATATA TGCAGAGCTG AAGCCCAAAG TCCTGTTACA GTCACCTCCA
421 AGTGACTAA AGAATCATA CAAAACGTTTC TTTTAGAGAT AAAATCCAGT CATGCAGAAA
481 ATTAACACTA TTCCAACAAC CTGTATCCTG CAGGTCTTGA CATTGTGTTT TTTTGGGTTT
541 TTTTTTCGTT TGTGTTGTTG TTTTTTAAGA TCTTCAAAGT AACCAAGGGA TGATGGTAAA
601 AATAATATAA ATGATACTAA TTACATTTAA TCTTTATTGT AAGAGCTACC ACCTAATAAA
661 AAAATCAACT ACACAGTCAT GATTTAGTAT TTGTAAAGGA ATCCCAGGC TAACACTTTT
721 GTGACAGCCA ATTACAGTCA ATCCCGCAA GGAGTTTGCG AGCAGACCTT TGGAAAGGTA
781 CTGTTTTA CAATGAGTTA CAGATCTAAA AGCTTAGGAA GAAAAGCAGG
```


4.2. Electropherogram of pGL3-5Xap1 antisense strand sequenced with LUC_R primer

File: pGL3-APIX5-LUC-DS38-LUC_R.ab1



www.geospiza.com

Sample Name: pGL3-APIX5-LUC-DS38-LUC_R

Signal Strengths: A = 1521, C = 2286, G = 1128, T = 2595

Mobility: KB_3730_POP7_BDTv3.mob

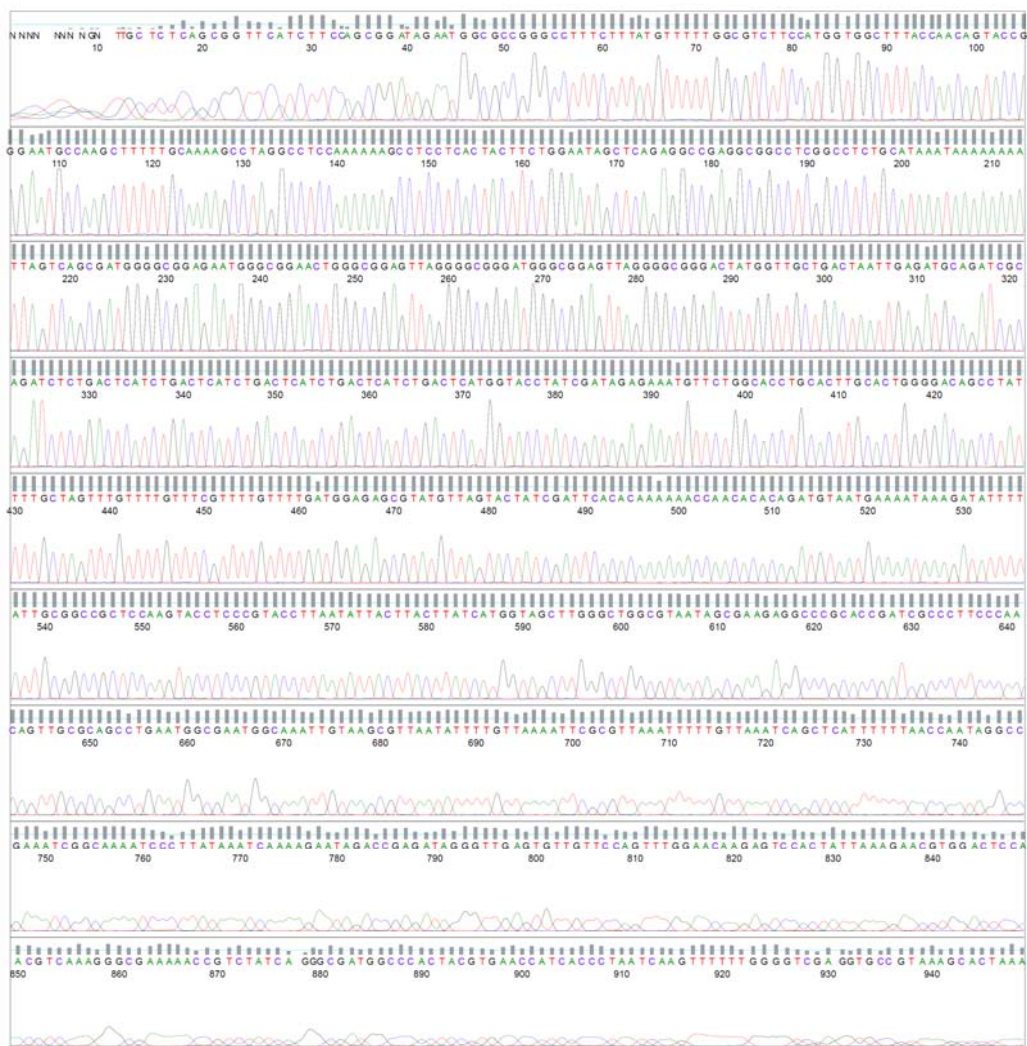
Lane/Cap#: 80

Spacing: 17.3422

Matrix: n/a

Comment: n/a

Direction: Native



4.3. 5Xap1 sequence (overhangs of BglII at 5'-end and KpnI at 3'-end were underlined)

5Xap1

55 bp

1 GATCTCTGAC TCATCTGACT CATCTGACTC ATCTGACTCA TCTGACTCAT
GGTAC

APPENDIX C
SEQUENCE ALIGNMENT

1. The alignment of U1557 sequence with the sequence 2,000 bases 5'-upstream of *runx2* gene and the gene promoter reported by Drissi et al. [25] (↑ indicates the mismatch position between U1557 and database;)

```

reported -----
database GAAGTCTAACATGCAAATTCAGAGTGGCGTGGATAAATGGCAAGAAATGCCTAGGAAATT
U1557 -----GAGTGGCGTGGATAAATGGCAAGAAATGCCTAGGAAATT

reported -----
database GGTCTGCTCGCCTTTATAATGTTTGTGAAAAATCCTCCATCGCTCCCAACTGATGAAAA
U1557 GGTCTGCTCGCCTTTATAATGTTTGTGAAAAATCCTCCATCGCTCCCAACTGATGAAAA

reported -----
database CAGGAAGCTCTATTTCATAAATGTGAAATTCACTGCCTATGATATATAATCATCCTAATAA
U1557 CAGGAAGCTCTATTTCATAAATGTGAAATTCACTGCCTATGATATATAATCATCCTAATAA

reported -----
database GAAAATGAGCTCTAGACATACATGTCCAAGAGGGCAAAGAAGAGATAGTTTCCCAAAGA
U1557 GAAAATGAGCTCTAGACATACATGTCCAAGAGGGCAAAGAAGAGATAGTTTCCCAAAGA

reported -----
database TGGTTTCAATTTCTCTTCTGAATCAGAATTAGCAAATCGAGACGACTAACATACTCTGTCT
U1557 TGGTTTCAATTTCTCTTCTGAATCAGAATTAGCAAATCGAGACGACTAACATACTCTGTCT
                ↑

reported -----
database GCGTGCATTATTCCTTACTACACACAGCATTGTGTAATTTATTTCAAAGCTTCCATTATA
U1557 GCGTGCATTATTCCTTACTACACACAGCATTGTGTAATTTATTTCAAAGCTTCCATTATA

reported -----
database AACAAAAAATACAGTTTCTGTTAACCCACTCTATTCTGAACATATGGAACTACTGAATA
U1557 AACAAAAAATACAGTTTCTGTTAACCCACTCTATTCTGAACATATGGAACTACTGAATA

reported -----
database TCTCATTATATATGCAGAGCTGAAGCCCAAAGTCCCTGTTACAGTCACCTTCCAAGCGGACT
U1557 TCTCATTATATATGCAGAGCTGAAGCCCAAAGTCCCTGTTACAGTCACCTTCCAAGTGGACT
                                               ↑

reported -----
database AAAGAATCATACAAAACGTTTCTTTTAGAGATAAAATCCAGTCATGCAGAAAATTAACAC
U1557 AAAGAATCATACAAAACGTTTCTTTTAGAGATAAAATCCAGTCATGCAGAAAATTAACAC

reported -----
database TATTCCAACAACCTGTATCCTGCAGGTCTTGACATTTGTTTTTTTGGGGTTTTTTTTT-G
U1557 TATTCCAACAACCTGTATCCTGCAGGTCTTGACATTTGTTTTTTTGGGGTTTTTTTTTGG
                                               ↑      ↑

reported -----
database TTTGTTTGTGTTTTTTAAGATCTTCAAAGTAACCAAGGGATGATGGTAAAAATAATAT
U1557 TTTGTTTGTGTTTTTTAAGATCTTCAAAGTAACCAAGGGATGATGGTAAAAATAATAT

```



```

reported      AAGGGGAAGCCACAGTGGTAGGCAGTCCCACTTTACTTTGAGTACTGTGAGGTCACAAA
database      AAGGGGAAGCCACAGTGGTAGGCAGTCCCACTTTACTTTGAGTACTGTGAGGTCACAAA
U1557        AAGGGGAAGCCACAGTGGTAGGCAGTCCCACTTTACTTTGAGTACTGTGAGGTCACAAA
*****

reported      CCACATGATTCTGTCTCTCCAGTAATAGTGCTTGCAAAAAATAGGAGTTTAAAGCTTTT
database      CCACATGATTCTGTCTCTCCAGTAATAGTGCTTGCAAAAAATAGGAGTTTAAAGCTTTT
U1557        CCACATGATTCTGTCTCTCCAGTAATAGTGCTTGCAAAAAATAGGAGTTTAAAGCTTTT
*****

reported      GCTTTTTGGATTGTGTGAATGCTTCATTGCGCTCACAAACAACCACAGAACCACAAGTG
database      GCTTTTTGGATTGTGTGAATGCTTCATTGCGCTCACAAACAACCACAGAACCACAAGTG
U1557        GCTTTTTGGATTGTGTGAATGCTTCATTGCGCTCACAAACAACCACAGAACCACAAGTG
*****
                ↑
reported      CGGTGCAAACCTTCTCCAGGAGGACAGCAAGGAGGCCCTGGTGTTTAAATGGTTAATCTC
database      CGGTGCAAACCTTCTCCAGGAGGACAGCAAGGAGGCCCTGGTGTTTAAATGGTTAATCTC
U1557        CGGTGCAAACCTTCTCCAGGAGGACAGCAAGGAGGCCCTGGTGTTTAAATGGTTAATCTC
*****

reported      TGCAGGTCACTACCAGCCA--
database      TGCAGGTCACTACCAGCCACC
U1557        TGCAGGTCACTACCAGCCA--
*****

```

2. The alignment of *runx2*-N sequence with the U1557 sequence

```

U1557      GAGTGGCGTGGATAAAATGGCAAGAAATGCCTAGGAAATTGGTCTGCTCGCCTTTATAATG
runx2_N    -----

U1557      TTTGTTGAAAAATCCTCCATCGCTCCCAACTGATGAAAACAGGAAGCTCTATTTCATAAAT
runx2_N    -----

U1557      GTGAAATTCACTGCCTATGATATATAATCATCCTAATAAGAAAATGAGCTCTAGACATAC
runx2_N    -----

U1557      ATGTCCAAGAGGGCAAAGAAGAGATAGTTTCCCAAAGATGGTTTCAATTCTCTTCTGAA
runx2_N    -----

U1557      TCAGAATTAGCAAATCGAGACGACTAACATACTCTGTCTGCGTGCATTATTCCCTACTAC
runx2_N    -----

U1557      ACACAGCATTTTGTAAATTTATTCAAAGCTTCCATTATAAACAAAAAATACAGTTTCTG
runx2_N    -----

U1557      TTAACCCACTCTATTCTGAACTATGGAACTACTGAATATCTCATTATATATGCAGAGCT
runx2_N    -----

U1557      GAAGCCCAAAGTCTGTACAGTCACTTCCAAGTGGACTAAAGAATCATACAAAACGTTT
runx2_N    -----

```

U1557 CTTTTAGAGATAAAATCCAGTCATGCAGAAAATTAACACTATCCAACAACCTGTATCCT
runx2_N -----

U1557 GCAGGTCTTGACATTTGTTTTTTTGGGTTTTTTTTTCGTTTGTGTTGTTTTTTAAG
runx2_N -----

U1557 ATCTTCAAAGTAACCAAGGGATGATGGTAAAAATAATAAATGATACTAATTACATTTA
runx2_N -----

U1557 ATCTTTATTGTAAGAGCTACCACCTAATAAAAAAATCAACTACACAGTCATGATTTAGTA
runx2_N -----

U1557 TTTGTAAAGGAATCCCCAGGCTAACACTTTTGTGACAGCCAATTACAGTCAATCCCGGCA
runx2_N -----TTACAGTCAATCCCGGCA

U1557 AGGAGTTTGCAGCAGACCTTTGGAAAGGTAACTGTTTTACAATGAGTTACAGATCTAC
runx2_N AGGAGTTTGCAGCAGACCTTTGGAAAGGTAACTGTTTTACAATGAGTTACAGATCTAC

U1557 AAGCTTAGGAAGACAAGCAGGAAAGAAGCAGCCACCCTGGGAAATCCGAAGCAGCCCTGA
runx2_N AAGCTTAGGAAGACAAGCAGGAAAGAAGCAGCCACCCTGGGAAATCCGAAGCAGCCCTGA

U1557 AAGTGATACAATCCCAAGATGTGACCCACTGCGAAGCAGCAGTTGTTTCAGAACGCTGCAC
runx2_N AAGTGATACAATCCCAAGATGTGACCCACTGCGAAGCAGCAGTTGTTTCAGAACGCTGCAC

U1557 TCACCTTGAACAGTTTTGCTCACTTTTCCATAGACATAATAATGAAGGAAAGAGAGGAGG
runx2_N TCACCTTGAACAGTTTTGCTCACTTTTCCATAGACATAATAATGAAGGAAAGAGAGGAGG

U1557 GGTAGAGAAAAGAGAAGAAAGAGCAGACGAGGGAAGGAGGGAAAGGGGGAGTAGGGAGGT
runx2_N GGTAGAGAAAAGAGAAGAAAGAGCAGACGAGGGAAGGAGGGAAAGGGGGAGTAGGGAGGT

U1557 GGTAGAAGGAAAACCTTAGCTGCAGAGTTCTGCTCTCCAAGTGCTTAACCTTACAGGA
runx2_N GGTAGAAGGAAAACCTTAGCTGCAGAGTTCTGCTCTCCAAGTGCTTAACCTTACAGGA

U1557 GTGTGGGCTCCTTCAGCATTGTATTCTATCCAAATCCTCATGAGTCACAAAAATTA
runx2_N GTGTGGGCTCCTTCAGCATTGTATTCTATCCAAATCCTCATGAGTCACAAAAATTA

U1557 AGCTATAACCTTCTGAATGCCAGGAAGGCCTCACCACAAGCCTTTTGTGAGAGGGGAGA
runx2_N AGCTATAACCTTCTGAATGCCAGGAAGGCCTCACCACAAGCCTTTTGTGAGAGGGGAGA

U1557 AAGGGAGGGGGAGGAAGGGAGAGAGAGGAAGGGAGGAAGGGAGAGAGAGCACCATAA
runx2_N AAGGGAGGGGGAGGAAGGGAGAGAGAGGAAGGGAGGAAGGGAGAGAGAGCACCATAA

U1557 GTAAAGAGACAGAAGGAAGGGAAGGGAGAGGACAACAGAAGAAAAGGGAGGGGAGGG
runx2_N GTAAAGAGACAGAAGGAAGGGAAGGGAGAGGACAACAGAAGAAAAGGGAGGGGAGGG

U1557 GAGAAGGAAAAAGATTGAGAAAAGGGAGGGGAGAGAAAAGGGGAAGCCACAGTGGTA
runx2_N GAGAAGGAAAAAGATTGAGAAAAGGGAGGGGAGAGAAAAGGGGAAGCCACAGTGGTA

U1557 GGCAGTCCCACCTTACTTTGAGTACTGTGAGGTCACAAACCACATGATTTCTGTCTCCA
runx2_N GGCAGTCCCACCTTACTTTGAGTACTGTGAGGTCACAAACCACATGATTTCTGTCTCCA


```

U1557      GTAATAGTGCTTGCAAAAAATAGGAGTTTAAAGCTTTTGCTTTTTGGATTGTGTGAGT
runx2_N    -----
U1557      GCTTCATTGCGCTCACAAACAACCACAGAACCACAAGTGCGGTGCAAACCTTCTCCAGGA
runx2_N    -----
U1557      GGACAGCAAGGAGGCCCTGGTGTTTAAATGGTTAATCTCTGCAGGTCACCTACCAGCCA
runx2_N    -----

```

3. The alignment of *runx2-F* sequence with the U1557 sequence

```

U1557      GAGTGGCGTGGATAAAATGGCAAGAAATGCCTAGGAAATGGTCTGCTCGCCTTTATAATG
runx2_F    -----AGGAAATGGTCTGCTCGCCTTTATAATG
                *****
U1557      TTGTTGAAAAATCCTCCATCGCTCCCAACTGATGAAAACAGGAAGCTCTATTCATAAAAT
runx2_F    TTGTTGAAAAATCCTCCATCGCTCCCAACTGATGAAAACAGGAAGCTCTATTCATAAAAT
                *****
U1557      GTGAAATTCACCTGCCTATGATATATAATCATCCTAATAAGAAAATGAGCTCTAGACATAC
runx2_F    GTGAAATTCACCTGCCTATGATATATAATCATCCTAATAAGAAAATGAGCTCTAGACATAC
                *****
U1557      ATGTCCAAGAGGGCAAAAGAAGAGATAGTTTCCCAAAGATGGTTTCAATTCTTCTTGAA
runx2_F    ATGTCCAAGAGGGCAAAAGAAGAGATAGTTTCCCAAAGATGGTTTCAATTCTTCTTGAA
                *****
U1557      TCAGAAATAGCAAATCGAGACGACTAACATACTCTGTCTGCGTGCATTATTCTTACTAC
runx2_F    TCAGAAATAGCAAATCGAGACGACTAACATACTCTGTCTGCGTGCATTATTCTTACTAC
                *****
U1557      ACACAGCATTTTGTAAATTTATTTCAAAGCTTCCATTATAAACAAAAAATACAGTTTCTG
runx2_F    ACACAGCATTTTGTAAATTTATTTCAAAGCTTCCATTATAAACAAAAAATACAGTTTCTG
                *****
U1557      TTAACCCACTCTATTCTGAACTATGGAACTACTGAAATATCTCATTATATATGCAGAGCT
runx2_F    TTAACCCACTCTATTCTGAACTATGGAACTACTGAAATATCTCATTATATATGCAGAGCT
                *****
U1557      GAAGCCCAAAGTCTGTACAGTCACTTCCAAGTGGACTAAAGAATCATACAAAACGTTT
runx2_F    GAAGCCCAAAGTCTGTACAGTCACTTCCAAGTGGACTAAAGAATCATACAAAACGTTT
                *****
U1557      CTTTLAGAGATAAAATCCAGTCATGCAGAAAATTAACACTATTCCAACAACCTGTATCCT
runx2_F    CTTTLAGAGATAAAATCCAGTCATGCAGAAAATTAACACTATTCCAACAACCTGTATCCT
                *****
U1557      GCAGGTCTTGACATTTGTTTTTTGGGTTTTTTTTTCGTTTGTGTTGTTTTTAAAG
runx2_F    GCAGGTCTTGACATTTGTTTTTTGGGTTTTTTTTTCGTTTGTGTTGTTTTTAAAG
                *****
U1557      ATCTTCAAAGTAACCAAGGGATGATGGTAAAAATAATATAAATGATACTAATTACATTTA
runx2_F    ATCTTCAAAGTAACCAAGGGATGATGGTAAAAATAATATAAATGATACTAATTACATTTA
                *****
U1557      ATCTTTATGTAGAGCTACCACCTAATAAAAAAATCAACTACACAGTCATGATTTAGTA
runx2_F    ATCTTTATGTAGAGCTACCACCTAATAAAAAAATCAACTACACAGTCATGATTTAGTA
                *****

```

U1557
runx2_F
TTTGTAAGGAATCCCCAGGCTAACACTTTTGTGACAGCCAATTACAGTCAATCCCGGCA
TTTGTAAGGAATCCCCAGGCTAACACTTTTGTGACAGCCAATTACAGTCAATCCCGGCA

U1557
runx2_F
AGGAGTTTGCAGCAGACCTTTGGAAAGGTAACTGTTTTACAATGAGTTACAGATCTAC
AGGAGTTTGCAGCAGACCTTTGGAAAGGTAACTGTTTTACAATGAGTTACAGATCTAA

U1557
runx2_F
AAGCTTAGGAAGACAAGCAGGAAAGAAGCAGCCACCCTGGGAAATCCGAAGCAGCCCTGA
AAGCTTAGGAAGAAAAGCAGGN-----

U1557
runx2_F
AAGTGATACAATCCCAAGATGTGACCCACTGCGAAGCAGCAGTTGTTTCAGAACGCTGCAC

U1557
runx2_F
TCACTTGAAACAGTTTTTGTCTCACTTTTCCATAGACATAATAATGAAGGAAAGAGAGGAG

U1557
runx2_F
GGTAGAGAAAAGAGAAGAAAGAGCAGACGAGGGAAGGAGGGAAGGGGGAGTAGGGAGGT

U1557
runx2_F
GGTAGAAAGGAAAACCTTAGCTGCAGAGTTCTGCTCTCCAAGTGCTTAACCTTACAGGA

U1557
runx2_F
GTGTGGGCTCCTTCAGCATTTGTATTCTATCCAAATCCTCATGAGTCACAAAAATTAAAA

U1557
runx2_F
AGCTATAACCTTCTGAATGCCAGGAAGGCCTCACCACAAGCCTTTTGTGACAGAGGGAGA

U1557
runx2_F
AAGGGAGGGGAGGAAGGGAGAGAGAGAGGAAGGGAGGAAGGGAGAGAGAGCACCATAA

U1557
runx2_F
GTAAAGAGACAGAAGGAAGGGAAGGGAGAGGACAACAGAAGAGAAAGGGAGGGGAGGG

U1557
runx2_F
GAGAAGGAAAAAGATTGAGAAAGAGGGAGGGGAGAGAGAAAGGGGAAGCCACAGTGGTA

U1557
runx2_F
GGCAGTCCCACCTTACTTTGAGTACTGTGAGGTCACAAACCACATGATTCTGTCTCTCCA

U1557
runx2_F
GTAATAGTGCTTGCAAAAAATAGGAGTTTTAAAGCTTTTGTCTTTTTTGGATTGTGTGAGT

U1557
runx2_F
GCTTCATTGCTCACAACAACCACAGAACCACAAGTGCGGTGCAAACTTTCTCCAGGA

U1557
runx2_F
GGACAGCAAGGAGGCCCTGGTGTTTAAATGGTTAATCTCTGCAGGTCACTACCAGCCA

APPENDIX D
STATISTICAL ANALYSIS

Abbreviation:

A1	2%FBS/TA+AA	C1	Insulin/TA+AA
A2	2%FBS/BMP2	C2	Insulin/BMP2
A3	2%FBS/BMP7	C3	Insulin/BMP7
A4	2%FBS/BMP2+BMP7	C4	Insulin/
B1	FGF2/ TA+AA	D1	FGF2+insulin/TA+AA
B2	FGF2/BMP2	D2	FGF2+insulin/BMP2
B3	FGF2/BMP7	D3	FGF2+insulin/BMP7
B4	FGF2/BMP2+BMP7	D4	FGF2+insulin/BMP2+BMP7

1. T-test of the expression of stem cell-associated genes of HBMSCs after serial passaging.

Group Statistics

	group	N	Mean	Std. Deviation	Std. Error Mean
<i>oct4</i>	passage2	4	1.0578	.06550	.03275
	passage5	4	.5371	.14251	.07125
<i>sox2</i>	passage2	4	1.0541	.32425	.16213
	passage5	4	.2366	.07871	.03936
<i>nanog</i>	passage2	4	1.0192	.22460	.11230
	passage5	4	.6512	.12322	.06161
<i>bst1</i>	passage2	4	1.0129	.18715	.09358
	passage5	4	2.9249	.16409	.08204
<i>fgf4</i>	passage2	4	1.0080	.15183	.07591
	passage5	4	.5943	.00787	.00393
<i>rex1</i>	passage2	4	1.0069	.11523	.05762
	passage5	4	1.0746	.31395	.15697
<i>tert</i>	passage2	4	1.0192	.22097	.11048
	passage5	4	2.7254	.89911	.44956

Independent Samples Test

		Levene's Test for Equality of Variances		t-test for Equality of Means						
		F	Sig.	t	df	Sig. (2-tailed)	Mean Difference	Std. Error Difference	95% Confidence Interval of the Difference	
									Lower	Upper
<i>oct4</i>	Equal variances assumed	1.965	.210	6.640	6	.001	.52071	.07842	.32882	.71259
	Equal variances not assumed			6.640	4.213	.002	.52071	.07842	.30726	.73415
<i>sox2</i>	Equal variances assumed	1.587	.255	4.901	6	.003	.81758	.16683	.40935	1.22581
	Equal variances not assumed			4.901	3.352	.012	.81758	.16683	.31685	1.31831
<i>nanog</i>	Equal variances assumed	2.801	.145	2.873	6	.028	.36797	.12809	.05454	.68140
	Equal variances not assumed			2.873	4.656	.038	.36797	.12809	.03124	.70470
<i>bst1</i>	Equal variances assumed	.438	.533	-15.364	6	.000	-1.91201	.12445	-2.21653	-1.60749
	Equal variances not assumed			-15.364	5.899	.000	-1.91201	.12445	-2.21780	-1.60622
<i>fgf4</i>	Equal variances assumed	5.642	.055	5.443	6	.002	.41373	.07601	.22773	.59973
	Equal variances not assumed			5.443	3.016	.012	.41373	.07601	.17255	.65491
<i>rex1</i>	Equal variances assumed	2.632	.156	-.405	6	.699	-.06773	.16721	-.47689	.34142
	Equal variances not assumed			-.405	3.794	.707	-.06773	.16721	-.54211	.40664
<i>tert</i>	Equal variances assumed	2.861	.142	-3.686	6	.010	-1.70616	.46293	-2.83891	-.57340
	Equal variances not assumed			-3.686	3.361	.029	-1.70616	.46293	-3.09380	-.31851

2. T-test of the expression of stem cell-associated genes and osteogenic genes of HBMSCs induced with FGF2 and/or insulin.

Group Statistics

group	N	Mean	Std. Deviation	Std. Error Mean	
<i>oct4</i>	non-induced	4	1.0578	.06550	.03275
	induced	4	.6452	.10412	.05206
<i>sox2</i>	non-induced	4	1.0541	.32425	.16213
	induced	4	2.2217	.57778	.28889
<i>nanog</i>	non-induced	4	1.0192	.22460	.11230
	induced	4	.8443	.13239	.06619
<i>bst1</i>	non-induced	4	1.0129	.18715	.09358
	induced	4	2.8920	.64383	.32192
<i>fgf4</i>	non-induced	4	1.0080	.15183	.07591
	induced	4	2.2288	.26043	.13022
<i>rex1</i>	non-induced	4	1.0069	.11523	.05762
	induced	4	1.0287	.29551	.14776
<i>tert</i>	non-induced	4	1.0192	.22097	.11048
	induced	4	.2394	.04550	.02275
<i>osc</i>	non-induced	6	1.0433	.05538	.02261
	induced	6	.4350	.04637	.01893
<i>alp</i>	non-induced	6	1.0350	.28933	.11812
	induced	6	.6483	.04070	.01662
<i>runx2</i>	non-induced	6	.9433	.13515	.05518
	induced	6	1.0700	.04980	.02033
<i>opn</i>	non-induced	6	1.1183	.08727	.03563
	induced	6	2.3883	.14552	.05941
<i>bsp</i>	non-induced	6	.9883	.09218	.03763
	induced	6	3.5100	.04427	.01807

Independent Samples Test

		Levene's Test for Equality of Variances		t-test for Equality of Means						
		F	Sig.	t	df	Sig. (2-tailed)	Mean Difference	Std. Error Difference	95% Confidence Interval of the Difference	
									Lower	Upper
<i>oct4</i>	Equal variances assumed	.292	.608	6.708	6	.001	.41259	.06151	.26209	.56309
	Equal variances not assumed			6.708	5.053	.001	.41259	.06151	.25498	.57020
<i>sox2</i>	Equal variances assumed	6.957	.039	-3.525	6	.012	-1.16759	.33127	-1.97819	-.35700
	Equal variances not assumed			-3.525	4.719	.019	-1.16759	.33127	-2.03463	-.30056
<i>nanog</i>	Equal variances assumed	2.215	.187	1.342	6	.228	.17495	.13036	-.14403	.49393
	Equal variances not assumed			1.342	4.860	.239	.17495	.13036	-.16307	.51297
<i>bst1</i>	Equal variances assumed	2.180	.190	-5.605	6	.001	-1.87910	.33524	-2.69940	-1.05879
	Equal variances not assumed			-5.605	3.503	.007	-1.87910	.33524	-2.86429	-.89390
<i>fgf4</i>	Equal variances assumed	.515	.500	-8.099	6	.000	-1.22081	.15073	-1.58963	-.85200
	Equal variances not assumed			-8.099	4.828	.001	-1.22081	.15073	-1.61246	-.82917
<i>rex1</i>	Equal variances assumed	1.999	.207	-.137	6	.895	-.02177	.15859	-.40983	.36629
	Equal variances not assumed			-.137	3.892	.898	-.02177	.15859	-.46696	.42343
<i>tert</i>	Equal variances assumed	2.978	.135	6.913	6	.000	.77984	.11280	.50382	1.05585
	Equal variances not assumed			6.913	3.254	.005	.77984	.11280	.43619	1.12348
<i>osc</i>	Equal variances assumed	.045	.837	20.631	10	.000	.60833	.02949	.54263	.67403
	Equal variances not assumed			20.631	9.700	.000	.60833	.02949	.54236	.67431
<i>alp</i>	Equal variances assumed	48.202	.000	3.242	10	.009	.38667	.11928	.12089	.65244
	Equal variances not assumed			3.242	5.198	.022	.38667	.11928	.08352	.68981
<i>runx2</i>	Equal variances assumed	3.858	.078	-2.154	10	.057	-.12667	.05880	-.25769	.00435
	Equal variances not assumed			-2.154	6.333	.072	-.12667	.05880	-.26874	.01540
<i>opn</i>	Equal variances assumed	.227	.644	-18.333	10	.000	-1.27000	.06927	-1.42435	-1.11565
	Equal variances not assumed			-18.333	8.185	.000	-1.27000	.06927	-1.42912	-1.11088
<i>bsp</i>	Equal variances assumed	1.683	.224	-60.404	10	.000	-2.52167	.04175	-2.61468	-2.42865
	Equal variances not assumed			-60.404	7.190	.000	-2.52167	.04175	-2.61985	-2.42348

3. ANOVA analysis of the MTT assay

ANOVA

MTT

	Sum of Squares	df	Mean Square	F	Sig.
Between Groups	.162	3	.054	42.153	.000
Within Groups	.010	8	.001		
Total	.172	11			

Multiple Comparisons

MTT

Tukey HSD

(I) group	(J) group	Mean Difference (I-J)	Std. Error	Sig.	95% Confidence Interval	
					Lower Bound	Upper Bound
2%FBS	FGF2	-.02198	.02924	.874	-.1156	.0717
	INSULIN	-.20113*	.02924	.001	-.2948	-.1075
	FGF2+INSULIN	-.27347*	.02924	.000	-.3671	-.1798
FGF2	2%FBS	.02198	.02924	.874	-.0717	.1156
	INSULIN	-.17915*	.02924	.001	-.2728	-.0855
	FGF2+INSULIN	-.25150*	.02924	.000	-.3451	-.1578
INSULIN	2%FBS	.20113*	.02924	.001	.1075	.2948
	FGF2	.17915*	.02924	.001	.0855	.2728
	FGF2+INSULIN	-.07234	.02924	.139	-.1660	.0213
FGF2 +INSULIN	2%FBS	.27347*	.02924	.000	.1798	.3671
	FGF2	.25150*	.02924	.000	.1578	.3451
	INSULIN	.07234	.02924	.139	-.0213	.1660

*. The mean difference is significant at the 0.05 level.

4. ANOVA analysis of the relative gene expression levels of RBMSCs induced with FGF2 and/or insulin.

ANOVA

		Sum of Squares	df	Mean Square	F	Sig.
<i>runx2</i>	Between Groups	21.722	3	7.241	41.167	.000
	Within Groups	1.407	8	.176		
	Total	23.129	11			
<i>osx</i>	Between Groups	4.348	3	1.449	9.303	.005
	Within Groups	1.246	8	.156		
	Total	5.594	11			

ANOVA

		Sum of Squares	df	Mean Square	F	Sig.
<i>bmp7</i>	Between Groups	8.422	3	2.807	51.610	.000
	Within Groups	.435	8	.054		
	Total	8.858	11			
<i>axin2</i>	Between Groups	8.354	3	2.785	26.271	.000
	Within Groups	.848	8	.106		
	Total	9.202	11			
<i>β-catenin</i>	Between Groups	33.630	3	11.210	12.957	.002
	Within Groups	6.921	8	.865		
	Total	40.551	11			
<i>dkk1</i>	Between Groups	334.761	3	111.587	6.266	.017
	Within Groups	142.473	8	17.809		
	Total	477.234	11			

Multiple Comparisons

Tukey HSD

Dependent Variable	(I) group	(J) group	Mean Difference (I-J)	Std. Error	Sig.	95% Confidence Interval	
						Lower Bound	Upper Bound
<i>runx2</i>	2%FBS	FGF2	.33637	.34243	.763	-.7602	1.4329
		INSULIN	-.25150	.34243	.881	-1.3481	.8451
		FGF2+INSULIN	-3.04128*	.34243	.000	-4.1379	-1.9447
	FGF2	2%FBS	-.33637	.34243	.763	-1.4329	.7602
		INSULIN	-.58787	.34243	.376	-1.6844	.5087
		FGF2+INSULIN	-3.37765*	.34243	.000	-4.4742	-2.2811
	INSULIN	2%FBS	.25150	.34243	.881	-.8451	1.3481
		FGF2	.58787	.34243	.376	-.5087	1.6844
		FGF2+INSULIN	-2.78978*	.34243	.000	-3.8864	-1.6932
	FGF2 +INSULIN	2%FBS	3.04128*	.34243	.000	1.9447	4.1379
		FGF2	3.37765*	.34243	.000	2.2811	4.4742
		INSULIN	2.78978*	.34243	.000	1.6932	3.8864
<i>osx</i>	2%FBS	FGF2	.55398	.32226	.375	-.4780	1.5860
		INSULIN	.01153	.32226	1.000	-1.0205	1.0435
		FGF2+INSULIN	-1.10186*	.32226	.037	-2.1339	-.0699
	FGF2	2%FBS	-.55398	.32226	.375	-1.5860	.4780
		INSULIN	-.54244	.32226	.391	-1.5744	.4896
		FGF2+INSULIN	-1.65583*	.32226	.004	-2.6878	-.6238
	INSULIN	2%FBS	-.01153	.32226	1.000	-1.0435	1.0205
		FGF2	.54244	.32226	.391	-.4896	1.5744
		FGF2+INSULIN	-1.11339*	.32226	.035	-2.1454	-.0814
	FGF2 +INSULIN	2%FBS	1.10186*	.32226	.037	.0699	2.1339
		FGF2	1.65583*	.32226	.004	.6238	2.6878

Dependent Variable	(I) group	(J) group	Mean Difference (I-J)	Std. Error	Sig.	95% Confidence Interval	
						Lower Bound	Upper Bound
		INSULIN	1.11339*	.32226	.035	.0814	2.1454
<i>bmp7</i>	2%FBS	FGF2	.54642	.19043	.080	-.0634	1.1562
		INSULIN	-.86296*	.19043	.008	-1.4728	-.2531
		FGF2+INSULIN	-1.65366*	.19043	.000	-2.2635	-1.0438
	FGF2	2%FBS	-.54642	.19043	.080	-1.1562	.0634
		INSULIN	-1.40937*	.19043	.000	-2.0192	-.7995
		FGF2+INSULIN	-2.20008*	.19043	.000	-2.8099	-1.5902
	INSULIN	2%FBS	.86296*	.19043	.008	.2531	1.4728
		FGF2	1.40937*	.19043	.000	.7995	2.0192
		FGF2+INSULIN	-.79071*	.19043	.014	-1.4005	-.1809
	FGF2	2%FBS	1.65366*	.19043	.000	1.0438	2.2635
		+INSULIN	2.20008*	.19043	.000	1.5902	2.8099
		INSULIN	.79071*	.19043	.014	.1809	1.4005
<i>axin2</i>	2%FBS	FGF2	.56784	.26583	.221	-.2835	1.4191
		INSULIN	-.30720	.26583	.668	-1.1585	.5441
		FGF2+INSULIN	-1.69849*	.26583	.001	-2.5498	-.8472
	FGF2	2%FBS	-.56784	.26583	.221	-1.4191	.2835
		INSULIN	-.87504*	.26583	.044	-1.7263	-.0237
		FGF2+INSULIN	-2.26633*	.26583	.000	-3.1176	-1.4150
	INSULIN	2%FBS	.30720	.26583	.668	-.5441	1.1585
		FGF2	.87504*	.26583	.044	.0237	1.7263
		FGF2+INSULIN	-1.39129*	.26583	.003	-2.2426	-.5400
	FGF2	2%FBS	1.69849*	.26583	.001	.8472	2.5498
		+INSULIN	2.26633*	.26583	.000	1.4150	3.1176
		INSULIN	1.39129*	.26583	.003	.5400	2.2426
<i>β-catenin</i>	2%FBS	FGF2	.36571	.75945	.961	-2.0663	2.7977
		INSULIN	-.70759	.75945	.789	-3.1396	1.7244
		FGF2+INSULIN	-3.87598*	.75945	.004	-6.3080	-1.4440
	FGF2	2%FBS	-.36571	.75945	.961	-2.7977	2.0663
		INSULIN	-1.07330	.75945	.526	-3.5053	1.3587
		FGF2+INSULIN	-4.24169*	.75945	.002	-6.6737	-1.8097
	INSULIN	2%FBS	.70759	.75945	.789	-1.7244	3.1396
		FGF2	1.07330	.75945	.526	-1.3587	3.5053
		FGF2+INSULIN	-3.16839*	.75945	.013	-5.6004	-.7364
	FGF2	2%FBS	3.87598*	.75945	.004	1.4440	6.3080
		+INSULIN	4.24169*	.75945	.002	1.8097	6.6737
		INSULIN	3.16839*	.75945	.013	.7364	5.6004
<i>dkk1</i>	2%FBS	FGF2	1.02403	3.44569	.990	-10.0103	12.0583
		INSULIN	.10328	3.44569	1.000	-10.9310	11.1376
		FGF2+INSULIN	-	3.44569	.037	-22.8214	-.7528
	FGF2	2%FBS	11.78709*				
		INSULIN	-1.02403	3.44569	.990	-12.0583	10.0103
		INSULIN	-.92075	3.44569	.993	-11.9551	10.1135

Dependent Variable	(I) group	(J) group	Mean Difference (I-J)	Std. Error	Sig.	95% Confidence Interval	
						Lower Bound	Upper Bound
		FGF2+INSULIN	-12.81112*	3.44569	.024	-23.8454	-1.7768
	INSULIN	2%FBS	-.10328	3.44569	1.000	-11.1376	10.9310
		FGF2	.92075	3.44569	.993	-10.1135	11.9551
		FGF2+INSULIN	-11.89037*	3.44569	.035	-22.9247	-.8561
	FGF2	2%FBS	11.78709*	3.44569	.037	.7528	22.8214
	+INSULIN	FGF2	12.81112*	3.44569	.024	1.7768	23.8454
		INSULIN	11.89037*	3.44569	.035	.8561	22.9247

*. The mean difference is significant at the 0.05 level.

5. ANOVA analysis of the relative gene expression levels of RBMSCs induced with 10 ng/ml BMP2, 10 ng/ml BMP7, or a combination of BMPs.

ANOVA

		Sum of Squares	df	Mean Square	F	Sig.
<i>runx2</i>	Between Groups	9.470	3	3.157	420.904	.000
	Within Groups	.060	8	.007		
	Total	9.530	11			
<i>osx</i>	Between Groups	1.484	3	.495	318.024	.000
	Within Groups	.012	8	.002		
	Total	1.497	11			
<i>bmp7</i>	Between Groups	1.900	3	.633	89.657	.000
	Within Groups	.057	8	.007		
	Total	1.957	11			
<i>axin2</i>	Between Groups	1.899	3	.633	24.555	.000
	Within Groups	.206	8	.026		
	Total	2.105	11			
<i>β-catenin</i>	Between Groups	4.995	3	1.665	256.215	.000
	Within Groups	.052	8	.006		
	Total	5.047	11			
<i>dkk1</i>	Between Groups	1.648	3	.549	38.929	.000
	Within Groups	.113	8	.014		
	Total	1.761	11			

Multiple Comparisons

Tukey HSD

Dependent Variable	(I) GROUP	(J) GROUP	Mean Difference (I-J)	Std. Error	Sig.	95% Confidence Interval	
						Lower Bound	Upper Bound
runx2	A1	A2	.18878	.07071	.106	-.0377	.4152
		A3	-1.94037*	.07071	.000	-2.1668	-1.7139
		A4	-1.29442*	.07071	.000	-1.5209	-1.0680
	A2	A1	-.18878	.07071	.106	-.4152	.0377
		A3	-2.12914*	.07071	.000	-2.3556	-1.9027
		A4	-1.48320*	.07071	.000	-1.7096	-1.2568
	A3	A1	1.94037*	.07071	.000	1.7139	2.1668
		A2	2.12914*	.07071	.000	1.9027	2.3556
		A4	.64594*	.07071	.000	.4195	.8724
	A4	A1	1.29442*	.07071	.000	1.0680	1.5209
		A2	1.48320*	.07071	.000	1.2568	1.7096
		A3	-.64594*	.07071	.000	-.8724	-.4195
osx	A1	A2	.19629*	.03220	.001	.0932	.2994
		A3	-.70298*	.03220	.000	-.8061	-.5999
		A4	-.42089*	.03220	.000	-.5240	-.3178
	A2	A1	-.19629*	.03220	.001	-.2994	-.0932
		A3	-.89927*	.03220	.000	-1.0024	-.7961
		A4	-.61717*	.03220	.000	-.7203	-.5140
	A3	A1	.70298*	.03220	.000	.5999	.8061
		A2	.89927*	.03220	.000	.7961	1.0024
		A4	.28210*	.03220	.000	.1790	.3852
	A4	A1	.42089*	.03220	.000	.3178	.5240
		A2	.61717*	.03220	.000	.5140	.7203
		A3	-.28210*	.03220	.000	-.3852	-.1790
bmp7	A1	A2	1.06285*	.06863	.000	.8431	1.2826
		A3	.38795*	.06863	.002	.1682	.6077
		A4	.75427*	.06863	.000	.5345	.9741
	A2	A1	-1.06285*	.06863	.000	-1.2826	-.8431
		A3	-.67489*	.06863	.000	-.8947	-.4551
		A4	-.30857*	.06863	.009	-.5284	-.0888
	A3	A1	-.38795*	.06863	.002	-.6077	-.1682
		A2	.67489*	.06863	.000	.4551	.8947
		A4	.36632*	.06863	.003	.1465	.5861
	A4	A1	-.75427*	.06863	.000	-.9741	-.5345
		A2	.30857*	.06863	.009	.0888	.5284
		A3	-.36632*	.06863	.003	-.5861	-.1465
axin2	A1	A2	.29466	.13110	.190	-.1252	.7145
		A3	-.78562*	.13110	.001	-1.2054	-.3658
		A4	-.27524	.13110	.232	-.6951	.1446
	A2	A1	-.29466	.13110	.190	-.7145	.1252
		A3	-1.08029*	.13110	.000	-1.5001	-.6605

Dependent Variable	(I) GROUP	(J) GROUP	Mean Difference (I-J)	Std. Error	Sig.	95% Confidence Interval		
						Lower Bound	Upper Bound	
	A3	A4	-.56990*	.13110	.011	-.9897	-.1501	
		A1	.78562*	.13110	.001	.3658	1.2054	
		A2	1.08029*	.13110	.000	.6605	1.5001	
	A4	A4	.51039*	.13110	.019	.0906	.9302	
		A1	.27524	.13110	.232	-.1446	.6951	
		A2	.56990*	.13110	.011	.1501	.9897	
	<i>β-catenin</i>	A1	A3	-.51039*	.13110	.019	-.9302	-.0906
			A2	.49128*	.06582	.000	.2805	.7021
			A4	-1.27307*	.06582	.000	-1.4839	-1.0623
		A2	A4	-.16538	.06582	.132	-.3762	.0454
			A1	-.49128*	.06582	.000	-.7021	-.2805
			A3	-1.76435*	.06582	.000	-1.9751	-1.5536
A3		A4	-.65666*	.06582	.000	-.8674	-.4459	
		A1	1.27307*	.06582	.000	1.0623	1.4839	
		A2	1.76435*	.06582	.000	1.5536	1.9751	
A4		A4	1.10769*	.06582	.000	.8969	1.3185	
		A1	.16538	.06582	.132	-.0454	.3762	
		A2	.65666*	.06582	.000	.4459	.8674	
<i>dkk</i>	A1	A3	-1.10769*	.06582	.000	-1.3185	-.8969	
		A2	.77743*	.09698	.000	.4669	1.0880	
		A4	.97461*	.09698	.000	.6640	1.2852	
	A2	A4	.73966*	.09698	.000	.4291	1.0502	
		A1	-.77743*	.09698	.000	-1.0880	-.4669	
		A3	.19718	.09698	.253	-.1134	.5077	
	A3	A4	-.03776	.09698	.979	-.3483	.2728	
		A1	-.97461*	.09698	.000	-1.2852	-.6640	
		A2	-.19718	.09698	.253	-.5077	.1134	
	A4	A4	-.23494	.09698	.150	-.5455	.0756	
		A1	-.73966*	.09698	.000	-1.0502	-.4291	
		A2	.03776	.09698	.979	-.2728	.3483	
		A3	.23494	.09698	.150	-.0756	.5455	

*. The mean difference is significant at the 0.05 level

6. ANOVA analysis of the relative gene expression levels after RBMSCs were sequentially treated with proliferation and differentiation factors.

6.1 *runx2*

ANOVA

runx2

	Sum of Squares	df	Mean Square	F	Sig.
Between Groups	5.690	15	.379	54.754	.000
Within Groups	.222	32	.007		
Total	5.912	47			

Multiple Comparisons

runx2

Tukey HSD

(I) GROUP	(J) GROUP	Mean Difference (I-J)	Std. Error	Sig.	95% Confidence Interval	
					Lower Bound	Upper Bound
A1	A2	1.06285*	.06796	.000	.8108	1.3149
	A3	.38795*	.06796	.000	.1359	.6400
	A4	.75427*	.06796	.000	.5023	1.0063
	B1	1.00519*	.06796	.000	.7532	1.2572
	B2	.54785*	.06796	.000	.2958	.7999
	B3	.72457*	.06796	.000	.4726	.9766
	B4	.09376	.06796	.988	-.1582	.3458
	C1	.15139	.06796	.673	-.1006	.4034
	C2	.67120*	.06796	.000	.4192	.9232
	C3	.04843	.06796	1.000	-.2036	.3004
	C4	-.01467	.06796	1.000	-.2667	.2373
	D1	.09418	.06796	.987	-.1578	.3462
	D2	.38434*	.06796	.000	.1323	.6363
	D3	.60434*	.06796	.000	.3523	.8563
D4	.62955*	.06796	.000	.3775	.8816	
A2	A1	-1.06285*	.06796	.000	-1.3149	-.8108
	A3	-.67489*	.06796	.000	-.9269	-.4229
	A4	-.30857*	.06796	.006	-.5606	-.0566
	B1	-.05765	.06796	1.000	-.3097	.1944
	B2	-.51499*	.06796	.000	-.7670	-.2630
	B3	-.33828*	.06796	.002	-.5903	-.0863
	B4	-.96908*	.06796	.000	-1.2211	-.7171
	C1	-.91145*	.06796	.000	-1.1635	-.6594
	C2	-.39165*	.06796	.000	-.6437	-.1396
	C3	-1.01442*	.06796	.000	-1.2664	-.7624
	C4	-1.07752*	.06796	.000	-1.3295	-.8255

(I) GROUP	(J) GROUP	Mean Difference (I-J)	Std. Error	Sig.	95% Confidence Interval	
					Lower Bound	Upper Bound
	D1	-.96867*	.06796	.000	-1.2207	-.7167
	D2	-.67851*	.06796	.000	-.9305	-.4265
	D3	-.45851*	.06796	.000	-.7105	-.2065
	D4	-.43330*	.06796	.000	-.6853	-.1813
A3	A1	-.38795*	.06796	.000	-.6400	-.1359
	A2	.67489*	.06796	.000	.4229	.9269
	A4	.36632*	.06796	.001	.1143	.6183
	B1	.61724*	.06796	.000	.3652	.8692
	B2	.15990	.06796	.592	-.0921	.4119
	B3	.33662*	.06796	.002	.0846	.5886
	B4	-.29419*	.06796	.011	-.5462	-.0422
	C1	-.23656	.06796	.084	-.4886	.0154
	C2	.28324*	.06796	.016	.0312	.5352
	C3	-.33952*	.06796	.002	-.5915	-.0875
	C4	-.40263*	.06796	.000	-.6546	-.1506
	D1	-.29378*	.06796	.011	-.5458	-.0418
	D2	-.00361	.06796	1.000	-.2556	.2484
	D3	.21639	.06796	.157	-.0356	.4684
	D4	.24159	.06796	.071	-.0104	.4936
	A4	A1	-.75427*	.06796	.000	-1.0063
A2		.30857*	.06796	.006	.0566	.5606
A3		-.36632*	.06796	.001	-.6183	-.1143
B1		.25092	.06796	.052	-.0011	.5029
B2		-.20642	.06796	.209	-.4584	.0456
B3		-.02970	.06796	1.000	-.2817	.2223
B4		-.66051*	.06796	.000	-.9125	-.4085
C1		-.60288*	.06796	.000	-.8549	-.3509
C2		-.08308	.06796	.996	-.3351	.1689
C3		-.70584*	.06796	.000	-.9578	-.4538
C4		-.76895*	.06796	.000	-1.0210	-.5169
D1		-.66010*	.06796	.000	-.9121	-.4081
D2		-.36993*	.06796	.001	-.6219	-.1179
D3		-.14993	.06796	.687	-.4019	.1021
D4		-.12473	.06796	.885	-.3767	.1273
B1		A1	-1.00519*	.06796	.000	-1.2572
	A2	.05765	.06796	1.000	-.1944	.3097
	A3	-.61724*	.06796	.000	-.8692	-.3652
	A4	-.25092	.06796	.052	-.5029	.0011
	B2	-.45734*	.06796	.000	-.7093	-.2053
	B3	-.28062*	.06796	.018	-.5326	-.0286
	B4	-.91143*	.06796	.000	-1.1634	-.6594
	C1	-.85380*	.06796	.000	-1.1058	-.6018
	C2	-.33400*	.06796	.002	-.5860	-.0820
	C3	-.95676*	.06796	.000	-1.2088	-.7048
	C4	-1.01987*	.06796	.000	-1.2719	-.7679

(I) GROUP	(J) GROUP	Mean Difference (I-J)	Std. Error	Sig.	95% Confidence Interval	
					Lower Bound	Upper Bound
	D1	-.91102*	.06796	.000	-1.1630	-.6590
	D2	-.62085*	.06796	.000	-.8729	-.3688
	D3	-.40085*	.06796	.000	-.6529	-.1488
	D4	-.37565*	.06796	.000	-.6277	-.1236
B2	A1	-.54785*	.06796	.000	-.7999	-.2958
	A2	.51499*	.06796	.000	.2630	.7670
	A3	-.15990	.06796	.592	-.4119	.0921
	A4	.20642	.06796	.209	-.0456	.4584
	B1	.45734*	.06796	.000	.2053	.7093
	B3	.17672	.06796	.432	-.0753	.4287
	B4	-.45409*	.06796	.000	-.7061	-.2021
	C1	-.39646*	.06796	.000	-.6485	-.1445
	C2	.12334	.06796	.893	-.1287	.3753
	C3	-.49942*	.06796	.000	-.7514	-.2474
	C4	-.56253*	.06796	.000	-.8145	-.3105
	D1	-.45368*	.06796	.000	-.7057	-.2017
	D2	-.16351	.06796	.557	-.4155	.0885
	D3	.05649	.06796	1.000	-.1955	.3085
	D4	.08169	.06796	.997	-.1703	.3337
	B3	A1	-.72457*	.06796	.000	-.9766
A2		.33828*	.06796	.002	.0863	.5903
A3		-.33662*	.06796	.002	-.5886	-.0846
A4		.02970	.06796	1.000	-.2223	.2817
B1		.28062*	.06796	.018	.0286	.5326
B2		-.17672	.06796	.432	-.4287	.0753
B4		-.63081*	.06796	.000	-.8828	-.3788
C1		-.57318*	.06796	.000	-.8252	-.3212
C2		-.05337	.06796	1.000	-.3054	.1986
C3		-.67614*	.06796	.000	-.9281	-.4241
C4		-.73924*	.06796	.000	-.9912	-.4872
D1		-.63039*	.06796	.000	-.8824	-.3784
D2		-.34023*	.06796	.002	-.5922	-.0882
D3		-.12023	.06796	.910	-.3722	.1318
D4		-.09502	.06796	.986	-.3470	.1570
B4		A1	-.09376	.06796	.988	-.3458
	A2	.96908*	.06796	.000	.7171	1.2211
	A3	.29419*	.06796	.011	.0422	.5462
	A4	.66051*	.06796	.000	.4085	.9125
	B1	.91143*	.06796	.000	.6594	1.1634
	B2	.45409*	.06796	.000	.2021	.7061
	B3	.63081*	.06796	.000	.3788	.8828
	C1	.05763	.06796	1.000	-.1944	.3096
	C2	.57743*	.06796	.000	.3254	.8294
	C3	-.04533	.06796	1.000	-.2973	.2067
	C4	-.10843	.06796	.958	-.3604	.1436

(I) GROUP	(J) GROUP	Mean Difference (I-J)	Std. Error	Sig.	95% Confidence Interval	
					Lower Bound	Upper Bound
	D1	.00041	.06796	1.000	-.2516	.2524
	D2	.29058*	.06796	.012	.0386	.5426
	D3	.51058*	.06796	.000	.2586	.7626
	D4	.53579*	.06796	.000	.2838	.7878
C1	A1	-.15139	.06796	.673	-.4034	.1006
	A2	.91145*	.06796	.000	.6594	1.1635
	A3	.23656	.06796	.084	-.0154	.4886
	A4	.60288*	.06796	.000	.3509	.8549
	B1	.85380*	.06796	.000	.6018	1.1058
	B2	.39646*	.06796	.000	.1445	.6485
	B3	.57318*	.06796	.000	.3212	.8252
	B4	-.05763	.06796	1.000	-.3096	.1944
	C2	.51980*	.06796	.000	.2678	.7718
	C3	-.10296	.06796	.972	-.3550	.1490
	C4	-.16607	.06796	.532	-.4181	.0859
	D1	-.05722	.06796	1.000	-.3092	.1948
	D2	.23295	.06796	.095	-.0191	.4850
	D3	.45295*	.06796	.000	.2009	.7050
	D4	.47815*	.06796	.000	.2261	.7302
	C2	A1	-.67120*	.06796	.000	-.9232
A2		.39165*	.06796	.000	.1396	.6437
A3		-.28324*	.06796	.016	-.5352	-.0312
A4		.08308	.06796	.996	-.1689	.3351
B1		.33400*	.06796	.002	.0820	.5860
B2		-.12334	.06796	.893	-.3753	.1287
B3		.05337	.06796	1.000	-.1986	.3054
B4		-.57743*	.06796	.000	-.8294	-.3254
C1		-.51980*	.06796	.000	-.7718	-.2678
C3		-.62277*	.06796	.000	-.8748	-.3708
C4		-.68587*	.06796	.000	-.9379	-.4339
D1		-.57702*	.06796	.000	-.8290	-.3250
D2		-.28686*	.06796	.014	-.5389	-.0349
D3		-.06686	.06796	1.000	-.3189	.1851
D4		-.04165	.06796	1.000	-.2937	.2104
C3		A1	-.04843	.06796	1.000	-.3004
	A2	1.01442*	.06796	.000	.7624	1.2664
	A3	.33952*	.06796	.002	.0875	.5915
	A4	.70584*	.06796	.000	.4538	.9578
	B1	.95676*	.06796	.000	.7048	1.2088
	B2	.49942*	.06796	.000	.2474	.7514
	B3	.67614*	.06796	.000	.4241	.9281
	B4	.04533	.06796	1.000	-.2067	.2973
	C1	.10296	.06796	.972	-.1490	.3550
	C2	.62277*	.06796	.000	.3708	.8748
	C4	-.06310	.06796	1.000	-.3151	.1889

(I) GROUP	(J) GROUP	Mean Difference (I-J)	Std. Error	Sig.	95% Confidence Interval	
					Lower Bound	Upper Bound
	D1	.04575	.06796	1.000	-.2063	.2978
	D2	.33591*	.06796	.002	.0839	.5879
	D3	.55591*	.06796	.000	.3039	.8079
	D4	.58112*	.06796	.000	.3291	.8331
C4	A1	.01467	.06796	1.000	-.2373	.2667
	A2	1.07752*	.06796	.000	.8255	1.3295
	A3	.40263*	.06796	.000	.1506	.6546
	A4	.76895*	.06796	.000	.5169	1.0210
	B1	1.01987*	.06796	.000	.7679	1.2719
	B2	.56253*	.06796	.000	.3105	.8145
	B3	.73924*	.06796	.000	.4872	.9912
	B4	.10843	.06796	.958	-.1436	.3604
	C1	.16607	.06796	.532	-.0859	.4181
	C2	.68587*	.06796	.000	.4339	.9379
	C3	.06310	.06796	1.000	-.1889	.3151
	D1	.10885	.06796	.956	-.1432	.3609
	D2	.39901*	.06796	.000	.1470	.6510
	D3	.61901*	.06796	.000	.3670	.8710
	D4	.64422*	.06796	.000	.3922	.8962
	D1	A1	-.09418	.06796	.987	-.3462
A2		.96867*	.06796	.000	.7167	1.2207
A3		.29378*	.06796	.011	.0418	.5458
A4		.66010*	.06796	.000	.4081	.9121
B1		.91102*	.06796	.000	.6590	1.1630
B2		.45368*	.06796	.000	.2017	.7057
B3		.63039*	.06796	.000	.3784	.8824
B4		-.00041	.06796	1.000	-.2524	.2516
C1		.05722	.06796	1.000	-.1948	.3092
C2		.57702*	.06796	.000	.3250	.8290
C3		-.04575	.06796	1.000	-.2978	.2063
C4		-.10885	.06796	.956	-.3609	.1432
D2		.29016*	.06796	.012	.0382	.5422
D3		.51016*	.06796	.000	.2582	.7622
D4		.53537*	.06796	.000	.2834	.7874
D2		A1	-.38434*	.06796	.000	-.6363
	A2	.67851*	.06796	.000	.4265	.9305
	A3	.00361	.06796	1.000	-.2484	.2556
	A4	.36993*	.06796	.001	.1179	.6219
	B1	.62085*	.06796	.000	.3688	.8729
	B2	.16351	.06796	.557	-.0885	.4155
	B3	.34023*	.06796	.002	.0882	.5922
	B4	-.29058*	.06796	.012	-.5426	-.0386
	C1	-.23295	.06796	.095	-.4850	.0191
	C2	.28686*	.06796	.014	.0349	.5389
	C3	-.33591*	.06796	.002	-.5879	-.0839

(I) GROUP	(J) GROUP	Mean Difference (I-J)	Std. Error	Sig.	95% Confidence Interval	
					Lower Bound	Upper Bound
	C4	-.39901*	.06796	.000	-.6510	-.1470
	D1	-.29016*	.06796	.012	-.5422	-.0382
	D3	.22000	.06796	.141	-.0320	.4720
	D4	.24521	.06796	.063	-.0068	.4972
D3	A1	-.60434*	.06796	.000	-.8563	-.3523
	A2	.45851*	.06796	.000	.2065	.7105
	A3	-.21639	.06796	.157	-.4684	.0356
	A4	.14993	.06796	.687	-.1021	.4019
	B1	.40085*	.06796	.000	.1488	.6529
	B2	-.05649	.06796	1.000	-.3085	.1955
	B3	.12023	.06796	.910	-.1318	.3722
	B4	-.51058*	.06796	.000	-.7626	-.2586
	C1	-.45295*	.06796	.000	-.7050	-.2009
	C2	.06686	.06796	1.000	-.1851	.3189
	C3	-.55591*	.06796	.000	-.8079	-.3039
	C4	-.61901*	.06796	.000	-.8710	-.3670
	D1	-.51016*	.06796	.000	-.7622	-.2582
	D2	-.22000	.06796	.141	-.4720	.0320
	D4	.02521	.06796	1.000	-.2268	.2772
	D4	A1	-.62955*	.06796	.000	-.8816
A2		.43330*	.06796	.000	.1813	.6853
A3		-.24159	.06796	.071	-.4936	.0104
A4		.12473	.06796	.885	-.1273	.3767
B1		.37565*	.06796	.000	.1236	.6277
B2		-.08169	.06796	.997	-.3337	.1703
B3		.09502	.06796	.986	-.1570	.3470
B4		-.53579*	.06796	.000	-.7878	-.2838
C1		-.47815*	.06796	.000	-.7302	-.2261
C2		.04165	.06796	1.000	-.2104	.2937
C3		-.58112*	.06796	.000	-.8331	-.3291
C4		-.64422*	.06796	.000	-.8962	-.3922
D1		-.53537*	.06796	.000	-.7874	-.2834
D2		-.24521	.06796	.063	-.4972	.0068
D3		-.02521	.06796	1.000	-.2772	.2268

*. The mean difference is significant at the 0.05 level.

6.2 osx

ANOVA

osx

	Sum of Squares	df	Mean Square	F	Sig.
Between Groups	5.126	15	.342	123.004	.000
Within Groups	.089	32	.003		
Total	5.215	47			

Multiple Comparisons

osx

Tukey HSD

(I) GROUP	(J) GROUP	Mean Difference (I-J)	Std. Error	Sig.	95% Confidence Interval	
					Lower Bound	Upper Bound
A1	A2	.19629*	.04304	.006	.0367	.3559
	A3	-.70298*	.04304	.000	-.8626	-.5434
	A4	-.42089*	.04304	.000	-.5805	-.2613
	B1	.43948*	.04304	.000	.2799	.5991
	B2	.32400*	.04304	.000	.1644	.4836
	B3	.25117*	.04304	.000	.0916	.4108
	B4	-.30582*	.04304	.000	-.4654	-.1462
	C1	-.41645*	.04304	.000	-.5760	-.2569
	C2	.06725	.04304	.964	-.0923	.2268
	C3	-.37316*	.04304	.000	-.5327	-.2136
	C4	-.11839	.04304	.344	-.2780	.0412
	D1	.26502*	.04304	.000	.1054	.4246
	D2	.03013	.04304	1.000	-.1295	.1897
	D3	-.06578	.04304	.970	-.2254	.0938
D4	-.49740*	.04304	.000	-.6570	-.3378	
A2	A1	-.19629*	.04304	.006	-.3559	-.0367
	A3	-.89927*	.04304	.000	-1.0588	-.7397
	A4	-.61717*	.04304	.000	-.7768	-.4576
	B1	.24319*	.04304	.000	.0836	.4028
	B2	.12771	.04304	.238	-.0319	.2873
	B3	.05489	.04304	.994	-.1047	.2145
	B4	-.50211*	.04304	.000	-.6617	-.3425
	C1	-.61273*	.04304	.000	-.7723	-.4532
	C2	-.12904	.04304	.225	-.2886	.0305
	C3	-.56945*	.04304	.000	-.7290	-.4099
	C4	-.31468*	.04304	.000	-.4743	-.1551
	D1	.06874	.04304	.957	-.0908	.2283
	D2	-.16616*	.04304	.035	-.3257	-.0066
	D3	-.26207*	.04304	.000	-.4216	-.1025
D4	-.69369*	.04304	.000	-.8533	-.5341	

(I) GROUP	(J) GROUP	Mean Difference (I-J)	Std. Error	Sig.	95% Confidence Interval	
					Lower Bound	Upper Bound
A3	A1	.70298*	.04304	.000	.5434	.8626
	A2	.89927*	.04304	.000	.7397	1.0588
	A4	.28210*	.04304	.000	.1225	.4417
	B1	1.14246*	.04304	.000	.9829	1.3020
	B2	1.02698*	.04304	.000	.8674	1.1866
	B3	.95416*	.04304	.000	.7946	1.1137
	B4	.39716*	.04304	.000	.2376	.5567
	C1	.28654*	.04304	.000	.1270	.4461
	C2	.77023*	.04304	.000	.6107	.9298
	C3	.32982*	.04304	.000	.1702	.4894
	C4	.58459*	.04304	.000	.4250	.7442
	D1	.96801*	.04304	.000	.8084	1.1276
	D2	.73311*	.04304	.000	.5735	.8927
	D3	.63720*	.04304	.000	.4776	.7968
D4	.20558*	.04304	.003	.0460	.3652	
A4	A1	.42089*	.04304	.000	.2613	.5805
	A2	.61717*	.04304	.000	.4576	.7768
	A3	-.28210*	.04304	.000	-.4417	-.1225
	B1	.86036*	.04304	.000	.7008	1.0199
	B2	.74489*	.04304	.000	.5853	.9045
	B3	.67206*	.04304	.000	.5125	.8316
	B4	.11506	.04304	.388	-.0445	.2746
	C1	.00444	.04304	1.000	-.1551	.1640
	C2	.48814*	.04304	.000	.3286	.6477
	C3	.04773	.04304	.999	-.1118	.2073
	C4	.30249*	.04304	.000	.1429	.4621
	D1	.68591*	.04304	.000	.5263	.8455
	D2	.45102*	.04304	.000	.2914	.6106
	D3	.35511*	.04304	.000	.1955	.5147
D4	-.07651	.04304	.907	-.2361	.0831	
B1	A1	-.43948*	.04304	.000	-.5991	-.2799
	A2	-.24319*	.04304	.000	-.4028	-.0836
	A3	-1.14246*	.04304	.000	-1.3020	-.9829
	A4	-.86036*	.04304	.000	-1.0199	-.7008
	B2	-.11548	.04304	.382	-.2751	.0441
	B3	-.18830*	.04304	.009	-.3479	-.0287
	B4	-.74530*	.04304	.000	-.9049	-.5857
	C1	-.85592*	.04304	.000	-1.0155	-.6963
	C2	-.37223*	.04304	.000	-.5318	-.2127
	C3	-.81264*	.04304	.000	-.9722	-.6531
	C4	-.55787*	.04304	.000	-.7174	-.3983
	D1	-.17445*	.04304	.022	-.3340	-.0149
	D2	-.40935*	.04304	.000	-.5689	-.2498
	D3	-.50526*	.04304	.000	-.6648	-.3457
D4	-.93688*	.04304	.000	-1.0965	-.7773	

(I) GROUP	(J) GROUP	Mean Difference (I-J)	Std. Error	Sig.	95% Confidence Interval	
					Lower Bound	Upper Bound
B2	A1	-.32400*	.04304	.000	-.4836	-.1644
	A2	-.12771	.04304	.238	-.2873	.0319
	A3	-1.02698*	.04304	.000	-1.1866	-.8674
	A4	-.74489*	.04304	.000	-.9045	-.5853
	B1	.11548	.04304	.382	-.0441	.2751
	B3	-.07282	.04304	.934	-.2324	.0868
	B4	-.62982*	.04304	.000	-.7894	-.4702
	C1	-.74045*	.04304	.000	-.9000	-.5809
	C2	-.25675*	.04304	.000	-.4163	-.0972
	C3	-.69716*	.04304	.000	-.8567	-.5376
	C4	-.44239*	.04304	.000	-.6020	-.2828
	D1	-.05897	.04304	.988	-.2186	.1006
	D2	-.29387*	.04304	.000	-.4534	-.1343
	D3	-.38978*	.04304	.000	-.5494	-.2302
	D4	-.82140*	.04304	.000	-.9810	-.6618
	B3	A1	-.25117*	.04304	.000	-.4108
A2		-.05489	.04304	.994	-.2145	.1047
A3		-.95416*	.04304	.000	-1.1137	-.7946
A4		-.67206*	.04304	.000	-.8316	-.5125
B1		.18830*	.04304	.009	.0287	.3479
B2		.07282	.04304	.934	-.0868	.2324
B4		-.55700*	.04304	.000	-.7166	-.3974
C1		-.66762*	.04304	.000	-.8272	-.5080
C2		-.18393*	.04304	.012	-.3435	-.0243
C3		-.62433*	.04304	.000	-.7839	-.4648
C4		-.36957*	.04304	.000	-.5291	-.2100
D1		.01385	.04304	1.000	-.1457	.1734
D2		-.22105*	.04304	.001	-.3806	-.0615
D3		-.31696*	.04304	.000	-.4765	-.1574
D4		-.74857*	.04304	.000	-.9082	-.5890
B4		A1	.30582*	.04304	.000	.1462
	A2	.50211*	.04304	.000	.3425	.6617
	A3	-.39716*	.04304	.000	-.5567	-.2376
	A4	-.11506	.04304	.388	-.2746	.0445
	B1	.74530*	.04304	.000	.5857	.9049
	B2	.62982*	.04304	.000	.4702	.7894
	B3	.55700*	.04304	.000	.3974	.7166
	C1	-.11062	.04304	.450	-.2702	.0490
	C2	.37307*	.04304	.000	.2135	.5327
	C3	-.06733	.04304	.964	-.2269	.0922
	C4	.18743*	.04304	.010	.0279	.3470
	D1	.57085*	.04304	.000	.4113	.7304
	D2	.33595*	.04304	.000	.1764	.4955
	D3	.24004*	.04304	.000	.0805	.3996
	D4	-.19158*	.04304	.008	-.3512	-.0320

(I) GROUP	(J) GROUP	Mean Difference (I-J)	Std. Error	Sig.	95% Confidence Interval	
					Lower Bound	Upper Bound
C1	A1	.41645*	.04304	.000	.2569	.5760
	A2	.61273*	.04304	.000	.4532	.7723
	A3	-.28654*	.04304	.000	-.4461	-.1270
	A4	-.00444	.04304	1.000	-.1640	.1551
	B1	.85592*	.04304	.000	.6963	1.0155
	B2	.74045*	.04304	.000	.5809	.9000
	B3	.66762*	.04304	.000	.5080	.8272
	B4	.11062	.04304	.450	-.0490	.2702
	C2	.48370*	.04304	.000	.3241	.6433
	C3	.04329	.04304	1.000	-.1163	.2029
	C4	.29805*	.04304	.000	.1385	.4576
	D1	.68147*	.04304	.000	.5219	.8410
	D2	.44658*	.04304	.000	.2870	.6062
	D3	.35067*	.04304	.000	.1911	.5102
	D4	-.08095	.04304	.866	-.2405	.0786
	C2	A1	-.06725	.04304	.964	-.2268
A2		.12904	.04304	.225	-.0305	.2886
A3		-.77023*	.04304	.000	-.9298	-.6107
A4		-.48814*	.04304	.000	-.6477	-.3286
B1		.37223*	.04304	.000	.2127	.5318
B2		.25675*	.04304	.000	.0972	.4163
B3		.18393*	.04304	.012	.0243	.3435
B4		-.37307*	.04304	.000	-.5327	-.2135
C1		-.48370*	.04304	.000	-.6433	-.3241
C3		-.44041*	.04304	.000	-.6000	-.2808
C4		-.18564*	.04304	.011	-.3452	-.0261
D1		.19778*	.04304	.005	.0382	.3574
D2		-.03712	.04304	1.000	-.1967	.1225
D3		-.13303	.04304	.189	-.2926	.0265
D4		-.56465*	.04304	.000	-.7242	-.4051
C3		A1	.37316*	.04304	.000	.2136
	A2	.56945*	.04304	.000	.4099	.7290
	A3	-.32982*	.04304	.000	-.4894	-.1702
	A4	-.04773	.04304	.999	-.2073	.1118
	B1	.81264*	.04304	.000	.6531	.9722
	B2	.69716*	.04304	.000	.5376	.8567
	B3	.62433*	.04304	.000	.4648	.7839
	B4	.06733	.04304	.964	-.0922	.2269
	C1	-.04329	.04304	1.000	-.2029	.1163
	C2	.44041*	.04304	.000	.2808	.6000
	C4	.25477*	.04304	.000	.0952	.4143
	D1	.63818*	.04304	.000	.4786	.7978
	D2	.40329*	.04304	.000	.2437	.5629
	D3	.30738*	.04304	.000	.1478	.4670
	D4	-.12424	.04304	.275	-.2838	.0353

(I) GROUP	(J) GROUP	Mean Difference (I-J)	Std. Error	Sig.	95% Confidence Interval	
					Lower Bound	Upper Bound
C4	A1	.11839	.04304	.344	-.0412	.2780
	A2	.31468*	.04304	.000	.1551	.4743
	A3	-.58459*	.04304	.000	-.7442	-.4250
	A4	-.30249*	.04304	.000	-.4621	-.1429
	B1	.55787*	.04304	.000	.3983	.7174
	B2	.44239*	.04304	.000	.2828	.6020
	B3	.36957*	.04304	.000	.2100	.5291
	B4	-.18743*	.04304	.010	-.3470	-.0279
	C1	-.29805*	.04304	.000	-.4576	-.1385
	C2	.18564*	.04304	.011	.0261	.3452
	C3	-.25477*	.04304	.000	-.4143	-.0952
	D1	.38342*	.04304	.000	.2238	.5430
	D2	.14852	.04304	.090	-.0111	.3081
	D3	.05261	.04304	.996	-.1070	.2122
D4	-.37901*	.04304	.000	-.5386	-.2194	
D1	A1	-.26502*	.04304	.000	-.4246	-.1054
	A2	-.06874	.04304	.957	-.2283	.0908
	A3	-.96801*	.04304	.000	-1.1276	-.8084
	A4	-.68591*	.04304	.000	-.8455	-.5263
	B1	.17445*	.04304	.022	.0149	.3340
	B2	.05897	.04304	.988	-.1006	.2186
	B3	-.01385	.04304	1.000	-.1734	.1457
	B4	-.57085*	.04304	.000	-.7304	-.4113
	C1	-.68147*	.04304	.000	-.8410	-.5219
	C2	-.19778*	.04304	.005	-.3574	-.0382
	C3	-.63818*	.04304	.000	-.7978	-.4786
	C4	-.38342*	.04304	.000	-.5430	-.2238
	D2	-.23490*	.04304	.000	-.3945	-.0753
	D3	-.33080*	.04304	.000	-.4904	-.1712
D4	-.76242*	.04304	.000	-.9220	-.6028	
D2	A1	-.03013	.04304	1.000	-.1897	.1295
	A2	.16616*	.04304	.035	.0066	.3257
	A3	-.73311*	.04304	.000	-.8927	-.5735
	A4	-.45102*	.04304	.000	-.6106	-.2914
	B1	.40935*	.04304	.000	.2498	.5689
	B2	.29387*	.04304	.000	.1343	.4534
	B3	.22105*	.04304	.001	.0615	.3806
	B4	-.33595*	.04304	.000	-.4955	-.1764
	C1	-.44658*	.04304	.000	-.6062	-.2870
	C2	.03712	.04304	1.000	-.1225	.1967
	C3	-.40329*	.04304	.000	-.5629	-.2437
	C4	-.14852	.04304	.090	-.3081	.0111
	D1	.23490*	.04304	.000	.0753	.3945
	D3	-.09591	.04304	.673	-.2555	.0637
D4	-.52753*	.04304	.000	-.6871	-.3679	

(I) GROUP	(J) GROUP	Mean Difference (I-J)	Std. Error	Sig.	95% Confidence Interval	
					Lower Bound	Upper Bound
D3	A1	.06578	.04304	.970	-.0938	.2254
	A2	.26207*	.04304	.000	.1025	.4216
	A3	-.63720*	.04304	.000	-.7968	-.4776
	A4	-.35511*	.04304	.000	-.5147	-.1955
	B1	.50526*	.04304	.000	.3457	.6648
	B2	.38978*	.04304	.000	.2302	.5494
	B3	.31696*	.04304	.000	.1574	.4765
	B4	-.24004*	.04304	.000	-.3996	-.0805
	C1	-.35067*	.04304	.000	-.5102	-.1911
	C2	.13303	.04304	.189	-.0265	.2926
	C3	-.30738*	.04304	.000	-.4670	-.1478
	C4	-.05261	.04304	.996	-.2122	.1070
	D1	.33080*	.04304	.000	.1712	.4904
	D2	.09591	.04304	.673	-.0637	.2555
D4	-.43162*	.04304	.000	-.5912	-.2720	
D4	A1	.49740*	.04304	.000	.3378	.6570
	A2	.69369*	.04304	.000	.5341	.8533
	A3	-.20558*	.04304	.003	-.3652	-.0460
	A4	.07651	.04304	.907	-.0831	.2361
	B1	.93688*	.04304	.000	.7773	1.0965
	B2	.82140*	.04304	.000	.6618	.9810
	B3	.74857*	.04304	.000	.5890	.9082
	B4	.19158*	.04304	.008	.0320	.3512
	C1	.08095	.04304	.866	-.0786	.2405
	C2	.56465*	.04304	.000	.4051	.7242
	C3	.12424	.04304	.275	-.0353	.2838
	C4	.37901*	.04304	.000	.2194	.5386
	D1	.76242*	.04304	.000	.6028	.9220
	D2	.52753*	.04304	.000	.3679	.6871
D3	.43162*	.04304	.000	.2720	.5912	

*. The mean difference is significant at the 0.05 level.

6.3 bmp7

ANOVA

bmp7

	Sum of Squares	df	Mean Square	F	Sig.
Between Groups	33.482	15	2.232	93.361	.000
Within Groups	.765	32	.024		
Total	34.247	47			

Multiple Comparisons

bmp7

Tukey HSD

(I) GROUP	(J) GROUP	Mean Difference (I-J)	Std. Error	Sig.	95% Confidence Interval	
					Lower Bound	Upper Bound
A1	A2	.18878	.12625	.975	-.2794	.6569
	A3	-1.94037 [*]	.12625	.000	-2.4085	-1.4722
	A4	-1.29442 [*]	.12625	.000	-1.7626	-.8263
	B1	.85426 [*]	.12625	.000	.3861	1.3224
	B2	.66799 [*]	.12625	.001	.1998	1.1361
	B3	.72547 [*]	.12625	.000	.2573	1.1936
	B4	.27009	.12625	.729	-.1981	.7382
	C1	-1.36393 [*]	.12625	.000	-1.8321	-.8958
	C2	.70755 [*]	.12625	.000	.2394	1.1757
	C3	.72849 [*]	.12625	.000	.2603	1.1966
	C4	-.15303	.12625	.997	-.6212	.3151
	D1	.23079	.12625	.888	-.2374	.6989
	D2	.22569	.12625	.903	-.2425	.6938
	D3	.77805 [*]	.12625	.000	.3099	1.2462
D4	.61751 [*]	.12625	.002	.1494	1.0857	
A2	A1	-.18878	.12625	.975	-.6569	.2794
	A3	-2.12914 [*]	.12625	.000	-2.5973	-1.6610
	A4	-1.48320 [*]	.12625	.000	-1.9513	-1.0151
	B1	.66549 [*]	.12625	.001	.1973	1.1336
	B2	.47921 [*]	.12625	.041	.0111	.9474
	B3	.53669 [*]	.12625	.013	.0685	1.0048
	B4	.08131	.12625	1.000	-.3868	.5495
	C1	-1.55271 [*]	.12625	.000	-2.0209	-1.0846
	C2	.51877 [*]	.12625	.019	.0506	.9869
	C3	.53971 [*]	.12625	.012	.0716	1.0079
	C4	-.34181	.12625	.369	-.8100	.1263
	D1	.04201	.12625	1.000	-.4261	.5102
	D2	.03691	.12625	1.000	-.4312	.5051
	D3	.58928 [*]	.12625	.004	.1211	1.0574
D4	.42873	.12625	.101	-.0394	.8969	
A3	A1	1.94037 [*]	.12625	.000	1.4722	2.4085
	A2	2.12914 [*]	.12625	.000	1.6610	2.5973
	A4	.64594 [*]	.12625	.001	.1778	1.1141
	B1	2.79463 [*]	.12625	.000	2.3265	3.2628
	B2	2.60835 [*]	.12625	.000	2.1402	3.0765
	B3	2.66584 [*]	.12625	.000	2.1977	3.1340
	B4	2.21045 [*]	.12625	.000	1.7423	2.6786
	C1	.57644 [*]	.12625	.006	.1083	1.0446
	C2	2.64792 [*]	.12625	.000	2.1798	3.1161
	C3	2.66886 [*]	.12625	.000	2.2007	3.1370
	C4	1.78733 [*]	.12625	.000	1.3192	2.2555

(I) GROUP	(J) GROUP	Mean Difference (I-J)	Std. Error	Sig.	95% Confidence Interval	
					Lower Bound	Upper Bound
	D1	2.17116 ⁺	.12625	.000	1.7030	2.6393
	D2	2.16605 ⁺	.12625	.000	1.6979	2.6342
	D3	2.71842 ⁺	.12625	.000	2.2503	3.1866
	D4	2.55788 ⁺	.12625	.000	2.0897	3.0260
A4	A1	1.29442 ⁺	.12625	.000	.8263	1.7626
	A2	1.48320 ⁺	.12625	.000	1.0151	1.9513
	A3	-.64594 ⁺	.12625	.001	-1.1141	-.1778
	B1	2.14869 ⁺	.12625	.000	1.6805	2.6168
	B2	1.96241 ⁺	.12625	.000	1.4943	2.4306
	B3	2.01989 ⁺	.12625	.000	1.5517	2.4880
	B4	1.56451 ⁺	.12625	.000	1.0964	2.0327
	C1	-.06951	.12625	1.000	-.5377	.3986
	C2	2.00197 ⁺	.12625	.000	1.5338	2.4701
	C3	2.02291 ⁺	.12625	.000	1.5548	2.4911
	C4	1.14139 ⁺	.12625	.000	.6732	1.6095
	D1	1.52521 ⁺	.12625	.000	1.0571	1.9934
	D2	1.52011 ⁺	.12625	.000	1.0520	1.9883
	D3	2.07248 ⁺	.12625	.000	1.6043	2.5406
	D4	1.91193 ⁺	.12625	.000	1.4438	2.3801
	B1	A1	-.85426 ⁺	.12625	.000	-1.3224
A2		-.66549 ⁺	.12625	.001	-1.1336	-.1973
A3		-2.79463 ⁺	.12625	.000	-3.2628	-2.3265
A4		-2.14869 ⁺	.12625	.000	-2.6168	-1.6805
B2		-.18628	.12625	.978	-.6544	.2819
B3		-.12879	.12625	.999	-.5969	.3394
B4		-.58418 ⁺	.12625	.005	-1.0523	-.1160
C1		-2.21820 ⁺	.12625	.000	-2.6863	-1.7500
C2		-.14671	.12625	.998	-.6149	.3214
C3		-.12577	.12625	1.000	-.5939	.3424
C4		-1.00730 ⁺	.12625	.000	-1.4754	-.5391
D1		-.62347 ⁺	.12625	.002	-1.0916	-.1553
D2		-.62858 ⁺	.12625	.002	-1.0967	-.1604
D3		-.07621	.12625	1.000	-.5444	.3919
D4		-.23676	.12625	.868	-.7049	.2314
B2		A1	-.66799 ⁺	.12625	.001	-1.1361
	A2	-.47921 ⁺	.12625	.041	-.9474	-.0111
	A3	-2.60835 ⁺	.12625	.000	-3.0765	-2.1402
	A4	-1.96241 ⁺	.12625	.000	-2.4306	-1.4943
	B1	.18628	.12625	.978	-.2819	.6544
	B3	.05748	.12625	1.000	-.4107	.5256
	B4	-.39790	.12625	.168	-.8660	.0703
	C1	-2.03192 ⁺	.12625	.000	-2.5001	-1.5638
	C2	.03957	.12625	1.000	-.4286	.5077
	C3	.06051	.12625	1.000	-.4076	.5287
	C4	-.82102 ⁺	.12625	.000	-1.2892	-.3529

(I) GROUP	(J) GROUP	Mean Difference (I-J)	Std. Error	Sig.	95% Confidence Interval	
					Lower Bound	Upper Bound
	D1	-.43719	.12625	.087	-.9053	.0310
	D2	-.44230	.12625	.080	-.9104	.0259
	D3	.11007	.12625	1.000	-.3581	.5782
	D4	-.05048	.12625	1.000	-.5186	.4177
B3	A1	-.72547 [*]	.12625	.000	-1.1936	-.2573
	A2	-.53669 [*]	.12625	.013	-1.0048	-.0685
	A3	-2.66584 [*]	.12625	.000	-3.1340	-2.1977
	A4	-2.01989 [*]	.12625	.000	-2.4880	-1.5517
	B1	.12879	.12625	.999	-.3394	.5969
	B2	-.05748	.12625	1.000	-.5256	.4107
	B4	-.45538	.12625	.063	-.9235	.0128
	C1	-2.08940 [*]	.12625	.000	-2.5575	-1.6213
	C2	-.01792	.12625	1.000	-.4861	.4502
	C3	.00302	.12625	1.000	-.4651	.4712
	C4	-.87850 [*]	.12625	.000	-1.3467	-.4104
	D1	-.49468 [*]	.12625	.030	-.9628	-.0265
	D2	-.49978 [*]	.12625	.027	-.9679	-.0316
	D3	.05258	.12625	1.000	-.4156	.5207
	D4	-.10796	.12625	1.000	-.5761	.3602
	B4	A1	-.27009	.12625	.729	-.7382
A2		-.08131	.12625	1.000	-.5495	.3868
A3		-2.21045 [*]	.12625	.000	-2.6786	-1.7423
A4		-1.56451 [*]	.12625	.000	-2.0327	-1.0964
B1		.58418 [*]	.12625	.005	.1160	1.0523
B2		.39790	.12625	.168	-.0703	.8660
B3		.45538	.12625	.063	-.0128	.9235
C1		-1.63402 [*]	.12625	.000	-2.1022	-1.1659
C2		.43746	.12625	.087	-.0307	.9056
C3		.45840	.12625	.060	-.0097	.9266
C4		-.42312	.12625	.111	-.8913	.0450
D1		-.03930	.12625	1.000	-.5074	.4289
D2		-.04440	.12625	1.000	-.5125	.4237
D3		.50797 [*]	.12625	.023	.0398	.9761
D4		.34742	.12625	.344	-.1207	.8156
C1		A1	1.36393 [*]	.12625	.000	.8958
	A2	1.55271 [*]	.12625	.000	1.0846	2.0209
	A3	-.57644 [*]	.12625	.006	-1.0446	-.1083
	A4	.06951	.12625	1.000	-.3986	.5377
	B1	2.21820 [*]	.12625	.000	1.7500	2.6863
	B2	2.03192 [*]	.12625	.000	1.5638	2.5001
	B3	2.08940 [*]	.12625	.000	1.6213	2.5575
	B4	1.63402 [*]	.12625	.000	1.1659	2.1022
	C2	2.07148 [*]	.12625	.000	1.6033	2.5396
	C3	2.09242 [*]	.12625	.000	1.6243	2.5606
	C4	1.21090 [*]	.12625	.000	.7428	1.6790

(I) GROUP	(J) GROUP	Mean Difference (I-J)	Std. Error	Sig.	95% Confidence Interval	
					Lower Bound	Upper Bound
	D1	1.59472 [*]	.12625	.000	1.1266	2.0629
	D2	1.58962 [*]	.12625	.000	1.1215	2.0578
	D3	2.14199 [*]	.12625	.000	1.6738	2.6101
	D4	1.98144 [*]	.12625	.000	1.5133	2.4496
C2	A1	-.70755 [*]	.12625	.000	-1.1757	-.2394
	A2	-.51877 [*]	.12625	.019	-.9869	-.0506
	A3	-2.64792 [*]	.12625	.000	-3.1161	-2.1798
	A4	-2.00197 [*]	.12625	.000	-2.4701	-1.5338
	B1	.14671	.12625	.998	-.3214	.6149
	B2	-.03957	.12625	1.000	-.5077	.4286
	B3	.01792	.12625	1.000	-.4502	.4861
	B4	-.43746	.12625	.087	-.9056	.0307
	C1	-2.07148 [*]	.12625	.000	-2.5396	-1.6033
	C3	.02094	.12625	1.000	-.4472	.4891
	C4	-.86058 [*]	.12625	.000	-1.3287	-.3924
	D1	-.47676 [*]	.12625	.043	-.9449	-.0086
	D2	-.48186 [*]	.12625	.039	-.9500	-.0137
	D3	.07050	.12625	1.000	-.3976	.5387
	D4	-.09004	.12625	1.000	-.5582	.3781
	C3	A1	-.72849 [*]	.12625	.000	-1.1966
A2		-.53971 [*]	.12625	.012	-1.0079	-.0716
A3		-2.66886 [*]	.12625	.000	-3.1370	-2.2007
A4		-2.02291 [*]	.12625	.000	-2.4911	-1.5548
B1		.12577	.12625	1.000	-.3424	.5939
B2		-.06051	.12625	1.000	-.5287	.4076
B3		-.00302	.12625	1.000	-.4712	.4651
B4		-.45840	.12625	.060	-.9266	.0097
C1		-2.09242 [*]	.12625	.000	-2.5606	-1.6243
C2		-.02094	.12625	1.000	-.4891	.4472
C4		-.88152 [*]	.12625	.000	-1.3497	-.4134
D1		-.49770 [*]	.12625	.028	-.9658	-.0296
D2		-.50280 [*]	.12625	.026	-.9710	-.0347
D3		.04956	.12625	1.000	-.4186	.5177
D4		-.11098	.12625	1.000	-.5791	.3572
C4		A1	.15303	.12625	.997	-.3151
	A2	.34181	.12625	.369	-.1263	.8100
	A3	-1.78733 [*]	.12625	.000	-2.2555	-1.3192
	A4	-1.14139 [*]	.12625	.000	-1.6095	-.6732
	B1	1.00730 [*]	.12625	.000	.5391	1.4754
	B2	.82102 [*]	.12625	.000	.3529	1.2892
	B3	.87850 [*]	.12625	.000	.4104	1.3467
	B4	.42312	.12625	.111	-.0450	.8913
	C1	-1.21090 [*]	.12625	.000	-1.6790	-.7428
	C2	.86058 [*]	.12625	.000	.3924	1.3287
	C3	.88152 [*]	.12625	.000	.4134	1.3497

(I) GROUP	(J) GROUP	Mean Difference (I-J)	Std. Error	Sig.	95% Confidence Interval	
					Lower Bound	Upper Bound
	D1	.38382	.12625	.208	-.0843	.8520
	D2	.37872	.12625	.224	-.0894	.8469
	D3	.93109 [†]	.12625	.000	.4629	1.3992
	D4	.77054 [†]	.12625	.000	.3024	1.2387
D1	A1	-.23079	.12625	.888	-.6989	.2374
	A2	-.04201	.12625	1.000	-.5102	.4261
	A3	-2.17116 [†]	.12625	.000	-2.6393	-1.7030
	A4	-1.52521 [†]	.12625	.000	-1.9934	-1.0571
	B1	.62347 [†]	.12625	.002	.1553	1.0916
	B2	.43719	.12625	.087	-.0310	.9053
	B3	.49468 [†]	.12625	.030	.0265	.9628
	B4	.03930	.12625	1.000	-.4289	.5074
	C1	-1.59472 [†]	.12625	.000	-2.0629	-1.1266
	C2	.47676 [†]	.12625	.043	.0086	.9449
	C3	.49770 [†]	.12625	.028	.0296	.9658
	C4	-.38382	.12625	.208	-.8520	.0843
	D2	-.00510	.12625	1.000	-.4733	.4630
	D3	.54726 [†]	.12625	.010	.0791	1.0154
	D4	.38672	.12625	.199	-.0814	.8549
	D2	A1	-.22569	.12625	.903	-.6938
A2		-.03691	.12625	1.000	-.5051	.4312
A3		-2.16605 [†]	.12625	.000	-2.6342	-1.6979
A4		-1.52011 [†]	.12625	.000	-1.9883	-1.0520
B1		.62858 [†]	.12625	.002	.1604	1.0967
B2		.44230	.12625	.080	-.0259	.9104
B3		.49978 [†]	.12625	.027	.0316	.9679
B4		.04440	.12625	1.000	-.4237	.5125
C1		-1.58962 [†]	.12625	.000	-2.0578	-1.1215
C2		.48186 [†]	.12625	.039	.0137	.9500
C3		.50280 [†]	.12625	.026	.0347	.9710
C4		-.37872	.12625	.224	-.8469	.0894
D1		.00510	.12625	1.000	-.4630	.4733
D3		.55237 [†]	.12625	.009	.0842	1.0205
D4		.39182	.12625	.184	-.0763	.8600
D3		A1	-.77805 [†]	.12625	.000	-1.2462
	A2	-.58928 [†]	.12625	.004	-1.0574	-.1211
	A3	-2.71842 [†]	.12625	.000	-3.1866	-2.2503
	A4	-2.07248 [†]	.12625	.000	-2.5406	-1.6043
	B1	.07621	.12625	1.000	-.3919	.5444
	B2	-.11007	.12625	1.000	-.5782	.3581
	B3	-.05258	.12625	1.000	-.5207	.4156
	B4	-.50797 [†]	.12625	.023	-.9761	-.0398
	C1	-2.14199 [†]	.12625	.000	-2.6101	-1.6738
	C2	-.07050	.12625	1.000	-.5387	.3976
	C3	-.04956	.12625	1.000	-.5177	.4186

(I) GROUP	(J) GROUP	Mean Difference (I-J)	Std. Error	Sig.	95% Confidence Interval	
					Lower Bound	Upper Bound
	C4	-.93109 [*]	.12625	.000	-1.3992	-.4629
	D1	-.54726 [*]	.12625	.010	-1.0154	-.0791
	D2	-.55237 [*]	.12625	.009	-1.0205	-.0842
	D4	-.16055	.12625	.994	-.6287	.3076
D4	A1	-.61751 [*]	.12625	.002	-1.0857	-.1494
	A2	-.42873	.12625	.101	-.8969	.0394
	A3	-2.55788 [*]	.12625	.000	-3.0260	-2.0897
	A4	-1.91193 [*]	.12625	.000	-2.3801	-1.4438
	B1	.23676	.12625	.868	-.2314	.7049
	B2	.05048	.12625	1.000	-.4177	.5186
	B3	.10796	.12625	1.000	-.3602	.5761
	B4	-.34742	.12625	.344	-.8156	.1207
	C1	-1.98144 [*]	.12625	.000	-2.4496	-1.5133
	C2	.09004	.12625	1.000	-.3781	.5582
	C3	.11098	.12625	1.000	-.3572	.5791
	C4	-.77054 [*]	.12625	.000	-1.2387	-.3024
	D1	-.38672	.12625	.199	-.8549	.0814
	D2	-.39182	.12625	.184	-.8600	.0763
	D3	.16055	.12625	.994	-.3076	.6287

*. The mean difference is significant at the 0.05 level.

6.4 axin2

ANOVA

axin2

	Sum of Squares	df	Mean Square	F	Sig.
Between Groups	5.727	15	.382	3.807	.001
Within Groups	3.210	32	.100		
Total	8.937	47			

Multiple Comparisons

axin2

Tukey HSD

(I) GROUP	(J) GROUP	Mean Difference (I-J)	Std. Error	Sig.	95% Confidence Interval	
					Lower Bound	Upper Bound
A1	A2	.29466	.25859	.998	-.6642	1.2535
	A3	-.78562	.25859	.209	-1.7445	.1732
	A4	-.27524	.25859	.999	-1.2341	.6836

(I) GROUP	(J) GROUP	Mean Difference (I-J)	Std. Error	Sig.	95% Confidence Interval	
					Lower Bound	Upper Bound
	B1	.38227	.25859	.977	-.5766	1.3411
	B2	-.09807	.25859	1.000	-1.0569	.8608
	B3	.19744	.25859	1.000	-.7614	1.1563
	B4	-.41142	.25859	.959	-1.3703	.5474
	C1	-.44365	.25859	.927	-1.4025	.5152
	C2	.13981	.25859	1.000	-.8190	1.0987
	C3	-.40906	.25859	.960	-1.3679	.5498
	C4	-.17812	.25859	1.000	-1.1370	.7807
	D1	-.86030	.25859	.117	-1.8192	.0986
	D2	-.43932	.25859	.932	-1.3982	.5195
	D3	-.31027	.25859	.997	-1.2691	.6486
	D4	-.16900	.25859	1.000	-1.1279	.7899
A2	A1	-.29466	.25859	.998	-1.2535	.6642
	A3	-1.08029*	.25859	.016	-2.0391	-.1214
	A4	-.56990	.25859	.688	-1.5288	.3890
	B1	.08760	.25859	1.000	-.8713	1.0465
	B2	-.39273	.25859	.972	-1.3516	.5661
	B3	-.09722	.25859	1.000	-1.0561	.8616
	B4	-.70608	.25859	.356	-1.6649	.2528
	C1	-.73831	.25859	.290	-1.6972	.2205
	C2	-.15485	.25859	1.000	-1.1137	.8040
	C3	-.70372	.25859	.361	-1.6626	.2551
	C4	-.47278	.25859	.888	-1.4316	.4861
	D1	-1.15496*	.25859	.007	-2.1138	-.1961
	D2	-.73398	.25859	.298	-1.6928	.2249
	D3	-.60493	.25859	.600	-1.5638	.3539
	D4	-.46366	.25859	.901	-1.4225	.4952
A3	A1	.78562	.25859	.209	-.1732	1.7445
	A2	1.08029*	.25859	.016	.1214	2.0391
	A4	.51039	.25859	.822	-.4485	1.4692
	B1	1.16789*	.25859	.006	.2090	2.1267
	B2	.68755	.25859	.397	-.2713	1.6464
	B3	.98306*	.25859	.040	.0242	1.9419
	B4	.37421	.25859	.981	-.5847	1.3331
	C1	.34197	.25859	.992	-.6169	1.3008
	C2	.92544	.25859	.067	-.0334	1.8843
	C3	.37656	.25859	.980	-.5823	1.3354
	C4	.60751	.25859	.594	-.3514	1.5664
	D1	-.07468	.25859	1.000	-1.0335	.8842
	D2	.34630	.25859	.991	-.6126	1.3052
	D3	.47536	.25859	.884	-.4835	1.4342
	D4	.61663	.25859	.571	-.3422	1.5755
A4	A1	.27524	.25859	.999	-.6836	1.2341

(I) GROUP	(J) GROUP	Mean Difference (I-J)	Std. Error	Sig.	95% Confidence Interval	
					Lower Bound	Upper Bound
	A2	.56990	.25859	.688	-.3890	1.5288
	A3	-.51039	.25859	.822	-1.4692	.4485
	B1	.65750	.25859	.468	-.3014	1.6164
	B2	.17717	.25859	1.000	-.7817	1.1360
	B3	.47268	.25859	.888	-.4862	1.4315
	B4	-.13618	.25859	1.000	-1.0950	.8227
	C1	-.16841	.25859	1.000	-1.1273	.7904
	C2	.41505	.25859	.956	-.5438	1.3739
	C3	-.13382	.25859	1.000	-1.0927	.8250
	C4	.09712	.25859	1.000	-.8617	1.0560
	D1	-.58506	.25859	.651	-1.5439	.3738
	D2	-.16408	.25859	1.000	-1.1229	.7948
	D3	-.03503	.25859	1.000	-.9939	.9238
	D4	.10624	.25859	1.000	-.8526	1.0651
B1	A1	-.38227	.25859	.977	-1.3411	.5766
	A2	-.08760	.25859	1.000	-1.0465	.8713
	A3	-1.16789*	.25859	.006	-2.1267	-.2090
	A4	-.65750	.25859	.468	-1.6164	.3014
	B2	-.48034	.25859	.876	-1.4392	.4785
	B3	-.18483	.25859	1.000	-1.1437	.7740
	B4	-.79368	.25859	.197	-1.7525	.1652
	C1	-.82592	.25859	.154	-1.7848	.1329
	C2	-.24245	.25859	1.000	-1.2013	.7164
	C3	-.79133	.25859	.200	-1.7502	.1675
	C4	-.56038	.25859	.711	-1.5192	.3985
	D1	-1.24257*	.25859	.003	-2.2014	-.2837
	D2	-.82159	.25859	.160	-1.7804	.1373
	D3	-.69253	.25859	.385	-1.6514	.2663
	D4	-.55126	.25859	.733	-1.5101	.4076
B2	A1	.09807	.25859	1.000	-.8608	1.0569
	A2	.39273	.25859	.972	-.5661	1.3516
	A3	-.68755	.25859	.397	-1.6464	.2713
	A4	-.17717	.25859	1.000	-1.1360	.7817
	B1	.48034	.25859	.876	-.4785	1.4392
	B3	.29551	.25859	.998	-.6633	1.2544
	B4	-.31334	.25859	.997	-1.2722	.6455
	C1	-.34558	.25859	.991	-1.3044	.6133
	C2	.23789	.25859	1.000	-.7210	1.1967
	C3	-.31099	.25859	.997	-1.2698	.6479
	C4	-.08004	.25859	1.000	-1.0389	.8788
	D1	-.76223	.25859	.247	-1.7211	.1966
	D2	-.34125	.25859	.992	-1.3001	.6176
	D3	-.21219	.25859	1.000	-1.1711	.7467
	D4	-.07092	.25859	1.000	-1.0298	.8879

(I) GROUP	(J) GROUP	Mean Difference (I-J)	Std. Error	Sig.	95% Confidence Interval	
					Lower Bound	Upper Bound
B3	A1	-.19744	.25859	1.000	-1.1563	.7614
	A2	.09722	.25859	1.000	-.8616	1.0561
	A3	-.98306*	.25859	.040	-1.9419	-.0242
	A4	-.47268	.25859	.888	-1.4315	.4862
	B1	.18483	.25859	1.000	-.7740	1.1437
	B2	-.29551	.25859	.998	-1.2544	.6633
	B4	-.60886	.25859	.590	-1.5677	.3500
	C1	-.64109	.25859	.509	-1.6000	.3178
	C2	-.05763	.25859	1.000	-1.0165	.9012
	C3	-.60650	.25859	.596	-1.5654	.3524
	C4	-.37556	.25859	.981	-1.3344	.5833
	D1	-1.05774*	.25859	.020	-2.0166	-.0989
	D2	-.63676	.25859	.519	-1.5956	.3221
	D3	-.50771	.25859	.827	-1.4666	.4512
D4	-.36644	.25859	.984	-1.3253	.5924	
B4	A1	.41142	.25859	.959	-.5474	1.3703
	A2	.70608	.25859	.356	-.2528	1.6649
	A3	-.37421	.25859	.981	-1.3331	.5847
	A4	.13618	.25859	1.000	-.8227	1.0950
	B1	.79368	.25859	.197	-.1652	1.7525
	B2	.31334	.25859	.997	-.6455	1.2722
	B3	.60886	.25859	.590	-.3500	1.5677
	C1	-.03224	.25859	1.000	-.9911	.9266
	C2	.55123	.25859	.733	-.4076	1.5101
	C3	.00236	.25859	1.000	-.9565	.9612
	C4	.23330	.25859	1.000	-.7256	1.1922
	D1	-.44888	.25859	.921	-1.4077	.5100
	D2	-.02790	.25859	1.000	-.9868	.9310
	D3	.10115	.25859	1.000	-.8577	1.0600
D4	.24242	.25859	1.000	-.7164	1.2013	
C1	A1	.44365	.25859	.927	-.5152	1.4025
	A2	.73831	.25859	.290	-.2205	1.6972
	A3	-.34197	.25859	.992	-1.3008	.6169
	A4	.16841	.25859	1.000	-.7904	1.1273
	B1	.82592	.25859	.154	-.1329	1.7848
	B2	.34558	.25859	.991	-.6133	1.3044
	B3	.64109	.25859	.509	-.3178	1.6000
	B4	.03224	.25859	1.000	-.9266	.9911
	C2	.58346	.25859	.655	-.3754	1.5423
	C3	.03459	.25859	1.000	-.9243	.9935
	C4	.26554	.25859	.999	-.6933	1.2244
	D1	-.41665	.25859	.954	-1.3755	.5422
	D2	.00433	.25859	1.000	-.9545	.9632
	D3	.13338	.25859	1.000	-.8255	1.0922

(I) GROUP	(J) GROUP	Mean Difference (I-J)	Std. Error	Sig.	95% Confidence Interval	
					Lower Bound	Upper Bound
	D4	.27466	.25859	.999	-.6842	1.2335
C2	A1	-.13981	.25859	1.000	-1.0987	.8190
	A2	.15485	.25859	1.000	-.8040	1.1137
	A3	-.92544	.25859	.067	-1.8843	.0334
	A4	-.41505	.25859	.956	-1.3739	.5438
	B1	.24245	.25859	1.000	-.7164	1.2013
	B2	-.23789	.25859	1.000	-1.1967	.7210
	B3	.05763	.25859	1.000	-.9012	1.0165
	B4	-.55123	.25859	.733	-1.5101	.4076
	C1	-.58346	.25859	.655	-1.5423	.3754
	C3	-.54887	.25859	.739	-1.5077	.4100
	C4	-.31793	.25859	.996	-1.2768	.6409
	D1	-1.00011*	.25859	.034	-1.9590	-.0413
	D2	-.57913	.25859	.666	-1.5380	.3797
	D3	-.45008	.25859	.919	-1.4089	.5088
D4	-.30881	.25859	.997	-1.2677	.6501	
C3	A1	.40906	.25859	.960	-.5498	1.3679
	A2	.70372	.25859	.361	-.2551	1.6626
	A3	-.37656	.25859	.980	-1.3354	.5823
	A4	.13382	.25859	1.000	-.8250	1.0927
	B1	.79133	.25859	.200	-.1675	1.7502
	B2	.31099	.25859	.997	-.6479	1.2698
	B3	.60650	.25859	.596	-.3524	1.5654
	B4	-.00236	.25859	1.000	-.9612	.9565
	C1	-.03459	.25859	1.000	-.9935	.9243
	C2	.54887	.25859	.739	-.4100	1.5077
	C4	.23095	.25859	1.000	-.7279	1.1898
	D1	-.45124	.25859	.918	-1.4101	.5076
	D2	-.03026	.25859	1.000	-.9891	.9286
	D3	.09879	.25859	1.000	-.8601	1.0577
D4	.24007	.25859	1.000	-.7188	1.1989	
C4	A1	.17812	.25859	1.000	-.7807	1.1370
	A2	.47278	.25859	.888	-.4861	1.4316
	A3	-.60751	.25859	.594	-1.5664	.3514
	A4	-.09712	.25859	1.000	-1.0560	.8617
	B1	.56038	.25859	.711	-.3985	1.5192
	B2	.08004	.25859	1.000	-.8788	1.0389
	B3	.37556	.25859	.981	-.5833	1.3344
	B4	-.23330	.25859	1.000	-1.1922	.7256
	C1	-.26554	.25859	.999	-1.2244	.6933
	C2	.31793	.25859	.996	-.6409	1.2768
	C3	-.23095	.25859	1.000	-1.1898	.7279
	D1	-.68219	.25859	.409	-1.6410	.2767
	D2	-.26121	.25859	1.000	-1.2201	.6977

(I) GROUP	(J) GROUP	Mean Difference (I-J)	Std. Error	Sig.	95% Confidence Interval	
					Lower Bound	Upper Bound
	D3	-.13215	.25859	1.000	-1.0910	.8267
	D4	.00912	.25859	1.000	-.9497	.9680
D1	A1	.86030	.25859	.117	-.0986	1.8192
	A2	1.15496*	.25859	.007	.1961	2.1138
	A3	.07468	.25859	1.000	-.8842	1.0335
	A4	.58506	.25859	.651	-.3738	1.5439
	B1	1.24257*	.25859	.003	.2837	2.2014
	B2	.76223	.25859	.247	-.1966	1.7211
	B3	1.05774*	.25859	.020	.0989	2.0166
	B4	.44888	.25859	.921	-.5100	1.4077
	C1	.41665	.25859	.954	-.5422	1.3755
	C2	1.00011*	.25859	.034	.0413	1.9590
	C3	.45124	.25859	.918	-.5076	1.4101
	C4	.68219	.25859	.409	-.2767	1.6410
	D2	.42098	.25859	.951	-.5379	1.3798
	D3	.55003	.25859	.736	-.4088	1.5089
D4	.69131	.25859	.388	-.2676	1.6502	
D2	A1	.43932	.25859	.932	-.5195	1.3982
	A2	.73398	.25859	.298	-.2249	1.6928
	A3	-.34630	.25859	.991	-1.3052	.6126
	A4	.16408	.25859	1.000	-.7948	1.1229
	B1	.82159	.25859	.160	-.1373	1.7804
	B2	.34125	.25859	.992	-.6176	1.3001
	B3	.63676	.25859	.519	-.3221	1.5956
	B4	.02790	.25859	1.000	-.9310	.9868
	C1	-.00433	.25859	1.000	-.9632	.9545
	C2	.57913	.25859	.666	-.3797	1.5380
	C3	.03026	.25859	1.000	-.9286	.9891
	C4	.26121	.25859	1.000	-.6977	1.2201
	D1	-.42098	.25859	.951	-1.3798	.5379
	D3	.12905	.25859	1.000	-.8298	1.0879
D4	.27033	.25859	.999	-.6885	1.2292	
D3	A1	.31027	.25859	.997	-.6486	1.2691
	A2	.60493	.25859	.600	-.3539	1.5638
	A3	-.47536	.25859	.884	-1.4342	.4835
	A4	.03503	.25859	1.000	-.9238	.9939
	B1	.69253	.25859	.385	-.2663	1.6514
	B2	.21219	.25859	1.000	-.7467	1.1711
	B3	.50771	.25859	.827	-.4512	1.4666
	B4	-.10115	.25859	1.000	-1.0600	.8577
	C1	-.13338	.25859	1.000	-1.0922	.8255
	C2	.45008	.25859	.919	-.5088	1.4089
	C3	-.09879	.25859	1.000	-1.0577	.8601
	C4	.13215	.25859	1.000	-.8267	1.0910

(I) GROUP	(J) GROUP	Mean Difference (I-J)	Std. Error	Sig.	95% Confidence Interval	
					Lower Bound	Upper Bound
	D1	-.55003	.25859	.736	-1.5089	.4088
	D2	-.12905	.25859	1.000	-1.0879	.8298
	D4	.14127	.25859	1.000	-.8176	1.1001
D4	A1	.16900	.25859	1.000	-.7899	1.1279
	A2	.46366	.25859	.901	-.4952	1.4225
	A3	-.61663	.25859	.571	-1.5755	.3422
	A4	-.10624	.25859	1.000	-1.0651	.8526
	B1	.55126	.25859	.733	-.4076	1.5101
	B2	.07092	.25859	1.000	-.8879	1.0298
	B3	.36644	.25859	.984	-.5924	1.3253
	B4	-.24242	.25859	1.000	-1.2013	.7164
	C1	-.27466	.25859	.999	-1.2335	.6842
	C2	.30881	.25859	.997	-.6501	1.2677
	C3	-.24007	.25859	1.000	-1.1989	.7188
	C4	-.00912	.25859	1.000	-.9680	.9497
	D1	-.69131	.25859	.388	-1.6502	.2676
	D2	-.27033	.25859	.999	-1.2292	.6885
	D3	-.14127	.25859	1.000	-1.1001	.8176

*. The mean difference is significant at the 0.05 level.

6.5 β -catenin

ANOVA

β -catenin

	Sum of Squares	df	Mean Square	F	Sig.
Between Groups	10.926	15	.728	74.829	.000
Within Groups	.311	32	.010		
Total	11.237	47			

Multiple Comparisons

β -catenin

Tukey HSD

(I) GROUP	(J) GROUP	Mean Difference (I-J)	Std. Error	Sig.	95% Confidence Interval	
					Lower Bound	Upper Bound
A1	A2	.49128*	.08056	.000	.1926	.7900
	A3	-1.27307*	.08056	.000	-1.5718	-.9744
	A4	-.16538	.08056	.779	-.4641	.1333
	B1	.59906*	.08056	.000	.3004	.8978

(I) GROUP	(J) GROUP	Mean Difference (I-J)	Std. Error	Sig.	95% Confidence Interval	
					Lower Bound	Upper Bound
	B2	.23736	.08056	.247	-.0614	.5361
	B3	.43835*	.08056	.001	.1396	.7371
	B4	-.26285	.08056	.134	-.5616	.0359
	C1	-.21650	.08056	.380	-.5152	.0822
	C2	.25318	.08056	.171	-.0455	.5519
	C3	-.82197*	.08056	.000	-1.1207	-.5233
	C4	-.20564	.08056	.462	-.5043	.0931
	D1	-.08855	.08056	.999	-.3873	.2102
	D2	-.38150*	.08056	.004	-.6802	-.0828
	D3	.15645	.08056	.838	-.1423	.4552
	D4	-.51069*	.08056	.000	-.8094	-.2120
A2	A1	-.49128*	.08056	.000	-.7900	-.1926
	A3	-1.76435*	.08056	.000	-2.0631	-1.4656
	A4	-.65666*	.08056	.000	-.9554	-.3579
	B1	.10778	.08056	.991	-.1909	.4065
	B2	-.25392	.08056	.168	-.5526	.0448
	B3	-.05293	.08056	1.000	-.3516	.2458
	B4	-.75413*	.08056	.000	-1.0528	-.4554
	C1	-.70778*	.08056	.000	-1.0065	-.4091
	C2	-.23810	.08056	.243	-.5368	.0606
	C3	-1.31325*	.08056	.000	-1.6120	-1.0145
	C4	-.69692*	.08056	.000	-.9956	-.3982
	D1	-.57983*	.08056	.000	-.8785	-.2811
	D2	-.87278*	.08056	.000	-1.1715	-.5741
	D3	-.33483*	.08056	.017	-.6335	-.0361
	D4	-1.00197*	.08056	.000	-1.3007	-.7033
A3	A1	1.27307*	.08056	.000	.9744	1.5718
	A2	1.76435*	.08056	.000	1.4656	2.0631
	A4	1.10769*	.08056	.000	.8090	1.4064
	B1	1.87213*	.08056	.000	1.5734	2.1708
	B2	1.51042*	.08056	.000	1.2117	1.8091
	B3	1.71142*	.08056	.000	1.4127	2.0101
	B4	1.01021*	.08056	.000	.7115	1.3089
	C1	1.05657*	.08056	.000	.7579	1.3553
	C2	1.52625*	.08056	.000	1.2275	1.8250
	C3	.45110*	.08056	.000	.1524	.7498
	C4	1.06743*	.08056	.000	.7687	1.3661
	D1	1.18452*	.08056	.000	.8858	1.4832
	D2	.89156*	.08056	.000	.5929	1.1903
	D3	1.42952*	.08056	.000	1.1308	1.7282
	D4	.76238*	.08056	.000	.4637	1.0611
A4	A1	.16538	.08056	.779	-.1333	.4641
	A2	.65666*	.08056	.000	.3579	.9554

(I) GROUP	(J) GROUP	Mean Difference (I-J)	Std. Error	Sig.	95% Confidence Interval	
					Lower Bound	Upper Bound
	A3	-1.10769*	.08056	.000	-1.4064	-.8090
	B1	.76444*	.08056	.000	.4657	1.0631
	B2	.40273*	.08056	.002	.1040	.7014
	B3	.60373*	.08056	.000	.3050	.9024
	B4	-.09748	.08056	.997	-.3962	.2012
	C1	-.05112	.08056	1.000	-.3498	.2476
	C2	.41856*	.08056	.001	.1199	.7173
	C3	-.65659*	.08056	.000	-.9553	-.3579
	C4	-.04026	.08056	1.000	-.3390	.2584
	D1	.07683	.08056	1.000	-.2219	.3755
	D2	-.21613	.08056	.383	-.5148	.0826
	D3	.32183*	.08056	.025	.0231	.6205
	D4	-.34531*	.08056	.012	-.6440	-.0466
	B1	A1	-.59906*	.08056	.000	-.8978
A2		-.10778	.08056	.991	-.4065	.1909
A3		-1.87213*	.08056	.000	-2.1708	-1.5734
A4		-.76444*	.08056	.000	-1.0631	-.4657
B2		-.36170*	.08056	.007	-.6604	-.0630
B3		-.16071	.08056	.811	-.4594	.1380
B4		-.86191*	.08056	.000	-1.1606	-.5632
C1		-.81556*	.08056	.000	-1.1143	-.5168
C2		-.34588*	.08056	.012	-.6446	-.0472
C3		-1.42103*	.08056	.000	-1.7197	-1.1223
C4		-.80470*	.08056	.000	-1.1034	-.5060
D1		-.68761*	.08056	.000	-.9863	-.3889
D2		-.98056*	.08056	.000	-1.2793	-.6819
D3		-.44261*	.08056	.000	-.7413	-.1439
D4	-1.10975*	.08056	.000	-1.4085	-.8110	
B2	A1	-.23736	.08056	.247	-.5361	.0614
	A2	.25392	.08056	.168	-.0448	.5526
	A3	-1.51042*	.08056	.000	-1.8091	-1.2117
	A4	-.40273*	.08056	.002	-.7014	-.1040
	B1	.36170*	.08056	.007	.0630	.6604
	B3	.20099	.08056	.498	-.0977	.4997
	B4	-.50021*	.08056	.000	-.7989	-.2015
	C1	-.45385*	.08056	.000	-.7526	-.1551
	C2	.01583	.08056	1.000	-.2829	.3145
	C3	-1.05932*	.08056	.000	-1.3580	-.7606
	C4	-.44300*	.08056	.000	-.7417	-.1443
	D1	-.32590*	.08056	.022	-.6246	-.0272
	D2	-.61886*	.08056	.000	-.9176	-.3202
	D3	-.08091	.08056	1.000	-.3796	.2178
D4	-.74804*	.08056	.000	-1.0468	-.4493	
B3	A1	-.43835*	.08056	.001	-.7371	-.1396

(I) GROUP	(J) GROUP	Mean Difference (I-J)	Std. Error	Sig.	95% Confidence Interval	
					Lower Bound	Upper Bound
	A2	.05293	.08056	1.000	-.2458	.3516
	A3	-1.71142*	.08056	.000	-2.0101	-1.4127
	A4	-.60373*	.08056	.000	-.9024	-.3050
	B1	.16071	.08056	.811	-.1380	.4594
	B2	-.20099	.08056	.498	-.4997	.0977
	B4	-.70120*	.08056	.000	-.9999	-.4025
	C1	-.65485*	.08056	.000	-.9536	-.3561
	C2	-.18517	.08056	.627	-.4839	.1135
	C3	-1.26032*	.08056	.000	-1.5590	-.9616
	C4	-.64399*	.08056	.000	-.9427	-.3453
	D1	-.52690*	.08056	.000	-.8256	-.2282
	D2	-.81985*	.08056	.000	-1.1186	-.5211
	D3	-.28190	.08056	.081	-.5806	.0168
	D4	-.94904*	.08056	.000	-1.2477	-.6503
B4	A1	.26285	.08056	.134	-.0359	.5616
	A2	.75413*	.08056	.000	.4554	1.0528
	A3	-1.01021*	.08056	.000	-1.3089	-.7115
	A4	.09748	.08056	.997	-.2012	.3962
	B1	.86191*	.08056	.000	.5632	1.1606
	B2	.50021*	.08056	.000	.2015	.7989
	B3	.70120*	.08056	.000	.4025	.9999
	C1	.04636	.08056	1.000	-.2524	.3451
	C2	.51604*	.08056	.000	.2173	.8147
	C3	-.55911*	.08056	.000	-.8578	-.2604
	C4	.05721	.08056	1.000	-.2415	.3559
	D1	.17431	.08056	.714	-.1244	.4730
	D2	-.11865	.08056	.978	-.4174	.1801
	D3	.41931*	.08056	.001	.1206	.7180
D4	-.24783	.08056	.194	-.5465	.0509	
C1	A1	.21650	.08056	.380	-.0822	.5152
	A2	.70778*	.08056	.000	.4091	1.0065
	A3	-1.05657*	.08056	.000	-1.3553	-.7579
	A4	.05112	.08056	1.000	-.2476	.3498
	B1	.81556*	.08056	.000	.5168	1.1143
	B2	.45385*	.08056	.000	.1551	.7526
	B3	.65485*	.08056	.000	.3561	.9536
	B4	-.04636	.08056	1.000	-.3451	.2524
	C2	.46968*	.08056	.000	.1710	.7684
	C3	-.60547*	.08056	.000	-.9042	-.3068
	C4	.01086	.08056	1.000	-.2879	.3096
	D1	.12795	.08056	.959	-.1708	.4267
	D2	-.16501	.08056	.782	-.4637	.1337
	D3	.37295*	.08056	.005	.0742	.6717
D4	-.29419	.08056	.057	-.5929	.0045	

(I) GROUP	(J) GROUP	Mean Difference (I-J)	Std. Error	Sig.	95% Confidence Interval	
					Lower Bound	Upper Bound
C2	A1	-.25318	.08056	.171	-.5519	.0455
	A2	.23810	.08056	.243	-.0606	.5368
	A3	-1.52625*	.08056	.000	-1.8250	-1.2275
	A4	-.41856*	.08056	.001	-.7173	-.1199
	B1	.34588*	.08056	.012	.0472	.6446
	B2	-.01583	.08056	1.000	-.3145	.2829
	B3	.18517	.08056	.627	-.1135	.4839
	B4	-.51604*	.08056	.000	-.8147	-.2173
	C1	-.46968*	.08056	.000	-.7684	-.1710
	C3	-1.07515*	.08056	.000	-1.3739	-.7764
	C4	-.45882*	.08056	.000	-.7575	-.1601
	D1	-.34173*	.08056	.013	-.6404	-.0430
	D2	-.63469*	.08056	.000	-.9334	-.3360
	D3	-.09673	.08056	.997	-.3954	.2020
D4	-.76387*	.08056	.000	-1.0626	-.4652	
C3	A1	.82197*	.08056	.000	.5233	1.1207
	A2	1.31325*	.08056	.000	1.0145	1.6120
	A3	-.45110*	.08056	.000	-.7498	-.1524
	A4	.65659*	.08056	.000	.3579	.9553
	B1	1.42103*	.08056	.000	1.1223	1.7197
	B2	1.05932*	.08056	.000	.7606	1.3580
	B3	1.26032*	.08056	.000	.9616	1.5590
	B4	.55911*	.08056	.000	.2604	.8578
	C1	.60547*	.08056	.000	.3068	.9042
	C2	1.07515*	.08056	.000	.7764	1.3739
	C4	.61633*	.08056	.000	.3176	.9150
	D1	.73342*	.08056	.000	.4347	1.0321
	D2	.44046*	.08056	.000	.1418	.7392
	D3	.97842*	.08056	.000	.6797	1.2771
D4	.31128*	.08056	.034	.0126	.6100	
C4	A1	.20564	.08056	.462	-.0931	.5043
	A2	.69692*	.08056	.000	.3982	.9956
	A3	-1.06743*	.08056	.000	-1.3661	-.7687
	A4	.04026	.08056	1.000	-.2584	.3390
	B1	.80470*	.08056	.000	.5060	1.1034
	B2	.44300*	.08056	.000	.1443	.7417
	B3	.64399*	.08056	.000	.3453	.9427
	B4	-.05721	.08056	1.000	-.3559	.2415
	C1	-.01086	.08056	1.000	-.3096	.2879
	C2	.45882*	.08056	.000	.1601	.7575
	C3	-.61633*	.08056	.000	-.9150	-.3176
	D1	.11709	.08056	.980	-.1816	.4158
	D2	-.17586	.08056	.702	-.4746	.1228
	D3	.36209*	.08056	.007	.0634	.6608

(I) GROUP	(J) GROUP	Mean Difference (I-J)	Std. Error	Sig.	95% Confidence Interval	
					Lower Bound	Upper Bound
	D4	-.30505*	.08056	.041	-.6038	-.0063
D1	A1	.08855	.08056	.999	-.2102	.3873
	A2	.57983*	.08056	.000	.2811	.8785
	A3	-1.18452*	.08056	.000	-1.4832	-.8858
	A4	-.07683	.08056	1.000	-.3755	.2219
	B1	.68761*	.08056	.000	.3889	.9863
	B2	.32590*	.08056	.022	.0272	.6246
	B3	.52690*	.08056	.000	.2282	.8256
	B4	-.17431	.08056	.714	-.4730	.1244
	C1	-.12795	.08056	.959	-.4267	.1708
	C2	.34173*	.08056	.013	.0430	.6404
	C3	-.73342*	.08056	.000	-1.0321	-.4347
	C4	-.11709	.08056	.980	-.4158	.1816
	D2	-.29296	.08056	.059	-.5917	.0058
	D3	.24500	.08056	.208	-.0537	.5437
D4	-.42214*	.08056	.001	-.7209	-.1234	
D2	A1	.38150*	.08056	.004	.0828	.6802
	A2	.87278*	.08056	.000	.5741	1.1715
	A3	-.89156*	.08056	.000	-1.1903	-.5929
	A4	.21613	.08056	.383	-.0826	.5148
	B1	.98056*	.08056	.000	.6819	1.2793
	B2	.61886*	.08056	.000	.3202	.9176
	B3	.81985*	.08056	.000	.5211	1.1186
	B4	.11865	.08056	.978	-.1801	.4174
	C1	.16501	.08056	.782	-.1337	.4637
	C2	.63469*	.08056	.000	.3360	.9334
	C3	-.44046*	.08056	.000	-.7392	-.1418
	C4	.17586	.08056	.702	-.1228	.4746
	D1	.29296	.08056	.059	-.0058	.5917
	D3	.53795*	.08056	.000	.2392	.8367
D4	-.12919	.08056	.956	-.4279	.1695	
D3	A1	-.15645	.08056	.838	-.4552	.1423
	A2	.33483*	.08056	.017	.0361	.6335
	A3	-1.42952*	.08056	.000	-1.7282	-1.1308
	A4	-.32183*	.08056	.025	-.6205	-.0231
	B1	.44261*	.08056	.000	.1439	.7413
	B2	.08091	.08056	1.000	-.2178	.3796
	B3	.28190	.08056	.081	-.0168	.5806
	B4	-.41931*	.08056	.001	-.7180	-.1206
	C1	-.37295*	.08056	.005	-.6717	-.0742
	C2	.09673	.08056	.997	-.2020	.3954
	C3	-.97842*	.08056	.000	-1.2771	-.6797
	C4	-.36209*	.08056	.007	-.6608	-.0634
	D1	-.24500	.08056	.208	-.5437	.0537

(I) GROUP	(J) GROUP	Mean Difference (I-J)	Std. Error	Sig.	95% Confidence Interval	
					Lower Bound	Upper Bound
	D2	-.53795*	.08056	.000	-.8367	-.2392
	D4	-.66714*	.08056	.000	-.9658	-.3684
D4	A1	.51069*	.08056	.000	.2120	.8094
	A2	1.00197*	.08056	.000	.7033	1.3007
	A3	-.76238*	.08056	.000	-1.0611	-.4637
	A4	.34531*	.08056	.012	.0466	.6440
	B1	1.10975*	.08056	.000	.8110	1.4085
	B2	.74804*	.08056	.000	.4493	1.0468
	B3	.94904*	.08056	.000	.6503	1.2477
	B4	.24783	.08056	.194	-.0509	.5465
	C1	.29419	.08056	.057	-.0045	.5929
	C2	.76387*	.08056	.000	.4652	1.0626
	C3	-.31128*	.08056	.034	-.6100	-.0126
	C4	.30505*	.08056	.041	.0063	.6038
	D1	.42214*	.08056	.001	.1234	.7209
	D2	.12919	.08056	.956	-.1695	.4279
	D3	.66714*	.08056	.000	.3684	.9658

*. The mean difference is significant at the 0.05 level.

6.6 dkk1

ANOVA

dkk1

	Sum of Squares	df	Mean Square	F	Sig.
Between Groups	5.655	15	.377	16.069	.000
Within Groups	.751	32	.023		
Total	6.406	47			

Multiple Comparisons

dkk1

Tukey HSD

(I) GROUP	(J) GROUP	Mean Difference (I-J)	Std. Error	Sig.	95% Confidence Interval	
					Lower Bound	Upper Bound
A1	A2	.77743	.12507	.000	.3137	1.2412
	A3	.97461*	.12507	.000	.5108	1.4384
	A4	.73966*	.12507	.000	.2759	1.2034
	B1	.86702*	.12507	.000	.4033	1.3308
	B2	.90076*	.12507	.000	.4370	1.3645
	B3	.78213*	.12507	.000	.3184	1.2459
	B4	.69197*	.12507	.000	.2282	1.1557

(I) GROUP	(J) GROUP	Mean Difference (I-J)	Std. Error	Sig.	95% Confidence Interval	
					Lower Bound	Upper Bound
	C1	-.21945	.12507	.915	-.6832	.2443
	C2	.88741 [†]	.12507	.000	.4236	1.3512
	C3	.24625	.12507	.824	-.2175	.7100
	C4	.95536 [†]	.12507	.000	.4916	1.4191
	D1	.62956 [†]	.12507	.002	.1658	1.0933
	D2	.54541 [†]	.12507	.010	.0816	1.0092
	D3	.60348 [†]	.12507	.003	.1397	1.0672
	D4	.25205	.12507	.800	-.2117	.7158
A2	A1	-.77743 [†]	.12507	.000	-1.2412	-.3137
	A3	.19718	.12507	.962	-.2666	.6609
	A4	-.03776	.12507	1.000	-.5015	.4260
	B1	.08960	.12507	1.000	-.3742	.5534
	B2	.12333	.12507	1.000	-.3404	.5871
	B3	.00470	.12507	1.000	-.4591	.4685
	B4	-.08546	.12507	1.000	-.5492	.3783
	C1	-.99688 [†]	.12507	.000	-1.4606	-.5331
	C2	.10998	.12507	1.000	-.3538	.5737
	C3	-.53118 [†]	.12507	.013	-.9949	-.0674
	C4	.17793	.12507	.984	-.2858	.6417
	D1	-.14787	.12507	.997	-.6116	.3159
	D2	-.23202	.12507	.877	-.6958	.2317
	D3	-.17394	.12507	.987	-.6377	.2898
	D4	-.52538 [†]	.12507	.015	-.9891	-.0616
A3	A1	-.97461 [†]	.12507	.000	-1.4384	-.5108
	A2	-.19718	.12507	.962	-.6609	.2666
	A4	-.23494	.12507	.867	-.6987	.2288
	B1	-.10759	.12507	1.000	-.5713	.3562
	B2	-.07385	.12507	1.000	-.5376	.3899
	B3	-.19248	.12507	.968	-.6562	.2713
	B4	-.28264	.12507	.652	-.7464	.1811
	C1	-1.19406 [†]	.12507	.000	-1.6578	-.7303
	C2	-.08720	.12507	1.000	-.5510	.3766
	C3	-.72836 [†]	.12507	.000	-1.1921	-.2646
	C4	-.01925	.12507	1.000	-.4830	.4445
	D1	-.34505	.12507	.340	-.8088	.1187
	D2	-.42920	.12507	.094	-.8930	.0346
	D3	-.37112	.12507	.238	-.8349	.0926
	D4	-.72256 [†]	.12507	.000	-1.1863	-.2588
A4	A1	-.73966 [†]	.12507	.000	-1.2034	-.2759
	A2	.03776	.12507	1.000	-.4260	.5015
	A3	.23494	.12507	.867	-.2288	.6987
	B1	.12736	.12507	.999	-.3364	.5911
	B2	.16110	.12507	.994	-.3027	.6249
	B3	.04247	.12507	1.000	-.4213	.5062

(I) GROUP	(J) GROUP	Mean Difference (I-J)	Std. Error	Sig.	95% Confidence Interval	
					Lower Bound	Upper Bound
	B4	-.04770	.12507	1.000	-.5115	.4161
	C1	-.95911 [*]	.12507	.000	-1.4229	-.4954
	C2	.14775	.12507	.997	-.3160	.6115
	C3	-.49342 [*]	.12507	.028	-.9572	-.0297
	C4	.21569	.12507	.925	-.2481	.6795
	D1	-.11010	.12507	1.000	-.5739	.3537
	D2	-.19426	.12507	.966	-.6580	.2695
	D3	-.13618	.12507	.999	-.5999	.3276
	D4	-.48762 [*]	.12507	.032	-.9514	-.0239
B1	A1	-.86702 [*]	.12507	.000	-1.3308	-.4033
	A2	-.08960	.12507	1.000	-.5534	.3742
	A3	.10759	.12507	1.000	-.3562	.5713
	A4	-.12736	.12507	.999	-.5911	.3364
	B2	.03374	.12507	1.000	-.4300	.4975
	B3	-.08489	.12507	1.000	-.5487	.3789
	B4	-.17505	.12507	.986	-.6388	.2887
	C1	-1.08647 [*]	.12507	.000	-1.5502	-.6227
	C2	.02039	.12507	1.000	-.4434	.4841
	C3	-.62077 [*]	.12507	.002	-1.0845	-.1570
	C4	.08833	.12507	1.000	-.3754	.5521
	D1	-.23746	.12507	.858	-.7012	.2263
	D2	-.32162	.12507	.450	-.7854	.1421
	D3	-.26354	.12507	.748	-.7273	.2002
	D4	-.61497 [*]	.12507	.002	-1.0787	-.1512
B2	A1	-.90076 [*]	.12507	.000	-1.3645	-.4370
	A2	-.12333	.12507	1.000	-.5871	.3404
	A3	.07385	.12507	1.000	-.3899	.5376
	A4	-.16110	.12507	.994	-.6249	.3027
	B1	-.03374	.12507	1.000	-.4975	.4300
	B3	-.11863	.12507	1.000	-.5824	.3451
	B4	-.20879	.12507	.940	-.6726	.2550
	C1	-1.12021 [*]	.12507	.000	-1.5840	-.6564
	C2	-.01335	.12507	1.000	-.4771	.4504
	C3	-.65451 [*]	.12507	.001	-1.1183	-.1907
	C4	.05460	.12507	1.000	-.4092	.5184
	D1	-.27120	.12507	.711	-.7350	.1926
	D2	-.35535	.12507	.297	-.8191	.1084
	D3	-.29728	.12507	.576	-.7610	.1665
	D4	-.64871 [*]	.12507	.001	-1.1125	-.1850
B3	A1	-.78213 [*]	.12507	.000	-1.2459	-.3184
	A2	-.00470	.12507	1.000	-.4685	.4591
	A3	.19248	.12507	.968	-.2713	.6562
	A4	-.04247	.12507	1.000	-.5062	.4213
	B1	.08489	.12507	1.000	-.3789	.5487
	B2	.11863	.12507	1.000	-.3451	.5824

(I) GROUP	(J) GROUP	Mean Difference (I-J)	Std. Error	Sig.	95% Confidence Interval	
					Lower Bound	Upper Bound
	B4	-.09016	.12507	1.000	-.5539	.3736
	C1	-1.00158 [*]	.12507	.000	-1.4653	-.5378
	C2	.10528	.12507	1.000	-.3585	.5690
	C3	-.53588 [*]	.12507	.012	-.9996	-.0721
	C4	.17323	.12507	.987	-.2905	.6370
	D1	-.15257	.12507	.996	-.6163	.3112
	D2	-.23672	.12507	.861	-.7005	.2270
	D3	-.17865	.12507	.983	-.6424	.2851
	D4	-.53008 [*]	.12507	.013	-.9938	-.0663
B4	A1	-.69197 [*]	.12507	.000	-1.1557	-.2282
	A2	.08546	.12507	1.000	-.3783	.5492
	A3	.28264	.12507	.652	-.1811	.7464
	A4	.04770	.12507	1.000	-.4161	.5115
	B1	.17505	.12507	.986	-.2887	.6388
	B2	.20879	.12507	.940	-.2550	.6726
	B3	.09016	.12507	1.000	-.3736	.5539
	C1	-.91142 [*]	.12507	.000	-1.3752	-.4477
	C2	.19544	.12507	.964	-.2683	.6592
	C3	-.44572	.12507	.070	-.9095	.0180
	C4	.26339	.12507	.749	-.2004	.7271
	D1	-.06241	.12507	1.000	-.5262	.4014
	D2	-.14656	.12507	.998	-.6103	.3172
	D3	-.08848	.12507	1.000	-.5522	.3753
	D4	-.43992	.12507	.077	-.9037	.0238
C1	A1	.21945	.12507	.915	-.2443	.6832
	A2	.99688 [*]	.12507	.000	.5331	1.4606
	A3	1.19406 [*]	.12507	.000	.7303	1.6578
	A4	.95911 [*]	.12507	.000	.4954	1.4229
	B1	1.08647 [*]	.12507	.000	.6227	1.5502
	B2	1.12021 [*]	.12507	.000	.6564	1.5840
	B3	1.00158 [*]	.12507	.000	.5378	1.4653
	B4	.91142 [*]	.12507	.000	.4477	1.3752
	C2	1.10686 [*]	.12507	.000	.6431	1.5706
	C3	.46570 [*]	.12507	.048	.0019	.9295
	C4	1.17481 [*]	.12507	.000	.7110	1.6386
	D1	.84901 [*]	.12507	.000	.3853	1.3128
	D2	.76486 [*]	.12507	.000	.3011	1.2286
	D3	.82293 [*]	.12507	.000	.3592	1.2867
	D4	.47150 [*]	.12507	.043	.0077	.9353
C2	A1	-.88741 [*]	.12507	.000	-1.3512	-.4236
	A2	-.10998	.12507	1.000	-.5737	.3538
	A3	.08720	.12507	1.000	-.3766	.5510
	A4	-.14775	.12507	.997	-.6115	.3160
	B1	-.02039	.12507	1.000	-.4841	.4434
	B2	.01335	.12507	1.000	-.4504	.4771

(I) GROUP	(J) GROUP	Mean Difference (I-J)	Std. Error	Sig.	95% Confidence Interval	
					Lower Bound	Upper Bound
	B3	-.10528	.12507	1.000	-.5690	.3585
	B4	-.19544	.12507	.964	-.6592	.2683
	C1	-1.10686 [*]	.12507	.000	-1.5706	-.6431
	C3	-.64116 [*]	.12507	.001	-1.1049	-.1774
	C4	.06795	.12507	1.000	-.3958	.5317
	D1	-.25785	.12507	.774	-.7216	.2059
	D2	-.34200	.12507	.353	-.8058	.1218
	D3	-.28393	.12507	.646	-.7477	.1798
	D4	-.63536 [*]	.12507	.001	-1.0991	-.1716
C3	A1	-.24625	.12507	.824	-.7100	.2175
	A2	.53118 [*]	.12507	.013	.0674	.9949
	A3	.72836 [*]	.12507	.000	.2646	1.1921
	A4	.49342 [*]	.12507	.028	.0297	.9572
	B1	.62077 [*]	.12507	.002	.1570	1.0845
	B2	.65451 [*]	.12507	.001	.1907	1.1183
	B3	.53588 [*]	.12507	.012	.0721	.9996
	B4	.44572	.12507	.070	-.0180	.9095
	C1	-.46570 [*]	.12507	.048	-.9295	-.0019
	C2	.64116 [*]	.12507	.001	.1774	1.1049
	C4	.70911 [*]	.12507	.000	.2453	1.1729
	D1	.38331	.12507	.199	-.0804	.8471
	D2	.29916	.12507	.566	-.1646	.7629
	D3	.35724	.12507	.289	-.1065	.8210
	D4	.00580	.12507	1.000	-.4580	.4696
C4	A1	-.95536 [*]	.12507	.000	-1.4191	-.4916
	A2	-.17793	.12507	.984	-.6417	.2858
	A3	.01925	.12507	1.000	-.4445	.4830
	A4	-.21569	.12507	.925	-.6795	.2481
	B1	-.08833	.12507	1.000	-.5521	.3754
	B2	-.05460	.12507	1.000	-.5184	.4092
	B3	-.17323	.12507	.987	-.6370	.2905
	B4	-.26339	.12507	.749	-.7271	.2004
	C1	-1.17481 [*]	.12507	.000	-1.6386	-.7110
	C2	-.06795	.12507	1.000	-.5317	.3958
	C3	-.70911 [*]	.12507	.000	-1.1729	-.2453
	D1	-.32580	.12507	.429	-.7896	.1380
	D2	-.40995	.12507	.130	-.8737	.0538
	D3	-.35187	.12507	.311	-.8156	.1119
	D4	-.70331 [*]	.12507	.000	-1.1671	-.2395
D1	A1	-.62956 [*]	.12507	.002	-1.0933	-.1658
	A2	.14787	.12507	.997	-.3159	.6116
	A3	.34505	.12507	.340	-.1187	.8088
	A4	.11010	.12507	1.000	-.3537	.5739
	B1	.23746	.12507	.858	-.2263	.7012
	B2	.27120	.12507	.711	-.1926	.7350

(I) GROUP	(J) GROUP	Mean Difference (I-J)	Std. Error	Sig.	95% Confidence Interval	
					Lower Bound	Upper Bound
	B3	.15257	.12507	.996	-.3112	.6163
	B4	.06241	.12507	1.000	-.4014	.5262
	C1	-.84901 [†]	.12507	.000	-1.3128	-.3853
	C2	.25785	.12507	.774	-.2059	.7216
	C3	-.38331	.12507	.199	-.8471	.0804
	C4	.32580	.12507	.429	-.1380	.7896
	D2	-.08416	.12507	1.000	-.5479	.3796
	D3	-.02608	.12507	1.000	-.4898	.4377
	D4	-.37751	.12507	.217	-.8413	.0862
D2	A1	-.54541 [†]	.12507	.010	-1.0092	-.0816
	A2	.23202	.12507	.877	-.2317	.6958
	A3	.42920	.12507	.094	-.0346	.8930
	A4	.19426	.12507	.966	-.2695	.6580
	B1	.32162	.12507	.450	-.1421	.7854
	B2	.35535	.12507	.297	-.1084	.8191
	B3	.23672	.12507	.861	-.2270	.7005
	B4	.14656	.12507	.998	-.3172	.6103
	C1	-.76486 [†]	.12507	.000	-1.2286	-.3011
	C2	.34200	.12507	.353	-.1218	.8058
	C3	-.29916	.12507	.566	-.7629	.1646
	C4	.40995	.12507	.130	-.0538	.8737
	D1	.08416	.12507	1.000	-.3796	.5479
	D3	.05808	.12507	1.000	-.4057	.5218
	D4	-.29336	.12507	.596	-.7571	.1704
D3	A1	-.60348 [†]	.12507	.003	-1.0672	-.1397
	A2	.17394	.12507	.987	-.2898	.6377
	A3	.37112	.12507	.238	-.0926	.8349
	A4	.13618	.12507	.999	-.3276	.5999
	B1	.26354	.12507	.748	-.2002	.7273
	B2	.29728	.12507	.576	-.1665	.7610
	B3	.17865	.12507	.983	-.2851	.6424
	B4	.08848	.12507	1.000	-.3753	.5522
	C1	-.82293 [†]	.12507	.000	-1.2867	-.3592
	C2	.28393	.12507	.646	-.1798	.7477
	C3	-.35724	.12507	.289	-.8210	.1065
	C4	.35187	.12507	.311	-.1119	.8156
	D1	.02608	.12507	1.000	-.4377	.4898
	D2	-.05808	.12507	1.000	-.5218	.4057
	D4	-.35144	.12507	.313	-.8152	.1123
D4	A1	-.25205	.12507	.800	-.7158	.2117
	A2	.52538 [†]	.12507	.015	.0616	.9891
	A3	.72256 [†]	.12507	.000	.2588	1.1863
	A4	.48762 [†]	.12507	.032	.0239	.9514
	B1	.61497 [†]	.12507	.002	.1512	1.0787

(I) GROUP	(J) GROUP	Mean Difference (I-J)	Std. Error	Sig.	95% Confidence Interval	
					Lower Bound	Upper Bound
	B2	.64871*	.12507	.001	.1850	1.1125
	B3	.53008*	.12507	.013	.0663	.9938
	B4	.43992	.12507	.077	-.0238	.9037
	C1	-.47150*	.12507	.043	-.9353	-.0077
	C2	.63536*	.12507	.001	.1716	1.0991
	C3	-.00580	.12507	1.000	-.4696	.4580
	C4	.70331*	.12507	.000	.2395	1.1671
	D1	.37751	.12507	.217	-.0862	.8413
	D2	.29336	.12507	.596	-.1704	.7571
	D3	.35144	.12507	.313	-.1123	.8152

*. The mean difference is significant at the 0.05 level.

7. ANOVA analysis of the relative ALP activity of RBMSCs induced with FGF2 and insulin

ANOVA

ALP

	Sum of Squares	df	Mean Square	F	Sig.
Between Groups	.095	3	.032	72.465	.000
Within Groups	.003	8	.000		
Total	.098	11			

Multiple Comparisons

ALP

Tukey HSD

(I) GROUP	(J) GROUP	Mean Difference (I-J)	Std. Error	Sig.	95% Confidence Interval	
					Lower Bound	Upper Bound
2%FBS	FGF2	-.10818*	.01705	.001	-.1628	-.0536
	INSULIN	-.17191*	.01705	.000	-.2265	-.1173
	FGF2+INSULIN	.05489*	.01705	.049	.0003	.1095
FGF2	2%FBS	.10818*	.01705	.001	.0536	.1628
	INSULIN	-.06373*	.01705	.024	-.1183	-.0091
	FGF2+INSULIN	.16307*	.01705	.000	.1085	.2177
INSULIN	2%FBS	.17191*	.01705	.000	.1173	.2265
	FGF2	.06373*	.01705	.024	.0091	.1183
	FGF2+INSULIN	.22680*	.01705	.000	.1722	.2814
FGF2+INSULIN	2%FBS	-.05489*	.01705	.049	-.1095	-.0003
	FGF2	-.16307*	.01705	.000	-.2177	-.1085
	INSULIN	-.22680*	.01705	.000	-.2814	-.1722

*. The mean difference is significant at the 0.05 level.

8. ANOVA analysis of the relative ALP activity of sequentially induced RBMSCs using FGF2/insulin followed by BMPs

ANOVA

ALP

	Sum of Squares	df	Mean Square	F	Sig.
Between Groups	.840	15	.056	296.570	.000
Within Groups	.006	32	.000		
Total	.846	47			

Multiple Comparisons

ALP

Tukey HSD

(I) GROUP	(J) GROUP	Mean Difference (I-J)	Std. Error	Sig.	95% Confidence Interval	
					Lower Bound	Upper Bound
A1	A2	-.06260 [*]	.01122	.000	-.1042	-.0210
	A3	-.10010 [*]	.01122	.000	-.1417	-.0585
	A4	-.09146 [*]	.01122	.000	-.1331	-.0499
	B1	-.27270 [*]	.01122	.000	-.3143	-.2311
	B2	-.17759 [*]	.01122	.000	-.2192	-.1360
	B3	-.35610 [*]	.01122	.000	-.3977	-.3145
	B4	-.27365 [*]	.01122	.000	-.3152	-.2321
	C1	-.09926 [*]	.01122	.000	-.1409	-.0577
	C2	-.24529 [*]	.01122	.000	-.2869	-.2037
	C3	-.30870 [*]	.01122	.000	-.3503	-.2671
	C4	-.23315 [*]	.01122	.000	-.2747	-.1916
	D1	.12950 [*]	.01122	.000	.0879	.1711
	D2	-.00429	.01122	1.000	-.0459	.0373
	D3	-.00424	.01122	1.000	-.0458	.0374
D4	-.05140 [*]	.01122	.005	-.0930	-.0098	
A2	A1	.06260 [*]	.01122	.000	.0210	.1042
	A3	-.03750	.01122	.113	-.0791	.0041
	A4	-.02886	.01122	.449	-.0705	.0127
	B1	-.21010 [*]	.01122	.000	-.2517	-.1685
	B2	-.11498 [*]	.01122	.000	-.1566	-.0734
	B3	-.29350 [*]	.01122	.000	-.3351	-.2519
	B4	-.21104 [*]	.01122	.000	-.2526	-.1695
	C1	-.03666	.01122	.133	-.0782	.0049
	C2	-.18269 [*]	.01122	.000	-.2243	-.1411
	C3	-.24610 [*]	.01122	.000	-.2877	-.2045
	C4	-.17055 [*]	.01122	.000	-.2121	-.1290
	D1	.19211 [*]	.01122	.000	.1505	.2337
	D2	.05831 [*]	.01122	.001	.0167	.0999
	D3	.05836 [*]	.01122	.001	.0168	.1000

(I) GROUP	(J) GROUP	Mean Difference (I-J)	Std. Error	Sig.	95% Confidence Interval	
					Lower Bound	Upper Bound
	D4	.01120	.01122	1.000	-.0304	.0528
A3	A1	.10010 [†]	.01122	.000	.0585	.1417
	A2	.03750	.01122	.113	-.0041	.0791
	A4	.00864	.01122	1.000	-.0330	.0502
	B1	-.17260 [†]	.01122	.000	-.2142	-.1310
	B2	-.07749 [†]	.01122	.000	-.1191	-.0359
	B3	-.25600 [†]	.01122	.000	-.2976	-.2144
	B4	-.17355 [†]	.01122	.000	-.2151	-.1320
	C1	.00084	.01122	1.000	-.0408	.0424
	C2	-.14519 [†]	.01122	.000	-.1868	-.1036
	C3	-.20860 [†]	.01122	.000	-.2502	-.1670
	C4	-.13305 [†]	.01122	.000	-.1746	-.0915
	D1	.22960 [†]	.01122	.000	.1880	.2712
	D2	.09581 [†]	.01122	.000	.0542	.1374
	D3	.09586 [†]	.01122	.000	.0543	.1375
D4	.04869 [†]	.01122	.010	.0071	.0903	
A4	A1	.09146 [†]	.01122	.000	.0499	.1331
	A2	.02886	.01122	.449	-.0127	.0705
	A3	-.00864	.01122	1.000	-.0502	.0330
	B1	-.18124 [†]	.01122	.000	-.2228	-.1396
	B2	-.08612 [†]	.01122	.000	-.1277	-.0445
	B3	-.26464 [†]	.01122	.000	-.3062	-.2230
	B4	-.18219 [†]	.01122	.000	-.2238	-.1406
	C1	-.00780	.01122	1.000	-.0494	.0338
	C2	-.15383 [†]	.01122	.000	-.1954	-.1122
	C3	-.21724 [†]	.01122	.000	-.2588	-.1756
	C4	-.14169 [†]	.01122	.000	-.1833	-.1001
	D1	.22097 [†]	.01122	.000	.1794	.2626
	D2	.08717 [†]	.01122	.000	.0456	.1288
	D3	.08722 [†]	.01122	.000	.0456	.1288
D4	.04006	.01122	.069	-.0015	.0816	
B1	A1	.27270 [†]	.01122	.000	.2311	.3143
	A2	.21010 [†]	.01122	.000	.1685	.2517
	A3	.17260 [†]	.01122	.000	.1310	.2142
	A4	.18124 [†]	.01122	.000	.1396	.2228
	B2	.09511 [†]	.01122	.000	.0535	.1367
	B3	-.08340 [†]	.01122	.000	-.1250	-.0418
	B4	-.00095	.01122	1.000	-.0425	.0406
	C1	.17344 [†]	.01122	.000	.1318	.2150
	C2	.02741	.01122	.532	-.0142	.0690
	C3	-.03600	.01122	.150	-.0776	.0056
	C4	.03955	.01122	.076	-.0020	.0811
	D1	.40220 [†]	.01122	.000	.3606	.4438
	D2	.26841 [†]	.01122	.000	.2268	.3100
	D3	.26846 [†]	.01122	.000	.2269	.3101

(I) GROUP	(J) GROUP	Mean Difference (I-J)	Std. Error	Sig.	95% Confidence Interval	
					Lower Bound	Upper Bound
	D4	.22129 [†]	.01122	.000	.1797	.2629
B2	A1	.17759 [†]	.01122	.000	.1360	.2192
	A2	.11498 [†]	.01122	.000	.0734	.1566
	A3	.07749 [†]	.01122	.000	.0359	.1191
	A4	.08612 [†]	.01122	.000	.0445	.1277
	B1	-.09511 [†]	.01122	.000	-.1367	-.0535
	B3	-.17852 [†]	.01122	.000	-.2201	-.1369
	B4	-.09606 [†]	.01122	.000	-.1377	-.0545
	C1	.07833 [†]	.01122	.000	.0367	.1199
	C2	-.06771 [†]	.01122	.000	-.1093	-.0261
	C3	-.13111 [†]	.01122	.000	-.1727	-.0895
	C4	-.05556 [†]	.01122	.002	-.0972	-.0140
	D1	.30709 [†]	.01122	.000	.2655	.3487
	D2	.17329 [†]	.01122	.000	.1317	.2149
	D3	.17335 [†]	.01122	.000	.1318	.2149
D4	.12618 [†]	.01122	.000	.0846	.1678	
B3	A1	.35610 [†]	.01122	.000	.3145	.3977
	A2	.29350 [†]	.01122	.000	.2519	.3351
	A3	.25600 [†]	.01122	.000	.2144	.2976
	A4	.26464 [†]	.01122	.000	.2230	.3062
	B1	.08340 [†]	.01122	.000	.0418	.1250
	B2	.17852 [†]	.01122	.000	.1369	.2201
	B4	.08246 [†]	.01122	.000	.0409	.1240
	C1	.25684 [†]	.01122	.000	.2153	.2984
	C2	.11081 [†]	.01122	.000	.0692	.1524
	C3	.04740 [†]	.01122	.014	.0058	.0890
	C4	.12295 [†]	.01122	.000	.0814	.1645
	D1	.48561 [†]	.01122	.000	.4440	.5272
	D2	.35181 [†]	.01122	.000	.3102	.3934
	D3	.35186 [†]	.01122	.000	.3103	.3935
D4	.30470 [†]	.01122	.000	.2631	.3463	
B4	A1	.27365 [†]	.01122	.000	.2321	.3152
	A2	.21104 [†]	.01122	.000	.1695	.2526
	A3	.17355 [†]	.01122	.000	.1320	.2151
	A4	.18219 [†]	.01122	.000	.1406	.2238
	B1	.00095	.01122	1.000	-.0406	.0425
	B2	.09606 [†]	.01122	.000	.0545	.1377
	B3	-.08246 [†]	.01122	.000	-.1240	-.0409
	C1	.17439 [†]	.01122	.000	.1328	.2160
	C2	.02835	.01122	.477	-.0132	.0699
	C3	-.03505	.01122	.177	-.0766	.0065
	C4	.04050	.01122	.063	-.0011	.0821
	D1	.40315 [†]	.01122	.000	.3616	.4447
	D2	.26935 [†]	.01122	.000	.2278	.3109
	D3	.26941 [†]	.01122	.000	.2278	.3110

(I) GROUP	(J) GROUP	Mean Difference (I-J)	Std. Error	Sig.	95% Confidence Interval	
					Lower Bound	Upper Bound
	D4	.22224 [*]	.01122	.000	.1807	.2638
C1	A1	.09926 [*]	.01122	.000	.0577	.1409
	A2	.03666	.01122	.133	-.0049	.0782
	A3	-.00084	.01122	1.000	-.0424	.0408
	A4	.00780	.01122	1.000	-.0338	.0494
	B1	-.17344 [*]	.01122	.000	-.2150	-.1318
	B2	-.07833 [*]	.01122	.000	-.1199	-.0367
	B3	-.25684 [*]	.01122	.000	-.2984	-.2153
	B4	-.17439 [*]	.01122	.000	-.2160	-.1328
	C2	-.14603 [*]	.01122	.000	-.1876	-.1044
	C3	-.20944 [*]	.01122	.000	-.2510	-.1678
	C4	-.13389 [*]	.01122	.000	-.1755	-.0923
	D1	.22876 [*]	.01122	.000	.1872	.2704
	D2	.09497 [*]	.01122	.000	.0534	.1366
	D3	.09502 [*]	.01122	.000	.0534	.1366
D4	.04786 [*]	.01122	.013	.0063	.0894	
C2	A1	.24529 [*]	.01122	.000	.2037	.2869
	A2	.18269 [*]	.01122	.000	.1411	.2243
	A3	.14519 [*]	.01122	.000	.1036	.1868
	A4	.15383 [*]	.01122	.000	.1122	.1954
	B1	-.02741	.01122	.532	-.0690	.0142
	B2	.06771 [*]	.01122	.000	.0261	.1093
	B3	-.11081 [*]	.01122	.000	-.1524	-.0692
	B4	-.02835	.01122	.477	-.0699	.0132
	C1	.14603 [*]	.01122	.000	.1044	.1876
	C3	-.06341 [*]	.01122	.000	-.1050	-.0218
	C4	.01214	.01122	.999	-.0294	.0537
	D1	.37480 [*]	.01122	.000	.3332	.4164
	D2	.24100 [*]	.01122	.000	.1994	.2826
	D3	.24105 [*]	.01122	.000	.1995	.2826
D4	.19389 [*]	.01122	.000	.1523	.2355	
C3	A1	.30870 [*]	.01122	.000	.2671	.3503
	A2	.24610 [*]	.01122	.000	.2045	.2877
	A3	.20860 [*]	.01122	.000	.1670	.2502
	A4	.21724 [*]	.01122	.000	.1756	.2588
	B1	.03600	.01122	.150	-.0056	.0776
	B2	.13111 [*]	.01122	.000	.0895	.1727
	B3	-.04740 [*]	.01122	.014	-.0890	-.0058
	B4	.03505	.01122	.177	-.0065	.0766
	C1	.20944 [*]	.01122	.000	.1678	.2510
	C2	.06341 [*]	.01122	.000	.0218	.1050
	C4	.07555 [*]	.01122	.000	.0340	.1171
	D1	.43820 [*]	.01122	.000	.3966	.4798
	D2	.30441 [*]	.01122	.000	.2628	.3460
	D3	.30446 [*]	.01122	.000	.2629	.3461

(I) GROUP	(J) GROUP	Mean Difference (I-J)	Std. Error	Sig.	95% Confidence Interval	
					Lower Bound	Upper Bound
	D4	.25730 [†]	.01122	.000	.2157	.2989
C4	A1	.23315 [†]	.01122	.000	.1916	.2747
	A2	.17055 [†]	.01122	.000	.1290	.2121
	A3	.13305 [†]	.01122	.000	.0915	.1746
	A4	.14169 [†]	.01122	.000	.1001	.1833
	B1	-.03955	.01122	.076	-.0811	.0020
	B2	.05556 [†]	.01122	.002	.0140	.0972
	B3	-.12295 [†]	.01122	.000	-.1645	-.0814
	B4	-.04050	.01122	.063	-.0821	.0011
	C1	.13389 [†]	.01122	.000	.0923	.1755
	C2	-.01214	.01122	.999	-.0537	.0294
	C3	-.07555 [†]	.01122	.000	-.1171	-.0340
	D1	.36265 [†]	.01122	.000	.3211	.4042
	D2	.22886 [†]	.01122	.000	.1873	.2704
	D3	.22891 [†]	.01122	.000	.1873	.2705
D4	.18174 [†]	.01122	.000	.1402	.2233	
D1	A1	-.12950 [†]	.01122	.000	-.1711	-.0879
	A2	-.19211 [†]	.01122	.000	-.2337	-.1505
	A3	-.22960 [†]	.01122	.000	-.2712	-.1880
	A4	-.22097 [†]	.01122	.000	-.2626	-.1794
	B1	-.40220 [†]	.01122	.000	-.4438	-.3606
	B2	-.30709 [†]	.01122	.000	-.3487	-.2655
	B3	-.48561 [†]	.01122	.000	-.5272	-.4440
	B4	-.40315 [†]	.01122	.000	-.4447	-.3616
	C1	-.22876 [†]	.01122	.000	-.2704	-.1872
	C2	-.37480 [†]	.01122	.000	-.4164	-.3332
	C3	-.43820 [†]	.01122	.000	-.4798	-.3966
	C4	-.36265 [†]	.01122	.000	-.4042	-.3211
	D2	-.13380 [†]	.01122	.000	-.1754	-.0922
	D3	-.13374 [†]	.01122	.000	-.1753	-.0921
D4	-.18091 [†]	.01122	.000	-.2225	-.1393	
D2	A1	.00429	.01122	1.000	-.0373	.0459
	A2	-.05831 [†]	.01122	.001	-.0999	-.0167
	A3	-.09581 [†]	.01122	.000	-.1374	-.0542
	A4	-.08717 [†]	.01122	.000	-.1288	-.0456
	B1	-.26841 [†]	.01122	.000	-.3100	-.2268
	B2	-.17329 [†]	.01122	.000	-.2149	-.1317
	B3	-.35181 [†]	.01122	.000	-.3934	-.3102
	B4	-.26935 [†]	.01122	.000	-.3109	-.2278
	C1	-.09497 [†]	.01122	.000	-.1366	-.0534
	C2	-.24100 [†]	.01122	.000	-.2826	-.1994
	C3	-.30441 [†]	.01122	.000	-.3460	-.2628
	C4	-.22886 [†]	.01122	.000	-.2704	-.1873
	D1	.13380 [†]	.01122	.000	.0922	.1754
	D3	.00005	.01122	1.000	-.0415	.0416

(I) GROUP	(J) GROUP	Mean Difference (I-J)	Std. Error	Sig.	95% Confidence Interval	
					Lower Bound	Upper Bound
	D4	-.04711*	.01122	.015	-.0887	-.0055
D3	A1	.00424	.01122	1.000	-.0374	.0458
	A2	-.05836*	.01122	.001	-.1000	-.0168
	A3	-.09586*	.01122	.000	-.1375	-.0543
	A4	-.08722*	.01122	.000	-.1288	-.0456
	B1	-.26846*	.01122	.000	-.3101	-.2269
	B2	-.17335*	.01122	.000	-.2149	-.1318
	B3	-.35186*	.01122	.000	-.3935	-.3103
	B4	-.26941*	.01122	.000	-.3110	-.2278
	C1	-.09502*	.01122	.000	-.1366	-.0534
	C2	-.24105*	.01122	.000	-.2826	-.1995
	C3	-.30446*	.01122	.000	-.3461	-.2629
	C4	-.22891*	.01122	.000	-.2705	-.1873
	D1	.13374*	.01122	.000	.0921	.1753
	D2	-.00005	.01122	1.000	-.0416	.0415
D4	-.04717*	.01122	.015	-.0888	-.0056	
D4	A1	.05140*	.01122	.005	.0098	.0930
	A2	-.01120	.01122	1.000	-.0528	.0304
	A3	-.04869*	.01122	.010	-.0903	-.0071
	A4	-.04006	.01122	.069	-.0816	.0015
	B1	-.22129*	.01122	.000	-.2629	-.1797
	B2	-.12618*	.01122	.000	-.1678	-.0846
	B3	-.30470*	.01122	.000	-.3463	-.2631
	B4	-.22224*	.01122	.000	-.2638	-.1807
	C1	-.04786*	.01122	.013	-.0894	-.0063
	C2	-.19389*	.01122	.000	-.2355	-.1523
	C3	-.25730*	.01122	.000	-.2989	-.2157
	C4	-.18174*	.01122	.000	-.2233	-.1402
	D1	.18091*	.01122	.000	.1393	.2225
	D2	.04711*	.01122	.015	.0055	.0887
D3	.04717*	.01122	.015	.0056	.0888	

*. The mean difference is significant at the 0.05 level.

9. ANOVA analysis of the relative calcium deposition of RBMSCs induced with FGF2 and insulin

ANOVA

ARS

	Sum of Squares	df	Mean Square	F	Sig.
Between Groups	2.036	3	.679	77.961	.000
Within Groups	.070	8	.009		
Total	2.106	11			

Multiple Comparisons

ARS
Tukey HSD

(I) GROUP	(J) GROUP	Mean Difference (I-J)	Std. Error	Sig.	95% Confidence Interval	
					Lower Bound	Upper Bound
2%FBS	FGF2	-.90466*	.07618	.000	-1.1486	-.6607
	INSULIN	-1.01109*	.07618	.000	-1.2551	-.7671
	FGF2+INSULIN	-.92461*	.07618	.000	-1.1686	-.6806
FGF2	2%FBS	.90466*	.07618	.000	.6607	1.1486
	INSULIN	-.10643	.07618	.534	-.3504	.1375
	FGF2+INSULIN	-.01996	.07618	.993	-.2639	.2240
INSULIN	2%FBS	1.01109*	.07618	.000	.7671	1.2551
	FGF2	.10643	.07618	.534	-.1375	.3504
	FGF2+INSULIN	.08647	.07618	.680	-.1575	.3304
FGF2+INSULIN	2%FBS	.92461*	.07618	.000	.6806	1.1686
	FGF2	.01996	.07618	.993	-.2240	.2639
	INSULIN	-.08647	.07618	.680	-.3304	.1575

*. The mean difference is significant at the 0.05 level.

10. ANOVA analysis of the relative calcium deposition of sequentially induced RBMSCs using FGF2/insulin followed by BMPs

ANOVA

ARS

	Sum of Squares	df	Mean Square	F	Sig.
Between Groups	5.918	15	.395	31.131	.000
Within Groups	.406	32	.013		
Total	6.324	47			

Multiple Comparisons

ARS
Tukey HSD

(I) GROUP	(J) GROUP	Mean Difference (I-J)	Std. Error	Sig.	95% Confidence Interval	
					Lower Bound	Upper Bound
A1	A2	-1.53659*	.09192	.000	-1.8774	-1.1957
	A3	-1.48337*	.09192	.000	-1.8242	-1.1425
	A4	-1.10421*	.09192	.000	-1.4451	-.7634
	B1	-.65188*	.09192	.000	-.9927	-.3110
	B2	-.90466*	.09192	.000	-1.2455	-.5638
	B3	-.82483*	.09192	.000	-1.1657	-.4840
	B4	-.78492*	.09192	.000	-1.1258	-.4441

(I) GROUP	(J) GROUP	Mean Difference (I-J)	Std. Error	Sig.	95% Confidence Interval	
					Lower Bound	Upper Bound
	C1	-.71840*	.09192	.000	-1.0593	-.3776
	C2	-1.01109*	.09192	.000	-1.3519	-.6702
	C3	-1.17738*	.09192	.000	-1.5182	-.8365
	C4	-.99778*	.09192	.000	-1.3386	-.6569
	D1	-.70510*	.09192	.000	-1.0460	-.3642
	D2	-.92461*	.09192	.000	-1.2655	-.5838
	D3	-.88470*	.09192	.000	-1.2256	-.5439
	D4	-.54545*	.09192	.000	-.8863	-.2046
A2	A1	1.53659*	.09192	.000	1.1957	1.8774
	A3	.05322	.09192	1.000	-.2876	.3941
	A4	.43237*	.09192	.004	.0915	.7732
	B1	.88470*	.09192	.000	.5439	1.2256
	B2	.63193*	.09192	.000	.2911	.9728
	B3	.71175*	.09192	.000	.3709	1.0526
	B4	.75166*	.09192	.000	.4108	1.0925
	C1	.81818*	.09192	.000	.4773	1.1590
	C2	.52550*	.09192	.000	.1846	.8663
	C3	.35920*	.09192	.031	.0184	.7001
	C4	.53880*	.09192	.000	.1980	.8797
	D1	.83149*	.09192	.000	.4906	1.1723
	D2	.61197*	.09192	.000	.2711	.9528
	D3	.65188*	.09192	.000	.3110	.9927
	D4	.99113*	.09192	.000	.6503	1.3320
A3	A1	1.48337*	.09192	.000	1.1425	1.8242
	A2	-.05322	.09192	1.000	-.3941	.2876
	A4	.37916*	.09192	.018	.0383	.7200
	B1	.83149*	.09192	.000	.4906	1.1723
	B2	.57871*	.09192	.000	.2379	.9196
	B3	.65854*	.09192	.000	.3177	.9994
	B4	.69845*	.09192	.000	.3576	1.0393
	C1	.76497*	.09192	.000	.4241	1.1058
	C2	.47228*	.09192	.001	.1314	.8131
	C3	.30599	.09192	.117	-.0349	.6468
	C4	.48559*	.09192	.001	.1447	.8264
	D1	.77827*	.09192	.000	.4374	1.1191
	D2	.55876*	.09192	.000	.2179	.8996
	D3	.59867*	.09192	.000	.2578	.9395
	D4	.93792*	.09192	.000	.5971	1.2788
A4	A1	1.10421*	.09192	.000	.7634	1.4451
	A2	-.43237*	.09192	.004	-.7732	-.0915
	A3	-.37916*	.09192	.018	-.7200	-.0383
	B1	.45233*	.09192	.002	.1115	.7932
	B2	.19956	.09192	.709	-.1413	.5404
	B3	.27938	.09192	.209	-.0615	.6202

(I) GROUP	(J) GROUP	Mean Difference (I-J)	Std. Error	Sig.	95% Confidence Interval	
					Lower Bound	Upper Bound
	B4	.31929	.09192	.085	-.0216	.6601
	C1	.38581*	.09192	.015	.0450	.7267
	C2	.09313	.09192	1.000	-.2477	.4340
	C3	-.07317	.09192	1.000	-.4140	.2677
	C4	.10643	.09192	.998	-.2344	.4473
	D1	.39911*	.09192	.010	.0583	.7400
	D2	.17960	.09192	.832	-.1612	.5205
	D3	.21951	.09192	.568	-.1213	.5604
	D4	.55876*	.09192	.000	.2179	.8996
B1	A1	.65188*	.09192	.000	.3110	.9927
	A2	-.88470*	.09192	.000	-1.2256	-.5439
	A3	-.83149*	.09192	.000	-1.1723	-.4906
	A4	-.45233*	.09192	.002	-.7932	-.1115
	B2	-.25277	.09192	.345	-.5936	.0881
	B3	-.17295	.09192	.866	-.5138	.1679
	B4	-.13304	.09192	.981	-.4739	.2078
	C1	-.06652	.09192	1.000	-.4074	.2743
	C2	-.35920*	.09192	.031	-.7001	-.0184
	C3	-.52550*	.09192	.000	-.8663	-.1846
	C4	-.34590*	.09192	.044	-.6867	-.0050
	D1	-.05322	.09192	1.000	-.3941	.2876
	D2	-.27273	.09192	.238	-.6136	.0681
	D3	-.23282	.09192	.474	-.5737	.1080
D4	.10643	.09192	.998	-.2344	.4473	
B2	A1	.90466*	.09192	.000	.5638	1.2455
	A2	-.63193*	.09192	.000	-.9728	-.2911
	A3	-.57871*	.09192	.000	-.9196	-.2379
	A4	-.19956	.09192	.709	-.5404	.1413
	B1	.25277	.09192	.345	-.0881	.5936
	B3	.07982	.09192	1.000	-.2610	.4207
	B4	.11973	.09192	.993	-.2211	.4606
	C1	.18625	.09192	.794	-.1546	.5271
	C2	-.10643	.09192	.998	-.4473	.2344
	C3	-.27273	.09192	.238	-.6136	.0681
	C4	-.09313	.09192	1.000	-.4340	.2477
	D1	.19956	.09192	.709	-.1413	.5404
	D2	-.01996	.09192	1.000	-.3608	.3209
	D3	.01996	.09192	1.000	-.3209	.3608
D4	.35920*	.09192	.031	.0184	.7001	
B3	A1	.82483*	.09192	.000	.4840	1.1657
	A2	-.71175*	.09192	.000	-1.0526	-.3709
	A3	-.65854*	.09192	.000	-.9994	-.3177
	A4	-.27938	.09192	.209	-.6202	.0615
	B1	.17295	.09192	.866	-.1679	.5138
	B2	-.07982	.09192	1.000	-.4207	.2610

(I) GROUP	(J) GROUP	Mean Difference (I-J)	Std. Error	Sig.	95% Confidence Interval	
					Lower Bound	Upper Bound
	B4	.03991	.09192	1.000	-.3009	.3808
	C1	.10643	.09192	.998	-.2344	.4473
	C2	-.18625	.09192	.794	-.5271	.1546
	C3	-.35255*	.09192	.037	-.6934	-.0117
	C4	-.17295	.09192	.866	-.5138	.1679
	D1	.11973	.09192	.993	-.2211	.4606
	D2	-.09978	.09192	.999	-.4406	.2411
	D3	-.05987	.09192	1.000	-.4007	.2810
	D4	.27938	.09192	.209	-.0615	.6202
B4	A1	.78492*	.09192	.000	.4441	1.1258
	A2	-.75166*	.09192	.000	-1.0925	-.4108
	A3	-.69845*	.09192	.000	-1.0393	-.3576
	A4	-.31929	.09192	.085	-.6601	.0216
	B1	.13304	.09192	.981	-.2078	.4739
	B2	-.11973	.09192	.993	-.4606	.2211
	B3	-.03991	.09192	1.000	-.3808	.3009
	C1	.06652	.09192	1.000	-.2743	.4074
	C2	-.22616	.09192	.521	-.5670	.1147
	C3	-.39246*	.09192	.012	-.7333	-.0516
	C4	-.21286	.09192	.616	-.5537	.1280
	D1	.07982	.09192	1.000	-.2610	.4207
	D2	-.13969	.09192	.971	-.4805	.2012
	D3	-.09978	.09192	.999	-.4406	.2411
D4	.23947	.09192	.429	-.1014	.5803	
C1	A1	.71840*	.09192	.000	.3776	1.0593
	A2	-.81818*	.09192	.000	-1.1590	-.4773
	A3	-.76497*	.09192	.000	-1.1058	-.4241
	A4	-.38581*	.09192	.015	-.7267	-.0450
	B1	.06652	.09192	1.000	-.2743	.4074
	B2	-.18625	.09192	.794	-.5271	.1546
	B3	-.10643	.09192	.998	-.4473	.2344
	B4	-.06652	.09192	1.000	-.4074	.2743
	C2	-.29268	.09192	.157	-.6335	.0482
	C3	-.45898*	.09192	.002	-.7998	-.1181
	C4	-.27938	.09192	.209	-.6202	.0615
	D1	.01330	.09192	1.000	-.3275	.3542
	D2	-.20621	.09192	.663	-.5471	.1346
	D3	-.16630	.09192	.895	-.5071	.1746
D4	.17295	.09192	.866	-.1679	.5138	
C2	A1	1.01109*	.09192	.000	.6702	1.3519
	A2	-.52550*	.09192	.000	-.8663	-.1846
	A3	-.47228*	.09192	.001	-.8131	-.1314
	A4	-.09313	.09192	1.000	-.4340	.2477
	B1	.35920*	.09192	.031	.0184	.7001
	B2	.10643	.09192	.998	-.2344	.4473

(I) GROUP	(J) GROUP	Mean Difference (I-J)	Std. Error	Sig.	95% Confidence Interval	
					Lower Bound	Upper Bound
	B3	.18625	.09192	.794	-.1546	.5271
	B4	.22616	.09192	.521	-.1147	.5670
	C1	.29268	.09192	.157	-.0482	.6335
	C3	-.16630	.09192	.895	-.5071	.1746
	C4	.01330	.09192	1.000	-.3275	.3542
	D1	.30599	.09192	.117	-.0349	.6468
	D2	.08647	.09192	1.000	-.2544	.4273
	D3	.12639	.09192	.988	-.2145	.4672
	D4	.46563*	.09192	.001	.1248	.8065
C3	A1	1.17738*	.09192	.000	.8365	1.5182
	A2	-.35920*	.09192	.031	-.7001	-.0184
	A3	-.30599	.09192	.117	-.6468	.0349
	A4	.07317	.09192	1.000	-.2677	.4140
	B1	.52550*	.09192	.000	.1846	.8663
	B2	.27273	.09192	.238	-.0681	.6136
	B3	.35255*	.09192	.037	.0117	.6934
	B4	.39246*	.09192	.012	.0516	.7333
	C1	.45898*	.09192	.002	.1181	.7998
	C2	.16630	.09192	.895	-.1746	.5071
	C4	.17960	.09192	.832	-.1612	.5205
	D1	.47228*	.09192	.001	.1314	.8131
	D2	.25277	.09192	.345	-.0881	.5936
	D3	.29268	.09192	.157	-.0482	.6335
D4	.63193*	.09192	.000	.2911	.9728	
C4	A1	.99778*	.09192	.000	.6569	1.3386
	A2	-.53880*	.09192	.000	-.8797	-.1980
	A3	-.48559*	.09192	.001	-.8264	-.1447
	A4	-.10643	.09192	.998	-.4473	.2344
	B1	.34590*	.09192	.044	.0050	.6867
	B2	.09313	.09192	1.000	-.2477	.4340
	B3	.17295	.09192	.866	-.1679	.5138
	B4	.21286	.09192	.616	-.1280	.5537
	C1	.27938	.09192	.209	-.0615	.6202
	C2	-.01330	.09192	1.000	-.3542	.3275
	C3	-.17960	.09192	.832	-.5205	.1612
	D1	.29268	.09192	.157	-.0482	.6335
	D2	.07317	.09192	1.000	-.2677	.4140
	D3	.11308	.09192	.996	-.2278	.4539
D4	.45233*	.09192	.002	.1115	.7932	
D1	A1	.70510*	.09192	.000	.3642	1.0460
	A2	-.83149*	.09192	.000	-1.1723	-.4906
	A3	-.77827*	.09192	.000	-1.1191	-.4374
	A4	-.39911*	.09192	.010	-.7400	-.0583
	B1	.05322	.09192	1.000	-.2876	.3941
	B2	-.19956	.09192	.709	-.5404	.1413

(I) GROUP	(J) GROUP	Mean Difference (I-J)	Std. Error	Sig.	95% Confidence Interval	
					Lower Bound	Upper Bound
	B3	-.11973	.09192	.993	-.4606	.2211
	B4	-.07982	.09192	1.000	-.4207	.2610
	C1	-.01330	.09192	1.000	-.3542	.3275
	C2	-.30599	.09192	.117	-.6468	.0349
	C3	-.47228*	.09192	.001	-.8131	-.1314
	C4	-.29268	.09192	.157	-.6335	.0482
	D2	-.21951	.09192	.568	-.5604	.1213
	D3	-.17960	.09192	.832	-.5205	.1612
	D4	.15965	.09192	.921	-.1812	.5005
D2	A1	.92461*	.09192	.000	.5838	1.2655
	A2	-.61197*	.09192	.000	-.9528	-.2711
	A3	-.55876*	.09192	.000	-.8996	-.2179
	A4	-.17960	.09192	.832	-.5205	.1612
	B1	.27273	.09192	.238	-.0681	.6136
	B2	.01996	.09192	1.000	-.3209	.3608
	B3	.09978	.09192	.999	-.2411	.4406
	B4	.13969	.09192	.971	-.2012	.4805
	C1	.20621	.09192	.663	-.1346	.5471
	C2	-.08647	.09192	1.000	-.4273	.2544
	C3	-.25277	.09192	.345	-.5936	.0881
	C4	-.07317	.09192	1.000	-.4140	.2677
	D1	.21951	.09192	.568	-.1213	.5604
	D3	.03991	.09192	1.000	-.3009	.3808
	D4	.37916*	.09192	.018	.0383	.7200
D3	A1	.88470*	.09192	.000	.5439	1.2256
	A2	-.65188*	.09192	.000	-.9927	-.3110
	A3	-.59867*	.09192	.000	-.9395	-.2578
	A4	-.21951	.09192	.568	-.5604	.1213
	B1	.23282	.09192	.474	-.1080	.5737
	B2	-.01996	.09192	1.000	-.3608	.3209
	B3	.05987	.09192	1.000	-.2810	.4007
	B4	.09978	.09192	.999	-.2411	.4406
	C1	.16630	.09192	.895	-.1746	.5071
	C2	-.12639	.09192	.988	-.4672	.2145
	C3	-.29268	.09192	.157	-.6335	.0482
	C4	-.11308	.09192	.996	-.4539	.2278
	D1	.17960	.09192	.832	-.1612	.5205
	D2	-.03991	.09192	1.000	-.3808	.3009
	D4	.33925	.09192	.052	-.0016	.6801
D4	A1	.54545*	.09192	.000	.2046	.8863
	A2	-.99113*	.09192	.000	-1.3320	-.6503
	A3	-.93792*	.09192	.000	-1.2788	-.5971
	A4	-.55876*	.09192	.000	-.8996	-.2179
	B1	-.10643	.09192	.998	-.4473	.2344

(I) GROUP	(J) GROUP	Mean Difference (I-J)	Std. Error	Sig.	95% Confidence Interval	
					Lower Bound	Upper Bound
	B2	-.35920*	.09192	.031	-.7001	-.0184
	B3	-.27938	.09192	.209	-.6202	.0615
	B4	-.23947	.09192	.429	-.5803	.1014
	C1	-.17295	.09192	.866	-.5138	.1679
	C2	-.46563*	.09192	.001	-.8065	-.1248
	C3	-.63193*	.09192	.000	-.9728	-.2911
	C4	-.45233*	.09192	.002	-.7932	-.1115
	D1	-.15965	.09192	.921	-.5005	.1812
	D2	-.37916*	.09192	.018	-.7200	-.0383
	D3	-.33925	.09192	.052	-.6801	.0016

*. The mean difference is significant at the 0.05 level.

11. ANOVA analysis of the relative BMP2 secretion of proliferative induced RBMSCs.

ANOVA

BMP2

	Sum of Squares	df	Mean Square	F	Sig.
Between Groups	.715	7	.102	132.739	.000
Within Groups	.012	16	.001		
Total	.727	23			

Multiple Comparisons

BMP2

Tukey HSD

(I) G4	(J) G4	Mean Difference (I-J)	Std. Error	Sig.	95% Confidence Interval	
					Lower Bound	Upper Bound
2%FBS 24h	FGF2 24h	-.08619*	.02265	.026	-.1646	-.0078
	INSULIN 24h	-.25316*	.02265	.000	-.3316	-.1748
	FGF2+INSULIN 24h	-.09588*	.02265	.011	-.1743	-.0175
	2%FBS 72h	.29549*	.02265	.000	.2171	.3739
	FGF2 72h	.10980*	.02265	.003	.0314	.1882
	INSULIN 72h	.10138*	.02265	.007	.0230	.1798
	FGF2+INSULIN 72h	.24603*	.02265	.000	.1676	.3244
FGF2 24h	2%FBS 24h	.08619*	.02265	.026	.0078	.1646
	INSULIN 24h	-.16697*	.02265	.000	-.2454	-.0886
	FGF2+INSULIN 24h	-.00969	.02265	1.000	-.0881	.0687
	2%FBS 72h	.38169*	.02265	.000	.3033	.4601
	FGF2 72h	.19600*	.02265	.000	.1176	.2744
	INSULIN 72h	.18757*	.02265	.000	.1092	.2660
	FGF2+INSULIN 72h	.33222*	.02265	.000	.2538	.4106

(I) G4	(J) G4	Mean Difference (I-J)	Std. Error	Sig.	95% Confidence Interval	
					Lower Bound	Upper Bound
INSULIN 24h	2%FBS 24h	.25316*	.02265	.000	.1748	.3316
	FGF2 24h	.16697*	.02265	.000	.0886	.2454
	FGF2+INSULIN 24h	.15728*	.02265	.000	.0789	.2357
	2%FBS 72h	.54866*	.02265	.000	.4702	.6271
	FGF2 72h	.36297*	.02265	.000	.2846	.4414
	INSULIN 72h	.35454*	.02265	.000	.2761	.4330
	FGF2+INSULIN 72h	.49919*	.02265	.000	.4208	.5776
FGF2 +INSULIN 24h	2%FBS 24h	.09588*	.02265	.011	.0175	.1743
	FGF2 24h	.00969	.02265	1.000	-.0687	.0881
	INSULIN 24h	-.15728*	.02265	.000	-.2357	-.0789
	2%FBS 72h	.39138*	.02265	.000	.3130	.4698
	FGF2 72h	.20569*	.02265	.000	.1273	.2841
	INSULIN 72h	.19726*	.02265	.000	.1189	.2757
	FGF2+INSULIN 72h	.34191*	.02265	.000	.2635	.4203
2%FBS 72h	2%FBS 24h	-.29549*	.02265	.000	-.3739	-.2171
	FGF2 24h	-.38169*	.02265	.000	-.4601	-.3033
	INSULIN 24h	-.54866*	.02265	.000	-.6271	-.4702
	FGF2+INSULIN 24h	-.39138*	.02265	.000	-.4698	-.3130
	FGF2 72h	-.18569*	.02265	.000	-.2641	-.1073
	INSULIN 72h	-.19412*	.02265	.000	-.2725	-.1157
	FGF2+INSULIN 72h	-.04946	.02265	.409	-.1279	.0289
FGF2 72h	2%FBS 24h	-.10980*	.02265	.003	-.1882	-.0314
	FGF2 24h	-.19600*	.02265	.000	-.2744	-.1176
	INSULIN 24h	-.36297*	.02265	.000	-.4414	-.2846
	FGF2+INSULIN 24h	-.20569*	.02265	.000	-.2841	-.1273
	2%FBS 72h	.18569*	.02265	.000	.1073	.2641
	INSULIN 72h	-.00843	.02265	1.000	-.0868	.0700
	FGF2+INSULIN 72h	.13623*	.02265	.000	.0578	.2146
INSULIN 72h	2%FBS 24h	-.10138*	.02265	.007	-.1798	-.0230
	FGF2 24h	-.18757*	.02265	.000	-.2660	-.1092
	INSULIN 24h	-.35454*	.02265	.000	-.4330	-.2761
	FGF2+INSULIN 24h	-.19726*	.02265	.000	-.2757	-.1189
	2%FBS 72h	.19412*	.02265	.000	.1157	.2725
	FGF2 72h	.00843	.02265	1.000	-.0700	.0868
	FGF2+INSULIN 72h	.14465*	.02265	.000	.0662	.2231
FGF2 +INSULIN 72h	2%FBS 24h	-.24603*	.02265	.000	-.3244	-.1676
	FGF2 24h	-.33222*	.02265	.000	-.4106	-.2538
	INSULIN 24h	-.49919*	.02265	.000	-.5776	-.4208
	FGF2+INSULIN 24h	-.34191*	.02265	.000	-.4203	-.2635
	2%FBS 72h	.04946	.02265	.409	-.0289	.1279
	FGF2 72h	-.13623*	.02265	.000	-.2146	-.0578
	INSULIN 72h	-.14465*	.02265	.000	-.2231	-.0662

*. The mean difference is significant at the 0.05 level.

12. ANOVA analysis of the relative luciferase activity of FGF2 and/or insulin induced RBMSCs

ANOVA

		Sum of Squares	df	Mean Square	F	Sig.
RUNX2_N	Between Groups	27.752	3	9.251	299.401	.000
	Within Groups	.247	8	.031		
	Total	27.999	11			
RUNX2_F	Between Groups	3.322	3	1.107	150.527	.000
	Within Groups	.059	8	.007		
	Total	3.381	11			
AP1X5	Between Groups	1.943	3	.648	19.193	.001
	Within Groups	.270	8	.034		
	Total	2.213	11			
SRYX5	Between Groups	.565	3	.188	13.119	.002
	Within Groups	.115	8	.014		
	Total	.680	11			

Multiple Comparisons

Tukey HSD

Dependent Variable	(I) GROUP	(J) GROUP	Mean Difference (I-J)	Std. Error	Sig.	95% Confidence Interval	
						Lower Bound	Upper Bound
RUNX2_N	2%FBS	FGF2	.41287	.14352	.079	-.0467	.8725
		INSULIN	-3.05741 [*]	.14352	.000	-3.5170	-2.5978
		FGF2+INSULIN	-2.54028 [*]	.14352	.000	-2.9999	-2.0807
	FGF2	2%FBS	-.41287	.14352	.079	-.8725	.0467
		INSULIN	-3.47028 [*]	.14352	.000	-3.9299	-3.0107
		FGF2+INSULIN	-2.95315 [*]	.14352	.000	-3.4128	-2.4935
	INSULIN	2%FBS	3.05741 [*]	.14352	.000	2.5978	3.5170
		FGF2	3.47028 [*]	.14352	.000	3.0107	3.9299
		FGF2+INSULIN	.51713 [*]	.14352	.029	.0575	.9767
	FGF2+INSULIN	2%FBS	2.54028 [*]	.14352	.000	2.0807	2.9999
		FGF2	2.95315 [*]	.14352	.000	2.4935	3.4128
		INSULIN	-.51713 [*]	.14352	.029	-.9767	-.0575
RUNX2_F	2%FBS	FGF2	-.40332 [*]	.07003	.002	-.6276	-.1791
		INSULIN	-.81331 [*]	.07003	.000	-1.0376	-.5890
		FGF2+INSULIN	-1.42318 [*]	.07003	.000	-1.6475	-1.1989
	FGF2	2%FBS	.40332 [*]	.07003	.002	.1791	.6276
		INSULIN	-.40999 [*]	.07003	.002	-.6343	-.1857
		FGF2+INSULIN	-1.01985 [*]	.07003	.000	-1.2441	-.7956
	INSULIN	2%FBS	.81331 [*]	.07003	.000	.5890	1.0376
		FGF2	.40999 [*]	.07003	.002	.1857	.6343

Dependent Variable	(I) GROUP	(J) GROUP	Mean Difference (I-J)	Std. Error	Sig.	95% Confidence Interval	
						Lower Bound	Upper Bound
	FGF2+INSULIN	FGF2+INSULIN	-.60987*	.07003	.000	-.8341	-.3856
		2%FBS	1.42318*	.07003	.000	1.1989	1.6475
		FGF2	1.01985*	.07003	.000	.7956	1.2441
		INSULIN	.60987*	.07003	.000	.3856	.8341
AP1X5	2%FBS	FGF2	-.19705	.14998	.580	-.6773	.2832
		INSULIN	-.00275	.14998	1.000	-.4830	.4775
		FGF2+INSULIN	-.97730*	.14998	.001	-1.4576	-.4970
	FGF2	2%FBS	.19705	.14998	.580	-.2832	.6773
		INSULIN	.19430	.14998	.590	-.2860	.6746
		FGF2+INSULIN	-.78025*	.14998	.004	-1.2605	-.3000
	INSULIN	2%FBS	.00275	.14998	1.000	-.4775	.4830
		FGF2	-.19430	.14998	.590	-.6746	.2860
		FGF2+INSULIN	-.97455*	.14998	.001	-1.4548	-.4943
	FGF2+INSULIN	2%FBS	.97730*	.14998	.001	.4970	1.4576
		FGF2	.78025*	.14998	.004	.3000	1.2605
		INSULIN	.97455*	.14998	.001	.4943	1.4548
SRYX5	2%FBS	FGF2	.36802*	.09787	.023	.0546	.6814
		INSULIN	-.23921	.09787	.145	-.5526	.0742
		FGF2+INSULIN	.00027	.09787	1.000	-.3131	.3137
	FGF2	2%FBS	-.36802*	.09787	.023	-.6814	-.0546
		INSULIN	-.60723*	.09787	.001	-.9206	-.2938
		FGF2+INSULIN	-.36775*	.09787	.023	-.6812	-.0543
	INSULIN	2%FBS	.23921	.09787	.145	-.0742	.5526
		FGF2	.60723*	.09787	.001	.2938	.9206
		FGF2+INSULIN	.23948	.09787	.145	-.0739	.5529
	FGF2+INSULIN	2%FBS	-.00027	.09787	1.000	-.3137	.3131
		FGF2	.36775*	.09787	.023	.0543	.6812
		INSULIN	-.23948	.09787	.145	-.5529	.0739

*. The mean difference is significant at the 0.05 level.